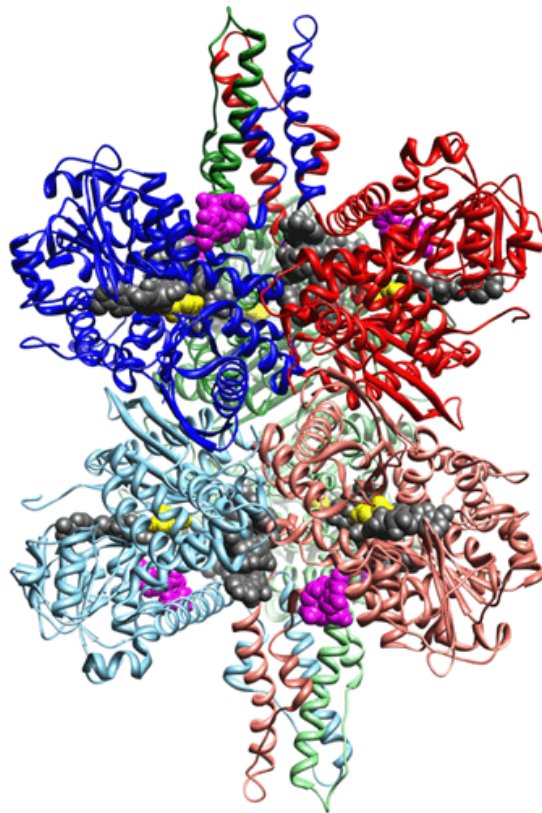UNIVERSITY OF CRETE
MEDICAL SCHOOL

FUNCTIONAL, STRUCTURAL AND GENETIC STUDIES ON HUMAN GLUTAMATE DEHYDROGENASES

Λειτουργικές, Δομικές και Γενετικές μελέτες των ανθρώπινων Γλουταμικών Αφυδρογονασών

Christina Dimovasili

PhD Thesis
September 2016

Three-Member Advisory Committee

Zaganas I. (Supervisor)
Kokkinidis M.
Tokatlidis K.

Seven-Member Examination Committee

Plaitakis A. (Emeritus Professor of Neurology, University of Crete)
Kokkinidis M. (Professor of Structural Biology, University of Crete)
Thermou K. (Professor of Pharmacology, University of Crete)
Kardasis D. (Professor of Biochemistry, University of Crete)
Tokatlidis K. (Professor of Medical School, Cathcart Chair of Biochemistry, University of Glasgow
Zaganas I. (Assistant Professor of Neurology, University of Crete)
Spanaki K. (Assistant Professor of Neurology, University of Crete)

1

To my true source of strength, my most beloved, Antonis Dimovasilis

Contents

Huge acknowledgements go to my colleagues, but most importantly friends, Lampro Mathioudaki and Mara Bourbouli for making this task pleasant, for the memorable moments we shared in the Neurology lab and beyond, and of course for the brainstorming, troubleshooting and their overall scientific input in this work.

Last but not least, I would like to thank my parents, George and Zografia, and my beloved brother Antonis, without whose love and support by any means, I would have never been able to achieve any of the goals I wished for, throughout all these years.

	Table of Abreviations		
AA	Amino Acid Aminotransferase	MNPs	Multiple Nucleotide Polymorphisms
AD	Alzheimer's Disease	mTOR	mechanistic Target of Rapamycin
ADP	Adenosine Diphosphate	MWCO	Molecular Weight Cut Off
ATP	Adenosine Triphosphate	NAD	Nicotinamide Adenine Dinucleotide
BCATm	Mitochondrial Branched Chain Aminotransferase	OXPHOS	Oxidative Phosphorylation
CNS	Central Nervous System	PAG	Phosphate-activated Glutaminase
Co-IP	Co-Immunoprecipitation	PAGE	Polyacrylimide Gel Electrophoresis
CRP	C-reactive Protein	PBS	Phosphate Buffer Saline
DES	Diethylstilbestrol	PD	Parkinson's DiseasePoly
DMSO	Dimethyl sulfoxide	PEG	Polyethynel Glycol
EAAT	Excitatory Amino Acid Transporter	PEP	Glyceraldehyde-3-Phosphate
EDTA	Ethylenediaminetetraacetic acid	PGA	3-Phosphoglycerate
EGCG	Epigallocatechin Gallate	PGAL	Glyceraldehyde-3-Phosphate
ETC	Electron Transfer Chain	PHC	Primary Health Care
ExAC	Exome Aggregation Consortium	RI	Refractive Intex
FAD	Flavin Adenine Dinucleotide	ROS	Reactive Oxygen Species
FBT	FlexiBacTurbo	SDS	Single Nucleotide Polymorphisms
FTD	Frontotemporal Dementia	SEC/MALS	Size Exclusion Chromatography/Multi Angle Light Scattering
GABA	Gamma-Aminobutyric Acid	SNPs	Single Nucleotide Polymorphisms
GAD	Glutamate Decarboxylase	TCA	Tricarboxylic Acid
GATK	Genome Analysis Toolkit	TMAP	Torrent Mapping Alignment Program
GDH	Glutamate Dehydrogenase	TNFα	Tumor Necrosis Factor
GLN	Glutamine	TRA	Triethanolamine
GLU	Glutamate	TVC	Torrent Variant Caller
GS	Glutamine Synthetase	UV	Ultra Violet
GTP	Guanosine-5'-Triphosphate	VaD	Vascular Dementia
GWAS	Genome-Wide Association Studies	VCF	Variant Call Format
HI/HA	Hyperammonemia/Hyperinsulinism	WES	Whole Exome Sequencing
HPLC	High Pressure Liquid Chromatography	α-KG	A-Ketoglutarate
IL-6	Interleukin 6		
LB	Lysogeny Broth		
LBD	Lewy Body Dementia		
MCI	Mild cognitive impairement		
MMSE	Mini Mental Status Examination		

Abstract

Background: Glutamate dehydrogenase (GDH) is an abundant mitochondrial enzyme which catalyzes the interconversion of glutamate to α-ketoglutarate. Humans possess two functional genes which encode for GDH, the ubiquitously expressed *GLUD1* (coding for hGDH1) and the tissue specific *GLUD2* (coding for hGDH2). The two iso-enzymes, although sharing all but 15 out of their 505 amino acids in their mature form, differ significantly in their regulation properties. hGDH2 is mainly detected on brain, kidney and testis, where it is found to co-localize with hGDH1 in the mitochondrial matrix. Both iso-enzymes operate by forming homo-hexamers, but it is currently unknown if they form hetero-hexamers at the areas where they co-localize. Besides their physiological role in metabolism, genetic alterations in the *GLUD1* and *GLUD2* genes have been associated with pathophysiological conditions. Specifically, mutations of the *GLUD1* gene lead to the hyperinsulinism / hyperammonemia syndrome, whereas a polymorphism in *GLUD2* has been associated with accelerated Parkinson's disease age of onset. Furthermore, there is evidence that hGDH plays a role in Alzheimer's disease associated neurodegeneration (as its overexpression leads to age associated degenerative changes in the mouse hippocampus), even though proof for this in human patients suffering from dementia is lacking.

Aims: Aim of this study is to further analyze hGDH1 and hGDH2 properties by employing functional, structural as well as genetic methods. Specifically, we investigated whether hGDH1 and hGDH2 are capable of forming hetero-hexamers when they are co-expressed, and what particular properties these complexes may have. Secondly, we aimed to obtain the so far unsolved crystal structure of hGDH2 which will enable us to perform a valid and accurate comparison with hGDH1 (the structure of which is already known). Lastly, we analyzed the genetic variations' spectrum of *GLUD1* and *GLUD2* genes in the well characterized Cretan Aging Cohort of 201 subjects, comprising of patients suffering from dementia and mild cognitive impairment (MCI), as well as of cognitive normal controls.

Methods: To accomplish the first part of our aims, we created hetero-hexameric hGDH complexes in Sf21 cells, using the Baculovirus expression system. We employed co-immunoprecipitation and affinity chromatography to discriminate between *in vitro* mixtures of separately expressed hGDHs and *in vivo* 1:1 co-expressed hGDHs. Then we performed a series of kinetic studies to characterize the possible hetero-hexamers' properties. For the second part, we produced hGDH2 in large-scale Sf21 cultures and

we purified it to homogeneity, before crystallization by repeated trials using different methods and reagents. For the genetic studies, we obtained Whole Exome Sequencing data from 201 Cretan elderly individuals, from which 100 suffered from dementia, 20 were classified as MCI and 81 were cognitive normal controls. After characterizing their dementia related genetic background, we focused on *GLUD1* and *GLUD2* genes in respect to their variations.

Results: In the present study we show that hGDHs can form, apart from homo-hexamers, hetero-hexameric complexes, when they are co-expressed. These hetero-hexamers possess unique enzymatic properties, which under specific conditions (absence of ADP, L-leucine activation, heat stability) are intermediate between the properties of pure hGDH1 and hGDH2 (and thus comparable to the 1:1 in vitro mixture of the two homo-hexamers), whereas they tend to resemble hGDH2's behavior in respect with GTP and DES inhibition. In the second part of the study, we managed for the first time to produce high-quality hGDH2 crystals of 3.2Å resolution for structure characterization. In the third part of the study (genetic analysis of *GLUD1* and *GLUD2* genes), we found the Ser498Ala *GLUD2* variant to be more common in controls (16.05%, n=81) than in patients with dementia (3.0%, n=100; p=0.003), and these results were verified by including in our analyses an additional local cohort.

Conclusion: Our study raises the possibility that hGDH1 and hGDH2 form hetero-hexamers in the cells where they are co-expressed. As the functional properties of these complexes are distinct from those of homo-hexamers, this association might provide versatility to human cells by equipping them with more than two iso-enzymes. Structural studies on hGDH2 are expected, not only to explore its particularities, but also to decipher the structural basis of its enzymatic differences from its highly homologous hGDH1 iso-enzyme. Finally, in the culturally and genetically homogeneous cohort of aged adults of the island of Crete, we found that the Ser498Ala *GLUD2* variant was associated with lower risk for dementia in our population.

Περίληψη

Ιστορικό: Η αφυδρογονάση του γλουταμικού (GDH) είναι ένα άφθονο μιτοχονδριακό ένζυμο που καταλύει την αλληλομετατροπή του γλουταμικού σε α-κετογλουταρικό. Οι άνθρωποι διαθέτουν δύο λειτουργικά γονίδια τα οποία κωδικοποιούν για GDH, το απανταχού εκφραζόμενο *GLUD1* (κωδικοποίηση για hGDH1) και το ιστο-ειδικό *GLUD2* (κωδικοποίηση για hGDH2). Τα δύο ισο-ένζυμα, αν και μοιράζονται όλα, πλην 15 από τα 505 αμινοξέα τους στην ώριμη μορφή τους, διαφέρουν σημαντικά στις ιδιότητες ρύθμισής τους. Η hGDH2 ανιχνεύεται κυρίως στον εγκέφαλο, στο νεφρό και στους όρχεις, όπου συνεντοπίζεται με τη hGDH1 στη μιτοχονδριακή μήτρα. Και τα δύο ισο-ένζυμα λειτουργούν σχηματίζοντας ομο-εξαμερών, αλλά είναι προς το παρόν άγνωστο κατά πόσον μπορούν να σχηματίσουν και λειτουργικά ετερο-εξαμερή στις περιοχές όπου συν-εντοπίζονται. Εκτός από το φυσιολογικό ρόλο των ενζύμων στο μεταβολισμό, γενετικές μεταβολές στα γονίδια *GLUD1* και *GLUD2* έχουν συσχετιστεί με παθοφυσιολογικές καταστάσεις. Συγκεκριμένα, οι μεταλλάξεις του γονιδίου *GLUD1* οδηγούν στο σύνδρομο υπερινσουλινισμό / υπεραμμωνιαιμία, ενώ ένας πολυμορφισμός στο *GLUD2* έχει συσχετισθεί με μικρότερη ηλικίας έναρξης της νόσου του Parkinson. Επιπλέον, υπάρχουν ενδείξεις ότι η hGDH παίζει κάποιο ρόλο στον νευροεκφυλισμό που σχετίζεται νόσο του Alzheimer (καθώς υπερέκφραση του αντίστοιχου γονιδίου οδηγεί σε σχετιζόμενες με το γήρας εκφυλιστικές μεταβολές στον ιππόκαμπο ποντικού), αν και απόδειξη για αυτό σε ανθρώπους ασθενείς που πάσχουν από άνοια δεν υπάρχει μέχρι σήμερα.

Στόχοι: Σκοπός της παρούσας μελέτης είναι η περαιτέρω ανάλυση των ιδιοτήτων των ενζύμων hGDH1 και hGDH2 χρησιμοποιώντας λειτουργικές, δομικές, καθώς και γενετικές μεθόδους. Συγκεκριμένα, ερευνήσαμε αν τα ένζυμα hGDH1 και hGDH2 είναι ικανά να σχηματίζουν ετερο-εξαμερή όταν συνεκφράζονται, και τι συγκεκριμένες ιδιότητες μπορεί να διαθέτουν αυτά τα μακρομόρια. Ένας δεύτερος στόχος ήταν να επιτύχουμε και να αναλύσουμε τη μέχρι σήμερα άλυτη κρυσταλλική δομή της hGDH2, η οποία θα μας επιτρέψει να πραγματοποιήσουμε μια έγκυρη και ακριβή σύγκριση με την hGDH1 (η δομή της οποίας είναι ήδη γνωστή). Τέλος, αναλύσαμε το φάσμα των γενετικών παραλλαγών των γονιδίων *GLUD1* και *GLUD2* γονιδίων στο καλά χαρακτηρισμένο Κρητικό Δείγμα Ηλικιωμένων 201 ατόμων, που αποτελείται από ασθενείς που πάσχουν από άνοια και ήπια γνωστική εξασθένηση (MCI), καθώς και από γνωστικά φυσιολογικά άτομα.

Μέθοδοι: Για να επιτευχθεί το πρώτο μέρος των στόχων μας, έχουμε δημιουργήσει hGDH ετερο-εξαμερή συμπλέγματα σε κύτταρα Sf21, χρησιμοποιώντας το σύστημα έκφρασης του βακουλοϊού. Πραγματοποιήσαμε πειράματα συν-ανοσοκατακρήμνισης και χρωματογραφίας συγγένειας για να διακρίνουμε μεταξύ των *in vitro* μιγμάτων χωριστά εκφρασμένων hGDHs και των *in vivo* 1:1 συν-εκφρασμένων hGDHs. Στη συνέχεια πραγματοποιήσαμε μια σειρά κινητικών δοκιμασιών για να χαρακτηρίσουμε τις ιδιότητες των πιθανών ετερο-εξαμερών. Για το δεύτερο μέρος των στόχων μας, παράχθηκε το ένζυμο hGDH2 σε Sf21 καλλιέργειες μεγάλης κλίμακας και κατόπιν καθαρίστηκε σε ομοιογένεια, πριν επιτευχθεί η κρυστάλλωσή του μέσω επαναλαμβανόμενων δοκιμών, χρησιμοποιώντας διαφορετικές μεθόδους και αντιδραστήρια. Για τις γενετικές μελέτες, αξιοποιήσαμε τα δεδομένα που προέκυψαν από την αλληλουχία ολόκληρου του εξώματος σε 201 άτομα του Κρητικού Δείγματος Ηλικιωμένων ατόμων, από τα οποία 100 έπασχαν από άνοια, 20 είχαν ταξινομηθεί ως MCI και 81 ήταν γνωστά φυσιολογικοί μάρτυρες. Μετά τον χαρακτηρισμό του γενετικού υπόβαθρου που σχετίζονται με την άνοια, επικεντρωθήκαμε στις παραλλαγές των γονιδίων *GLUD1* και *GLUD2*.

Αποτελέσματα: Στην παρούσα μελέτη δείξαμε ότι οι hGDHs μπορούν να σχηματίσουν, εκτός από ομο-εξαμερή, ετερο-εξαμερή σύμπλοκα, όταν συν-εκφράζονται. Αυτά ετερο-εξαμερή ένζυμα διαθέτουν μοναδικές ενζυμικές ιδιότητες, οι οποίες κάτω από συγκεκριμένες συνθήκες (απουσία ADP, L-λευκίνη ενεργοποίηση, θερμική σταθερότητα) είναι ενδιάμεσες μεταξύ των ιδιοτήτων του καθαρού hGDH1 και hGDH2 (και συνεπώς συγκρίσιμα με το 1:1 *in vitro* μίγμα των δύο ομο-εξαμερών μορφών), ενώ τείνουν να μοιάζουν με τη συμπεριφορά της hGDH2 σε σχέση με την αναστολή από GTP και από DES. Στο δεύτερο μέρος της μελέτης, επιτύχαμε για πρώτη φορά την παραγωγή υψηλής ποιότητας κρυστάλλων hGDH2 των 3.2Å για το χαρακτηρισμό της δομής της. Στο τρίτο μέρος της μελέτης (γενετική ανάλυση των *GLUD1* και *GLUD2* γονιδίων), βρήκαμε ότι η παραλλαγή Ser498Ala του *GLUD2* εμφανίζεται συχνότερα σε φυσιολογικούς μάρτυρες (16,05%, n = 81) από ό,τι σε ασθενείς με άνοια (3,0%, n = 100? p = 0,003), και τα αποτελέσματα αυτά επιβεβαιώθηκαν με τη συμπερίληψη μιας επιπλέον τοπικής ομάδας ηλικιωμένων ατόμων στις αναλύσεις μας.

Συμπέρασμα: Η μελέτη μας εγείρει την πιθανότητα ότι οι hGDH1 και hGDH2 σχηματίζουν ετερο-εξαμερή στα κύτταρα όπου συνεκφράζονται. Δεδομένου ότι οι λειτουργικές ιδιότητες αυτών των συμπλόκων είναι διακριτές από εκείνες των ομο-εξαμερών, η αλληλεπίδραση αυτή ενδέχεται να παρέχει ευελιξία στα ανθρώπινα

κύτταρα, εξοπλίζοντας τα με περισσότερα από δύο ισο-ένζυμα. Οι δομικές μελέτες της hGDH2 αναμένεται, όχι μόνο να εξερευνήσουν τις ιδιαιτερότητές του, αλλά και να αποκρυπτογραφήσει τη δομική βάση των ενζυμικών διαφορών του από το υψηλά ομόλογο της ισο-ένζυμο hGDH1. Τέλος, στην πολιτισμικά και γενετικά ομοιογενή ομάδα της των ηλικιωμένων ατόμων του νησιού της Κρήτης, βρήκαμε ότι η παραλλαγή Ser498Ala του *GLUD2* σχετίζεται με μειωμένο κίνδυνο για άνοια στον πληθυσμό μας.

The connection between mitochondrial dysfunction and neurodegenerative processes has lately become more and more well established. Numerous pieces of evidence have come together to greatly expand our understanding of the role of mitochondria in the pathogenesis of neurodegenerative diseases. Interestingly, mitochondria dysfunction and oxidative stress occur early in most major neurodegenerative disorders. Together with the biochemical processes, mitochondrial DNA mutations, also contribute to ageing which is essentially the greatest risk factor of these disorders. The propensity of mitochondrial dysfunction to affect primarily the brain has been explained by the different tissue requirements for mitochondrial function, or, in other words, different energy requirements. CNS functions strongly depend on efficient mitochondrial function, because brain tissue has a high energy demand. Energy requirements are covered by the energy-bearing molecule of the cell, namely ATP. Mitochondria are involved in ATP supply to cells through a chain of reactions comprising oxidative phosphorylation (OXPHOS).

Beyond this essential role, mitochondria are responsible for other crucial functions as well. They are involved in the synthesis of key molecules, in response to oxidative stress, in apoptosis and in dynamic movements required for correct respiratory activity and metabolic efficiency through fusion/fission. Therefore, mitochondria contain many redox enzymes to fulfil their functions. However, naturally occurring inefficiencies of redox procedures such as oxidative phosphorylation, generate reactive oxygen species (ROS) which can cause several damages in cellular structures (Lin et al. 2006).

Towards the direction of studying mitochondrial enzymes which are implicated in energy metabolism, we ought to focus on glutamate dehydrogenases. Mammalian glutamate dehydrogenase (GDH) is an abundant mitochondrial enzyme (constituting up to 10% of the total matrix protein) that catalyzes the reversible conversion of glutamate to α-ketoglutarate and ammonia, employing NADP(H) and NAD(H) as cofactors (Zaganas et al. 2009). The enzyme interconnects the Krebs cycle with amino-acid metabolism, lying at the crossroads of several important metabolic pathways. The levels of the main allosteric regulators of the enzyme (ADP, GTP, and L-leucine) reflect the cellular energy charge, suggesting that the activity of the enzyme depends heavily on the energy status of the cell.

1. BRAIN ENERGY METABOLISM

Human brain, although occupying only 2% of total body weight, is one of the most energy-consuming organs, utilizing 25% of total glucose intakes and 20% of available oxygen. Unlike other tissues which process glucose via various metabolic pathways, neural tissue entirely oxidizes glucose to CO_2 and water through its sequential processing by glycolysis, the tricarboxylic acid (TCA) cycle and oxidative phosphorylation. Complete oxidation of one glucose molecule provides the cell with an energy load of 30-36 ATP molecules, and the procedure not only is vital but also it is highly effective at meeting the energy demands of the restless neuron.

Regarding the energy distribution at the cellular level, neurons are by far the most demanding cell type, since they are being allocated more than 80% of brain energy, while glia require only 5-15%. Indeed, in contrast to other cell types that use their energy to fuel their baseline general cellular processes (which include DNA replication, protein synthesis, vessel transportation and communication with other cells etc.), neurons are burdened with the complex, yet vital, signaling operation. The main energy consuming procedure in brain is the maintenance of ionic gradients, across the plasma membrane, which are disrupted during excitability. This is predominantly achieved through the activity of NA^+ and K^+-ATPase ionic pumps, which, as stated by their name, function with ATP-mediated activation. The largest proportion of energy consumed accounts for glutamate-mediated neurotransmission, whereas resting potential maintenance is a less intensive process. Apart from the abovementioned neuronal obligations, these cells need extra energy to synthesize the molecules needed for neurotransmission on a constant basis. Moreover, in cases of long neurons, there is the additional charge of axonal transport of molecules that need to be delivered from cell body to terminal synapses (Belanger et al. 2008).

Since glucose is the main energy substrate of the brain, under normal conditions, the processes involved in its metabolism will be briefly discussed. As in all tissues, the first step of glucose metabolism in brain is glycolysis, a procedure that catabolizes glucose to two molecules of pyruvate, producing a net amount of two ATP molecules (Fig.1). At the pyruvate level, the sequence of events towards further carbon metabolism can follow two different directions: the aerobic or the anaerobic pathway (Belanger et al. 2008).
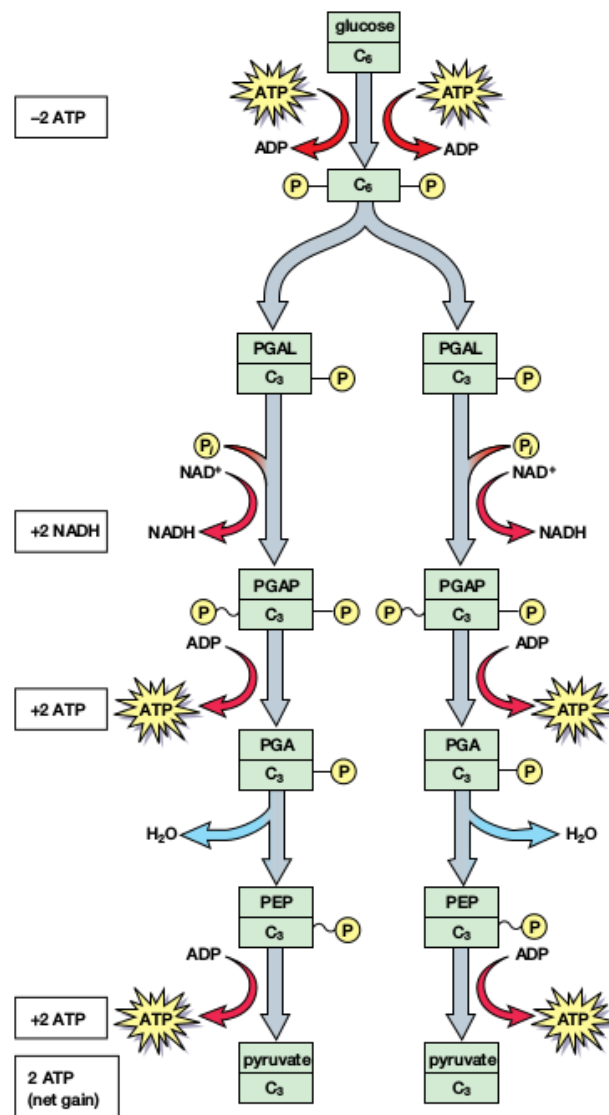
Figure 1: Glycolysis. Glucose phosphorylation, using ATP, is regulated by hexokinase, an enzyme inhibited by glucose 6-phosphate. Glucose 6-phosphate either enters glycolysis or is stored as glycogen. Glucose 6-phosphate is then rearranged to form fructose-6-phosphate. At this point, another ATP molecule phosphorylates (by phosphofructokinase) fructose-6-phosphate, producing fructose-1,6-diphosphate. In turn, this molecule is split into two PGAL (glyceraldehyde-3-phosphate). PGAL is oxidized and is then again phosphorylated, forming PGAP. Two ADP molecules each remove one phosphate group from each PGAP to form PGA (3-phosphoglycerate). Next, the two PGA molecules are each oxidized, forming two water molecules and two PEP (phosphoenolpyruvate) molecules. Finally, two ADP molecules are used by pyruvate kinase to remove the remaining phosphate group from each PEP molecule. The result is the production of two ATP molecules and two pyruvate molecules. http://biology.reachingfordreams.com/cellular-energy/cellular-respiration/glycolysis.html

Under aerobic circumstances, pyruvate enters the mitochondrion where it is decarboxylated by pyruvate dehydrogenase to produce acetyl-CoA. The latter, in turn, enters a fundamental series of reactions which produce three molecules of NADH, one FADH$_2$ and one GTP, and which collectively consist the TCA cycle (Fig.2) (Belanger et al. 2008).
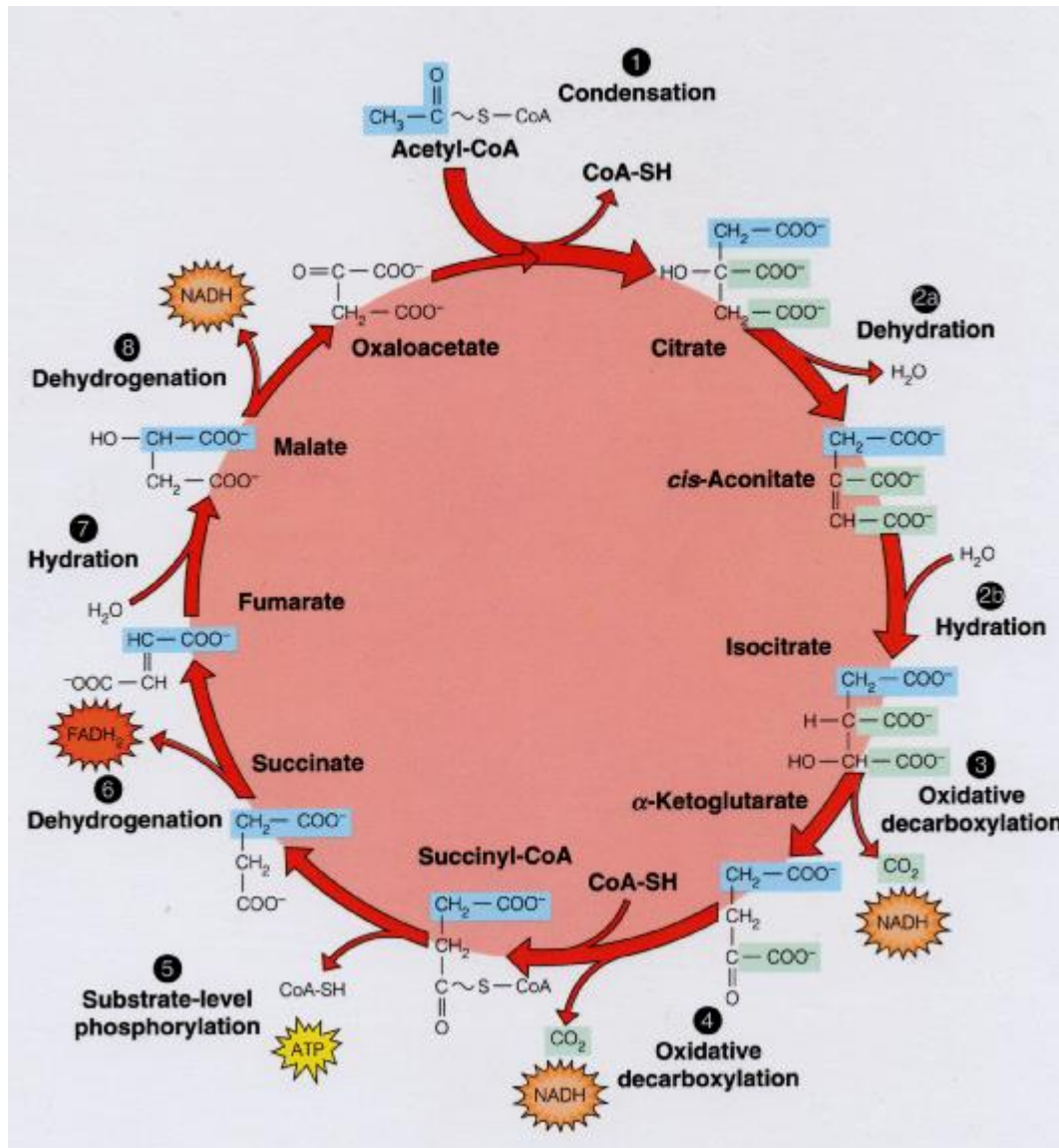
Figure 2: Tricarboxylic acid cycle (TCA cycle). Through catabolism of sugars, fats, and proteins acetyl-CoA is produced and enters the citric acid cycle. Other steps of the cycle are also fed by catabolism of several amino acids. The reactions of the cycle result in the production of high energy molecules such as 3 NADH, 1 FADH2, and 1 GTP. TCA regulations are accordingly accomplished by high levels of energy indices (ATP and NADH). https://www3.nd.edu/~aseriann/tcacfates.html

The generated NADH and FADH$_2$ are subsequently used as electron donors by the oxidative phosphorylation pathway. Oxygen, according to which the procedure is

called aerobic, serves as the final electron acceptor. The H^+ gradient created across the inner mitochondrial membrane, following electron exchanging, ultimately leads ATP synthase to generate energy-rich ATP molecules (Fig.3) (Belanger et al. 2008).
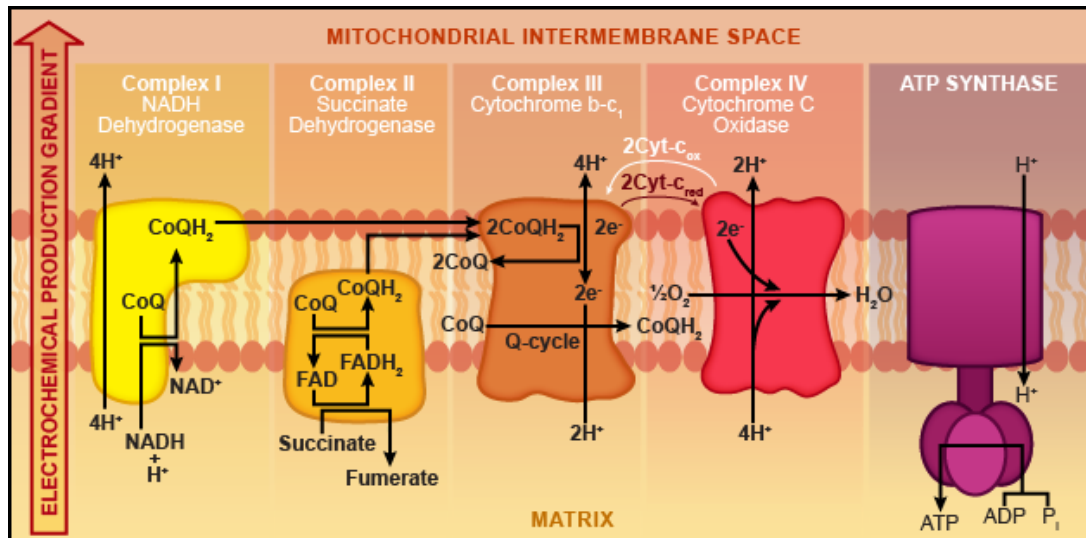
Figure 3: NADH and $FADH_2$ donate electrons to protein complexes (I, II, III and IV), constituting the electron transfer chain (ETC), located in the inner mitochondrial membrane. Oxygen is the terminal electron acceptor, which also combines with free protons to produce water. Electron transfer results in a respective proton (H^+) movement towards the other side of the inner mitochondrial membrane. A steady stream of H^+ moving back across the inner membrane of the mitochondria provides the power to ATP synthase, which ultimately produces ATP. http://www.shmoop.com/cell-respiration/oxidative-phosphorylation.html

On the anaerobic branch of metabolism, pyruvate is converted to lactate through the action of lactate dehydrogenase. Lactate is predominantly released by a cell population that act as supportive and nourishing companions of neurons, namely the astrocytes. The metabolic compartmentation that occurs during neuronal activation has been extensively studied and the resulting motif suggests that following synaptic neurotransmission and subsequent glutamate uptake by astrocytes, the latter respond by taking up glucose from circulation and stimulating glycolysis to produce lactate. Lactate is then transferred to neurons where it serves as energy substrate (Fig.4) (Belanger et al. 2008).

Hence, apart from glucose, lactate and pyruvate can also compensate for energy deprivation in neurons. It is also recognized that ketone bodies can serve as an alternative source of energy under conditions of starvation.
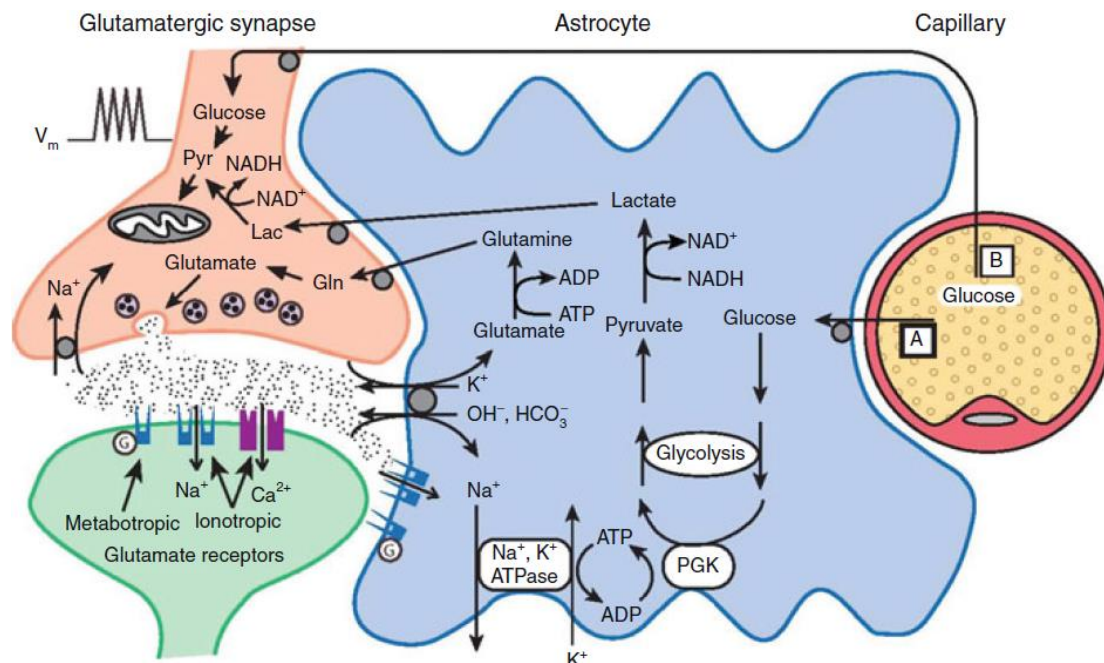
Figure 4: Glutamate-induced glycolysis in astrocytes during neuronal activation. At glutamatergic synapses, presynaptically released glutamate depolarizes postsynaptic neurons by acting at specific receptor subtypes. The action of glutamate is terminated by an efficient glutamate uptake system located primarily in astrocytes. Glutamate is co-transported with Na^+, resulting in an increase in the intra-astrocytic concentration of Na+, leading to an activation of the astrocyte Na^+/K^+-ATPase. Activation of Na+/K+-ATPase subsequently stimulates glycolysis. For each glucose molecule entering astrocytes from circulation, two ATP molecules are produced through glycolysis, and two lactate molecules are released. Within the astrocyte, ATP is used to fuel the next Na+/K+-ATPase pump opening, and to convert glutamate to glutamine by glutamine synthase. Once released by astrocytes, lactate can be taken up by neurons and serve as an energy substrate. Direct glucose uptake into neurons under basal conditions can also occur (arrow labeled B) (Pellerin and Magistretti 1994).

2. *MAMMALIAN GLUTAMATE DEHYDROGENASE AND ITS ROLE*

Glutamate dehydrogenase catalyze the reversible oxidative deamination of L-glutamate to α-ketoglutarate, employing NAD(P)H as a cofactor (Fig.5). GDH holds a critical role in cell metabolism, interconnecting carbon and nitrogen metabolism, regulating glutamate concentration and contributing to energy homeostasis.
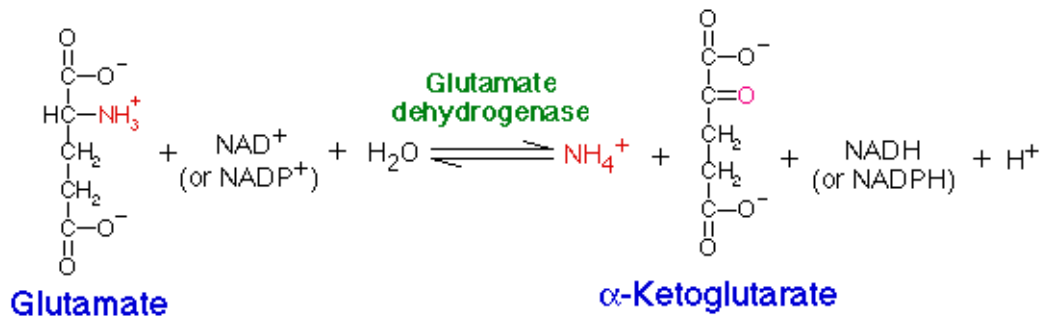
Figure 5: GDH catalyzes the reversible NAD(P)$^+$-linked oxidative deamination of L-glutamate into alpha ketoglutarate and ammonia.
http://www.chem.uwec.edu/Webpapers2005/mintermm/pages/GDH.html

The reaction equilibrium favors the reductive amination of α-ketoglutarate to glutamate, as indicated by the comparison of the Km for α-ketoglutarate with that for glutamate, with the latter being much bigger (Adeva et al. 2012). This is explained by the fact that many less complex organisms, such as plants and microbes, use GDH to integrate ammonia nitrogen in organic compounds, in order to synthesize their amino acids *de novo*. In animals, however, where the main source of amino acids is through direct nutrition, the enzyme is primarily used for the catabolic reaction of oxidative deamination of glutamate to α-ketoglutarate, thereby connecting the amino acid metabolism with citric acid cycle. Although the reaction equilibrium still favors the reductive amination of ketoglutarate in mammals, shortage of free ammonia in the intracellular environment ultimately switches GDH reaction to the direction of the oxidative deamination.

Glutamate dehydrogenase's importance for the cell lies on the interconnection of glutamate metabolism with the TCA cycle (Plaitakis et al. 2013). In fact, it would not be an exaggeration to postulate that through glutamate transactions, GDH provides a significant path for the reversible conversion of amino acids to alpha-keto acids, thus connecting the amino acid metabolism with carbohydrate metabolism. Even though cellular metabolomics are enriched with another enzymatic family that also deaminates amino acids, namely the transaminases, this category of reactions does not involve oxidation/reduction of molecules and yet transaminases transfer nitrogen groups from one amino acid to another, thus no free ammonium is released or incorporated to other compounds. In summary, GDH reaction mediates four basic functions, which are amino acid biosynthesis, ammonia metabolism, glutamate scavenging, and energy homeostasis.

The reaction of GDH is one of the main ammonia integration pathways in metabolism and *de novo* amino acid synthesis (Hudson and Daniel 1993). In turn, glutamate can serve as precursor for other amino acids through the function of transaminases and other enzymes. Although, as already mentioned, the reaction equilibrium favors, in general, the reductive amination direction, in mammals GDH does not normally operate in the same direction due to the significantly low ammonia concentration in the cell. However, under the presence of pathological conditions with concomitant increasing ammonia concentrations, liver GDH can operate towards the reductive amination of α-ketoglutarate, contributing to urea cycle enzymes' and glutamine synthase role in ammonia incorporation (Cooper 2011).

Nevertheless, by operating primarily in the direction of oxidative deamination, GDH still has an important role in protein degradation and in ammonia homeostasis. Through deamination of glutamate it contributes to the metabolism of most amino acids. Indeed, during amino acid catabolism, alpha-amino group is transferred by aminotransferases to α-ketoglutarate in order to form glutamate, which is then oxidatively deaminated by GDH. Through the latter's reaction $NH4^+$ is produced, which is subsequently converted to urea and excreted.

The principal role of GDH in mammals, though, seems to be the catabolism of amino acids for energy production. This is strongly supported by the fact that the enzyme's allosteric regulators (ADP, GTP, NADH, L-leucine to name a few) are tightly connected with the energy status of the cell. In fact, energy shortage, as sensed from high ADP concentration, and in parallel high amino acid -such as L-leucine- load can drive glutamate, through GDH pathway, to be further metabolized by TCA cycle. On the contrary, intense activity of TCA cycle, producing GTP and NADH, implies an adequacy of energy sources and thus GDH is rendered inhibited. In this respect, it is assumed that glutamate dehydrogenase may function as an energy sensor that can readily respond to the energy needs of the cell.

Of note, GDH functions seem to be specified according to the needs of different tissues where it is expressed. Thus, for example, in the proximal renal tubules, GDH may indirectly participate in ammonia excretion mechanisms (Spanaki and Plaitakis, 2012), while, in beta pancreatic cells it is involved in insulin secretion. In the brain, where glutamate plays a fundamental role as a neurotransmitter, GDH is particularly important, as we shall see below.

In the brain, GDH seems to be involved in the metabolism of glutamate, as indicated by the fact that the enzyme is present in high concentrations on areas with dense glutamatergic innervation (Aoki et al. 1987). GDH is predominantly found proximate to glutamatergic synapses, and specifically at the astrocytic projections, as shown by immunohistochemical studies (Subbalakshmi and Murthy 1985, Aoki et al. 1987, Rothe et al. 1994, Spanaki et al. 2010). Glutamate is the main excitatory neurotransmitter in the CNS, and it plays a principal role in neural activation. It is present in a large population of synapses and it is crucial for cognitive functions of the brain such as memory and learning, but also for sensorimotor functions. Moreover, glutamate is a precursor of another major neurotransmitter of inhibitory character this time, namely gamma-aminobutyric acid (GABA), through the action of glutamate decarboxylase (GAD).

GDH's action in brain is not yet well established. However, it is assumed that it is not strongly involved in the synthesis of glutamate, as it seems to function towards oxidative deamination and glutamate catabolism (Cooper et al. 1979, Sonnewald et al. 1997) and its activity is tightly restrained by allosteric control (Kuo et al. 1994). In fact, glutamate synthesis in neurons is believed to occur either by α-ketoglutarate through transamination reactions, or by glutamine through the action of glutaminase. However, GDH seems to be involved in the removal of the synaptically released glutamate (Fig.6). In more details, after its release in the synaptic slot, glutamate is ingested from surrounding astrocytes via its special receptors, EAAT1 and EAAT2. The main glutamate recycling pathway is the so called glutamate-glutamine cycle (Daikhin and Yudkoff 2000). According to it, glutamate is predominantly converted to glutamine by glutamate synthase (localized exclusively in astrocytes). Glutamine is then transferred back to neighboring where it is once again converted to glutamate, a reaction mediated by glutaminase. An alternative route of glutamate processing in the astrocyte is its conversion to α-ketoglutarate, mainly by transamination, and its subsequent catabolism through the Krebs cycle (Shen 2005). But during intense glutamatergic transmission, in combination with a respective increase in energy expenditure, GDH action can direct> 50% glutamate to TCA cycle (McKenna et al. 1996; Westergaard et al. 1996; Sonnewald et al. 1997). It is obvious that in such circumstances the oxidative deamination outweighs transamination. Specifically, GDH mediated catabolism of glutamate anticipates for the energy deprivation consumed in glutamate recycling (the reaction of glutamine synthase requires ATP, but also the transfer of glutamate by EAAT2 and EAAT1 carriers occurs concurrently with the energy-consuming sodium transport process, mediated by K + / Na + -ATPase). On the other hand, GDH reaction

produces ammonia which can be then used as a substrate for synthase glutamine. According to this model, GDH deficiency could theoretically contribute to impaired energy homeostasis in the astrocytes, resulting in incomplete removal of glutamate from the synaptic slot and, ultimately, in glutamate excitotoxicity (McKenna et al. 2007).

Finally, GDH is not expected to function towards ammonia removal for the brain, as glutamine synthase is the dominant enzyme that serves this scope. (Butterworth et al. 2002).
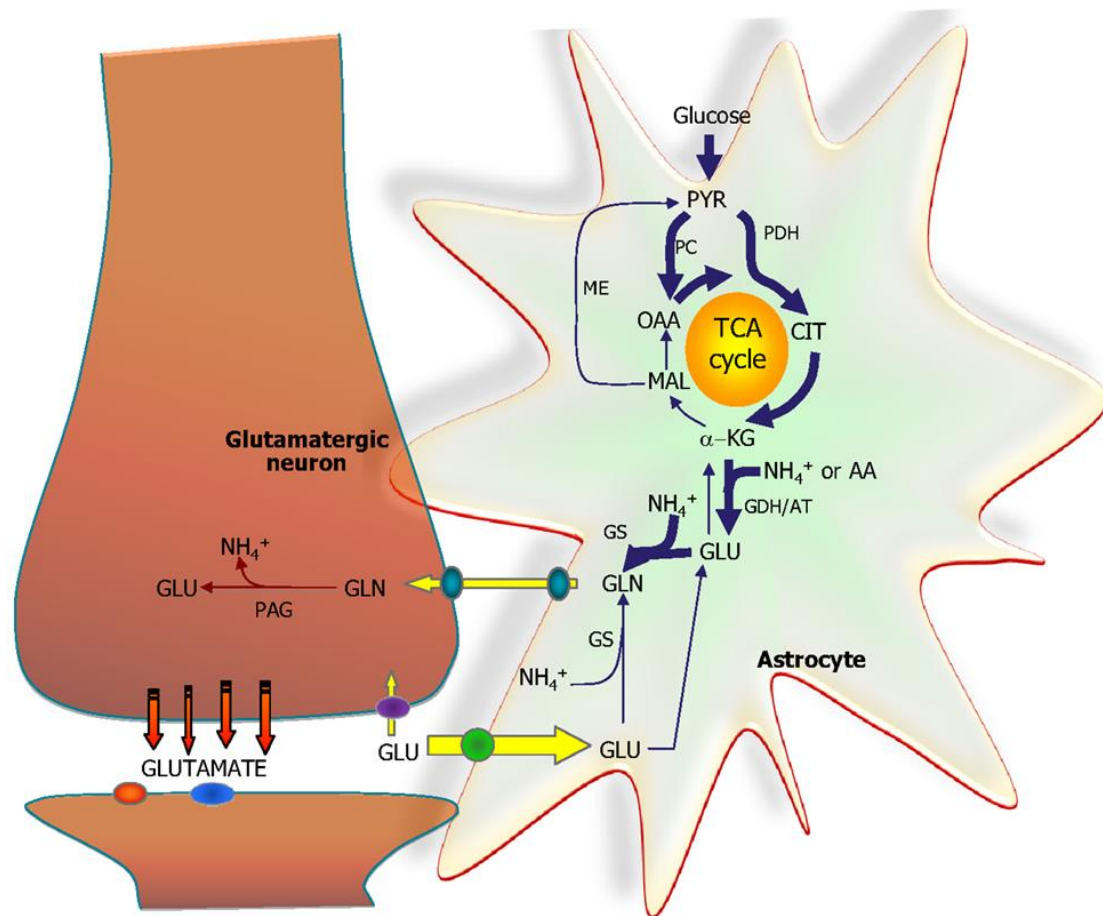
Figure 6: GDH involvement in glutamate recycling. Astrocytic glycolysis and TCA cycle result in the synthesis of α-ketoglutarate (α-KG), allowing synthesis of glutamate (GLU) catalyzed by either glutamate dehydrogenase (GDH) or an amino acid aminotransferase (AA). Glutamate is used for synthesis of glutamine (GLN) catalyzed by glutamine synthetase (GS). Glutamine is transferred to the glutamatergic neuron where it is used by phosphate-activated glutaminase (PAG). Released glutamate is taken up into the astrocyte and transformed into glutamine completing the glutamate-glutamine cycle (Schousboe et al. 2013).

3. GLUTAMATE DEHYDROGENASE'S EVOLUTION

Glutamate dehydrogenases (GDHs) compose a family of metabolic enzymes which are met in almost every organism and which have therefore been a subject of intense research over the past 60 years. Invariably, all GDHs consist of four to six subunits each of which consists of an approximately 450 to 500 amino acid long peptide chain. The subunits are not necessarily identical though. Tetrameric GDHs use NADH while hexameric can use both NADPH and NADH, and this preference seems to be relevant to their functioning direction: NADH specific enzymes are catabolic while NADPH specific are anabolic oriented. Generally, even though the reaction catalyzed by GDH is reversible, there is a preference towards the deamination direction, as Km for ammonium is high. In some simple organisms such as *T. Cruzi* (Carneiro and Caldas 1983; Barderi et al. 1998), *N. Crassa* (Veronese et al. 1974; Blumenthal et al. 1975), *P. Aeruginosa* (Smits et al. 1984; Lu and Abdelal 2001), though, there have been found different GDHs which display different subunit composition and which put through different functions. In eukaryotic organisms, GDHs localize in the matrix of mitochondria, where they are ultimately functional (Mastorodemos et al. 2009).

According to the phylogenetic tree of GDH genes (Andersson and Roger 2003), tetrameric GDHs are grouped in classes GDH-3 and GDH-4, while the hexameric GDHs in classes GDH-1 and GDH-2. During hexameric GDH evolution, the catalytic site of GDH has remained highly conservative. On the contrary, in ciliate protozoa branch, a new 50-amino acid long structure appeared, probably due to a random genetic insertion (Fig.7). This small structure would form the so called antenna, which dramatically equipped GDH with a tightly allosterically regulating mechanism. Therefore, unlike bacterial, which have a short loop instead of antenna, GDHs with antenna can efficiently "sense" and "communicate" with their microenvironment and act accordingly. In fact, ciliate protozoa have a slightly smaller antenna than the one which is present later in the Animalia kingdom, although other members of Protista have a bacterial-like GDH (Banerjee et al. 2003). Studies on Tetrahymena, revealed that GDH could be activated by ADP and inhibited by palmitoyl-CoA. Mammalian GDH in particular is prone to allosteric regulation by a range of small molecules including ADP, GTP, L-leucine, palmitoyl-CoA and others. While the antenna is not necessary for regulators' binding, nor for catalytic activity per se, without it all forms of GDH regulation is lost, except for L-leucine activation. This is because, at least for the two major regulators which are ADP and GTP, these exert their effect through abortive complexes, NAD(P)H·GLU and NAD(P)·A-KG. Specifically, ADP which acts as an

activator of GDH, destabilizes abortive complexes while GTP exerts its inhibiting effects by stabilizing them. The urge for the evolution of this regulatory mechanism coincides with the partial moving of fatty acid oxidation procedures from peroxisomes to mitochondria. The changing environment conditions, which were then enriched with new metabolites, required a more fine-tuned enzyme to respond accordingly to the new demands (Banerjee et al. 2003; Allen et al. 2004, Smith and Stanley 2008).

Although, as mentioned above, in simple organisms different molecules with GDH activity have been detected, in most mammals there is only one active GDH. Bright exception to this rule is the humans and modern apes, which less than 23 million years ago acquired a second GDH encoding gene which produces a second functional GDH enzyme, as it is discussed later in this introduction. The needs which drove to the genesis of an extra glutamate dehydrogenase are far from understood, however, the event seems to coincide with a general increase in brain size and complexity.
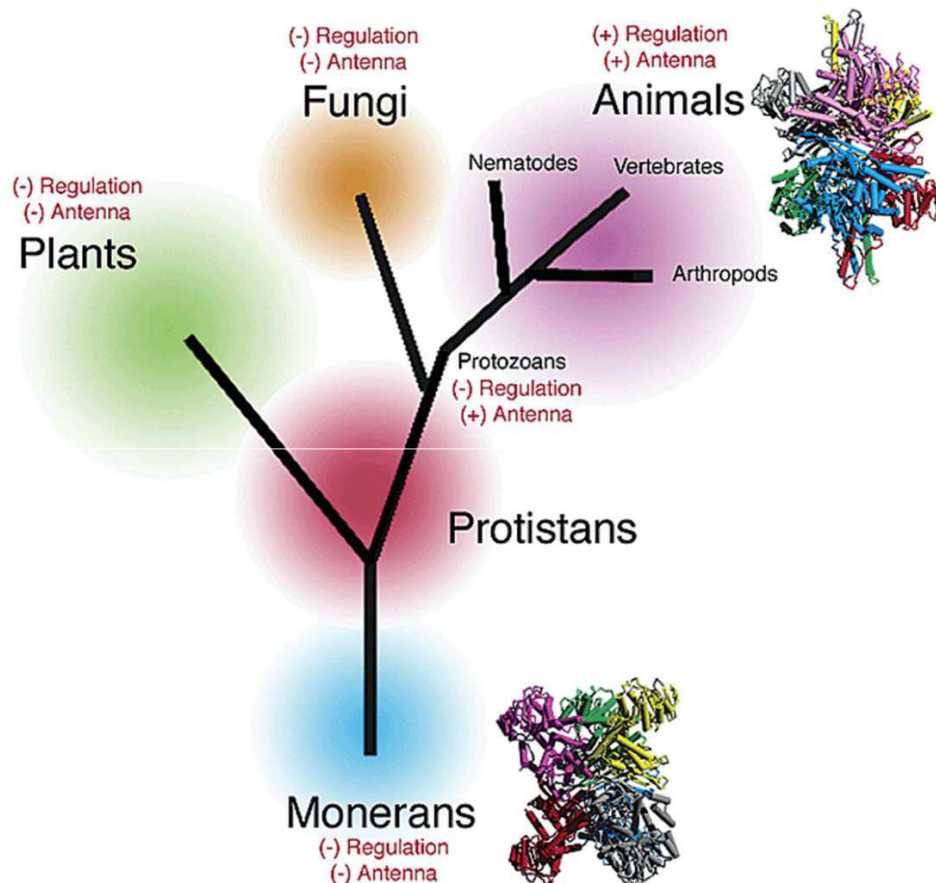
Figure 7: Schematic representation of the evolution of the antenna and the allosteric regulation by purines for GDH (Banerjee et al. 2003).

4. MAMMALIAN GLUTAMATE DEHYDROGENASE' S STRUCTURE

The structure of glutamate dehydrogenase has been resolved for several organisms, by X-ray crystallography. Specifically, in mammals, Smith et al. have obtained images of bovine GDH and human GDH1, in various states: the enzyme's apo-form (Smith et al. 2002), in complex with glutamate, NADH and GTP (Peterson and Smith 1999), in complex with α-ketoglutarate and NAD^+ (Smith et al. 2001), in complex with ADP (Banerjee et al. 2003) as well as with other hydrophobic inhibitors (Li et al. 2011; Li et al. 2009).

Mammalian glutamate dehydrogenase forms symmetrical homo-hexamers (Fig.8), each subunit of which has a molecular weight of ~ 56kDa and is comprised of ~ 500 amino acids (505 for human, 501 for bovine). In each subunit there are three discrete domains

a) a glutamate binding region towards the N terminus,

b) a NAD binding domain, and

c) a regulatory domain, which includes the antenna (amino acids 402-447 for human form) and the pivot helix (amino acids 449-475).

Antenna is a perturbing structure that projects from the top of the NAD(P)H binding domain. It comprises of an ascending 21 amino-acid long alpha helix (amino acids 403-422) and a descending component (amino acids 425- 447), ending with a small alpha helix (amino acids 438-445). The antennae of the three subunits that are on the same side of the hexamer are intertwined together.

On each subunit, two distinct regions are formed, based on the separation by a long slit, which is essentially the catalytic cleft. The first region, consisting of amino acids 4-204 and 428-453, corresponds to glutamate binding site, while the second (residues 205-427), which has a characteristic nucleotide binding pattern, corresponds to coenzyme binding site. Upon substrate binding, the coenzyme binding site is rotated around the pivot helix, resulting in a generalized conformational change that ultimately leads to catalytic cleft closing. Extensive configuration changes follow this movement, as observed at the antenna region which rotates around its axis, while its descending short helix is concurrently compressed, just as a spring.

NAD$^+$ binding site lies within an extended area of the GDH monomer's catalytic cleft. The coenzyme has a second, allosteric binding site. Glutamate also binds to the catalytic cleft with γ-carboxyl group interacting with lysine 94, and α-carboxyl group with lysine 118. When NAD$^+$ site "closes" on the ligands, its nicotinamide ring is moved next to glutamate and lysine 130, thus displacing water molecules and creating a convenient hydrophobic environment. Of note, GDH catalytic cleft and the mechanism of its reaction, are highly conserved among species, based on previous crystallographic analysis on simple organisms such as *Clostridium symbiosum* (Stillman et al. 1993; 1999).
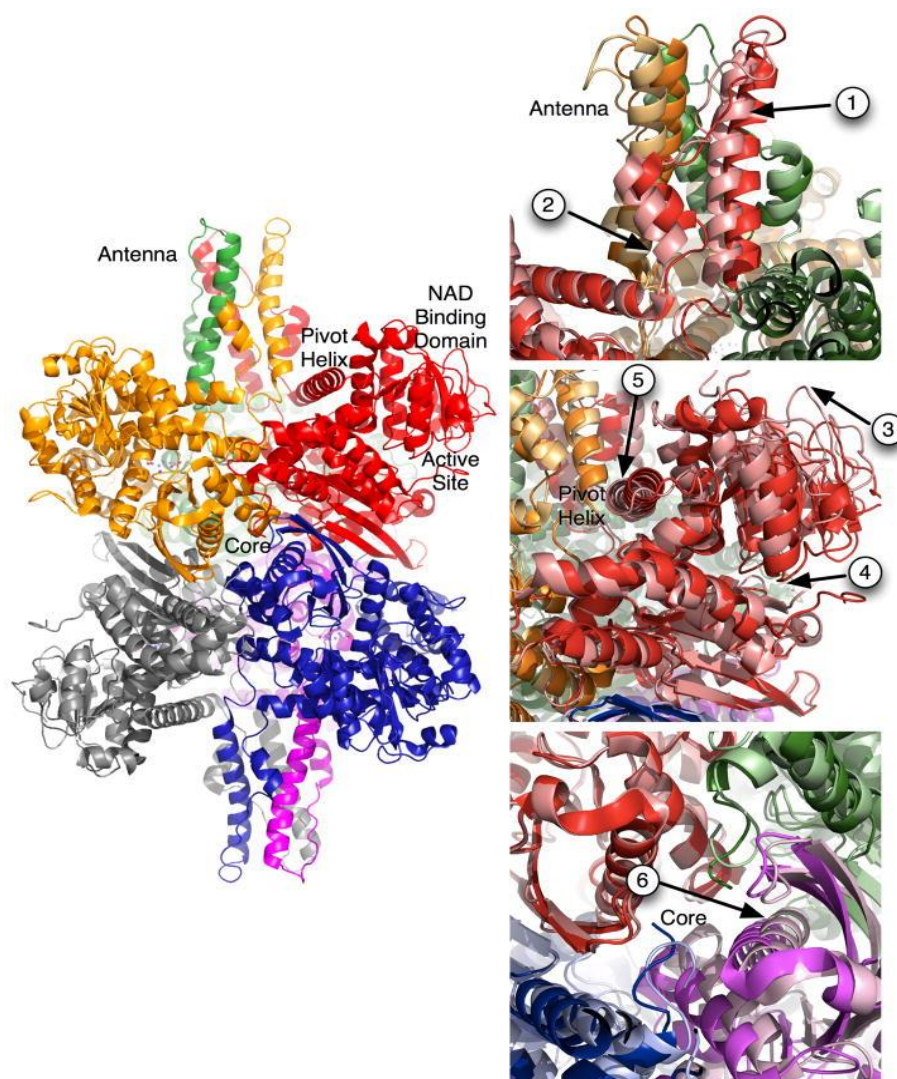
Figure 8: Structure of mammalian GDH. On the left is the structure of hexameric GDH apoform, with each subunit represented by a different color. On the right side are magnified views of the regions of GDH that exhibit large conformational changes as the catalytic cleft opens and closes. The darker colored parts refer to the closed conformation of GDH and the lighter represent the open conformation. The arrows highlight the key movement points during catalysis (obtained from Li et al. 2012).

5. MAMMALIAN GLUTAMATE DEHYDROGENASE'S REGULATION

GTP is a major inhibitor of mammalian GDH, and it exerts its control towards the oxidative deamination of glutamate (Frieden 1959; Frieden 1962). GTP mediated regulation seems to be serving the elimination of TCA cycle and amino acid catabolism when there is energy overload. Thus, GTP produced from an overactive TCA cycle functions as a negative feedback for the enzyme that feeds the same metabolic pathway with α-ketoglutarate. Histidine 213, arginine 221, arginine 265, arginine 269, lysine 293, glutamate 296, lysine 450, and histidine 454 are essential for the inhibitor binding on GDH (Fig.9). Notably, GTP can only bind on the closed conformation of the enzyme, namely when both substrate and coenzyme are already bound. Thus, the inhibition is achieved through the creation of an abortive complex, essentially by stabilizing the closed conformation and blocking the release of the product.

The main activator of GDH, ADP, is also indicative of the energy status of the cell (Frieden 1959). It acts at the opposite direction of GTP, in a sense that it activates GDH to produce more α-ketoglutarate which will be directed to TCA cycle, when the energy stores are depleted. According to Banerjee et al. (2003), ADP interacts with glutamine 89, arginine 90, aspartate 123, serine 397 and arginine 463 of one subunit as well as with lysine 391 and arginine 400 of the neighboring subunit (Fig.9). ADP acts by facilitating the catalytic cleft opening and the product release respectively, thereby antagonizing GTP inhibition.
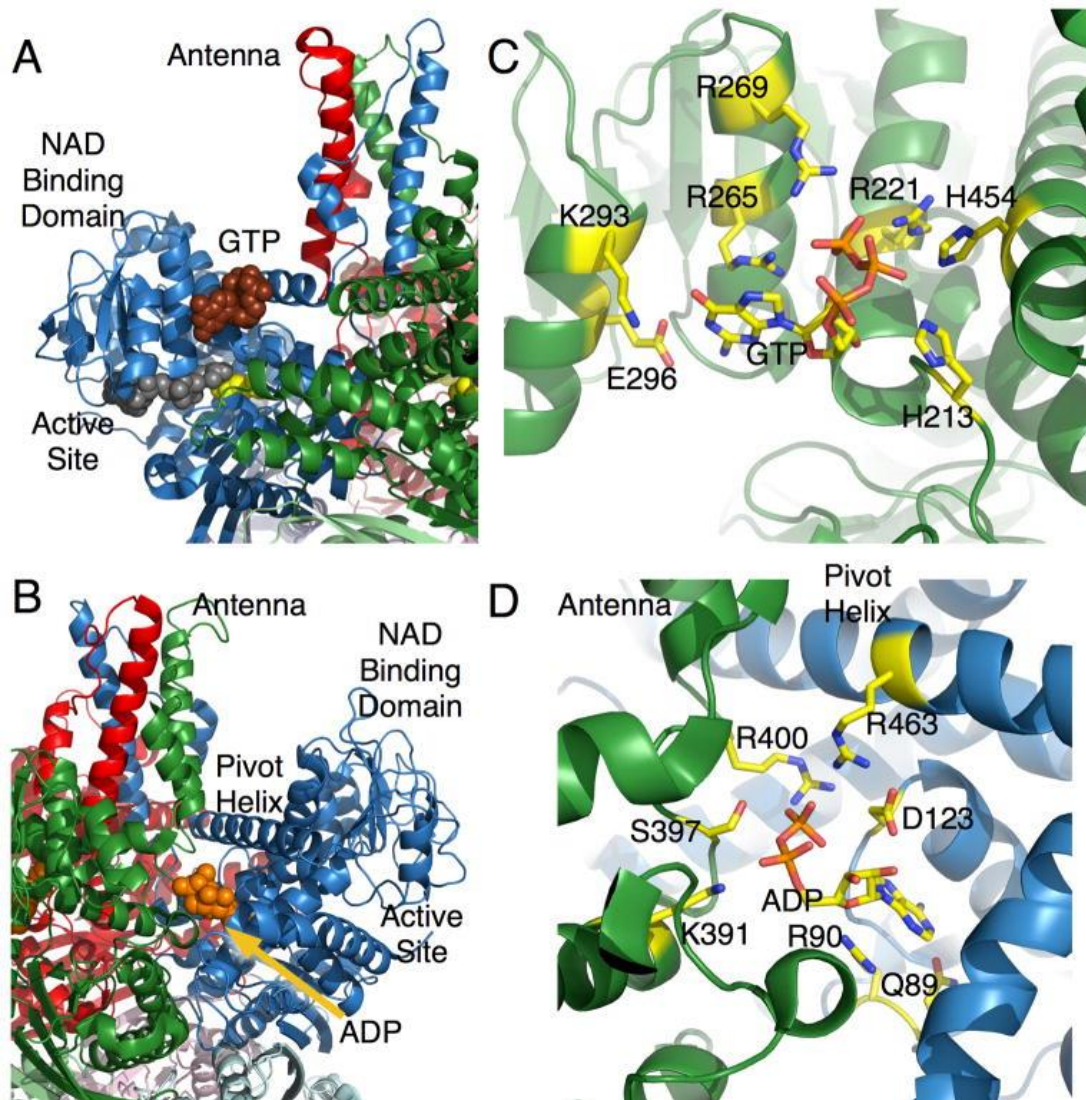
Figure 9: Locations of the main GDH allosteric regulators' binding sites. A) GTP is bound to the closed conformation of GDH. GTP is represented by the brown spheres, coenzyme in grey, and glutamate in yellow. B) ADP (orange) binds behind the catalytic cleft, under the pivot helix. C) Magnification of GTP bound to GDH. D) Magnification of ADP bound to GDH (obtained from Li et al. 2012).

Another important GDH activator is L-leucine (Yielding and Tomkins, 1961). It has been proposed that this amino acid's levels is an indicator of other amino acids' source adequacy in the cell, thus it might act by leading GDH to catabolism of glutamate, in an attempt to reach a new equilibration. Tomita et al. (2011) have identified the important amino acid residues mediating L-leucine's binding on GDH from *Thermus thermophilus*, and the respective human GDH positions are arginine 151 and aspartate 185. Leucine activation seems to be associated with extensive conformational changes of the enzyme structure during catalysis. This becomes apparent from experiments with substitutions at the antenna area, which were adequate to attenuate

L-leucine activation (Zaganas et al. 2002). However, deletion of the entire antenna has little effect on L-leucine activation while it eliminates ADP and GTP regulatory effects (Allen et al. 2004).

Palmitoyl-CoA is part of the system that mediates fatty acids transportation to mitochondria for β-oxidation. This compound also appears to inhibit the enzyme (Kawaguchi and Bloch 1976; Fahien and Kmiotek 1981), probably by eliminating amino acid catabolism when sufficient energy sources, through fatty acid metabolism, can compensate for cell requirements. Palmitoyl-CoA inhibition appears to also be dependent upon the antenna domain. In contrast to plants and fungi, animals perform β-oxidation of medium and long chain fatty acids mainly in the mitochondria. Therefore, it has been proposed that the antenna evolved to link fatty acid and amino acid catabolism in the mitochondria (Allen et al. 2004).

Another group of GDH inhibitors consists of steroid hormones, such as estradiol, progesterone and testosterone (Yielding and Tomkins 1960; Colon et al. 1986; Li et al. 2007), although at higher concentrations than the ones that are normally present in the cell. It has been proposed that these compounds bind to the 'core' of the hexamer, among its subunits (Li et al. 2009), although crystallographic data are not available. Binding of these hormones seems to favor the "closed" conformation of the enzyme, in the same way GTP functions.

Apart from its role in GDH reaction *per se*, the coenzyme appears to have a regulatory role, although the latter is achieved through binding at a different region. Increasing concentrations of NADH (but not NADPH) have been observed to inhibit GDH, while low concentrations of its oxidized form, NAD^+, seem to act as an activating mechanism (Frieden 1959a; Dalziel and Engel 1968). The second, allosteric coenzyme binding site is identical with that of ADP binding site, as it was crystallographically proved (Smith et al. 2001, Banerjee et al. 2003). Thus, although these allosteric regulators use the same binding site, NADH and ADP exert the opposite effect. NADH shows cooperativity with GTP and it favors the closed conformation of the enzyme, whereas ADP binding displaces NADH and facilitates the opening of the catalytic cleft.

Finally, evidence shows that some polyphenolic compounds such as epigallocatechin gallate and epicatechin gallate contained in green tea are potent inhibitors of human glutamate dehydrogenase (Li al. 2006; 2007), by binding at the ADP regulatory site (Li et al. 2011).

Besides the enzyme's allosteric regulators abovementioned, there is a large number of putatively regulatory substances. Nevertheless the mechanisms by which they control GDH remain elusive. Indicatively, inhibitory effects have been revealed for various antipsychotics (Shemisa and Fahien 1971; Tamir et al. 1981; Couee and Tipton 1990), thyroxine (Caughey et al. 1957; DiPrisco et al. 1965), and a series of metals such as silver, zinc, magnesium, aluminum and manganese (Hellerman et al. 1958; Fahien et al. 1985; Fahien et al.1990; Kuo et al. 1994; Zatta et al. 2000; Yang et al. 2003). Nevertheless, the concentrations of most of them are rather unlikely to be met in mitochondria under physiological conditions. Still, microenvironment clusters of these substances can exert a fine tuning role on GDH control.

To complete the list of GDH effectors, it is important to include the solution characteristics in which the enzyme is measured *in vitro*. It appears that oxidative deamination of glutamate is optimally performed at alkaline pH ~ 8.5-9.0, while the optimum pH for the reductive amination of α-ketoglutarate is usually around 7.8-8.0 (Hudson and Daniel. 1993). Furthermore, at low pH (~ 7.0) ADP activation seems to be reversed (Bailey et al. 1982) while GTP inhibition is not significantly affected in a pH range from 7.0 to 9.0 (Smith and Piszkiewicz 1973). Buffer constitution and concentration also play a role in the stability of the *in vitro* preparations of GDH. In Tris-Acetate solution, the enzyme was often unstable, unlike in sodium phosphate solutions where it was fairly stable (Engel and Dalziel 1969). However, in high phosphate concentrations the inhibitory effect of GTP was found eliminated (DiPrisco and Strecker 1969).

6. MULTIPLICITY OF HUMAN GLUTAMATE DEHYDROGENASES

Early studies had provided supporting evidence that in the human brain two forms of GDH exist and that they exhibit different thermal stability (Plaitakis et al. 1984). Later on, Hussain et al. (1989) using 2D electrophoresis, detected 4 GDH isoproteines. It was already known that GDH1 in human was the expression product of *GLUD1* gene (Mavrothalassitis et al. 1988; Anagnou et al. 1993; Deloukas et al. 1993). Following these data, a family of several *GLUD1*-like genes was discovered along with a number of different transcripts (Mavrothalassitis et al. 1988; Michaelidis et al. 1993) but at that time, it was not clear whether, they represented functional genes or pseudogenes. Eventually, a new *GLUD*-derived cDNA was isolated from a retina cDNA library, which

was coded by an intronless gene located on chromosome X. That gene was named *GLUD2*, and was found to produce a protein expressed in the human retina, testes and, to a lesser extent, in the brain (Shashidharan et al. 1994).

It was thus proposed that in human glutamate dehydrogenase is encoded by two discrete genes named *GLUD1* and *GLUD2*. *GLUD1* is the orthologue glutamate dehydrogenase gene found in all mammals. *GLUD2* is an exclusive evolutionary privilege of humans and great apes such as gibbon, chimpanzee and gorilla. A number of pseudogenes (*GLUDP2A*, *GLUDP2B*, *GLUDP2C*, *GLUDP3*, *GLUDP5* on chromosome 10 and *GLUDP4* on chromosome 18) is also present in the human genome (Michaelidis et al. 1993). The majority of these pseudogenes appear to have arisen by gene duplication mechanisms, such as retroposition.

GLUD1 is a 13-exon gene which expands on a 45kb long genomic region and is located on the long arm of chromosome 10 (10q23.3). It is ubiquitously expressed and it is transcribed in a 1674 bp long mRNA (without UTR). The first exon (540 bp), which is the largest, contains, apart from the 5'-UTR sequence, the coding sequence for a mitochondrial leader peptide and the first 91 codons of the mature hGDH1 protein.
GLUD2, on the other hand, is an intronless gene which locates on the long arm of chromosome X (Xq24) and spans a genomic region of only 2.5kb. It produces a single transcript and has a selective pattern of expression, being detectable only in brain, testis, kidney and retina. Lack of introns is explained by the fact that *GLUD2* arose from an incident of retroposition of *GLUD1*'s transcript to chromosome X which happened less than 23 million years ago (Shashidharan et al. 1994; Burki and Kaessmann 2004).

Each of human *GLUD* genes is able to produce a different isoenzyme with glutamate dehydrogenase activity, namely hGDH1 and hGDH2 respectively. Both *GLUD* genes code for a 558-amino acid long peptide. Of these 558 amino acids, the first 53 located on the N-terminus of the protein correspond to a leader peptide sequence, responsible for the transport of the enzyme to the interior of the mitochondria (Kotzamani and Plaitakis 2012; Mastorodemos et al. 2009), where both isoenzymes are functional (Aoki et al. 1987; Rothe et al. 1994; Mastorodemos et al. 2009). The leader peptide is subsequently cleaved and the remaining 505 amino acids form the monomeric human GDH. The two unprocessed isoenzymes differ in 9 out of the 53 amino acids of the leader peptide. In fact, some of these amino acid changes seem to have equipped

hGDH2 with a more efficient transport mechanism in the mitochondrion (Rosso et al. 2008).

Concerning the 505 amino acids comprising the mature protein, the two isoenzymes differ in only 15 amino acids (Fig.10), showing 97% homology. Therefore, any differences in the functional properties between hGDH1 and hGDH2 must be attributed to these 15 amino acid differences.

Studies on the evolution and establishment of *GLUD2* revealed the presence of the gene in a series of primates (Burki and Kaessman 2004). Based on the phylogenetic tree of the primates and the detection of the gene in different species, it was concluded that the retroposition event happened after the separation of the genealogical branches of the great apes of the Old World and the African green monkey, but before the separation of human and gibbon branches, dating between 23 and 18 million years ago (Fig.11). Specifically, the amino acid changes Ala3Val, Glu34Lys, Asp142Glu, Ser174Asn, Arg443Ser, Gly456Ala and Asn498Ser occurred immediately after the retroposition event whereas amino acid changes Val3Leu, Arg39Gln, Lys299Arg, Ser331Thr, Met370Leu and Arg470His, occurred after the separation of the gibbon branch (Fig.11). Among many other incidences of gene duplication via retroposition which invariably produce non-functional pseudogenes, this particular event luckily established the creation of a new gene. It is rational that the two genes, *GLUD1* and *GLUD2*, share a large proportion of their sequence, yet random mutagenesis and positive natural selection acted towards the prevalence of specific alterations which equipped the new gene with unique characteristics.

Of note, the birth of *GLUD2* coincides with a period of increased neural structural and functional complexity, as well as an increase in brain size, in the human and great ape ancestor (Burki and Kaessmann 2004). Since higher neuronal activity has probably coevolved with greater brain size, *GLUD2* may have contributed to enhanced brain function in humans and apes by facilitating higher neurotransmitter flux (Vallender et al. 2008). This is further supported by the fact that there is decreased activity of this retrogene in neurodegenerative disorders (Plaitakis et al. 2000). Consequently, *GLUD2* may have been important for the evolution of increased cognitive capacities in hominoids.

Figure 10: Comparison of the two mature human glutamate dehydrogenases' sequences. The 15 out of 505 amino acid residues that differentiate one from another are marked in red. Detailed amino acid changes: Ala3Leu, Glu34Lys, Arg39Gln, Asp142Glu, Ile166Val, Ser174Asn, Gly247Arg, Ala321Val, Ser331Thre, Met370Leu, Met415Leu, Arg443Ser, Gly456Ala, Arg470His, Asn498Ser (from Kanavouras K. thesis, 2012).
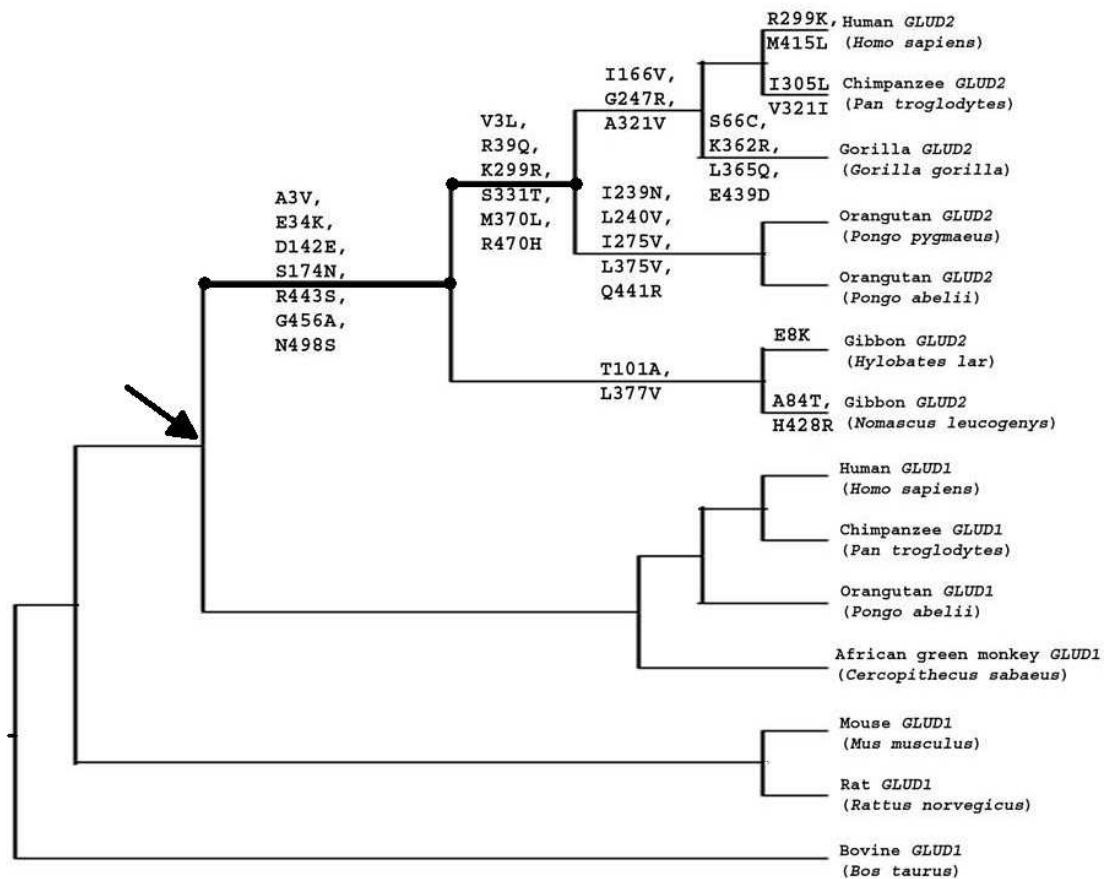
Figure 11: Phylogenetic tree showing the evolution of *GLUD2*. The black arrow indicates the point of *GLUD2* separation from *GLUD1*, after the retroposition event ~ 18-23 million years ago. Immediately after *GLUD2* genesis, the amino acid changes occurred, were established by positive natural selection (Shashidharan and Plaitakis 2014).

.

7. FUNCTIONAL DIFFERENCES BETWEEN HUMAN GDH1 AND GDH2

Human glutamate dehydrogenase 2 discovery has arisen questions regarding its differences with its "sister" isoprotein, hGDH1. In an attempt to answer these questions, Shashidharan al. (1994; 1997) expressed recombinant human GDHs in a eukaryotic protein production system which employs *Spodoptera frugiperda* (Sf9 / Sf21) cell cultures. A number of comparative enzymatic studies have thenceforth been performed at either crude cell extracts (Shashidharan et al. 1997; Plaitakis et al. 2000), or purified enzyme preparations (Plaitakis et al. 2003; Mastorodemos et al. 2005).

Initial kinetic analyses showed that hGDH1 and hGDH2 share quite similar catalytic properties, such as Vmax and Km for the enzyme substrates (Plaitakis et al. 2000; 2003; Kanavouras et al. 2007). Given their high sequence similarity, sharing all but 15

of 505 amino acids in their mature form, one would expect that these isoenzymes function in a similar way. When looking at their enzymatic properties though, hGDH1 and hGDH2 differ markedly in their basal catalytic activity, regulatory properties, optimal pH and relative resistance to heat inactivation.

As it was previously discussed, ADP is the main activator of mammalian glutamate dehydrogenase. This observation is true for both human enzymes too. Indeed, in the presence of 1 mM ADP, human GDHs show comparable maximal specific activities, according to measurements on crude enzymatic preparations (Shashidharan et al. 1997). However, it has been repeatedly proven that the two isoenzymes differ markedly in their basal catalytic activity (Fig.12), which is estimated in the absence of ADP (or other effectors) and expressed as percentage of their maximal activity (Shashidharan et al. 1997; Plaitakis et al. 2000; 2003; Zaganas et al. 2009). In contrast to the wild-type hGDH1, which maintains about 35–40 % of its maximal activity at baseline, hGDH2 shows very little basal catalytic activity (2–8 % of its maximal). This basal activity seems to be enhanced at increasing enzyme concentrations *in vitro*, but still remains significantly lower than that of hGDH1 (Kanavouras et al. 2007).

Despite this low basal activity, hGDH2 is remarkably responsive to activation by ADP and L-leucine. Given that the two isoenzymes show comparable maximal activity and hGDH2 has much lower basal activity than hGDH1, the proportional activation of hGDH2 by 1 mM ADP is significantly higher (Fig.12). However, the affinity of ADP for hGDH2 (as measured by the SC_{50} values, i.e. the ADP concentration at which ADP activation is 50 % of the maximal activation) is lower than that for hGDH1. Physiological L-leucine concentrations (67.5-125 uM) activate hGDH2 less intensively than ADP, yet this activation is again proportionally greater compared to that of hGDH1, although the two isoenzymes show comparable affinity for this amino-acid. But at this range of leucine concentrations, the addition of small quantities of ADP (10, 25, or 50 uM) allowed the leucine mediated activation of hGDH2 to reach significant levels, a finding not replicated at the same magnitude for hGDH1. Thus for hGDH2, ADP and leucine, even though at low concentrations, exhibited a strong synergistic behavior, which was not observable for hGDH1 (Kanavouras et al. 2007). Total dependence on available ADP levels permits the recruitment of the enzyme under conditions of low cellular energy (high ADP/ATP ratio), such as those occurring under glutamatergic neurotransmission that is highly energy consuming (Plaitakis and Zaganas 2001; Attwel and Laughlin 2001; Schousboe et al. 2011). The average concentration of ADP in human cells and fluids is 137 uM (Traut 1994), however, the ADP concentration

inside mitochondria can fluctuate between 1 and 9 mM depending on the energy adequacy (Wheeler and Mathews 2011). Moreover, the ability of L-leucine to sensitize hGDH2 to ADP activation may permit the enzyme to respond to small changes in ADP concentration, even in the absence of an overt local energy deficit.

While hGDH1 is markedly sensitive to GTP, hGDH2 is resistant to this compound either in the absence or in the presence of the enzyme activators ADP and L-leucine. In the absence of allosteric activators, hGDH1 is strongly inhibited by GTP (IC_{50} ~ 0.2 uM) (Plaitakis et al. 2000; Zaganas and Plaitakis 2002). Under the same conditions hGDH2 is remarkably resistant to GTP, with IC_{50} being at least 20 times higher (Plaitakis et al. 2000). ADP is shown to attenuate the inhibitory effect of GTP. Specifically, at 0.1 mM ADP, IC_{50} is ~ 0.6 uM for hGDH1 and ~20 mM for hGDH2, and at 1.0 mM ADP, IC_{50} is ~ 2.5 uM for hGDH1 and ~ 300 uM for hGDH2. L-leucine can also alleviate the inhibitory effect of GTP, although to a lesser extent (Plaitakis et al. 2000). GTP resistance for hGDH2 might have a profound biological value. hGDH2 may have evolved to perform an additional role in the nervous system, such as metabolism of glutamate irrespectively of the energy status of the cell (Zaganas et al. 2012). Thus, hGDH2 could produce or catabolize glutamate as a neurotransmitter even under conditions of high energy charge (high GTP levels due to enhanced Krebs cycle function), that are prone to fully inactivate hGDH1.

Hill plot analyses further showed that, in contrast to the co-operative behavior of hGDH1, GTP binding to hGDH2 was non co-operative (Kanavouras et al. 2007). This is expressed by the shape of the GTP inhibition curve, which for hGDH1 is sigmoidal (Hill coefficient> 1.9) whereas for hGDH2 is almost hyperbolic (Hill coefficient <1). In macromolecular means, positive cooperativity indicates the ease with which additional molecules (eg GTP) can be bound on the enzyme after the first one achieves binding. Early observations by Plaitakis et al. (1984) had revealed that the two isoforms of human GDH present different sensitivity to heat inactivation. Indeed, later studies employed thermal tests on both enzymatic preparations and confirmed that hGDH2 is much more heat sensitive than its heat stable isoenzyme hGDH1 (Shashidharan et al.1997). As demonstrated by Yang et al. (2004), the thermal resistance of both enzymes and their mutants can be restored with the addition of ADP and / or L-leucine before the enzymes are exposed to the thermal effect.
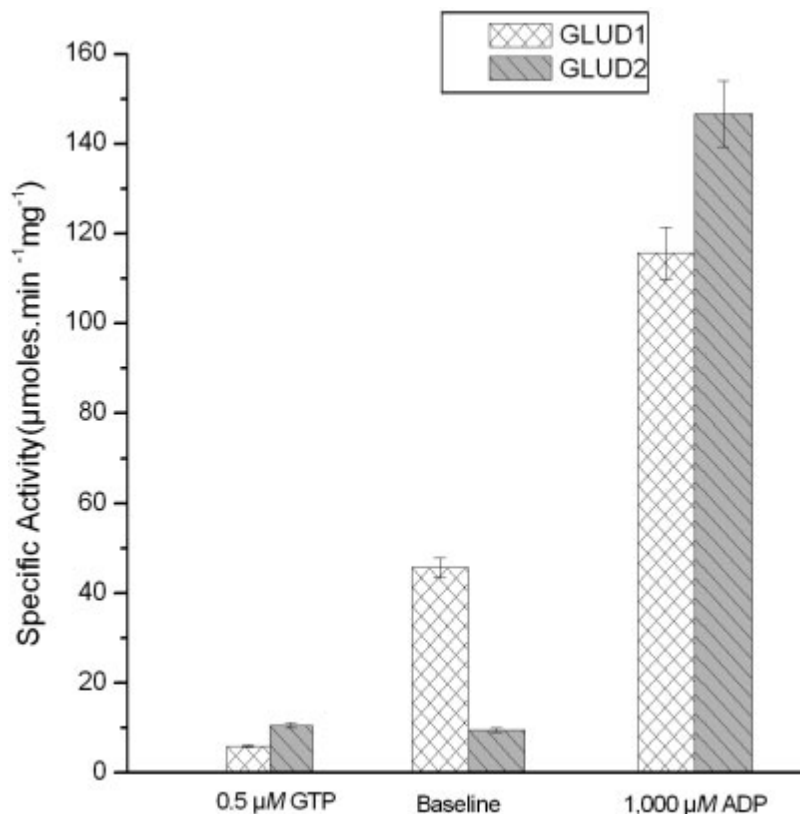
Figure 12: Specific activities of recombinant hGDH1 and hGDH2, assayed in the absence of allosteric modulators (Baseline), or in the presence of either 0.5 uM GTP or 1mM ADP. Enzyme activity was measured in the direction of reductive amination of α-ketoglutarate in 50 mM TRA buffer, pH 8.0 (Mastorodemos et al. 2005).

Regarding the effect of pH on human GDH activity, hGDH1 displays its maximal activity at pH 7.75-8 while hGDH2 prefers slightly more acidic pH, as it optimally functions at pH 7.5. Under baseline conditions (in the absence of ADP), hGDH1's activity is higher at pH 8, while hGDH2 has its highest basal activity at pH 7.8. This differences observed in the optimal functioning pH suggest that hGDH2 might have been adapted to better respond under the acidic conditions occurring after neurotransmission and glutamate uptake, in the nerve tissue (Bouvier et al. 1992; Poitry et al. 2000).

Female steroidal hormones have also been shown to inhibit human GDHs, although at higher concentrations than normal tissue levels of these compounds. Studies on the effects of estrogens on recombinant hGDH1 and hGDH2 revealed that these hormones interact more potently with hGDH2 than with hGDH1 (Borompokas et al. 2010). In details, when inhibitory assays were performed in the absence of other effectors, hGDH2 was 18-fold more sensitive to the synthetic estrogen diethylstilbestrol (DES) or to the naturally occurring 17 beta-estradiol than hGDH1. Other female hormones, such as estriol and progesterone also inhibited the wild-type hGDH2 more

strongly than the wild-type hGDH1, but at higher concentrations than those required for DES or for 17-beta-estradiol (Borompokas et al. 2010). The sensitivity of hGDH2 to estrogens relates to the propensity of the enzyme to assume under base-line conditions a closed conformation while ADP antagonizes estrogen inhibition by helping the catalytic cleft to open. Taken together, these findings imply that regulation of hGDH2 may be achieved by the opposing actions of estrogens and ADP, akin to the regulation of hGDH1 by the antagonistic effects of GTP and ADP (Borompokas et al. 2010).

hGDH2 is also more potently inhibited by neuroleptic drugs compared to hGDH1. Studies using highly purified recombinant human GDHs revealed that haloperidol had a significantly higher affinity for hGDH2. Similarly, perphenazine interacted more potently with hGDH2 than with the wild-type hGDH1 (Plaitakis et al. 2011). Since the concentrations of haloperidol needed for hGDH2 inhibition are close to the steady-state levels found in the plasma and erythrocytes of patients receiving doses of 5–20 mg, these studies suggest that the interaction of these anti-psychotic agents with hGDH2 may be physiologically relevant (Couee and Tipton, 1990).

Other potent effectors that differentially inhibit isoenzyme hGDH1 and hGDH2 include Palmitoyl-CoA, spermidine (a polyamine) and EGCG (epigallocatechin gallate, a green tea compound). All the above mentioned induce a concentration-dependent inhibition of hGDH isozymes, especially evident for hGDH2. In contrast, hGDH1 appears to be less sensitive (Choi et al. 2007; Plaitakis et al. 2011; Spanaki et al. 2012).

8. STRUCTURAL BASIS OF THE DIFFERENCES BETWEEN HUMAN GDHs

Although the structure of hGDH1 is thoroughly studied by X-ray crystallography (Smith et al. 2002), such data are not yet available for hGDH2. Nevertheless, site directed mutagenesis on *GLUD1* cDNA at sites that differ from *GLUD2* cDNA have been performed to identify the amino acid changes that conferred unique properties to hGDH2 (Zaganas and Plaitakis 2002; Yang et al. 2004; Kanavouras et al. 2007). From a simplified point of view, two evolutionary amino acid changes were critical for the acquirement of the characteristic regulatory properties of hGDH2: Arg443Ser and Gly456Ala.

Specifically, substitution of Arg443 by Ser rendered the enzyme practically inactive under baseline conditions and subject to activation by rising ADP and L-leucine levels. Additionally, the same amino acid change was found responsible for the observed hGDH2 heat-lability. Nevertheless, when wild type hGDH2 and Arg443Ser-hGDH1 mutant were kinetically compared, this alteration could not replicate the exact enzymatic characteristics which are attributed to it. Wild type hGDH2 showed higher basal activity (Fig.14), it was activated by lower concentrations of ADP, it was amenable to activation by L-leucine in the absence of ADP and it was less heat labile than the mutant (Kanavouras et al. 2007). Also, Arg443Ser mutant was even more sensitive to neuroleptics and estrogens than wild type hGDH2 (Plaitakis et al. 2011). Arg443 holds a critical position on the enzyme's regulatory domain (Fig.13), since it is located in the small descending helix of the antenna that is subject to intense conformational changes during catalysis.

The second crucial amino acid substitution that differentiated hGDH2 from hGDH1 was Gly456Ala. This replacement rendered hGDH2 resistant to GTP inhibition and abolished the cooperative binding of this allosteric inhibitor (Fig.15) (Zaganas and Plaitakis 2002). Gly456 is also located on the regulatory domain of GDH, but, this time, on the pivot helix (Fig.13).

While the abovementioned single amino acid replacements have recreated some basic regulatory properties of wild type hGDH2, they are not sufficient to explain all of its characteristics. In fact, neither the double hGDH1 mutant, carrying both Arg443Ser and Gly456Ala, was able to reproduce hGDH2 behavior, as it showed intermediate properties between single mutants and the wild type enzyme (Kanavouras et al. 2007). Therefore, even though determinant for hGDH2-specific properties, the combined action of these two substitutions cannot compensate for hGDH2 functional signature. On the contrary, additional amino acid changes, acting in concert with Arg443Ser and Gly456Ala, must have been responsible for the establishment of hGDH2's particularities.

Later studies towards the elucidation of which amino acid changes were essential for hGDH2 regulatory evolution, revealed that two additional substitutions, Ser174Asn and Met370Leu, when studied in combination with Arg443Ser and Gly456Ala, contribute to the unique properties of hGDH2. Also, Arg39Gln, Ser174Asn, Met370Leu and Gly456Ala were sufficient to modify the extreme effects of Arg443Ser on various aspects of hGDH2 regulation (discussed above) (Plaitakis et al. 2011).
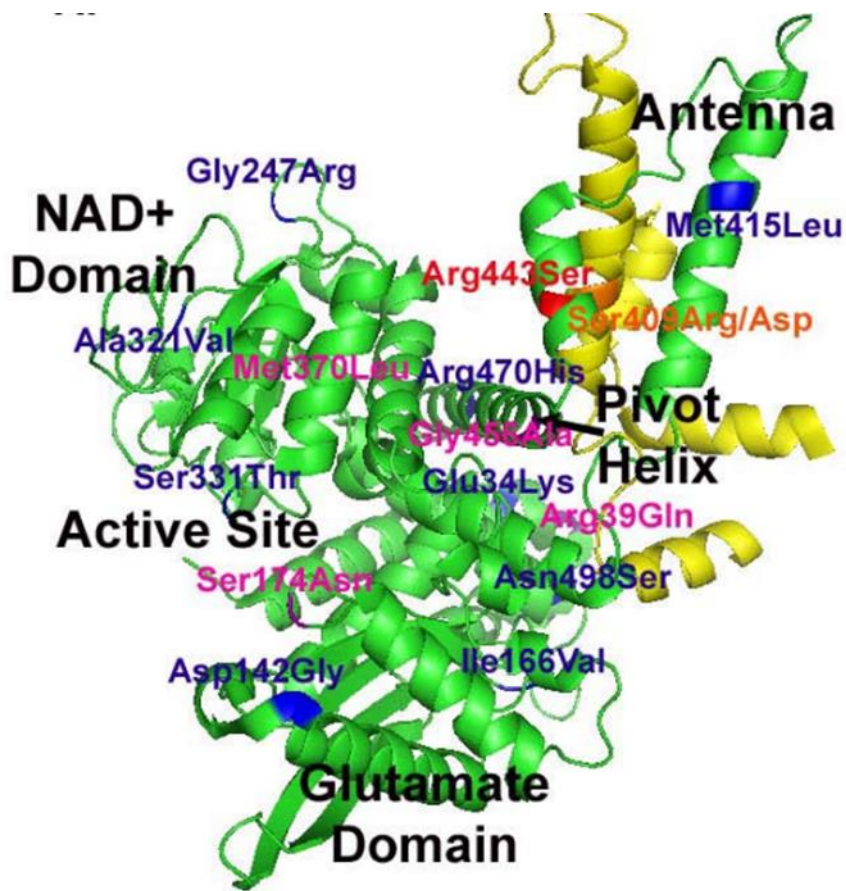
Figure 13: Comparison of hGDH1 and hGDH2 sequences. For simplicity, only one of the six subunits that compose the hGDH1 hexamer is shown (PDB code: 1L1F). Residues at sites of difference between hGDH1 and hGDH2 are shown in different colors. The main functional parts of the subunit (NAD+ binding domain, glutamate binding domain, active site, pivot helix and antenna) are also shown (from Borobokas et. al 2010).
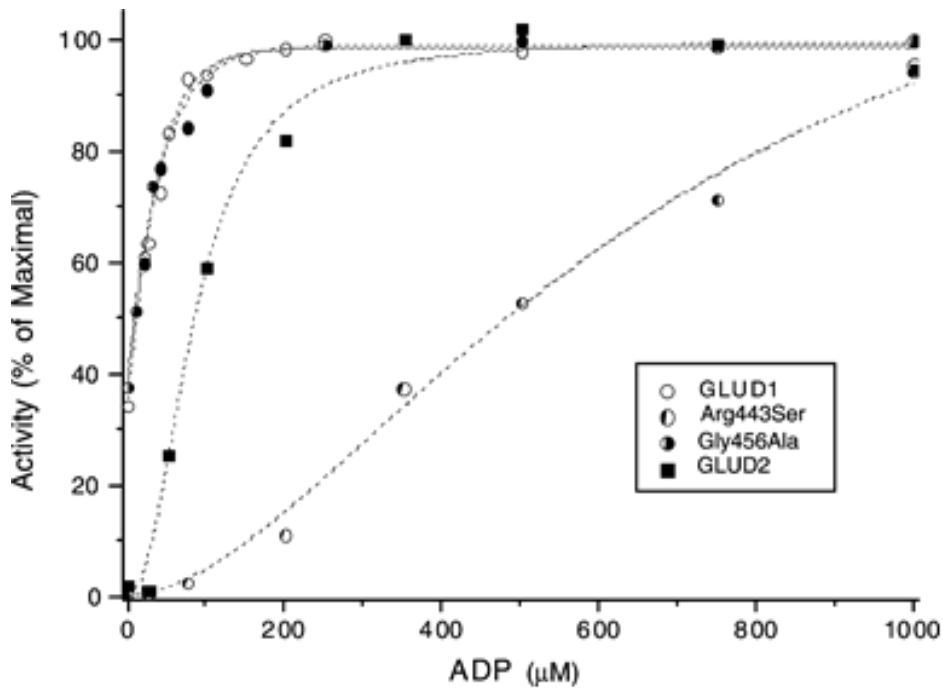
Figure 14: Comparison of ADP activation curves of the Gly456Ala and Arg443Ser mutants and of the wild-type human GDHs. GDH activity was measured in the direction of reductive amination of α-ketoglutarate in TRA, pH 8.0, buffer in the presence of increasing concentrations of ADP (from Plaitakis et al. 2003).
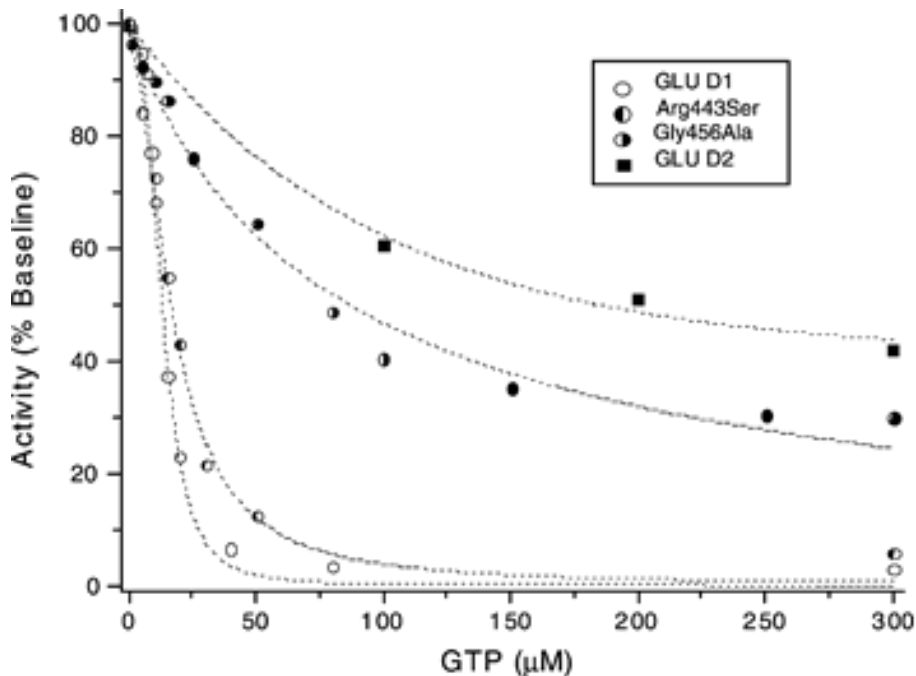
Figure 15: Comparison of inhibition curves of the Gly456Ala and Arg443Ser mutants and of the wild-type human GDHs. GDH activity was measured in the direction of reductive amination of α-ketoglutarate in TRA, pH 8.0, buffer in the presence of increasing concentrations of GTP (from Plaitakis et al. 2003).

9. EXPRESSION PATTERN AND SUBCELLULAR LOCALIZATION OF HUMAN GDHs

The tissue expression pattern, which is characterized either by the existence or the number of a gene's transcripts in a particular tissue, is indicative of the needs each region has, that can be satisfied by this particular gene's products. Following GLUD1 cloning, four different transcripts of the gene were identified by hybridization studies. GLUD1 was found to be ubiquitously expressed, although a different magnitude of hGDH1 activity was detected in the different tissues. GLUD2 mRNA was detected only in brain, testis and retina (Shashidharan et al. 1994). Later studies which aimed at the detection of hGDH proteins, were facilitated by the development of a hGDH2 specific antibody, since anti-hGDH1 antibodies were already commercially available. The task was not easy, given that the two isoenzymes differ in only a handful of amino acids, which are spread throughout the proteins' length, but a 12 amino acid long peptide including Arg443Ser change was found appropriate to discriminate between those two. Hence, Western blot experiments revealed that hGDH2 is expressed in human testis, brain and kidney, and was represented by the appearance of a higher hGDH band which migrated at 58kDa instead of 56kDa which was previously known for hGDH1. Specifically, testis contains almost equal amounts of hGDH1 and hGDH2 while brain contains substantially higher amounts of hGDH1 (Zaganas et al. 2012). Even more detailed results arose from immune-histochemistry experiments which aimed at the identification of cellular expression of hGDH2 in testicular and brain tissues. Interestingly, hGDH2 was detected in the cytoplasm of Sertoli and Leydig cells from testicular tissue and in astrocytes from brain tissue (Spanaki et al. 2015; Spanaki et al. 2014). All of the abovementioned cells are responsible for the constant support and nourishment of the high energy consuming neighboring cells, namely spermatogonia and neurons. Since the expression pattern reflects different needs of a protein, it would be safe to assume that these particular cells need to compensate for the augmented energy consumption via an extra GDH which is nevertheless governed by a distinct regulation motif for ultimate fine tuning of the metabolic procedures they accomplish. Concerning subcellular localization, several studies including subcellular fractionation, immune-electron microscopy and GFP-confocal microscopy have indicated that GDHs localize mainly in the mitochondria, and in fact in the mitochondria matrix (Mastorodemos et al. 2009; Rosso et al. 2008). GDH besides bears a 53-amino acid long guide peptide on its N' end, which is capable to drive it to the mitochondria, and is removed thereafter. Characteristically, cell lines overexpressing hGDH1-GFP and

hGDH2-GFP, produced a punctate mitochondria-like image under confocal microscopy.

10. GLUTAMATE DEHYDRGENASE'S QUARTENARY STRUCTURES IN HUMAN AND OTHER ORGANISMS

Protein subunit interaction is a critical phenomenon in regulation and catalysis. Thousands of such interactions are theoretically possible in a combinatorial manner. The subunit interaction to form a fully functional quaternary protein structure is mainly based on three factors, which are the inter-subunit H-bonds, the hydrophobic effect and the interphase size (Zhanhua et al. 2005). According to existing findings, GDH isoenzymes have been reported to form hetero-hexamers in some organisms, such as *Thermus thermophilus* (Tomita et al. 2011). Indeed, this eubacterium possesses two putative GDH encoding genes, producing GdhB and GdhA enzymes which share approximately 46 % identity in their amino acid sequence. It was revealed that its GDH holoenzyme functions as a hetero-oligomer, where GdhB and GdhA function as catalytic and regulatory subunits, respectively.

Human GDHs, as previously mentioned, function in the mitochondrial matrix. According to cellular biology norms, prior entering the mitochondrion, they should present an unfolded monomeric formation (enriched with the leader peptide on the N' terminus) which is aided by molecular chaperons to approach the target organelle. It is assumed that following their import in mitochondria, the leader peptide is removed and they are driven in the matrix which provides the suitable environment for their ultimate folding and function (Kotzamani and Plaitakis 2012). There, the separate subunits must be able to meet their counterparts and, through protein-specific interactions, to acquire their mature hexameric conformation. We can only hypothesize on this model, since there have not been supporting evidence on the precise mechanism so far. For the two human isoenzymes, it is inevitable to suspect that such homologous isoenzymes as hGDH1 and hGDH2, would be able to form both homo- and hetero-hexamers when both subunits would be available in the cell milieu. This matter is not yet elucidated, but since it has occupied the biggest part of the present thesis, it will not be further discussed at this section.

It has been proposed that the enzymes that are responsible for catalyzing sequential reactions in several metabolic pathways are highly organized in supramolecular complexes termed metabolons (Srere 2000). The advantages of such a supramolecular assembly include efficient channeling of substrates between enzymes,

and targeting the assembly of the interacting proteins to the appropriate intracellular structure. Regarding protein complexes in which GDH putatively participate, it could be anticipated that other enzymes of the mitochondrial matrix that are associated with GDH in a manner of "substrate donor-product acceptor" relationship (e.g. glutamine synthase, amino acid aminotransferase) possibly form large metabolic complexes. There are, indeed, recent indications (Islam et al. 2010; Hutson et al. 2011), that, in order to meet even more easily the catabolic needs, glutamate dehydrogenase forms a loose complex with mitochondrial aminotransferase branched amino acid (BCATm). GDH1 can participate functionally in this metabolon, creating a kinetically more efficient channeling of BCATm products to the oxidative pathway. By the combined action of BCATm and GDH1, a BCAA nitrogen group is efficiently channeled to glutamate, which is oxidatively deaminated by hGDH1 producing α-ketoglutarate. The interaction between BCATm and GDH1 also enhances leucine stimulation of hGDH1 activity, presumably by promoting an allosteric change in hGDH1.

11. CLINICAL SIGNIFICANCE OF HUMAN GLUTAMATE DEHYDROGENASES

Apart from being an intriguing enzyme research-wise, GDH has attracted the clinical interest too, as it has been found to participate in the manifestation of some human diseases, such as hyperammonemia/hyperinsulinism (HI/HA) syndrome and Parkinson's disease.

The most well established relation between GDH and human disease is that of HI/HA. Patients suffering from this syndrome are usually infants and present with hypoglycemia episodes accompanied with epileptic seizures, mainly following a protein rich meal. An additional feature of this condition is the concurrent elevation of ammonia levels 2-5 times higher than normal (hyperammonemia). In most cases hyperammonemia is considered asymptomatic, as patients do not show toxicity (Stanley et al. 1998; De Lonlay et al. 2001).

In pancreatic beta cells, GDH is involved in the regulation of insulin secretion, as factors that activate GDH, such as leucine, are associated with an increase in insulin secretion (and vice versa) (Fahien et al. 1988). Insulin secretion is a process controlled by energy metabolites. Specifically, glucose metabolism increases the ATP/ADP ratio in the cytoplasm which leads to closure of ATP-sensitive K^+ channels and subsequent depolarization of the cell membrane. The depolarization allows Ca_2^+ ions to enter the cell through specific ionotropic channels, and to stimulate insulin exocytosis. GDH

reaction, producing α-ketoglutarate, also contributes to energy boosting by feeding the TCA cycle, thus leading to increased ATP/ADP ratio. This mechanism is suppressed by the tonic inhibitory effect of GTP (also produced by the TCA cycle) on GDH. During fasting, with the consequent reduction of cell stocks of glucose and ATP, the oxidation of glutamate is enhanced by rising levels of ADP (and the catabolism of the amino acids in general), providing energy to the cell and maintaining insulin secretion at normal rates. The mechanism by which mutated GDH leads to HI/HA can be explained by the fact that decreased sensitivity to GTP inhibition, along with GDH over-activation by L-leucine after a protein rich meal cause excessive insulin secretion by pancreatic β-cells (Fig.16) (Stanley 2011).
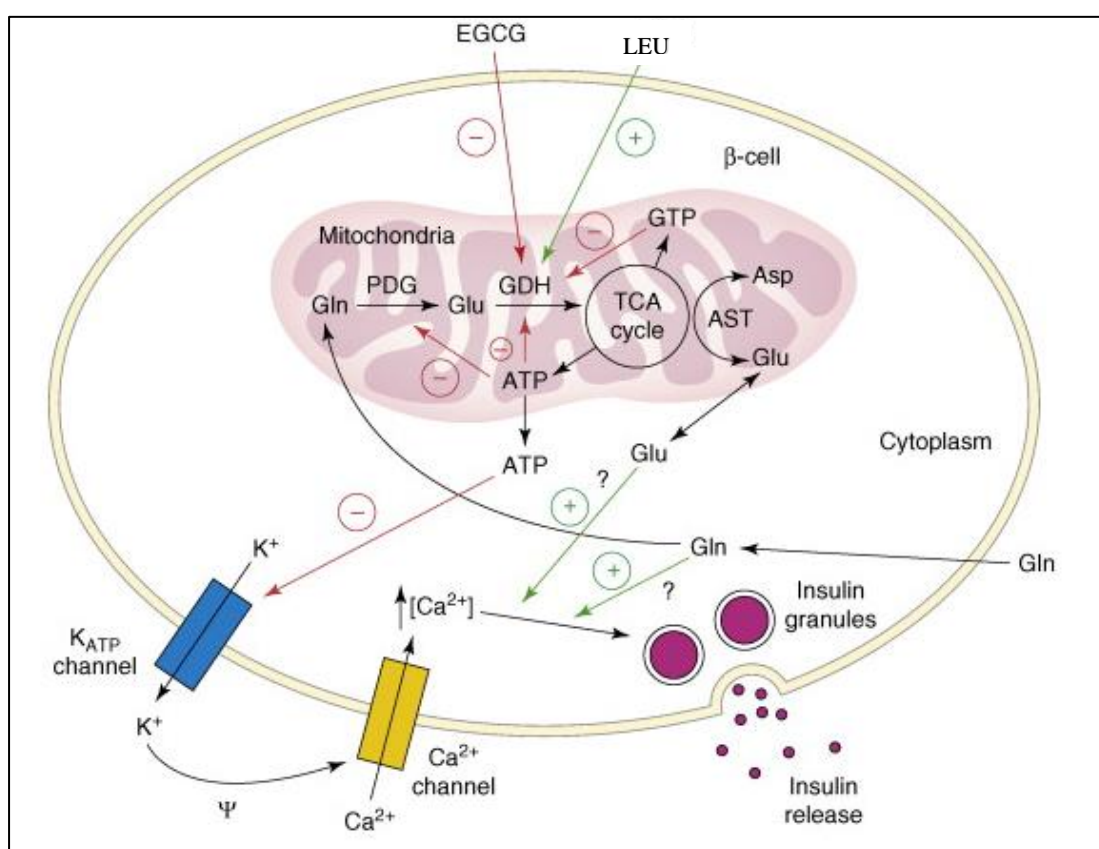
Figure 16: Role of GDH in HI/HA syndrome. In energy-depleted beta-cells (low ATP/ADP), the major energy source is glutaminolysis and GDH. L-leucine promotes GDH activation, thus providing the ATP signal necessary for insulin secretion. GDH inhibitors (GTP) normally block this process. However in HI/HA cases, GTP inhibition is abolished through mutations on GLUD1 which make hGDH1 unresponsive (Smith and Stanley 2008).

HI/HA syndrome is associated with dominantly expressed missense mutations on *GLUD1* (Stanley et al. 1998). All relevant mutations reported are single amino acid substitutions, which occur either in the GTP binding site or in the antenna region. Both

regions are crucial for allosteric regulation and in particular in this condition, the regulation of GDH by GTP is found to be impaired. These mutations are characterized as gain-of-function, since they lead to an overactive GDH enzyme, and they mostly occur *de novo*, while ⅓ of them are inherited. Mutations in exons 6, 7 and some in exon 12 are located on the pivot helix, thus being directly involved in the GTP binding site. Mutations in exons 11 and 12 are found to impair the antenna region, and probably act indirectly by inhibiting the conformational changes caused by GTP binding. Accompanying basal activity disruption has also been reported for some of these alterations (Ser445Leu causes a significantly increased basal activity, whereas Ser448Pro leads to a very reduced one). Interestingly, a particular mutation, Asn410Thr, does not seem to impair GTP inhibition, instead it significantly increases the basal enzyme activity (Kelly and Stanley 2001; Stanley et al. 1998; MacMullen et al. 2001; Miki et al. 2000; Stanley et al. 2000; Tanizawa et al. 2002; DeLonlay et al. 2001; Santer et al. 2001; Yorifuji et al. 1999; Fujioka et al. 2001; Yasuda et al. 2001; Aso et al. 2011; Kapoor et al. 2009)

One of the main clinical manifestations that accompany HI/HA syndrome is epilepsy, as already mentioned. Indeed, mutations causing hyperactivity of hGDH, could lead to the development of epilepsy. The mechanism underlying this relation indicates that the hyperactive GDH can lead to a depletion of glutamate and a consequent depletion of GABA neurotransmitter (Raizen et al. 2005), which is normally synthesized in neuronal cells from glutamate through the action of glutamate decarboxylase (GAD). GABA is the main inhibitory neurotransmitter in the central nervous system (CNS), reducing neuronal excitability throughout the nervous system and regulating muscle tone. Therefore, GABA levels' elimination can result in epileptic seizures as well as dystonic phenotypes (Plaitakis et al. 2013).

Another thoroughly studied example of GDH involvement in the pathophysiology of human diseases, is that of Parkinson's disease. Parkinson's disease exhibits multifactorial etiology. Among others, mitochondrial dysfunction has been repeatedly reported over the years to be associated with the onset of the disease. GDH's implication in this condition arose from the finding that a single nucleotide substitution on GLUD2 gene was related to earlier onset of Parkinson's disease, in male hemizygous patients (Plaitakis et al. 2010). T1492G variant of GLUD2, which causes an Ala445Ser change in the respective hGDH2 enzyme, interacts significantly with the time of manifestation of the disease, accelerating the disease onset by 6 – 13 years in men. That mutation in hGDH2, causes a gain of function in the enzyme's basal activity

as it seems to represent reduced sensitivity on GTP inhibition, but also high sensitivity on suppressing modification by estrogens. Plaitakis' research team studied this particular amino acid change enzymatically and they resulted that the mutant enzyme showed an increased basal activity, strong resistance to GTP inhibition but higher sensitivity to estrogens. Mainly male patients are affected by the effect of the mutation, because on the one hand, it is X-linked inherited and on the other side female patients are partially protected by tight regulation of GDH from estrogens (Plaitakis et al. 2010; 2011). We can only hypothesize about Ala445-hGDH2 variation on human brain but, it is likely that augmentation of glutamate oxidation could accelerate an ongoing degenerative process in PD by altering the compartmented metabolism of glutamate in brain and/or by increasing ROS production (Plaitakis et al. 2010).

Several studies have also related the deregulation of glutamate homeostasis in the development of age related neurodegenerative diseases, such as Alzheimer's disease (AD) (Kulijewicz - Nawrot et al. 2013; Olabarria et al. 2011).

Bao et al. (2009), by generating transgenic mice overexpressing GDH, they showed that glutamate release was enhanced in specific brain regions such as striatum and hippocampal CA1 region. These observations were accompanied by progressive neurodegeneration findings in many brain areas of transgenic mice, which expanded to other brain regions with aging progression. Specifically, they ascertained a significant reduction in the number of dendritic spines and axonal nerve terminals in CA1 hippocampal region. In Alzheimer's disease, hippocampus is one of the first regions impaired in brain, with memory loss and disorientation being among the early symptoms of the disease. Hence, it is hypothesized that GDH1 overexpression can accelerate age-related neuronal loss and dendritic dysfunction, findings similar to those previously observed in Alzheimer's disease (Bao X. et al. 2009; Wang X. et al. 2014).

12. STUDIES ON ALTERED GLUD1 EXPRESSION

In an attempt to further unravel GDH impact on cellular metabolism, some studies were focused on either deleting or overexpressing *GLUD1* gene in various models. Indicatively, Carobbio et al. (2009) by generating transgenic mice with β-cell-specific GDH deletion concluded that GDH is critical for full development of the insulin secretory response. Specifically, they observed that GDH appears to account for about 40% of glucose-stimulated insulin secretion. In these knock-out mice, the reduced

insulin secretory capacity resulted in lower plasma insulin levels in response to both feeding and glucose load, while body weight gain was preserved.

Later on, Frigerio et al. (2012) generated CNS-specific GDH-null mice to investigate the importance of this enzyme for the neural tissue. The knock-out mice did not present altered synaptic transmission nor behavioral problems, however they exhibited deficient oxidative catabolism of glutamate in astrocytes. In fact, brain glutamate levels remained unchanged, whereas glutamine levels were increased. This pattern was favored by upregulation of astrocyte glutamate and glutamine transporters and of enhanced activity of glutamine synthase.

Another group used transgenic mice modified to overexpress GDH1 in order to elucidate how GDH levels are crucial for normal brain function. They revealed that increased GDH expression in neural cells resulted in upregulation of glutamate release and consequently, excitotoxicity. The mice were exhibiting a phenotype similar to progressive neurodegeneration (Bao et al. 2009).

Lastly, Wang et al. (2014) have examined the impact of GDH in gene expression of wild type and GDH overexpressing transgenic mice, during development and aging. They firstly depicted that GDH overexpression leads to excess synaptic release of glutamate. By analyzing the whole genome expression in the hippocampus of these mice, they showed that glutamate hyperactivity caused gene expression changes in that region. Genes that were mainly differentially expressed in transgenic mice during development and aging were associated with synaptic function, cytoskeleton formation, protein ubiquitination, calcium signaling, neuron projection and mitochondria function.

Recently in our laboratory, we have produced some interesting data of GDH1 and GDH2 overexpression in mammalian cell lines. Specifically, stable HEK293 lines over expressing hGDH1 or hGDH2, display lower death rates in different time points of their lifespan as compared to wild-type cells (Lampros Mathioudakis, unpublished data). Our next aim is to further elucidate the metabolic impact expansion of hGDH expression disequilibrium in these cells. At the same time, we aim to create stable hGDH1 and/or hGDH2 knock out HEK293 cell lines, by employing CRISPR/Cas9 technology and already available constructs for disruption of each gene (*GLUD1*, *GLUD2*) in order to study how their deletion affects cellular metabolism and survival (Christina Kosmopoulou, unpublished data).

13. RECENT FINDINGS ON GLUTAMATE DEHYDROGENASE'S ROLE

Except for its participation in complex metabolic processes, recent findings have indirectly connected GDH with cell signaling pathways as well. Beyond that, and as a natural consequence, GDH's association with cancer development was also studied, since it is well established that cancer is related to abnormal signaling procedures.

One of the major signaling pathways in mammalian cells involves mTOR which, following some combinations of signals, is able to regulate growth, aging and metabolism. Recently mTOR activation was connected with glutaminolysis processes, which mediates the recruitment of mTOR to lysosomes and its subsequent activation, in response to glutamine and leucine. Both abovementioned amino acids, are associated with GDH, the former as a precursor of glutamate, which is GDH's substrate, and the latter as GDH's activator. Hence, both amino acids trigger GDH to catabolize glutamate towards α-ketoglutarate production, which ultimately mediates mTOR activation (Duran et al. 2012).

Regarding GDH implications in cancer, a recent study by Chen et al. (2014) reported an association of *GLUD2* with secondary glioblastoma. Mutations of IDH1 (isocitrate dehydrogenase 1) are commonly found in patients with this brain tumor, and these events are recognized as early causative. Both *GLUD1* and *GLUD2* were found overexpressed in IDH1-gliomas. Furthermore, a particular mutation, IDH1 R132H, which otherwise exhibits growth-inhibitory effects on glioma tumors, was shown to be abrogated by the presence of *GLUD2* which promoted cells' growth and metabolite influx in murine glioma progenitor cells. The mechanism by which this is possible is speculated to be through the supplementation of α-ketoglutarate to the TCA cycle via GDH reaction, and the subsequent support of lipid synthesis which enables cancer cells to survive. In addition, IDH1 R132H gliomas lack BCAT1 which helps them maintain high concentrations of α-ketoglutarate and leucine, thus higher GDH activity. The preference of hGDH2 over hGDH1 to mediate the processes could be explained by the fact that *GLUD2*'s optimum pH suits better the glioma acidified environment. Besides, *GLUD2* was evolved concurrently with the prefrontal cortex where IDH1 R132H glioma most commonly occurs.

Aim of this study is to advance our knowledge on the structural properties and structure-function relationships of hGDHs, towards deciphering the metabolic implications these relationships might have. Additionally, we sought to examine the variants of *GLUD1* and *GLUD2* genes in a Greek population of aged adults, as obtained from whole exome sequencing data available in our laboratory. Each of these aims along with the need for their accomplishment are analyzed below.

As discussed in the introduction section, while in most mammals GDH is encoded by a single gene, GDH in humans and other apes exists in two isoforms, named human GDH type 1 (hGDH1) and human GDH type 2 (hGDH2), respectively. Despite their high amino-acid sequence similarity, the two isoenzymes differ significantly in their enzymatic properties (Plaitakis et al. 2000). Specifically, while hGDH1 is sensitive to GTP inhibition and maintains 40% of its maximal activity in the absence of allosteric activators, hGDH2 is GTP-resistant and shows negligible unstimulated (basal) activity. Most of the functional differences between the two isoenzymes can be attributed to only 2 amino acid substitutions, namely Arg443Ser and Gly456Ala. These amino acid changes occurred immediately after the emergence of the hGDH2 enzyme from its paralogue hGDH1 though a retroposition event in the common ancestor of humans and modern apes (Burki and Kaessman 2004). Apart from their enzymatic properties, the two enzymes also differ in their tissue compartmentation. Specifically, hGDH1 is a ubiquitously expressed enzyme, while hGDH2 is mainly present in brain and testis. Interestingly, in these tissues hGDH2 is found in the nourishing and supporting cells which are the astrocytes and Sertoli cells, respectively. hGDH2 activity is also detectable in kidneys and retina (Zaganas et al. 2012; Spanaki et al. 2010).

It is currently unknown whether these hGDH isoforms can interact in the tissues where they are co-expressed (by forming hetero-hexamers) and what further metabolic adaptations the particular tissues/cells might be equipped with, due to this possible interaction. Supporting evidence has revealed that such an interaction is indeed possible, as *Thermus thermophilus* GDH isoenzymes are able to form hetero-hexamers which are critical for the holoenzyme's function and regulation (Tomita et al. 2011). Given that the subunit interaction depends on physical factors such as inter-subunit H-bonds, hydrophobicity and interphase size (Zhanhua et al. 2005), we can anticipate that such homologous isoenzymes as human GDHs are, would be able to

form both homo- and hetero-hexamers when both subunit types are available in the cell milieu. Since protein subunit interaction has important implications in regulation and catalysis and beyond that, a protein's quaternary structure is crucial for its very folding and function, it is intriguing to investigate the nature and importance of hGDH1 and hGDH2 possible interaction. As the functional properties of hetero-hexamers may be distinct from those of homo-hexamers, this association may provide versatility to human cells by equipping them with more than two isoenzymes.

Given the importance of the GDH enzyme for cellular metabolism and the complexity of its catalytic properties and allosteric regulation, there have been numerous efforts to solve its structure by X-ray crystallography. However, while the structure of bovine (boGDH1) and human (hGDH1) hexamer was ultimately solved both in unbound form and in complex with various substrates and allosteric regulators (Smith et al. 2002; Peterson and Smith 1999; Smith et al. 2001; Banerjee et al. 2003), the structural properties of hGDH2 (and thus the basis of its functional diversity from hGDH1) remain unknown. Previous attempts for hGDH2 crystallization involved its recombinant production in bacterial cultures, which resulted in large enzyme aggregations in the cytosol, incapable of folding properly (Kokkinidis M, unpublished data). Later attempts employing chaperon-mediated clearance resulted in obtaining even more complex macromolecular structures, rendering hGDH2 crystallization even more laborious. The persistent resistance of the hGDH2 isoenzyme to numerous crystallization efforts is also due to its extreme sensitivity to various conditions that affect its stability (including small changes in the temperature and the pH of the containing buffer). Thus, in the context of structural studies, it is interesting to study GDH native conformations under changing pH conditions *in vitro*. Acquiring the crystal structure of hGDH2 is pivotal for understanding the structural basis of its dramatic functional differences compared to the hGDH1 enzyme. This will be achieved through comparison of the two crystal structures and will provide evidence on the evolutionary adaptation of the newly formed hGDH2 isoenzyme to its new functional role. These new functional properties enabled the persistence of the enzyme during primate evolution, by conferring an evolutionary advantage. This will provide an example of how these primate proteins evolved, not only at sequence and functional level, but also at structural level.

Along with the establishment of the implications of mitochondrial dysfunction in human degenerative disorders, there is increasing evidence that deregulation of human hGDH1 and hGDH2 isoenzymes putatively leads to neuronal dysfunction and degeneration. This evidence stems from the following observations: 1) mutations in

hGDH1 that render the enzyme overactive (gain-of function) are associated with epilepsy (Raizen et al. 2005); 2) a gain-of–function variant in *GLUD2* (overactive enzyme) accelerates the commencement of PD (Plaitakis et al. 2010) and 3) over-expression of hGDH1 in transgenic mice leads to age-dependent degenerative changes in the CA1 region of the hippocampus (Bao et al. 2009). The latter observations, along with data showing *GLUD2* transcripts in human hippocampus, have raised the possibility that GDH deregulation may be associated with AD onset. These possibilities will be explored in the present study, in which *GLUD1* and *GLUD2* genetic variations' spectrum will be assessed in a large Cretan Aging Cohort, whose whole exome sequence data are already available in our laboratory as the outcome of a large interdisciplinary program (Thalis-MNSAD, P.I. A. Vgontzas).

Summarily, the specific questions we intend to answer in the present study are:

1) Whether the two isoforms hGDH1 and hGDH2 can form hetero- hexamers when recombinantly co-expressed in Sf21 cell cultures.

2) What are the enzymatic properties and optimal functioning conditions of the possible hGDH1/2 hetero-hexamers in comparison with wt-hGDH1 and wt-hGDH2 as well as with hGDH1/hGDH2 *in vitro* mix

3) Under which conditions can hGDH2 form crystals and what are the properties of these crystal structures (in collaboration with Dr. Kokkinidis group).

4) Which is the genetic variation spectrum of *GLUD1* and *GLUD2* genes in the Cretan Aging Cohort, and how are they related to dementia (collaboration with Thalis-MNSAD program of Neurology laboratory).

To address the first two aims, we have recombinantly co-expressed hGDH1 and hGDH2 in Sf21 cultures using the Baculovirus expression system, and we have performed co-immunoprecipitation and affinity chromatography studies in order to investigate the formation of possible hetero-complexes. Subsequently, we extensively studied the enzymatic properties of the possible hetero-hexamers under multiple conditions, by comparing it with wild type human GDHs and with an *in vitro* mix of both isoenzymes in their pure homo-hexameric form.

In order to approach the unsolved issue of hGDH2 crystal structure (third specific aim), we performed a large scale production of the protein in Sf21 cultures. Then we performed sequential chromatographic preparations to obtain a highly purified enzyme solution, which was concentrated and subjected to crystallization trials by the method of "hanging-drop vapour-diffusion". The most compact crystals were harvested and

frozen. Subsequently, in collaboration with Prof. M. Kokkinidis lab, the crystals were subjected to X-ray diffraction which, after *in silico* analyses, provided us with some initial structural data. Additionally, we studied the conformation of hGDH enzymes under different pH conditions, using size exclusion chromatography on line with multi angle light scattering (SEC/MALS).

For the last (fourth) specific aim of the present study, we have performed whole exome sequencing (WES) on 100 patients with dementia, 20 with MCI and 81 cognitively normal controls, having in our disposal a total of 201 full exomes, each comprising of information on the exons and intron/exon boundaries of 20,000 genes. Of these, we focused on *GLUD1* and *GLUD2* genetic variations in order to elucidate their frequency in the Cretan aging sample and their association with dementia and to uncover unique uncharacterized variants.

1. PROTEIN PRODUCTION

Recombinant hGDH1 and hGDH2 proteins are produced in Sf21 cells using the Baculovirus expression system, as previously described (Shashidharan et al. 1994). The human cDNAs for hGDH1 and hGDH2 have been subcloned into suitable plasmid vectors, named pVL1393 and pVL1392, respectively (these constructs have been created in the context of previous projects and were kindly provided for the purposes of the current study) [3]. They have subsequently been combined with linearized baculovirus DNA (Baculogold, BD, Pharmingen), downstream of the powerful polyhedrin promoter that has allowed the production of potentially unlimited amounts of the human protein. This initial (P1) generation of viruses and its subsequent generations that are at store, are used for protein production.

The Sf21 cell culture is usually initiated at the level of 5ml in one T25 culture flask (2.8x106 cells) and gradually reaches 1-2 L cultures in Erlenmeyer or spinner flasks for large scale protein production. Sf21 cell line requires Grace's Insect medium supplemented with FBS and, optionally, gentamycin. The cells are kept at a 27°C – incubator, displaying a duplication time of approximately 24h. They are usually transfected with the viral stock when they are at the exponential phase of their growth (~75% confluency) and they are incubated with this virus-containing medium for 4-5 days. The cells are then harvested, centrifuged and their pellets (containing the recombinantly expressed human GDH isoenzyme) are kept at -80oC for future use.

For cell lysis and homogenization, the cell pellets are re-suspended in a lysis buffer containing Tris-HCl, NaCl, EDTA (pH 7.4), Triton 1% and protease inhibitors, and are homogenized by a suitable tissue homogenizer. The obtained crude cell extracts are subsequently used for protein purification. Protein expression levels in the crude extracts are assessed by measurement of the specific activity of the enzyme (measurement of the GDH activity per mg protein of the extract spectrophotometrically at 340 nm in TRA pH 8, with the supply of the specific substrates –NADPH-and activators –ADP- for the reaction) or by Western Blot using the specific antibodies for each protein (anti-GDH1, anti-GDH2 or anti-GDH). The extended protocols used for this part are described below.

<u>Sf21 cell culture</u>

Sf21 are large circular-shaped cells that derive from ovaries of the insect Spodoptera frugiperda. They are widely used for recombinant protein production due to their high efficiency in generating large amounts of proteins in comparison with human cell lines, and their easy manipulation. They were selected for expression of human GDH, as they constitute a eukaryotic expression system that provides means for normal protein processing and post-translational modifications, allowing native protein conformation to take place.

Although Sf21 cells possess an endogenous GDH, it is strictly NAD(H)-specific. Thus, wild type Sf21 cell lysates show zero GDH activity when assayed in the presence of NADP(H) as cofactor.

Sf21 cells are kept in suitable cryovials containing 60% culture medium, 30% FBS and 10% DMSO (as cryo-protectant), at -80°C for six months or at liquid nitrogen for years. To initiate a cell culture, the vials need to be quickly thawed in a 37°C preheated water bath, while being gently shaken. Once thawed, the cells must immediately be added in a T25 culture flask filled with 5ml full culture medium consisting of Grace's Insect medium, 10% FBS and, optionally, 100ug/ml gentamicin (Life Technologies, USA, CA), and are allowed to adhere on the flask's surface for 45 minutes, in a 27°C incubator. Most cells die at that step due to the thawing shock and the excess DMSO contained in their freezing medium, phenomenon which allows them to renew. After 45 minutes the medium (together with the dead cells) is removed and is replaced with 5ml fresh medium. Sf21 display a duplication time of approximately 24h.The cells are allowed to grow in a 27°C incubator until they reach confluency, covering 90% of the flask's surface.

The culture is then expanded by splitting cells in more, or larger, culture flasks (usually 1:3 dilution). Fresh medium is added in the confluent flask, and cells are detached from the surface mechanically, either by using cells scrapers or by rinsing medium on them. They are divided in different flasks and adequate fresh medium is added so as to cover them up.

Sf21 cells are also capable to grow as a suspension culture, in suitable Erlenmeyer or spinner flasks. Growth in Erlenmeyer flasks requires a shaking incubator and the

addition of a surfactant (Pluronic 10% F-68, Life Technologies, USA, CA) to avoid cell rupture due to shear forces. Cell growth is monitored by adding 10ul culture sample in a Neubauer chamber and counting them under light microscope. Maximum cell density to ensure proper cell growth is approximately 2×10^6/ml.

<u>Sf21 culture transfection</u>

DNA from a transfer vector containing the target gene (pvl1392 for *GLUD1* and pvl1393 for *GLUD2*) is transfected into Spodoptera frugiperda cells along with Bsu36 I-digested BacPAK6 viral DNA. In vivo homologous recombination between the plasmid and viral DNAs rescues the viral DNA and in the process transfers the target gene to the viral genome. Baculovirus DNA and transfection reagent were available from Clontech (CA, USA).

1. Dilute the plasmid DNA to 100 ng/µl with TE (10 mM Tris-HCl pH 8.0, 1 mM EDTA).
2. Seed a 6-well culture plate with 1×10^6 exponentially growing Sf21 cells per well, and incubate at 27°C for ~30 minutes.
3. Remove the old medium from the cells and add 2 ml Grace's plain Medium. Swirl gently, remove the medium again and add 2 ml Grace's plain Medium. Incubate at room temperature for 10–30 minutes while the Bacfectin-DNA mixture is prepared, as described in the following steps.
4. Make the following additions to two sterile polystyrene tubes:

	Cotransfection	Control
Sterile H$_2$O	86 ul	91 ul
Plasmid DNA	(100 ng/ul) 5 ul	5 ul
BacPAK6 viral DNA	5 ul	—

Gently flick the tubes to mix solutions
5. Add 4 ul of Bacfectin to the DNAs and mix gently. Incubate at room temperature for 15 minutes to allow the Bacfectin to form complexes with the DNA.
6. Meanwhile, remove the medium from the cell monolayers and add 1.5 ml Grace's plain Medium.
7. Add the Bacfectin-DNA mixture dropwise to the medium while gently swirling the dish to mix. Incubate at 27°C for 5 hours.
8. Add 1.5 ml Grace's Complete Medium, containing 10% fetal bovine serum and antibiotics to each well. Incubate at 27°C.

9. Approximately 72 hours after addition of the Bacfectin DNA mixture to the cells, harvest and centrifuge cells at 1500 rpm for 10 minutes, transfer the supernatant, which contains viruses produced by the transfected cells, to a sterile container and store at 4°C.

The recombinant viruses which were released from the cells in the culture medium were thenceforth used for following transfections, after they were first amplified in larger cell cultures (usually at the T75cm^2 level, ~8 x 10^6 cells at confluency).

Baculovirus DNA isolation and validation

In order to establish the feasibility of our experiments, it is wise to regularly check whether Baculovirus has maintained its genome integrity, especially within the gene of interest, as viruses are generally prone to mutations. For that purpose Baculovirus DNA is isolated and subjected to PCR with primers binding at either side of the gene of interest. The PCR product is then validated through sequencing using the same set of primers.

For Baculovirus DNA isolation:

1. Aspirate ~6ml of viral stock in a new sterile falcon tube. Centrifuge at 5000 rpm for 5 minutes. Transfer supernatant to a clean tube.
2. Add equal volume of ice cold 20% PEG solution. Agitate the mix gently and let it cool on ice for 30 minutes.
3. Centrifuge at 13000g for 10 minutes
4. Discard supernatant. Add 400ul FG1 buffer (from Flexigene DNA kit, Qiagen, Germany) to the remaining pellet, and mix by pipetting up and down.
5. Add equal volume (400ul) of buffer FG2 (from Flexigene DNA kit, Qiagen, Germany) and 1% protease (4ul). Incubate at 65°C for 10 minutes.
6. Add 800ul isopropanol. Centrifuge at 13000g for 20 minutes.
7. Discard supernatant. Add 800ul 70% ethanol solution to the pellet. Vortex briefly. Centrifuge at 13000g for 20 minutes.
8. Discard supernatant. Dry pellet by reversing tubes on absorbing paper (do not let pellet over dry, as it becomes difficult to resuspend).
9. Resuspend pellet in 50ul FG3 (from Flexigene DNA kit, Qiagen, Germany) buffer, vortex briefly. Incubate at 65°C for 30 minutes.

Once the desired DNA is obtained, its concentration (in ng/ul) is measured at nanodrop. The sample is stored at -20°C.

For amplification of the desired DNA sequences (here *GLUD1* and *GLUD2* genes) and subsequent validation through Sanger sequencing, we performed PCR using GLUD specific sets of primers. Because GLUD cDNAs were >1500bp long, we used four sets of primers spanning the whole length of this sequence and we produced two overlapping PCR products. Specifically, for GLUD inserts in the Baculovirus DNA, we used the following primers:

Primer	Sequence	Tm
Polyhedrin Forward	AAATGATAACCATCTCGC	54.9
Klio2as	TGATCTTGGCTTTGACTCTG	60.6
Polyhedrin Reverse	GTCCAAGTTTCCCTG	50.9
Klio2s	ACAAGTGTGCAGTGGTTGAT	60.7

PCR reactions and thermocycler programs used are described below:

MIX A		MIX B	
Buffer C Kapa Taq 5X	8ul	Buffer C Kapa Taq 5X	8ul
MgCl$_2$ 25mM	4ul	MgCl$_2$ 25mM	4.8ul
dNTPs 2mM	4ul	dNTPs 2mM	4ul
Primer Forward (polyhF) 5pmol/ul	4ul	Primer Forward (Klio2s) 5pmol/ul	4ul
Primer Reverse (Klio2as) 5pmol/ul	4ul	Primer Reverse (polyhR) 5pmol/ul	4ul
Kapa Taq DNA polymerase	0.5ul	Kapa Taq DNA polymerase	0.5ul
DNA template (Baculovirus DNA) ~ 50ng/ul	3ul	DNA template (Baculovirus DNA) ~ 50ng/ul	3ul
ddH$_2$O	12.5ul	ddH$_2$O	11.7ul
Final volume	40ul	Final volume	40ul

	PROGRAM A			PROGRAM B		
Initial denaturation	95°C	5'		95°C	5'	
Denaturation	95°C	1'		95°C	1'	
Annealing	55°C	1'	30X	52°C	1'	30X
Elongation	72°C	1'		72°C	1'	
Final elongation	72°C	10'		72°C	10'	
Storage	4°C	∞		4°C	∞	

For verification of the results, 2 ul of the PCR products were mixed with 4x orange G loading dye, were loaded on 1% agarose gels containing gel red (Gel RED Nucleic Acid 10,000X, Biotium, CA, USA) (3ul/100ml agarose solution) and run at 100V before they were visualized under UV light.

The verified products were cleaned up using PCR clean up and gel extraction kit from Macherey-Nagel following the provided protocol:

1. For very small sample volumes < 30 ul adjust the volume of the reaction mixture to 50–100 ul with water.

2. Mix 1 volume of sample with 2 volumes of Buffer NTI

3. Place a NucleoSpin® Gel and PCR Clean-up Column into a Collection Tube (2 ml) and load up to 700 ul sample.

4. Centrifuge for 30 s at 11,000 x g. Discard flow-through and place the column back into the collection tube. Load remaining sample if necessary and repeat the centrifugation step.

5. Add 700 ul Buffer NT3 to the NucleoSpin® Gel and PCR Clean-up Column. Centrifuge for 30 s at 11,000 x g. Discard flow-through and place the column back into the collection tube.

6. Repeat step 5.

7. Centrifuge the empty column for 1 minute at 11,000 x g to remove Buffer NT3 completely.

8. Place the NucleoSpin® Gel and PCR Clean-up Column into a new 1.5 ml microcentrifuge tube. Add 15–30 ul Buffer NE and incubate at 70ºC) for 1 minute. Centrifuge for 1 minute at 11,000 x g.

In order to remove PCR by-products (or digestion fragments) we perform gel extraction. For gel extraction we follow the same procedure as above, after we have isolated the DNA band we are interested in from the gel, and we have melt the gel piece by adding 2 volumes of NTI (based on the gel weight in mg) at 50ºC.

The cleaned-up DNA is used for Sanger sequencing validation. For this purpose 20ul DNA of final concentration at least 50ng/ul, together with specific primers (usually the same sets as those used for PCR) at a final concentration of 10pmol/ul, are packed and sent at Macrogen sequencing services (Netherlands). The results are then assessed by BLAST alignment, using as a template sequence the cDNA of each gene.

<u>Cell harvesting and lysate processing</u>

As already mentioned, Sf21 culture was used for human GDH enzymes' production. Following 3-4 day incubation with the viral stock, cell cultures reach their maximal protein production threshold before they start to decay. This is the critical point at which the cells are harvested for protein isolation. Either adherent or suspension cultures are put into falcon tubes and are centrifuged at 1500 rpm for 10 minutes at room temperature. The resulting supernatant, containing medium, dead cells and viral particles, is discarded while the cell pellet is further processed. Cell pellets are re-suspended in lysis buffer (10mM Tris-HCl, 0.5M NaCl, 0.5mM EDTA (pH 7.4), Triton 1% and 1X protease inhibitors), and are homogenized with a suitable tissue homogenizer. The lysate is allowed to cool on ice for at least 30 minutes, before it is once again centrifuged at 10000g, for 10 minutes, at 4°C. This time the supernatant, containing the crude cell extract, is transferred into clean tubes and is kept at 4°C for future usage.

2. BACULOVIRUS GLUD1/GLUD2 GENERATION

To reduce the phenomenon of unequal expression due to different expression capacity of the viruses while trying to recombinantly produce the putative GDH heterohexamer, we ought to create a single Baculovirus which would produce hGDH1/2 at a stable proportion of 1:1. For this purpose the BacToBac system was employed, by which, using the pFastBacDual plasmid that carries both GLUD1 and GLUD2 cDNAs under equally strong promoters (polyhedrin and p10 respectively), we managed to transpose them into a Baculovirus DNA sequence-bacmid and to transfect Sf21 cultures with equal amounts of the abovementioned genes (Fig.17). pFastBacDual-GLUD1/GLUD2 construct was supplied from ATG-Biosynthetics (Germany) (Fig.18), along with the specific strain flexiBacTurbo-containing E.coli (FBT).

After amplification of the plasmid in a DH10b E.coli strain culture, using Ampicillin and Gentamicin selection, and midi prep purification using Macherey-Nagel (Germany) kit, large amounts of DNA were obtained which was subsequently used to transform the specific FBT cells. FBT cells contain the so called bacmid, which is a >135kb circular Baculovirus DNA and a helper plasmid which serves in the transposition of the genes of interest from the pFastBac plasmid to the bacmid. Since the transposition sites are located at either sides of a lacZ gene, the recombinant bacmids are then selected by

their white color in an X-gal/IPTG agar plate. The positive colonies are amplified and the bacmids are isolated by midi prep, before they are further evaluated by PCR using primers that bind at both sides of the insert. Finally, recombinant bacmids in combination with Cellfectin II reagent are used to transfect Sf21 cultures in order to produce the P1 Baculovirus after 4 days of incubation. P1 is then used to upscale the transfection and thus the protein expression.

Blue silver stained acrylamide gels and western blots using the non-discriminating hGDH antibody in transfected Sf21 crude extracts, proved that hGDH1 and hGDH2 isoenzymes were indeed expressed at a 1:1 proportion.

As a next step, pFastBacDual-GLUD1/GLUD2 was manipulated to carry single GLUD genes, by cutting off either GLUD1 or GLUD2, in order to be used for hGDH1-specific and hGDH2-specific Baculovirus generation and, thereby, separate enzyme production. Detailed protocols of this section are discussed below.
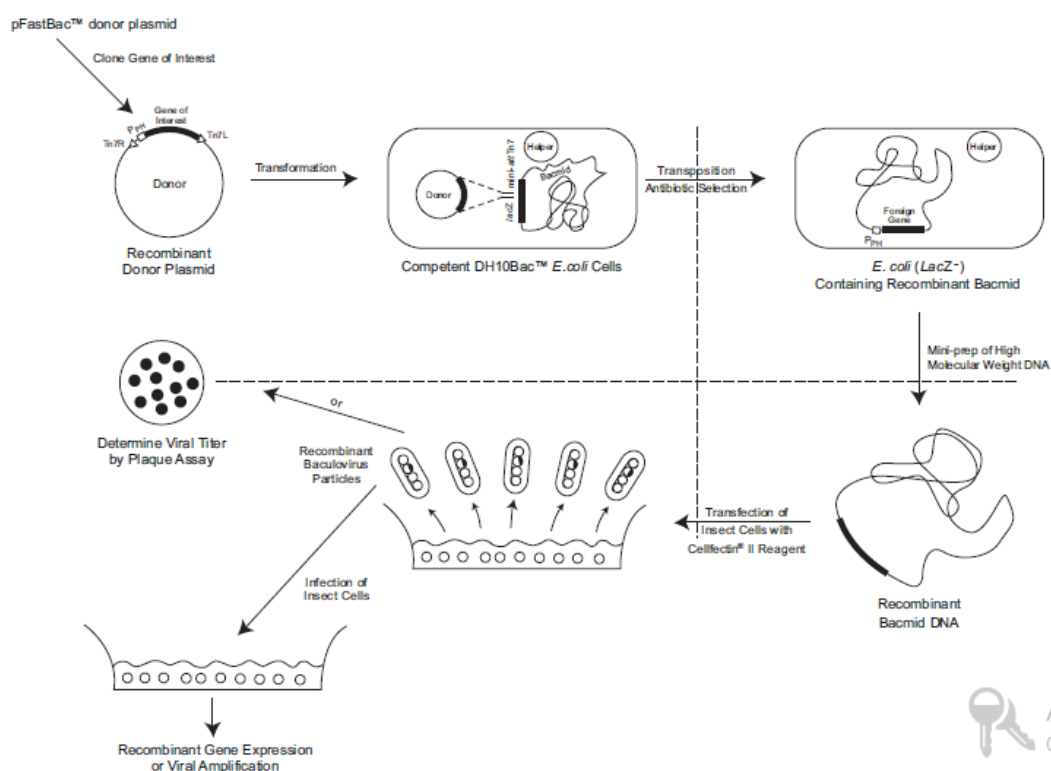
Figure 17: Bac-to-Bac Baculovirus expression system. The genes of interest are cloned into pFastBac vector, which is then used to transform FBT E.coli cultures (containing bacmid and helper plasmid). The recombinant bacmid positive colonies are picked and grown O/N, and the bacmid DNA is isolated. The bacmid is used to transfect Sf21 cultures with cellfectin II reagent, and P1 Baculovirus is generated. P1 is finally used for upscaling of protein expression.
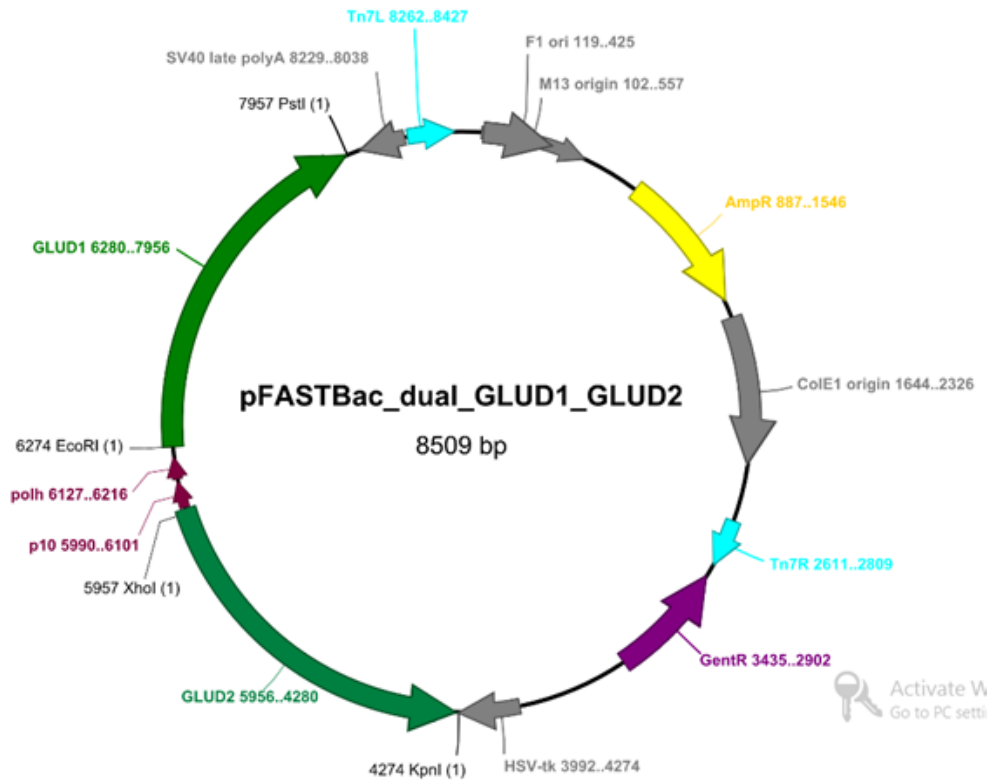
Figure 18: pFastBacDual-GLUD1/GLUD2 construct. GLUD1 cDNA was inserted downstream the polyhedrin promoter, at the multiple cloning site of the plasmid between restriction sites EcoRI-PstI, while GLUD2 was inserted back-to-back to GLUD1, downstream promoter p10 and between restriction sites XhoI-KpnI.

pFastBacDual vectors amplification

4ug of pFastBacDual was provided in lyophilized form from ATG Biosynthetics (Germany). Initially it was diluted at a final concentration of 150ng/ul and a small quantity (~3ng) was used to transform DH10b bacterial cells for subsequent amplification of the vector.

The transformation method selected was electroporation. In order to generate electrocompetent cells, 100ml of LB* medium (1lt: 10gr yeast extract, 5gr bactotryptone, 5gr NaCl, pH 7.0) were inoculated with DH10b cells and the cultured was allowed to grow in a 37°C shaking incubator, until the optical density of the culture reaches 0.6 at 600 nm.

Afterwards:

1. Cells are incubated on ice for 15 minutes
2. Centrifuge at 4000 rpm, 4°C for 15 minutes

3. Remove supernatant and dissolve the bacterial pellet in 100ml of ice cold sterile nanopure H_2O

4. Centrifuge at 4000 rpm, 4°C for 15 minutes

5. Remove supernatant and dissolve the bacterial pellet in 50ml of ice cold sterile nanopure H_2O

6. Centrifuge at 4000 rpm, 4°C for 15 minutes

7. Remove supernatant and dissolve the bacterial pellet in 25ml of ice cold sterile nanopure H_2O

8. Centrifuge at 4000 rpm, 4°C for 15 minutes

9. Remove supernatant and dissolve the bacterial pellet in 10ml of ice cold sterile nanopure H_2O

10. Centrifuge at 3500 rpm, 4°C for 15 minutes

11. Remove supernatant and dissolve the pellet in ~1ml ice cold 10% v/v glycerol solution

12. Electrocompetent cells are stored in aliquots of ~50ul at -80°C

For electroporation, 1μl of the plasmid DNA (~20ng) are mixed with the cells. Subsequently, the mix is transferred in an electroporation cuvette, which has previously been UV-sterilized and ice frozen. Electroporation is performed at 2500 V for 5msec. This allows the cells to temporarily allow plasmids enter the bacterial membrane. Afterwards, the cells are transferred in tubes supplied with 1ml of LB medium (1lt: 10gr tryptone, 5gr yeast extract, 10gr NaCl, pH 7.0), and incubation occurs at a 37°C shaking incubator for 1hr. The culture is centrifuged at 11000g for 1 minute, most of the supernatant (~800ul) is removed, and the pellet is resuspented to in the remaining volume. Finally cells are plated on petri dishes with LB medium, agar (12gr/lt of LB) and the appropriate selection antibiotics (here: Ampicillin 100ug/ml, Gentamycin 7ug/ml). Cells are allowed to grow colonies in a 37°C incubator, overnight.

The next day, colonies that originate from cells which have acquired the desired plasmid, have grown in the LB-agar plate, as they are antibiotic resistant. Single colonies are selected and are picked from the plate using a sterile pipette tip, and are transferred in a tube with 3ml LB and appropriate antibiotics. They are allowed to grow in a 37°C shaking incubator overnight. A small volume of the culture (~500ul) is used to create 15% glycerol stocks, for long term storage at -80°C, while 100-150ul are inoculated in 100ml LB (1/1000 starter culture dilution) with antibiotics, and are once again allowed to grow overnight. The next day plasmids are isolated and purified using the midi-prep kit by Macherey-Nagel (Germany):

1. Pellet the cells by centrifugation at 6,000 x g for 20 minutes at 4 °C and discard the supernatant completely.

2. Resuspend the cell pellet completely in 8 ml Resuspension Buffer RES + RNase A by pipetting the cells up and down or vortexing the cells.

3. Add 8 ml Lysis Buffer LYS to the suspension. Mix gently by inverting the tube 5 times. Incubate the mixture at room temperature (18–25 °C) for 5 minutes.

4. Equilibrate a NucleoBond® Xtra Column together with the inserted column filter 12 ml with Equilibration Buffer EQU. Apply the buffer onto the rim of the column filter Allow the column to empty by gravity flow.

5. Add 8 ml Neutralization Buffer NEU to the suspension and immediately mix the lysate gently by inverting the tube until blue samples turns colorless.

6. Centrifuge at 6,000 x g for 15 minutes to clarify the lysate. Aspirate supernatant carefully and load it on the column. Allow the column to empty by gravity flow.

7. Wash the NucleoBond® Xtra Column Filter and NucleoBond® Xtra Column with 5 ml Equilibration Buffer EQU.

8. Discard NucleoBond® Xtra Column Filter by turning the column upside down.

9. Wash the NucleoBond® Xtra Column with 8 ml Wash Buffer WASH.

10. Preheat Buffer ELU to 50 °C. Elute the plasmid DNA with 5 ml Elution Buffer ELU. Collect the eluate in a 15 ml tube.

11. Freeze isopropanol at -20°C. Add 3.5 ml isopropanol to precipitate the eluted plasmid DNA. Vortex thoroughly! Centrifuge at 15,000 x g for 30 minutes at 4 °C. Carefully discard the supernatant.

12. Add 2 ml room-temperature 70 % ethanol to the pellet.
Centrifuge at 15,000 x g for 5 minutes at room temperature. Carefully remove ethanol completely from the tube with a pipette tip. Allow the pellet to dry at room temperature for 10–15 minutes.

13. Dissolve the DNA pellet in an appropriate volume (usually 200-400ul) of sterile H_2O. DNA concentration and purity are measured at nanodrop and plasmid DNA is stored at -20°C.

Recombinant bacmid generation

When the desired amount of pFastBacDual plasmid is obtained, it is used for transfection of FBT E.coli strains. FBT bacteria are processed in a way that apart from their genomic DNA, they also contain a helper plasmid carrying sequences coding for trasposases and tetracyclin resistance, and a large (>135kb) bacmid DNA that

essentially comprises Baculovirus genomic DNA and also bares a gene for kanamycin resistance and a lacZ gene located between two sites of transposition elements. To make FBT competent cells, we follow a quick protocol:

1. Inoculate a fresh starter 3ml-LB FBT culture (overnight at 27°C).
2. The next day, inoculate 30-40ul of culture in 1.5ml LB*, and allow it to grow for 3-4 hours at 27°C. In the meanwhile, prepare ice-cold sterile ddH$_2$O.
3. Pellet the cells by centrifugation at 11,000 x g, at 2°C for 1 minute. Discard supernatant. Resuspend pellet in 1ml ice cold steride ddH$_2$O.
4. Repeat step 3 x 3 times.
5. After the last centrifugation, discard most of the ddH$_2$O volume, and leave 20-30ul in which resuspent the cell pellet.
FBT cells are ready to use-only for electroporation.

After electroporation with pFastBacDual, FBT cells are plated on petri dishes supplied with LB, agar, appropriate antibiotics (100ug/ml ampicillin, 50ug/ml kanamycin, 7ug/ml gentamycin and 10ug/ml tetracyclin), X-gal (100ug/ml) and IPTG (40ug/ml). Selection of the desired colonies is based on the discrimination between blue and white colonies. If transposition of cDNA of interest is successfully accomplished on bacmid, lacZ gene must have been disrupted thus producing only white colonies in the presence of X-gal and IPTG. Selected colonies are grown and their bacmid DNA is isolated by midi prep, as previously described.

pFastBac*GLUD1* and pFastBac*GLUD2* vectors construction

In order to ensure similar conditions of transfection, we then constructed pFastBac vectors, and respective bacmids, so as to express single cDNAs (*GLUD1* and *GLUD2* separately). To achieve that, we cut off from pFastBacDual each cDNA with suitable restriction enzymes that surround it. We specifically used XhoI-KpnI to cut off *GLUD2* and create a pFastBacGLUD1 vector, and EcoRI-PstI to cut off *GLUD1* and create a pFastBacGLUD2 vector. For each double digestion, two extra single digestions were performed in order to ensure that the restriction sites are single cutters, and digestions will not interrupt any other sequence within the construct. Digestion reactions are shown below, and they took place at 37°C for 2 hours.

	EcoRI/PstI digestion	EcoRI digestion	PstI digestion	XhoI/KpnI digestion	XhoI digestion	PstI digestion
BSA 10X	8ul	2ul	2ul	8ul	2ul	2ul
Neb3 buffer	8ul	2ul	2ul	-	-	-
Neb1 buffer	-	-	-	8ul	2ul	2ul
EcoRI	2ul	1ul	-	-	-	-
PstI	2ul	-	1ul	-	-	-
XhoI	-	-	-	2ul	1ul	-
KpnI	-	-	-	2ul	-	1ul
pFastBacDual/	1ul	1ul	1ul	1ul	1ul	1ul
GLUD1GLUD2	(1ug/ul)	(250ng/ul)	(250ng/ul)	(1ug/ul)	(250ng/ul)	(250ng/ul)
ddH$_2$O	55ul	14ul	14ul	55ul	14ul	14ul
Final Volume	80ul	20ul	20ul	80ul	20ul	20ul

Following successful double digestions, the linearized vectors, containing each cDNA separately, were cleaned up by PCR clean-up kit Macherey-Nagel (as described earlier). DNA fragments with 5' overhangs are blunted by filling in a recessed 3' terminus with DNA polymerase in the presence of dNTPs. The reaction takes place at room temperature for 30 minutes.

dNTPs	3ul
Blunt buffer	3ul
Blunting enzyme (T$_4$ DNA polymerase)	1ul
pFastBacGlud1 or pFastBacGlud2	~20ul (from digestion clean up)
ddH$_2$O	3ul
Final Volume	30ul

Immediately after blunting, we proceed to ligation of the resulting linearized-blunt ended vectors, to generate circular and thus functional recombinant molecules. DNA ligases catalyze the formation of a phosphodiester bond between the 3' hydroxyl and 5' phosphate of adjacent DNA residues (with either blunt or cohesive ends). Ligation takes place overnight at 16°C.

T$_4$ ligase buffer	2ul
T$_4$ ligase	1ul
pFastBacGlud1 or pFastBacGlud2	15ul (from blunting)
ddH$_2$O	2ul
Final Volume	20ul

Ligation reaction is cleaned up by PCR clean-up kit of Macherey-Nagel, and is ultimately used to transform DH10b cells. Plasmid DNA is extracted from selected colonies by mini-prep kit of Macherey-Nagel, for further evaluation prior usage:

1. Harvest bacterial cells pellets by centrifuging the culture at 11,000 x g for 30 seconds. Discard supernatant.

2. For cell lysis, add 250 ul Buffer A1 and resuspend pellet. Then add 250 ul Buffer A2, invert tubes 6-8 times. Incubate at RT for no more than 5 minutes. Finally, add 300 ul Buffer A3.

3. Centrifuge lysate at 11,000 x g, for 5 minutes, for clarification of the lysate. Aspirate supernatant carefully and discard the pellet.

4. Load supernatant on a nucleospin DNA binding column, centrifuge at 11000 x g for 30 seconds. Discard flow through.

5. Add 500 ul Buffer AW and centrifuge at 11,000 x g, for 30 seconds. Discard flow through.

6. Add 500 ul Buffer A4 and centrifuge at 11,000 x g, for 30 seconds. Discard flow through.

7. Dry nucleopsin column by an additional centrifugation at 11,000 x g, for 1 minute.

6. Elute DNA by adding 50 ul Buffer AE, incubating at 70°C for 2 minutes and centrifuge at 14,000 x g for 1 minute. Transfer the plasmid DNA-containing flow through in clean tubes and store at -20°C.

Plasmid DNA's concentration and purity is estimated by nanodrop. Digestion tests, employing restriction enzymes for sites surrounding the specific insert (EcoRI-PstI for *GLUD1*, and XhoI-KpnI for *GLUD2*), are performed in order to discriminate true from false positive colonies. Once confirmed as positive, plasmid DNA is sent for sequencing at Macrogen (Netherlands) along with insert specific sites of primers. The plasmids are subsequently amplified by midi-prep and are used to transfect FBT cultures and respective *GLUD1*- and *GLUD2*- bacmids.

Primer	Sequence	Tm
Glud2_XhoI_F	GCCGCGCTCGAGATGTAC	67.2
Glud2_KpnI_R	CCATGATCCATGGTACCCTATGT	65.4
Glud1_EcoRI_F	GTGGCCGAATTCATGTAC	58.9
Glud1_PstI_R	TGATCCATCTGCAGCTAGT	58.5

3. PROTEIN PURIFICATION

According to standard protocols used in our laboratory, GDH purification is a four-step procedure including two ammonium sulfate precipitation cuts, hydrophobic interaction chromatography and, finally, hydroxyapatite chromatography [6]. Ammonium sulfate precipitations provide separation of the desired cell lysate fraction from other organelles and membranes of the cell. Specifically, the supernatant of the cell lysate is subjected to a 30% ammonium sulfate precipitation and the new supernatant obtained is subjected to a 65% ammonium sulfate precipitation. Finally, the pellet from the last cut is resuspended in a 15% ammonium sulfate solution (in Tris-HCl, pH 6).
The first chromatography step performed uses phenyl-sepharose which displays hydrophobic interaction with the proteins present in the cell extracts. For maximum performance, phenyl-sepharose is always cleaned and degassed before use. Typically, a 15ml chromatography column is used that is almost fully packed with phenyl-sepharose. The column is pre-equilibrated with a 15% ammonium sulfate solution before loading the sample. Elution is performed by a 15% ammonium sulfate solution-90% ethylene-glycol solution gradient, provided by a gradient mixer. Verification of protein-containing fractions is then performed by spectrophotometric measurement of the enzyme reaction.

The desired fractions from hydrophobic interaction chromatography are pooled together and dialyzed against 200mM KCl solution using a dialysis membrane with MWCO 7000. The post-dialysis sample is then subjected to hydroxyapatite chromatography (usually ~5ml hydroxyapatite in sodium phosphate pH 6.8 buffer, packed in a small column). The column is equilibrated with 50mM sodium phosphate pH 6.8, before sample loading. The enzymes are finally eluted with a 50mM sodium phosphate pH 6.8-400mM sodium phosphate pH 6.8 gradient. Verification of protein-containing fractions is performed as in previous steps, using enzymatic methods. The desired fractions containing the purified protein are once again pooled into one, which is then used for sample concentration.

4. ENZYMATIC ASSAYS

To determine the enzymatic properties of GDH isoenzymes a series of enzymatic assays were performed initally on crude cell extracts and extensively on purified proteins. The enzyme reactions were performed under varying concentrations of the studied substrate or allosteric modifier maintaining the concentrations of other reaction agents stable.

Enzymatic assays of human GDHs were performed spectrophotometrically at 340 nm in the reductive amination direction (Colon et al. 1986). The method is based on reduction of the absorbance of NADPH (with absorption spectrum top at 340nm), as a result of its concentration reduction, during the reaction. The reaction rate was measured as change in absorbance per unit of time (ratio dA340nm/dt), normally for 30 seconds. The standard reaction mixture of 1 ml final volume, contained 50 mM triethanolamine-HCl buffer pH 8, 100 mM ammonium acetate, 100 uM NADPH and 2.6 mM EDTA. Enzyme reaction is initiated with the addition of α-ketoglutarate to obtain a final concentration of 10 mM. Where not otherwise indicated, reactions were performed at 25°C. For maximal activity, ADP is added in the reaction at 1 mM, since hGDH2 shows very little activity in the absence of ADP. Different concentration of ADP are used in cases where the focus is on the basal behavior of the enzymes. In all kinetic studies, the reference point for enzymes' concentration was that at which the reaction rate, in the presence of 1 mM ADP was approximately 0.1 units/minute. For hGDH1, hGDH2 and hGDH1/hGDH2 possible hetero-hexamer, it was assumed that the resulting reaction rate was the result of a single enzyme unit kinetics. In contrast, to achieve the desired reaction rate for hGDH1+hGDH2 in vivo mix, we combined separate purified enzyme preparations at such quantities that each one conferred 50% of maximal activity.

Basal activity

For basal activity measurement purified enzyme preparations were assayed in the absence of allosteric regulators, using such amount of enzymes that the reaction rate in the presence of 1 mM ADP is approximately 0.1 units/minute. Basal activity was expressed as percentage of the maximum (basal/maximal), as measured in the presence of 1 mM ADP. Due to artefacts caused by low temperatures during the

performance of these measurements, we switched the reaction temperature to 37°C by preheating TRA buffer before use.

GTP inhibition

The study of GTP inhibition on recombinant enzymes was possible by adding, in the reaction mix, GTP in various concentrations and such amount of enzyme that the reaction rate in the absence of GTP was approximately 0.1. To compare the inhibition patterns among different enzyme preparations, Hill coefficient (h) and IC_{50} index are estimated. The former refers to the degree of cooperativity of GDH subunits to GTP whereas the latter refers to the GTP concentration at which reaction speed is Vmax/2 (Vmax is the initial reaction velocity). $IC_{50} \pm SE$ was calculated from the graphic representations of GTP inhibition, using Origin. Hill coefficient (h) for collaborative inhibition of GTP was based on the Hill equation of Hill: $dA340nm/min = [GTP]^h / (K+[GTP]^h)$.

Activation by L-leucine

To study the activation of recombinant enzymes by L-leucine, gradually elevating concentrations of L-leucine (0-6 mM) were added in the reaction mix, and enough enzyme so that reaction rate as measured under maximal activity conditions was about 0.1. Moreover, to study the cooperativity effect of ADP with L-leucine, various concentrations of the amino acid (0-9 mM) were added to the reaction mixture containing different constant concentrations of ADP (0, 0.025, 0.05 mM).

Divalent cations' inhibition

For the kinetic studies with Mn, 0.25–3mM of $MnCl_2$ (M3634, Sigma, St.Louis, MO, USA) was added to the reaction mixture. Similar concentrations of $CaCl_2$ (C5080, Sigma, St.Louis, MO, USA) and $MgCl_2$ (#5833, Merck, Darmstadt, Germany) were used for studying the effect of Ca and Mg, respectively. The reaction mixture, of 1ml final volume, contained 50mM triethanolamine pH8, 100mM ammonium acetate and 100µM NADPH, while it was lacking EDTA. As a control, EDTA was added in the reaction buffer (at a concentration of 2.6mM) and the Mn kinetic studies were repeated for both iso-enzymes.

70

Thermal lability

For thermal inactivation studies purified enzyme preparations were heated at 47.5°C on a heating block, and small quantities were removed at certain time points (every 20 minutes) in order to be measured immediately, in the presence of 1mM ADP.

DES inhibition

The inhibitory effect of diethylstilbestrol was studied by adding to the reaction mix varying concentrations of this steroid hormone in the presence of 1mM ADP, while keeping the concentrations of the remaining components constant. Amount of purified enzymes was such that the initial reaction rate in the absence of inhibitor was about 0.1. Since DES is soluble in ethylen glycol, assays using only the solvent served as a negative control.

Buffer composition and pH range

In order to study the optimal functioning conditions of the different enzymes, we replaced the standard buffer TRA 50mM pH 8 with buffers of alternative characteristics. Specifically, we tried different concentrations of Tris-HCl and NaHPO4 buffers while maintaining pH at 8, to examine under which conditions ours enzymes and particularly the possible hetero-hexamer was more stable. To decipher which are the optimal functioning pH conditions, we used different TRA pHs ranging from 6-9 to test the maximal GDH activities (in the presence of 1mM ADP), and $NaHPO_4$ pHs ranging from 7-8 to test the basal activities.

5. STATISTICAL ANALYSIS

Diagrams of different kinetic studies were available from Origin 6.0. Statistical analysis of the differences observed in the enzymatic assays was performed by student t-test, in order to compare the values obtained from different enzymes. Statistical significance was assumed to be any $p < 0.05$.

6. PROTEIN ELECTROPHORESIS

Polyacrylamide gel electrophoresis is a widely used technique which exploits the difference in electrophoretic mobility of a protein mix, to separate and study a molecule of interest. It could be used to study either subunits of a denatured protein (SDS PAGE) or a protein in its native form (BLUE NATIVE PAGE). SDS PAGE is often used in combination with Western blot analyses, in order to precisely identify the particular molecule of interest within the complex protein cocktail resulting from a cell lysate. For the purposes of our study we employed different electrophoresis methods to describe our proteins, as described below.

SDS PAGE (denaturing polyacrylamide gel electrophoresis)

In order to characterize and compare the molecular weight and electrophoretic behavior of hGDHs, the different enzyme preparations were handled according standard protocols and were loaded on two-phase1,5mm-thick well polyacrylamide gels which were prepared as follows

RESOLVING GEL 10%	STACKING GEL 4%
ddH2O 4.1 ml	ddH2O 6.1 ml
30% bis/acrylamide 3.3 ml	30% bis/acrylamide 1.3 ml
gel buffer *1.5 Tris-HCl ph 8.8 2.5 ml	gel buffer *0.5 Tris-HCl ph 6.8 2.5 ml
10% SDS 100 ul	10% SDS 100 ul
10% APS 50 ul	10% APS 50 ul
TEMED 5 ul	TEMED 10 ul

After determining the protein sample volume, 4X loading dye with 4% mercaptoethanol and 1X loading dye up to 40µl are added. The samples are heated at 95 C for 4-5 minutes and subsequently loaded on the gel, together with a protein ladder. Approximately, 1 L of 1X running buffer (10X running buffer: 30.3 gr Tris base, 144 gr glycine, 10 gr SDS, pH 8.3) is added in the electrophoretic device, and the samples are electrophoresed for 30 minutes at 100 V (through the stacking gel) and for another 1 hour and 45 minutes at 150 V. After that, the separating gel is removed from the device and is processed according the respective protocols of either blues silver staining or western blot.

Blue silver staining

In order to visualize the protein mixture that has run on a gel, and also to evaluate the clarity of our sample or even to relatively quantify the amount of a protein, blue silver staining is a suitable and sensitive method to use. Purified protein preparations were used for this protocol. The polyacrylamide gels are processed for 30-60 minutes with a 30%-methanol, 10% acetic acid solution, and are subsequently washed several times with ddH$_2$O. Then, they are stained O/N with a 0,12% Coomassie Blue G-250 solution (0.12% dye, 10% ammonium sulfate, 10% phosphoric acid , 20% methanol), and after several ddH$_2$O washes the proteins become visible.

Western Blot

Usually whole cell lysates were used for this procedure. After electrophoresis, the proteins are transferred on a nitrocellulose membrane. Specifically, the separating gel I placed in a so called "sandwich" consisting of a sponge, 3 pieces of whatman filter paper, the gel, a nitrocellulose (or other if differently specified) membrane, 3 more pieces of filter paper and a last sponge. The "sandwich" is put in the respective transfer device, which is filled with ice cold transfer buffer (20% MethOH, 10% 10X running buffer), and is run for 1 hour at 310 mA.

The nonspecific sites on the membrane are blocked by a 5% milk solution in 1x PBS-tween (10x PBS: 1.37 M NaCl, 27mM KCl, 100 mM Na$_2$HPO$_4$, 18mM KH$_2$PO$_4$), for 1 hour at room temperature, before it is treated with the primary antibody, (diluted in 5% milk in PBS-tween) which in our case is the anti-GDH (1:500) nonspecific antibody (polyclonal, ABNOVA, Taiwan) that recognizes both human GDHs and originates from mouse. The membrane is incubated with the primary antibody O/N at 4 C on a shaker. The secondary antibody is anti-mouse (used in dilution 1:5000, in 5% milk-PBS tween) which recognizes all proteins that are generated in mice, namely only our primary antibody here, and which is HRP (horseradish peroxidase) conjugated. Incubation with the secondary antibody lasts 1 hour at room temperature. All the nonspecific bindings are washed away after every antibody incubation step with PBS-tween buffer treatment. The final step for protein visualization is the incubation of the membrane with ECL kit which is essentially a 1:1 mixture of peroxide (HRP's substrate) and a signal enhancer solution, and the results are developed on a photograph film.

<u>Blue Native-PAGE</u>

Non-denaturing gels are used to study proteins their folded state. Thus, the electrophoretic mobility depends on both their molecular weight and their native shape. The polyacrylamide gels are characterized by gradient concentration, with thicker gel layers placed on bottom. Gradient gels are made by mixing different acrylamide concentration solutions using a gel gradient mixer, while the stacking gel is made separately and added on top. For hGDHs electrophoresis, 1,5mm midi (and maxi) polyacrylamide gels of 5-12% concentration, were used and were prepared as follows

<u>RESOLVING GEL 5%</u>
ddH2O 6.6 ml
30% bis/acrylamide 3.375 ml
3x gel buffer 5.025 ml
*1.5M 6-aminohexanoic acid, 75mM imidazole, ph 7
10% APS 50 ul
TEMED 5 ul

<u>RESOLVING GEL 12%</u>
ddH2O 1.125 ml
30% bis/acrylamide 6 ml
3x gel buffer 5.025 ml
87% glycerol 2.85 ml
10% APS 50 ul
TEMED 5 ul

<u>STACKING GEL</u>
ddH2O 3.33 ml
30% bis/acrylamide 0.7 ml
3x gel buffer ml
10% APS 50 ul
TEMED 5 ul

Purified enzyme preparations' volumes were estimated to represent at least 1 ng of protein, and 10x and 1x sample buffers are added to a final desirable volume. The gel is placed on the electrophoretic apparatus, samples and appropriate ladder are loaded on it and anode (25mM imidazole, ph 7) and cathode (50mM Tricine, 7,5mM imidazole, 0.02% Coomassie G-250, ph 7) running buffers fill the respective lower and upper tanks. Electrophoresis lasts 2.5 hours or even O/N, at 300V, and subsequently the gel is removed from the apparatus and is destained in a 40% methanol, 10% acetic acid solution. The proteins become visible after several hours.

7. CO-IMMUNOPRECIPITATION EXPERIMENTS

For the co-immunoprecipitation experiments anti-hGDH2 specific antibody was employed, which originated from rabbit, in combination with protein A sepharose beads (Protein A-Sepharose from Staphylococcus aureus, P3391-250MG, Sigma). Initially a pre-clearing step is performed on crude Sf21 lysates, with protein A sepharose alone, in order to remove any nonspecific protein binding on the sepharose beads. Subsequently, the samples are incubated with the specific antibody and finally the protein A beads is added in the mixture. Protein A-Sepharose has the capacity to link with antibodies and the binding occurs between Protein A and Fc portion of the IgG molecule leaving antigen specific sites free. Thus the complex that is generated consists of protein A sepharose beads-antibody-protein of interest. Since sepharose beads have the tendency to precipitate, they also provoke the proteins to precipitate along. Several centrifugations for washing away of the other cell lysate components follow. To extract the samples from the beads an SDS loading buffer is added to the mixture before it is boiled for 5 minutes and centrifuged once again. The resulting supernatant contains the proteins which are specifically precipitated after the IP procedure, and which are visualized by western blotting using a non-specific anti-GDH antibody (polyclonal, ABNOVA, Taiwan) , originating from mouse. It is critical to use antibodies that have been produced in different animals, otherwise the secondary antibody for Western blot will reveal immunoglobulins which are also contained in the sample from the Co-IP step, apart from proteins of interest.

Sepharose beads' washing before use

Sepharose beads should be washed in Lysis Buffer (without detergent) prior to use. Lysis Buffer is the same one used for cell lysis (described earlier).
1. Aspirate 1ml sepharose beads from stock (50%)
2. Centrifuge at 14,000 rpm for 1 minute. Discard supernatant.
3. Dilute beads in 1ml Lysis Buffer without detergent.
4. Repeat steps 2 and 3 two more times.
5. Dilute the sepharose beads in 1ml Lysis Buffer without detergent. Store at 4ºC.

<u>Sample preclearing</u>

The samples should be precleared before Co-IP, so that any non specific binding could be eliminated.

1. Add 30ul sepharose beads per 1ml of sample (bead amount should be >25ul in order for the pellet to be visible).

2. Incubate for >2hours at 4°C, on a rotating machine.

3. Centrifuge at 14,000 rpm for 1 minute at 4°C.

4. Transfer supernatant to a fresh tube.

<u>Co-immunoprecipitation</u>

1. Add 5ul anti-GDH2 antibody in the precleared sample.

2. Incubate overnight at 4°C, on a rotating machine.

3. The following day add 30ul sepharose beads in the sample.

4. Incubate at 4°C, on a rotating machine for 2-3 hours

5. Centrifuge at 14,000 rpm, 4°C for 2 minutes.

6. Aspirate carefully and discard supernatant. Dilute pellet in 1ml Triton 1% Lysis Buffer (with protease inhibitors). Mix by inverting the tubes several times.

7. Repeat steps 5 and 6 two more times.

8. Centrifuge at 14,000 rpm, 4°C for 2 minutes.

9. Aspirate carefully and discard supernatant. Dilute pellet in 1ml Lysis Buffer (without Triton – it can reduce SDS power in the loading buffer). Mix by inverting the tubes several times.

10. Centrifuge at 14,000 rpm, 4°C for 2 minutes.

11. Aspirate carefully and discard supernatant. Leave a small amount of supernatant.

12. Centrifuge at 14,000 rpm, 4°C for 30 seconds.

13. Aspirate carefully and discard supernatant.

14. To extract the proteins from the beads, add ~40ul 2X SDS loading buffer, and boil at 100°C for 5 minutes.

15. Centrifuge at 14,000 rpm for 5 minutes. Load the whole supernatant on a 10% acrylamide gel.

8. GTP-AFFINITY CHROMATOGRAPHY

Affinity chromatography relies on the principle that a molecule of interest is characterized by a defined property, which differentiates it from the heterogeneous group of molecules in a solution and which can be exploited during an affinity purification process. For our project purposes, γ-Amino-octyl-GTP prepacked columns (AC-106, Jena Bioscience) were used, which are essentially composed of a stationary phase of agarose conjugated with GTP. The particular molecule is employed because, as discussed in the introduction section, the two isoenzymes hGDH1 and hGDH2 differ significantly in their regulation by GTP (Zaganas and Plaitakis 2002) and they can thus be separated according to this feature. Specifically, hGDH1 is particularly sensitive to inhibition by GTP while hGDH2 is rather resistant, a difference that reflects their affinity with the nucleotide. Thus, hGDH1 is expected to bind on the GTP resin and be released by a gradually increasing ionic strength elution process, while hGDH2 is expected to be eluted on the flow through.

Before our samples are submitted in GTP chromatography, they are processed by 2 cuts of ammonium sulfate precipitation and a phenyl-sepharose chromatography, as described above, in order to become semi-purified and to reduce nonspecific bindings and false results, since a variety of proteins have also affinity for GTP. 60-80 enzyme units were used for affinity chromatography, after spectrophotometrical estimation. In vitro mixture of hGDH1 and hGDH2 contained a 1:1 ratio of each enzyme. The semi-purified protein sample is dialyzed against a buffer that consists of 50mM KCl, 100mM Tris-HCl, 1mM EDTA (pH 7.15). GTP column is equilibrated with 3 volumes of the same buffer, and then the sample is loaded while the fractions collection starts immediately. The bound proteins are finally eluted with a 50mM KCl pH 7.15-400mM KCl pH 7.15 gradient, and they are identified by the enzymatic assay described previously.

The resin is finally regenerated with 2–3 column volumes of alternating high pH (0.1 M Tris-HCl + 0.5 M NaCl, pH 8.5) and low pH (0.1 M sodium acetate + 0.5 M NaCl, pH 6.0) buffers. This procedure should is repeated 3 times followed by re-equilibration. Short-term storage of GTP-agarose is allowed in 20% ethanol solution at 4°C.

9. PROTEIN CONCENTRATION

For crystallography and SEC/MALS purposes the purified protein needs to be highly concentrated. Specifically, crystallography trials require at least 10mg/ml and SEC/MALS 5mg/ml of pure protein. Thus, the dilute protein pool is subjected to repeated centrifugations at 5000 rpm into specific protein concentrators supplied with ultrafiltration membrane with separating capacity of a maximum of 100KDa (in specific, centrifugal filter units with ultracell regenerated cellulose membrane and 50KDa or 100KDa cut off, able to provide both fast spin times and ultra-high recoveries). In the process of purification and concentration of the hGDH1 and hGDH2 proteins, it is safe to use either 50KDa or 100KDa cut off membranes since the enzyme's molecular weight as a hexamer is 300KDa.

10. SIZE EXCLUSION CHROMATOGRAPHY ON LINE WITH MULTI ANGLE LIGHT SCATTERING (SEC/MALS)

In the case of hGDH2, the size exclusion chromatography on line with multi-angle light scattering is used to study the formation of multimers and the degradation products of the enzyme under different pH. The purified enzymes are dialyzed overnight against 100mM $NaHPO_4$ buffers of different pH, in the range of 6-8. Then they are concentrated down to 5mg/ml (total protein: 200microgr) injected in the SEC system which is previously equilibrated with at least 2 column volumes the same buffer. As the sample passes through the column its differently sized conformations are separated and as they pass from MALS, their MW, size and quantity are characterized via the light scattering, UV and RI detectors. Since the separated products which can be collected, there is the opportunity to study the possible activity of conformations other than the hexameric. These studies are performed using a Shimadzu HPLC system with an isocratic pump connected via a size exclusion column Superdex 200HR10/30 column (Pharmacia), of 24ml, to a Multi angle Light Scattering instrument (DAWN HELEOSII, Wyatt). Software (ASTRA) is available from Wyatt for the data analysis of the LS, QELS in connection with the UV and RI which are detected by the HPLC detectors. The size exclusion chromatography column we are currently using is a Superdex 200 column and has an optimum separation range for globular proteins between 10KDa and 600KDa.

11. X-RAY CRYSTALLOGRAPHY (in collaboration with Dr. Kokkinidis group)

The crystallization of an enzyme such as hGDH2 is a very sensitive process that depends, among other factors, on the homogeneity of the material. Using a protein crystallization robot (OrynxNano by Douglas instruments), crystallizing GDH2 was succeeded in at least ten different conditions (crystallization kits JBScreen JCSG++ HTS, Structure Screen 1,2 MD1-30, 1-31, 1-32, 136 and MIDAS). One of the conditions was chosen to upscale the crystallization experiment in larger volumes. Selected crystallization conditions for hGDH2 were screened using the hanging-drop vapor-diffusion method in 24-well Linbro cell-culture plates. The drops were made up of 2 ul protein solution of 9.7 mg/ml, mixed with an equal volume of reservoir solution and were equilibrated against 1000 ul reservoir solution at 291 K. Initial crystallization screening was performed using commercially available crystallization kits including Structure Screen 1 and 2, Grid screen Ammonium Sulfate, Grid screen MPD, Grid screen PEG 6000, GBS screen 3, 6, 7, 8, 9, 10, Grid screen PEG ion, MEB FAK and Natrix screen, from Molecular Dimensions. Data quality crystals were obtained with 8% PEG 8000, 15% MPD, 0.4M NaCl and 0.1M phosphate buffer pH 7.

12. GENETIC ANALYSES OF GLUD1 AND GLUD2 GENES

In the context of a parallel large genetic study of Thalis-MNSAD program, we have collected DNA samples from 385 participants (patients with dementia, mild cognitive impairment and cognitively normal controls), after informed consent. All these subjects have been thoroughly characterized, through structured questionnaires, neuropsychological evaluations and biomarker (IL6, CRP, TNFα and cortisol) measurements. Subsequently, we have performed whole exome sequencing (WES) on and partially analyzed the results of this WES for 100 patients with dementia, 20 with MCI and 81 cognitively normal controls. Specifically, we have analyzed and interpreted coding regions (exons) of all the genes of the human genome (97% CCDS, >19,000 reference genes in RefSeq) using targeted amplification and sequencing of exons using the Ion Torrent Technology.

This has allowed us to create a large database that includes extensive high quality phenotypic and genotypic data that we are in the process of analyzing.

The participants in for the genetic study were selected from the Cretan Aging Cohort, an initial sample of 3,140 community-dwelling adults, aged 60-100 years, who were recruited from a representative set of Primary Health Care (PHC) facilities in the district of Heraklion, Crete, Greece (Zaganas et al. in preparation). Consenting individuals were invited to attend a structured interview based on a detailed questionnaire, that included the Mini Mental Status Examination (MMSE) and questions on demographics (i.e. age, gender, marital status, education, place of residence), current physical and mental health problems and medication use. On the basis of the MMSE score, a universal cutoff of 23/24 points was used for referral of patients for further evaluation. In the second phase of the study, those participants showing potential cognitive impairment as defined by a MMSE score of <24 (n=636) were referred for a thorough neuropsychiatric and neuropsychological assessment to establish a final diagnosis. Among those with MMSE >24, a sub- group of 181 participants (matched for place of residence with the MMSE <24 group) were also invited for the same evaluation. This second phase of the study also employed detailed questionnaires in the context of a semi-structured interview to assess the medical and other determinants of health status for each individual in detail. Neuropsychological assessment was performed by trained neuropsychologists, using a battery of validated tests that evaluated among others, memory, visuoconstructive ability, speech, visuomotor processing, attention, executive functions, depressive symptomatology and anxiety, quality of life, daily functional capacity and behavioral disturbances.

All information obtained through history, physical and mental status examination, neuropsychological examination, questionnaires, as well as all other additional data (imaging studies, laboratory results) available, was reviewed by a certified neurologist (I.Z.) and a neuropsychologist (A.S.) and consensus diagnoses were reached using published criteria and taking into account the reports from the clinicians that had examined the patients, as well as the neuropsychologists' reports. For the diagnosis of dementia and MCI, the DSM-IV criteria (Diagnostic and Statistical Manual of Mental Disorders, 4th edition, 1994) and the IWG (Winblad et al. 2004) criteria were used, respectively. Probable Alzheimer' disease (AD), vascular dementia (VaD), Lewy body dementia (LBD), behavioral variant frontotemporal dementia (FTD) and other types of frontotemporal dementia were diagnosed according to published criteria (Zaganas et al. in preparation).

<u>Family history information</u>

Among the 636 participants with a low MMSE score (<24) and the 2,504 with MMSE >24 points, 344 and 161, respectively, underwent detailed neuropsychiatric evaluation in the second phase of the study. As part of this assessment of these 405 participants, a detailed family history for dementia and other neuropsychiatric diseases was obtained both through the semistructured questionnaire described above and also in the context of a special second interview of the patient and/or his caregivers. The family history collected from each participant and their caregivers included the names, ages and, when dead, age and cause of death of up to 3rd degree relatives. The presence and age at onset of neuropsychiatric diseases (including dementia) was also recorded. On the basis of this information, detailed family trees were constructed using the software HaploPainter 1.043.

<u>Biological sample collection and DNA extraction</u>

For the genetic analyses, whole peripheral blood from consenting participants was collected in EDTA vacutainer tubes which were rushed on ice to the laboratory and stored at -20oC until DNA extraction. In total, blood was collected from 385 individuals (107 participants with dementia, 161 with MCI and 117 controls). Genomic DNA was extracted from 200µl of whole peripheral blood by processing with the QIAamp DNA Blood Mini kit, Qiagen (CA, USA). DNA concentration and purity were assessed spectrophotometrically at 260/280 nm. Each DNA sample was coded through unique identifiers, to ensure the anonymity of the participants and traceability of the sample, and was stored at -20oC for future analyses.

<u>Whole Exome Sequencing (WES)</u>

Out of these 385 individuals with blood sample available, 201 were selected to be characterized by WES in this study. From these 201 well-characterized individuals, 100 were dementia patients, with 95 (95.0%) of those being affected by AD. In addition, we included 81 individuals that were classified as cognitively normal controls and 20 individuals that were diagnosed with MCI. The geographic origin (place of residence) within Heraklion, Crete prefecture of the genotyped participants is shown in figure 19.
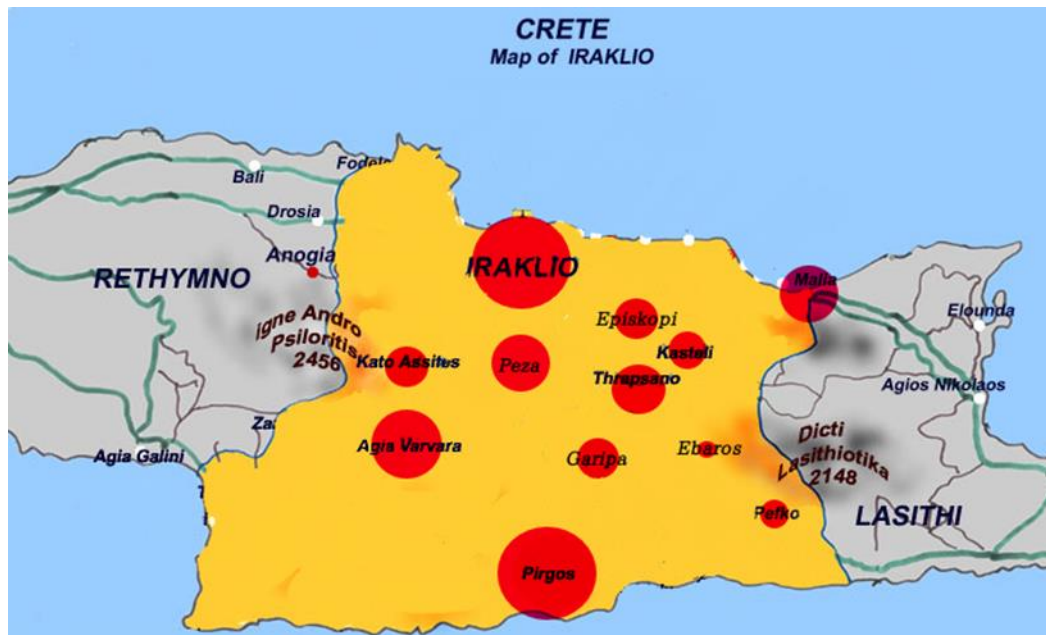
Figure 19: Geographic origin (place of residence) of genotyped Cretan Aging Cohort participants within Heraklion, Crete prefecture (n=201). Depicted on the map of Heraklion, Crete district are the places where participants included in the genetic substudy resided. The size of the cycle is proportional to the number of participants genotyped.

WES was performed at the Institute of Molecular Biology and Biotechnology (IMBB, FORTH) in collaboration with the team of Minotech Genomics Facility (Dr. D. Kafetzopoulos lab). WES sequencing reactions were performed with Ion Torrent technology in a Proton system (ThermoFisher Scientific, MA, USA) using a PI chip (Ion PI chip v3, 2 samples/chip). The process is outlined as follows:

Library preparation and template sequencing

100ng of genomic DNA extracted from each sample by the Neurology Lab team will be given to the specialized scientists at Minotech Genomics Facility, who will proceed with the determination of its quantity and quality using Qubit™ quantitation assay. The construction of libraries and barcoding will be performed using Ion AmpliseqTM Exome kit (ThermoFisher Scientific) and Ion XpressTM kit (ThermoFisher Scientific), respectively. The Ion AmpliSeq™ Exome technology provides a workflow that targets ~33 Mb of coding Exons in 12 primer pools (293,904 primers pairs -24,500-plex PCR) for highly specific enrichment of exons within the human genome. The total design coverage including padding and flanking regions is ~58 Mb. The technology enables high-efficiency enrichment, with more than 90% on-target bases and more than 90% bases covered at 20x. Unamplified libraries will be quantified and purified using qPCR

Ion Library Taqman quantitation kit and Agencourt AMPure XP reagent (ThermoFisher Scientific), respectively. Finally, sequencing reactions will be performed using Ion PI Hi-Q sequencing 200 kit following amplification of the corresponding libraries with Ion PI Hi-Q OT2 200 kit (Thermo Fisher Scientific).

<u>Variant calling and annotation</u>

Primary data analysis is performed with Torrent Suite™ Software that uses the Torrent Mapping Alignment Program (TMAP), a modified format of Burrows-Wheeler Aligner (BWA) algorithm for ION technology, assuring the successful base-calling and alignment of sequences to the designed regions of the human reference genome 19 (hg19). The output of sequence alignment is a binary format (.BAM file) of storing aligned sequences (.SAM file) containing the mapped reads with accompanied quality control metrics.

Detection of variants is performed with Torrent Variant Caller (TVC), a modified format of Genome Analysis Toolkit (GATK) optimized to exploit the underlying flow signal in the statistical model to evaluate variants in the sample. This plugin accepts as input the .BAM file generated by Torrent Suite Software and produces as output a list of Single and Multiple Nucleotide Polymorphisms (SNPs, MNPs) and Copy Number Variations (Insertions/Deletions) called in the sample. The output file, a tab-separated Variant Call Format file (.VCF), is produced by the application of appropriate filters/parameters in order to achieve best detection of variants (i.e. low stringency to minimize false negatives and germ-line settings optimized for high frequency variants) and the data metrics of the called variants (e.g. chromosomal coordinates, quality score, minimum coverage and strand bias).

<u>Validation</u>

Whole exome sequencing technologies, as all methods, are prone to false positive results concerning mainly *indel* mutations. This is due to their inability of amplifying correctly genomic regions which are located on the end of an amplicon or within GC rich stretches. Thereby, it is mandatory that before reporting a genetic alteration, regardless of whether it is novel or known, we ensure it is genuine, by targeted Sanger sequencing or other genotyping methods.

All variants in *APP, PSEN1, PSEN2, GLUD1, GLUD2* and *APOE* detected by WES and reported in this study were validated by Sanger sequencing. Specifically, primers sets were designed for each variant using Ensembl (http://www.ensembl.org/index.html), Primer3 (http://bioinfo.ut.ee/primer3-0.4.0/) and OligoEvaluator (http://www.oligoevaluator.com/OligoCalcServlet) and were ordered from Macrogen OligoSynthesis service (Korea). Specific sets of primers are shown at Table 1. Regions carrying the variants of interest were amplified by PCR and were cleaned up by Macherey-Nagel (Germany) PCR clean up and gel extraction kit. Finally, PCR products were sequenced by Macrogen Standard Sequencing service (Netherlands).

Table 1: Primer sets for WES results validation by Sanger sequencing in APP, PSEN1, PSEN2, APOE, GLUD1 and GLUD2 genes.

Variant	Primers (5'→3')
APP p.Glu686Gly	Forward: ATGTCCCCTGCATTTAAGAA
	Reverse: CATCATGGAAGCACACTGAT
APP p.Val375Ile	Forward: CAGTGTCTCATGGTGTTCTC
	Reverse: TTTGGCTTTCTGGAAATG
APP Asn195Asp	Forward: GCAGTGAGAAGAGTACCAACT
	Reverse: TCTGAGGCTGAACACAAA
PSEN1 p.Glu318Gly	Forward: TTTGTGTGGAGAAATGATGG
	Reverse: TGACCAAAGAAAGACGATAAAA
PSEN2 p.Arg29His	Forward: CAGGAAAGTGGAACAAGGTC
	Reverse: TCCTATGAAACCCTGCAGAT
PSEN2 p.Arg62His	Forward: AAAAATCCGTGCATTACAT
	Reverse: ATTCTTCTCTGTGTAGAAGCG
PSEN2 p.Cys391Arg	Forward: TTCTTTTTCCATTCTGTGC
	Reverse: CAGAGGGAAGAGAAGAAATG
APOE p.Gly195Asp	Forward: GGCACGGCTGTCCAAGGA
	Reverse: GGCACGGCTGTCCAAGGA
GLUD1 p.Asp341Gly	Forward: GACTCTTGCTGTCCTATACCAG
	Reverse: TGGTATGTGCAGTATGTGCC
GLUD2 p.Asp414Gly	Forward: ATGAAGGAAGCATCTTGGAG
	Reverse: TGTCAGGAGAGAAAGGGATT
GLUD2 p.Gly35Arg	Forward: AGTCTGAGAAAGCGCACC
	Reverse: TCCTTCACCAACTTGTCCTC

Specifically, for *APOE* genotyping PCR/RFLP was employed, as originally described by Kim et al. (2010). *APOE* alleles ε2, ε3, and ε4 which are separated by the presence of either arginine or cysteine at positions 130 and 176 of the respective apolipoprotein E. In more details, ε3 produces p.Cys130/Arg176 (c.388T, c.526T), ε4 is characterized by rs429358 and produces p.Arg130/Arg176 (c.388C, c.526T), and ε2 is characterized by rs7412 and produces p.Cys130/Cys176 (c.388T, c.526C).

25ul reaction volume PCRs were performed with:

100 ng purified genomic DNA
0.5 µM apoEf1 primer (5'-GGCACGGCTGTCCAAGGA-3')
0.5 µM apoEr1 (5'-CTCGCGGATGGCGCTGAG-3')
200 µM dNTPs
1 M betaine
2 mM MgCl$_2$
2.5 U Kapa Taq DNA polymerase
5X reaction buffer C

The amplification was initiated at 95◦C for 2 min, followed by 35 cycles of 95◦C for 30 s, 63◦C for 30 s, and 72◦C for 30 s, and then a final extension at 72◦C for 7 min. The resulting PCR products were treated with restriction enzyme HhaI, for 2 hours at 37ºC. The restriction fragments were identified with 13% polyacrylamide gel electrophoresis, run for 70 minutes at 120 volt, and 3X gel red (Gel Red Nucleic Acid 10,000X, Biotium, CA, USA) post-electrophoresis staining (~25ml per gel, overnight at RT). For 13% polyacrilimide gels we used:

5X TBE	2.4ml
30% bis/acr	5.2ml
dH$_2$O	4.4ml
10% APS	200ul
TEMED	10ul

For *GLUD2* Ser498Ala polymorphism (formerly known as Ser445Ala, where the N-53 leader peptide was not counted in the full length mature enzyme), we also employed a PCR/RFLP method which has been previously described by Plaitakis et al. (2010).

Specifically, the region containing the respective T1492G variant was amplified using:

100 ng purified genomic DNA
0.25 µM Klio5s primer (5'-TGAATGCTGGAGGAGTGACA-3')
0.25 µM Klio5as primer (5'-TGGATTGACTTGAGAATGG-3')
200 µM dNTPs
5% DMSO
1.25 mM $MgCl_2$
2.5 U Kapa Taq DNA polymerase
5X reaction buffer C,
in a final volume of 20ul.

The amplification was initiated at 95°C for 5 min, followed by 35 cycles of 95°C for 1 min, 56°C for 1 min, and 72°C for 1 min, and then a final extension at 72°C for 10 min. The resulting PCR products were treated with AciI restriction enzyme at 37°C, for 12 hours. Results were visualized by 1% agarose gel electrophoresis, run at 120 volt for 1 hour.

Especially for the extension of the Ser498Ala *GLUD2* variant genotyping, a second local cohort was used, that has been established through the Interreg "ΣΚΕΨΗ" research program (Simos et al. in preparation). This cohort consists of elders, also residents of the prefecture of Heraklion, Crete, who either responded to advertisements in local media inviting persons aged 50 years or older to be tested for "memory and other cognitive difficulties they may be experiencing" or were referred for neuropsychological testing by local physicians. Participants in this cohort were characterized and diagnosis was reached in a manner essentially identical to that described above for the Cretan Aging Cohort. In our study, 232 of these participants were genotyped for the Ser498Ala *GLUD2* variant.

Bioinformatics and Statistical Analysis

Further data analysis was performed either manually on the vcf files containing the raw sequencing data, using in-house created gene panels for dementia or by employing the Ingenuity Variant Analysis software, Qiagen (CA, USA; Fig. 20). Specifically, manual variant annotation was performed by integrating clinical information with published phenotypic data. In addition, we used phenotypic relevant gene panels, which were created in-house consulting public available databases [ClinVar, Ensembl

(GRCh37.p13) and OMIM]. Pathogenicity of the reported variants was also assessed using the Polyphen2 (http://genetics.bwh.harvard.edu/cgi-bin/ggi/ggi2.cgi) algorithm.
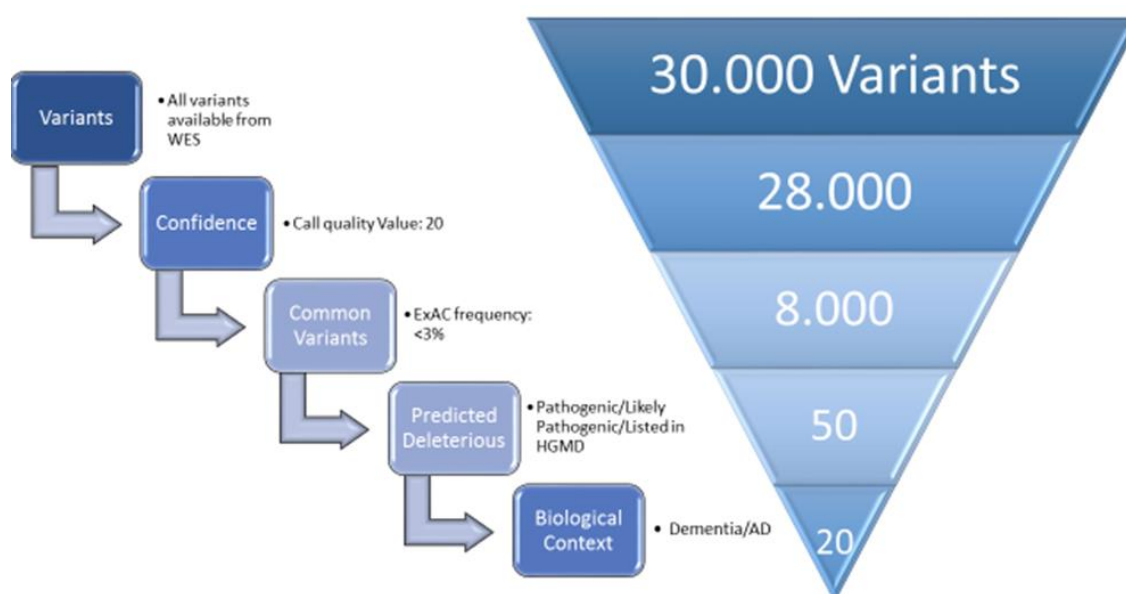
Figure 20: Variant identification pipeline based on IVA filters. Confidence Filter, set at minimum 20, allows filtering out variants of low quality. Common Variants filter, with a value of maximum 3%, excludes variants that are commonly observed in the population, according to ExaC browser (Exome Aggregation Consortium). Predicted Deleterious filter provides quick identification of variants classified as "pathogenic" or "likely pathogenic", according to ACMG criteria (© American College of Medical Genetics and Genomics; Richards C et al. 2015). Finally, biological context filter is designed to identify variants that have been associated (directly or indirectly) with the respective pathogenic condition.

Statistical analysis of *APOE* allelic distribution and *GLUD2* S498A variant among cases with dementia, MCI and controls, was performed by the χ^2 and Fisher's exact tests, using a significance level of p=0.05. Also, a t test was used to assess differences in age and education between participant groups.

1. THE TWO ISOFORMS hGDH1 AND hGDH2 CAN FORM HOMO- OR HETERO- HEXAMERS WHEN RECOMBINANTLY CO-EXPRESSED IN SF21 CELL CULTURES.

Following the sequence of questions described at the "aim" section of the present study, the first part of results concerns the investigation of whether the two glutamate dehydrogenases are able to create hetero-hexamers, when they are co-expressed in Sf21 cell cultures. This question was approached using two different techniques, which are both based on affinity relationships, in order to provide a more solid support to our findings. In our case, affinity relationships are the safest approach to study possible hetero-hexameric structures, because it is otherwise difficult to discriminate between hGDH1 and hGDH2, since the two isoenzymes share many common characteristics. Specifically, co-immunoprecipitation experiments using anti-hGDH2 specific antibody and affinity chromatography using a GTP-conjugated resin were applied on either crude or on semi-purified enzyme preparations originating from Sf21 transfected cultures. In order to study the existence of GDH hetero-hexamers, a fundamental assumption was made: in case these hetero-molecules exist, they will have to operate as a unit as opposed to a simple mixture of two different enzymes (hGDH1 + hGDH2), which should operate independently and maintain their unique properties. For this reason, particular attention was given to comparison of these two enzymatic preparations.
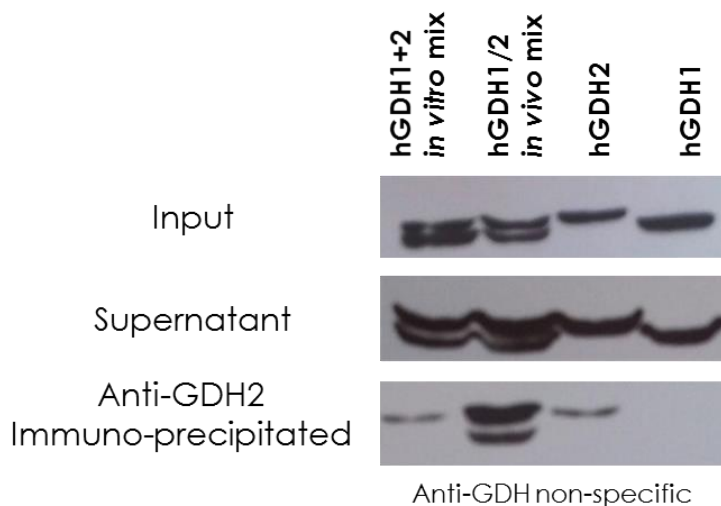
Co-Immunoprecipitation experiments

Co-immunoprecipitation experiments were performed on crude Sf21 cell extracts overexpressing hGDH1, hGDH2, hGDH1 and hGDH2 concurrently, and on mixed cell extracts where we combined hGDH1 and hGDH2 *in vitro* (hGDH1+2). A specific anti-hGDH2 antibody was used to examine which of these enzymatic samples were able to precipitate due to their affinity with it, when assayed through Co-IPs. Results were visualized by western blots using a non-specific GDH antibody which can bind to both hGDH1 and hGDH2. For all samples subjected to Co-IPs, both precipitants and supernatants from first centrifugation step (after incubation with the specific antibody

and the sepharose beads) were kept and assayed by western blot, so that the efficiency of the method could be concurrently assessed. As expected, recombinantly overexpressed hGDH2 alone was able to precipitate along with its specific antibody, which was, in turns, bound on protein A sepharose beads. As a result, western blot revealed a hGDH2 specific band at ~58kDa at the sample originating from Co-IP pellet. hGDH1 on the contrary, remained in the supernatant since it has no affinity for anti-hGDH2 antibody, and was thus absent from Co-IP pellet, as confirmed by western blot. Anti-GDH non-specific antibody was able to bind to hGDH1 contained in the supernatant fraction, which is a quality control which ensures that the enzyme was not present in the Co-IP pellet.

Interestingly, results showed that the cell lysate produced by co-expression of hGDH1 and hGDH2 in Sf21 culture, derived a structure consisting of both enzymes, which could be recognized by the anti-hGDH2 antibody, and which was precipitated as a whole. Western blot showed that in the Co-IP fraction, both isoforms were immunoblotted by non-specific anti-GDH antibody. In contrast, when the two cell extracts derived from separate overexpression of hGDH1 and hGDH2, were in vitro (and thus after expression) mixed, only hGDH2 was able to be recognized and precipitated by its specific antibody. Indeed, hGDH1 was detectable only in supernatant (Fig.21).

We can safely assume that in the case of hGDH1/hGDH2 co-expression, hGDH1 became visible in the Co-IP pellet, because it must have been part of a complex consisting of both hGDH1 and hGDH2 subunits. It seems that it was in fact hGDH2 subunits that caused hGDH1 subunits to precipitate along with anti-GDH2 specific antibody, as they were closely associated with each other.

Concerning Co-IP efficiency, pilot experiments focusing on the quantity of reagents (mainly anti-GDH2 antibody and cell extract amounts) have been performed to standardize the actual experimental conditions. Nevertheless, even under the optimal conditions, there has been significant protein excess that remained to the supernatant and was not able to precipitate by the method.

Figure 21: Co-Immunoprecipitation experiments. Crude Sf21 extracts overexpressing human GDHs were immunoprecipitated with anti-hGDH2 antibody and visualized via western blotting using the anti-GDH nonspecific antibody. hGDH2 was precipitated when expressed alone (hGDH2, hGDH1+2 in vitro mix) and so was hGDH1/hGDH 2 in vivo mix (after co-expression). Supernatants from intermediate steps of the experiment were also assessed with western blot in order to compare the efficiency among different lysates.

GTP-affinity chromatography

Affinity chromatography, using prepacked columns with GTP conjugated-agarose, was applied on semi-purified enzyme preparations (after 2 cuts of ammonium sulfate precipitation and a hydrophobic chromatography), resulting from the same cell extracts as above (for Co-IPs). The reason for semi-purified enzymes' need for these sets of experiments was that GTP agarose is a rather sensitive material, prone to destabilization, so it would be a risk to our results to overload it with extra material. This method was chosen due to the selectivity of GTP to bind strongly to hGDH1, since it is its most potent inhibitor (Zaganas and Plaitakis 2002). On the other hand, hGDH2 is practically tolerant to GTP inhibition, and the affinity for this molecule should be accordingly low. In other words, GTP affinity is putatively a means of discriminating the two isoenzymes, and it was interesting to investigate how intermediate molecules such as the possible hetero-hexamer would respond to this assay.

As expected, hGDH1 which has a high affinity for GTP and is strongly inhibited by it (Zaganas and Plaitakis 2002), was bound on the resin and was only eluted by gradually increasing the ionic strength of KCl buffer which was applied on the column. By increasing the ionic strength of the buffer, interactions between the enzyme and the

immobilized substrate become weaker, before they reach a point at which affinity is not adequate to sustain binding. Indeed, a relatively high KCl concentration was required to antagonize and ultimately detach the enzyme from GTP (Fig.22). hGDH1 was therefore undetectable in the initial fractions collected from chromatography, as confirmed by enzymatic assays on each fraction separately.
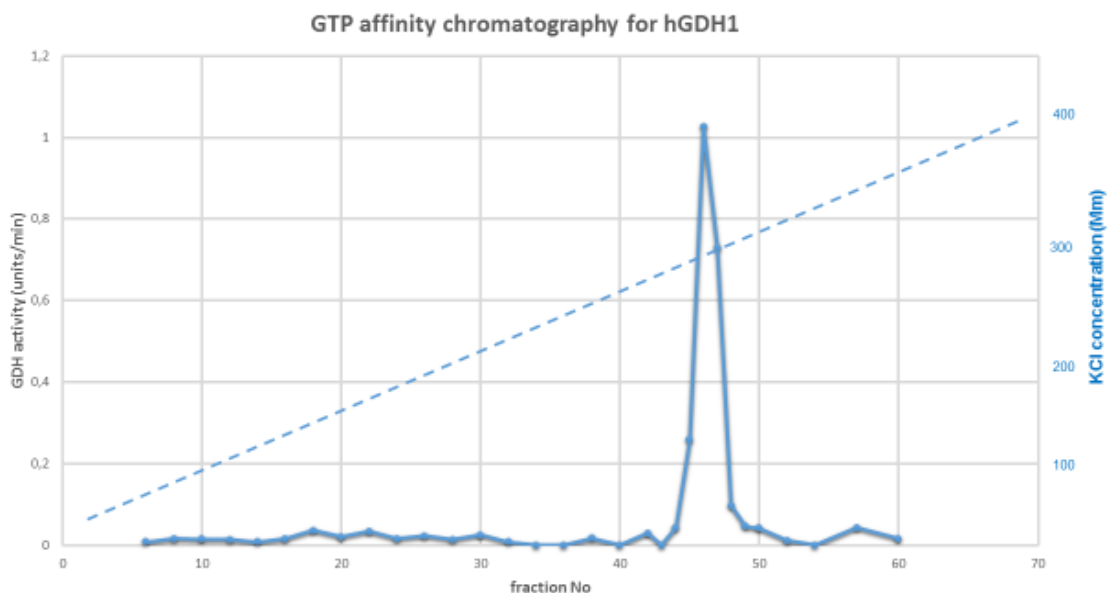
Figure 22: GTP affinity chromatography assay for semi-purified hGDH1 preparation. Recombinant hGDH1, being GTP-inhibition responsive, was able to bind to a GTP-resin column being eluted with a KCl gradient (50mM-400mM).

In contrast, when hGDH2 was subjected to GTP-affinity chromatography, it was immediately eluted in the flow through, being incapable to bind on the resin. Even before KCl gradient solution was applied on the column, hGDH2 had passed through the resin and it was detectable in early fraction by enzymatic assays (Fig.23). Although crystallographic data are not yet available to support this hypothesis, hGDH2 shows low affinity for GTP, since only a high concentration of the inhibitor is able to exert an effect on this isoenzyme (Zaganas and Plaitakis 2002).
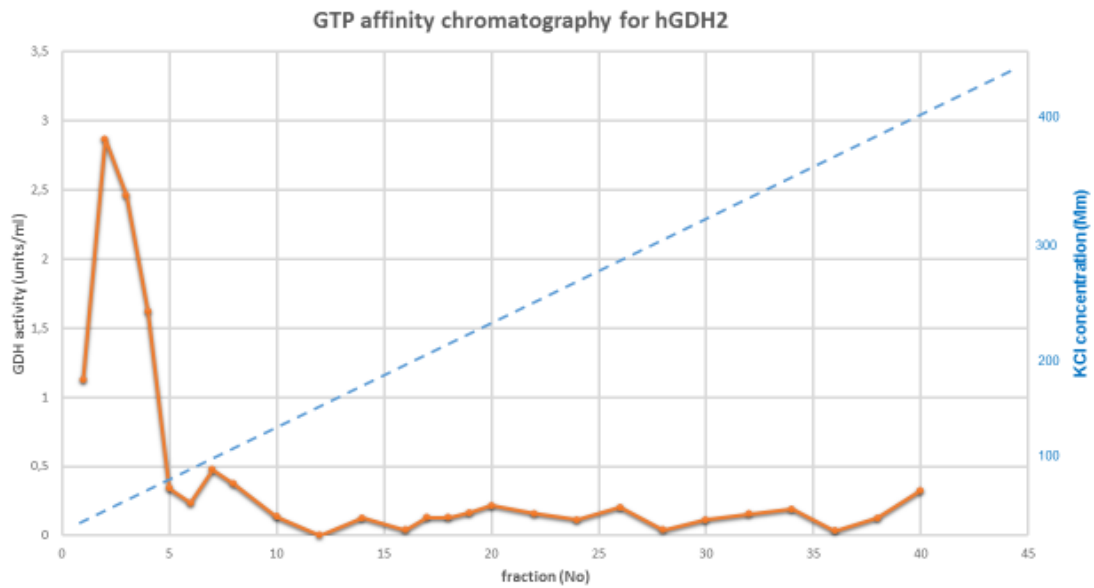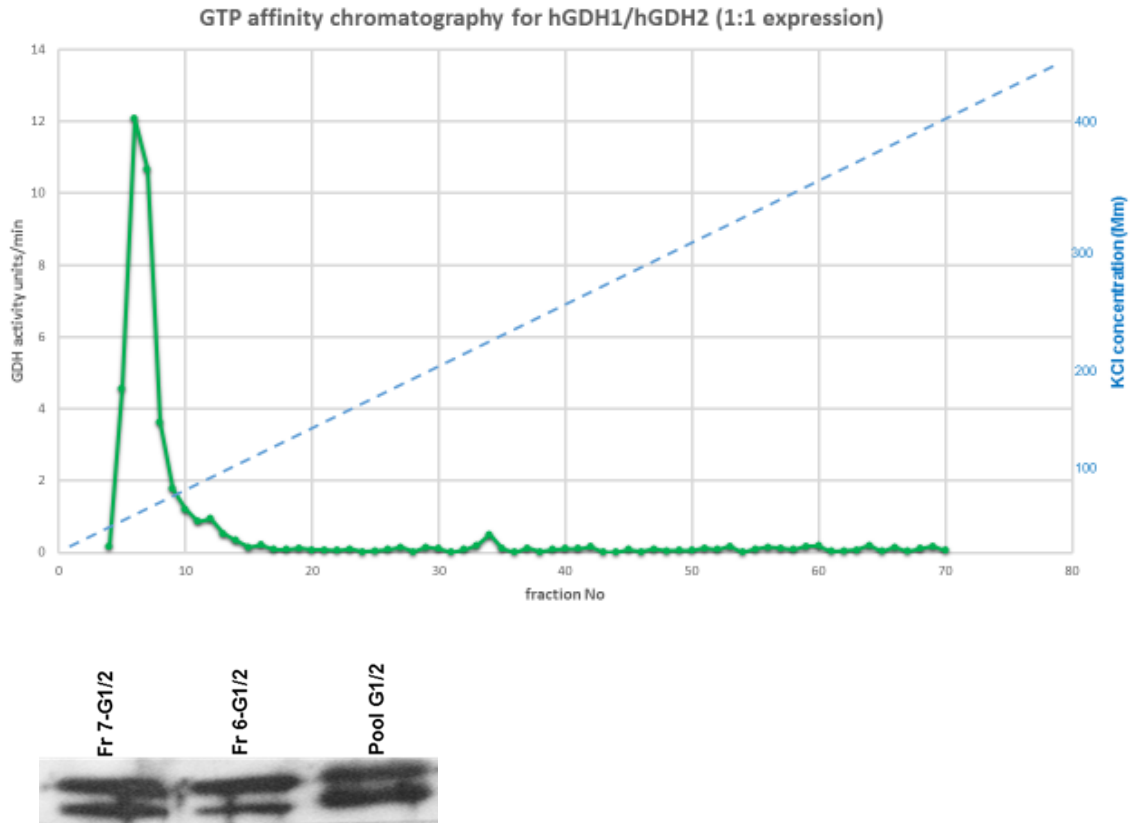
Figure 23: GTP affinity chromatography assay for semi-purified hGDH2 preparation. Recombinant hGDH2, being GTP-inhibition tolerant, failed to bind to the GTP column, being recovered in the flow through.

Impressively, enzyme preparations resulting from 1 hGDH1: 1 hGDH2 co-expression displayed an intriguing elution pattern when subjected to GTP-affinity chromatography. Specifically, the possible hetero-hexamer followed hGDH2 response to the assay, namely it was majorly eluted in the flow through of GTP column. Although presumably hGDH1's presence in the structure was expected to confer some degree of affinity to GTP, this was not the case here. Lacking a structural model, we can only assume that the possible hetero-hexameric conformation is such that does not allow hGDH1 subunits to interact as potently with GTP as homo-hexameric hGDH1 (Fig.24).

Figure 24: (Up) GTP affinity chromatography assay for semi-purified enzyme preparation resulting from 1 hGDH1: 1hGDH2 co-expression in Sf21 culture. Co-expressed hGDH1 and hGDH2, presumably forming hetero-hexamer GDH structures, were eluted as a single peak from GTP column, mimicking hGDH2 response to the assay. (Down) Western blot of peak fractions resulting from GTP chromatography (fr6,7 G1/2) and GDH preparation prion to chromatography (pool G1/2), using anti-GDH non specific antibody (able to bind to both human GDHs). The sample loaded on GTP column (pool) clearly consists of equal amounts of the two isoenzymes.

In order to establish the validity of these results, the possible hetero-hexamer's behavior was again compared with a simple in vitro mixture of enzyme preparations resulting from separate hGDH1 and hGDH2 overexpressing Sf21 cultures. The semi-purified enzymes were mixed in a 1:1 ratio, according to enzymatic estimations. When subjected to GTP-affinity chromatography assay, the mix showed two distinct elution patterns, one resembling hGDH1 and the other resembling hGDH2 (Fig.25). In details, hGDH2 was enzymatically detected in the flow through while hGDH1 was accordingly detected after the application of a KCl gradient in later fractions. Identification of each enzyme in the two resulting peaks was achieved by GTP kinetic assay, by which the first peak representing the flow through of unbound proteins, was particularly resistant to GTP inhibition, whereas the second peak was GTP sensitive. This finding implies

that each isoenzyme in the mixture functions as if it is subjected separately to the assay. In fact, GTP chromatography could as well offer, for instance, as a means to separate the two isoforms from tissues were they are co-expressed. Thus, in an in vitro mix of human GDHs each enzyme is able to maintain its unique properties, unlike the putative hetero-hexamer which functions as a single enzyme with distinct elution pattern. GTP-affinity chromatography results are summarized in figure 26.
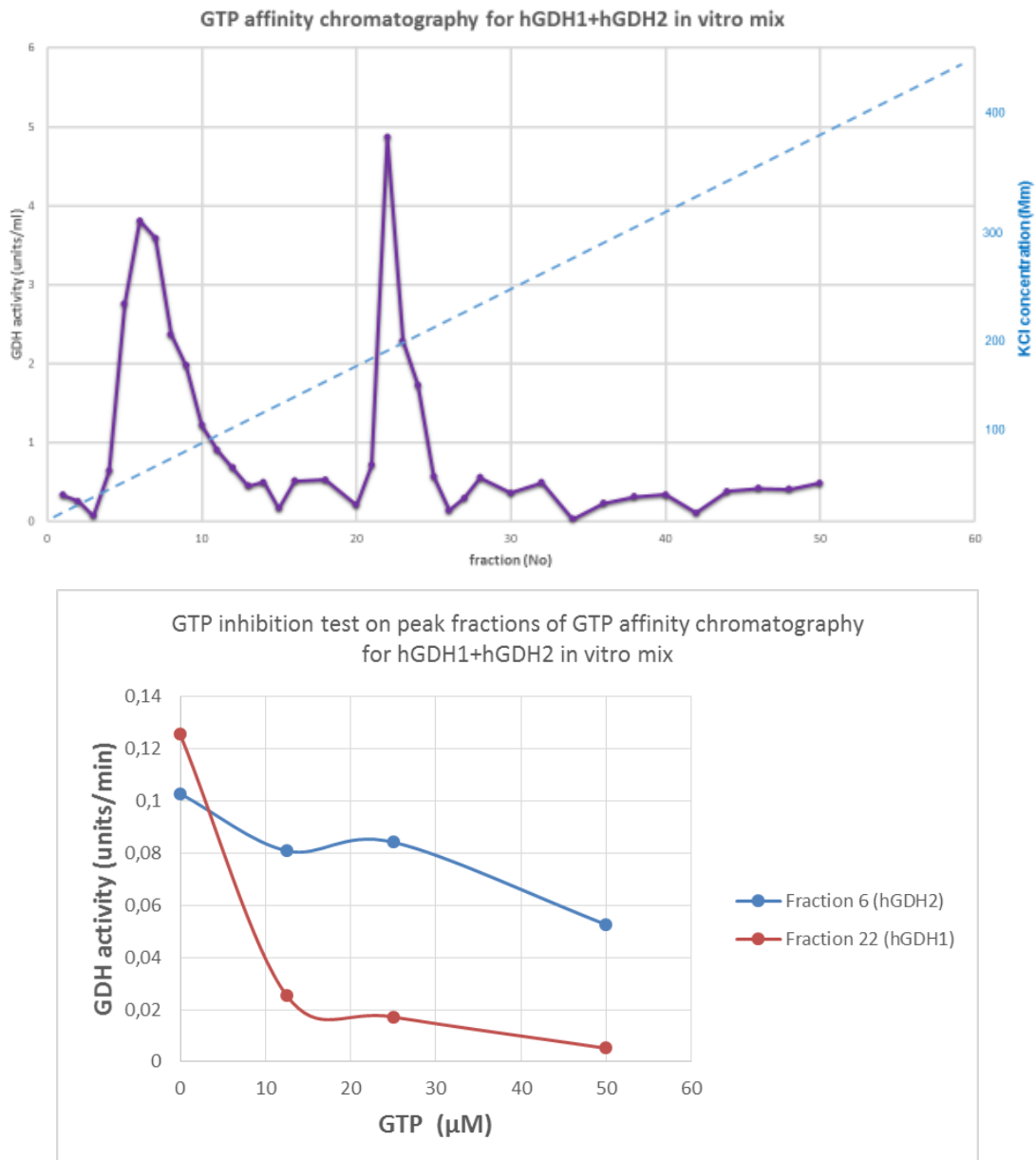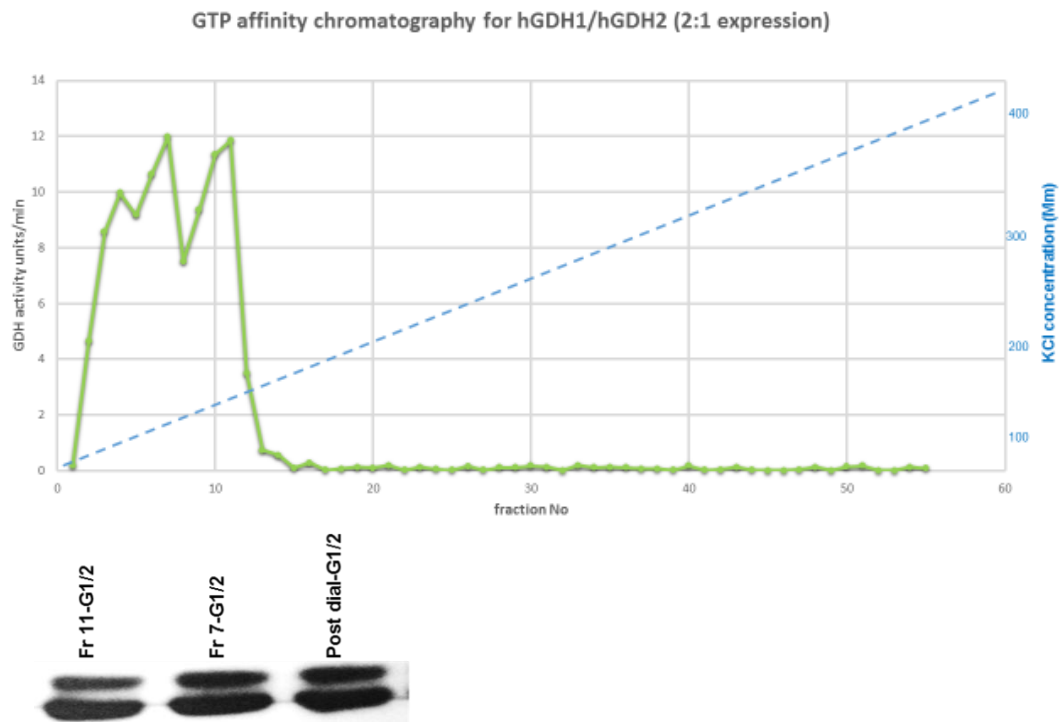

Figure 25: (Up) GTP affinity chromatography assay for in vitro mixture of semi-purified hGDH1 and hGDH2. When hGDH1 and hGDH2 were mixed in vitro, two separate peaks were recovered from the GTP column corresponding to the hGDH1 and hGDH2 homo-hexamers. (Down) Identification of each enzyme contained in the two different chromatography peaks by GTP inhibition kinetics.
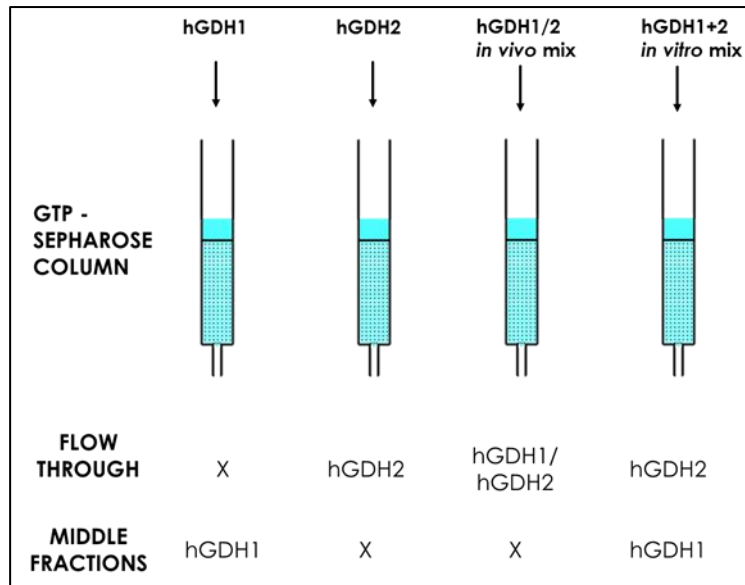
Figure 26: Cartoon representation of the GTP-affinity chromatography experiments on different human GDH preparations.

Although in testis hGDH1 and hGDH2 are expressed in a 1:1 ratio (Zaganas et al. 2012), in other tissues such as brain, hGDH2 expression is significantly lower than that of hGDH1. In an attempt to reproduce tissue GDH levels but also to provide support to our findings concerning hetero-hexamers existence, we co-expressed the two isoenzymes in Sf21 cultures in ratios other than 1:1. Using different amounts of viral stocks, we managed to produce 1 hGDH2: 2 hGDH1 and 1 hGDH2: 10 hGDH1 expression ratios at the protein levels, as was roughly estimated by western blots. When these samples were subjected to affinity chromatography, an interesting observation was made. The excess of hGDH1 enzyme that might have not participated in the hetero-hexameric formation, was normally bound on the column and depending on its quantity, it was eluted in different KCl concentrations. Thus, in these enzyme preparations the elution pattern constituted of two peaks, one representing the possible hetero-hexamer which was detectable in the flow through, as also observed in 1:1 expression, and one representing the excess hGDH1 that was bound on the resin, acting as single hGDH1 preparation (Fig.27, 28).

Figure 27: (Up) GTP affinity chromatography assay for semi-purified enzyme preparation resulting from 2 hGDH1: 1 hGDH2 co-expression in Sf21 culture. Unlike 1 hGDH1: 1 hGDH2 co-expression sample which eluted as a single peak from GTP chromatography, 2 hGDH1: 1 hGDH2 was somewhat less monodisperse, showing a second developing peak reflecting hGDH1 excess binding. (Down) Western blot of peak fractions resulting from GTP chromatography (fr7,11 G1/2) and GDH preparation prion to chromatography (post dial G1/2), using anti-GDH non specific antibody (able to bind to both human GDHs). The sample loaded on GTP column (post dial) consists of roughly 2 hGDH1: 1 hGDH2 ratio of the two isoenzymes.
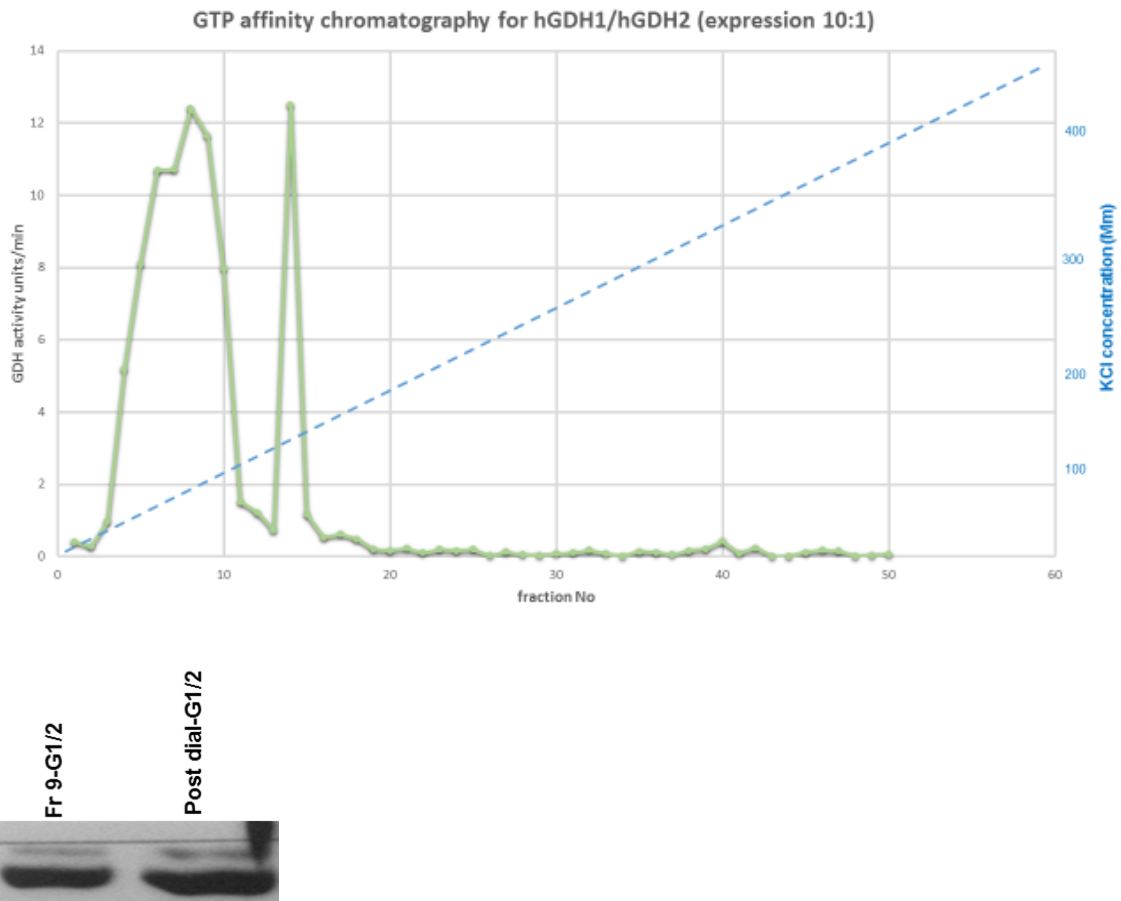
Figure 28: (Up) GTP affinity chromatography assay for semi-purified enzyme preparation resulting from 10 hGDH1: 1 hGDH2 co-expression in Sf21 culture. 10 hGDH1: 1 hGDH2 sample was eluted from GTP chromatography as two peaks. The second peak, reflecting hGDH1 excess binding, which was starting to develop at 2:1 expression (Fig.26) was here definitely present. (Down) Western blot of peak fractions resulting from GTP chromatography (fr9 G1/2) and GDH preparation prion to chromatography (post dial G1/2), using anti-GDH non specific antibody (able to bind to both human GDHs). The sample loaded on GTP column (post dial) consists of roughly 10 hGDH1: 1 hGDH2 ratio of the two isoenzymes.

2. ELECTROPHORESES STUDIES ON HUMAN GDHs

Blue native PAGE electrophoresis for the separation of hGDHs

According to previous findings (Dr. Kostis Kanavouras PhD thesis), hGDH1 and hGDH2 are expected to display a slightly different electrophoretic mobility when they run on a native polyacrylamide gel, since they also display different mobility on SDS gels and they are speculated to have subtle differences in their native form conformation. Blue native electrophoresis was primarily employed to examine whether it could be an efficient method to discriminate hetero-hexameric from homo-hexameric

GDHs. Pilot experiments were performed with the two different homo-hexamers, and an in vitro mixture of them. Prior electrophoresis, samples were purified to homogeneity.

Given that both human isoenzymes form hexamers consisting of 56-58kDa subunits, their native molecular weight was consistent with the hexameric form, although due to technical difficulties it appeared slightly bigger than ~340kDa. Theoretically, hGDH1 should have a native molecular weight of 336kDa and hGDH2 of 348kDa. Nevertheless, such a difference (12kDa) was not detectable by the means used in the present blue native PAGE assay (Fig.29). An in vitro mix of hGDH1 and hGDH2 was also loaded on the same gel, but showed the same mobility as the separate hGDHs, while the separation of the two enzymes was not achieved. Different gel sizes and electrophoresis durations were employed in several efforts to optimize the protocol for hGDHs, yet hGDH1 and hGDH2 were always behaving in a similar way under native conditions. In addition, boGDH was used as a positive control, and appeared to run at similar molecular weights as hGDHs, which provides a proof that all native forms are of similar mass and thus subunit composition (hexamers). In light of these results, it was unfortunately infeasible to use this method for identification of possible GDH hetero-hexamers, since it was impossible to detect the subtle possible difference between the hetero-hexamer and homo-hexamer forms of hGDHs. However, the results established the feasibility of our experiments concerning the homogeneity of our samples and their proper folding, which were extremely important factors for the subsequent structural studies.
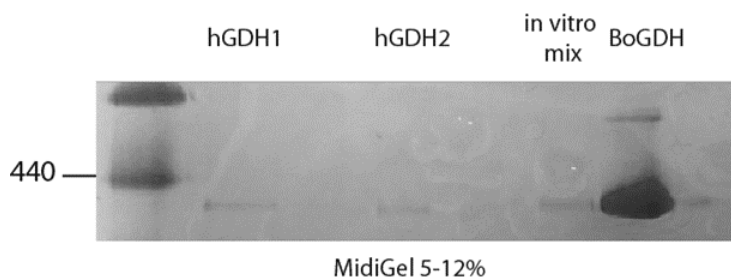
Figure 29: Blue native PAGE on human GDHs. Purified hGDH preparations (hGDH1, hGDH2, hGDH1 + hGDH2 in vitro mix) and industrially available boGDH were loaded on a non-denaturing polyacrylamide gel. All run at similar molecular weights, which are in accordance with their expected hexameric conformation. Despite several optimizations though, the two iso-enzymes were not able to separate with this technique.

For purposes of validity of the enzymatic assays that followed, it was mandatory that the expression of each hGDH isoenzyme in co-expression experiments was in a stable absolute ratio of 1:1. This is an important precondition for our enzymatic studies, since its needs to be ensured that hetero-hexamer's response to different effectors is a result of a monodisperse sample's behavior, and no excess hGDH1 or hGDH2 interferes with this response. Equal isoenzymes' expression was indeed achieved using a single expression vector, pFastBacDual, containing both *GLUD1* and *GLUD2* genes under equally powerful promoters (p10 and polyhedrin), and Bac-to-Bac expression system described in methods section. In order to verify the 1:1 expression, both blue silver stained acrylamide gels and western blots using the nonspecific anti-GDH antibody, were performed. Interestingly, hGDH1 and hGDH2 have been reported to display different electrophoretic mobility when separated in an SDS polyacrylamide gel, although they have similar molecular weight, so they could both be distinctly visible. In fact, hGDH1 runs at approximately 58kDa while hGDH2 lies just above it, at 56kDa. Results showed that hGDH1 and hGDH2 were equally represented in the possible hetero-hexamer hGDH1/2 preparation (Fig.30). As control, a 1:1 in vitro mix of the isoenzymes was used, for which the relative quantity of each enzyme was estimated enzymatically prior to loading.
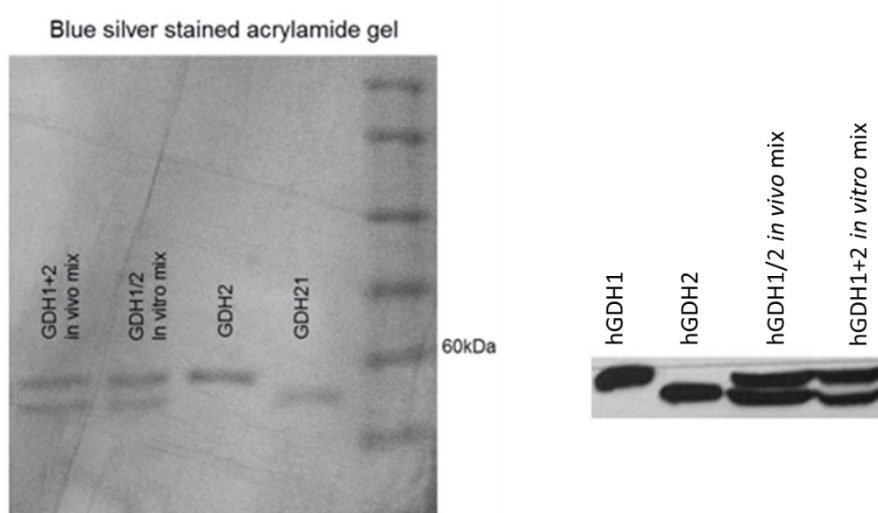
Figure 30: SDS electrophoresis studies for the verification of hGDH1/2 possible hetero-hexamer's 1:1 co-expression. Blue silver stained acrylamide gels (left) as well as western blot experiments using anti-GDH antibody (right) showed an equal expression of each isoenzyme when they were co-expressed in Sf21 using the bac-to-bac expression system.

3. DESCRIPTION OF THE ENZYMATIC PROPERTIES AND OPTIMAL FUNCTIONING CONDITIONS OF THE POSSIBLE hGDH1/2 HETERO-HEXAMERS.

Having verified a 1:1 expression of hGDH isoenzymes, the protein production was then scaled up and the enzymes were purified to homogeneity according to routine protocols previously used to purify each enzyme separately. Subsequently, a series of comparative kinetic studies were performed in order to study primarily whether the possible hetero-hexameric hGDH was acting in the same way as a simple in vitro mix of hGDH1 and hGDH2, or it had its own distinct properties. Secondly it was important to determine the precise conditions under which the possible hetero-hexamer can optimally function. All sets of enzymatic studies were replicated at least in 3 different experiment sessions.

All enzymatic studies were performed with highly purified enzymatic preparations from cell extracts from baculovirus-infected Sf21 cells. These preparations displayed measurable GDH activity when assayed in the presence of NADPH, originating from the exogenous (recombinantly expressed) hGDH1 and hGDH2 (Shashidharan et al. 1994). In addition, in accordance with previous findings (Shashidharan et al. 1997), hGDH2 showed, in the absence of allosteric activators (ADP and L-leucine), very low basal activity compared to hGDH1; this activity was fully restored, as expected, by the addition of 1 mM ADP.

GTP inhibition

In accordance with preceding studies (Plaitakis et al. 2000; Zaganas and Plaitakis 2002), in the presence of 1mM ADP, hGDH1 was strongly inhibited by GTP (IC_{50} 27.72093 ±1.08399 uM). Under the same conditions hGDH2 was remarkably resistant to GTP, with IC50 being at least 18 times higher than that of hGDH1 (IC_{50} 493.3376 ±87.07413 uM). The enzymatic preparation resulting from hGDH1 and hGDH2 recombinant co-expression presented a distinct inhibition pattern by GTP, with an IC_{50} value which leaned towards pure hGDH2 isoform (144.33416 ±9.83684 uM). In comparison, the in vitro mixture of purified hGDH1 and hGDH2 enzymes displayed an intermediate inhibition behavior, with its inhibition curve lying between the two pure isoforms. The mixture's response to GTP differed markedly from the possible hetero-hexamer's response, with its IC_{50} value being ~2,4 times lower than the latter

100

(60.58676 ±5.79904 uM). Indeed, the IC_{50} values between the possible hetero-hexamer and the in vitro mix of human GDHs differ in a statistically significant level (p=0.0003). Thereby, hGDH1/2 seems to operate in a distinct manner, than a simple enzyme mixture. The possible hetero-hexamer's response to GTP inhibition also differs significantly from the respective homo-hexameric hGDHs (Table 2), underlying that this enzyme is able to function in a unique pattern under changing GTP levels. In addition, there is an apparent difference in their GTP inhibition pattern since the possible hetero-hexamer's curve displays a tendency to diverge from that of but as much from that of hGDH2 (Fig.31). In more details, regarding Hill coefficient, which refers to the cooperativity of the enzyme's subunits, and, accordingly to how steep the inhibition curve is, the tendency of the possible hetero-hexamer to respond to GTP similarly to hGDH2 is even more profound (Table 2). The differences observed between Hill coefficient values of hGDH1/2 and hGDH2 do not differ significantly (p=0.5308), unlike those between hGDH1/2 and hGDH1 which reach a notable significance level (p=0.001). The mixture of pure homo-hexamers also presented a similar Hill coefficient with hGDH1/2 and differences with the homo-hexamers, but still it is profoundly more distant from hGDH2 response than the possible hetero-hexamer. Interestingly, two-way-ANOVA statistic test, by which each curve point was assessed separately between different GTP inhibition responses, revealed that when GTP was added in concentration over 25uM, a statistical significance was valid between hGDH1/2 possible hetero-hexamer's and hGDH1+2 mixture activity differences.
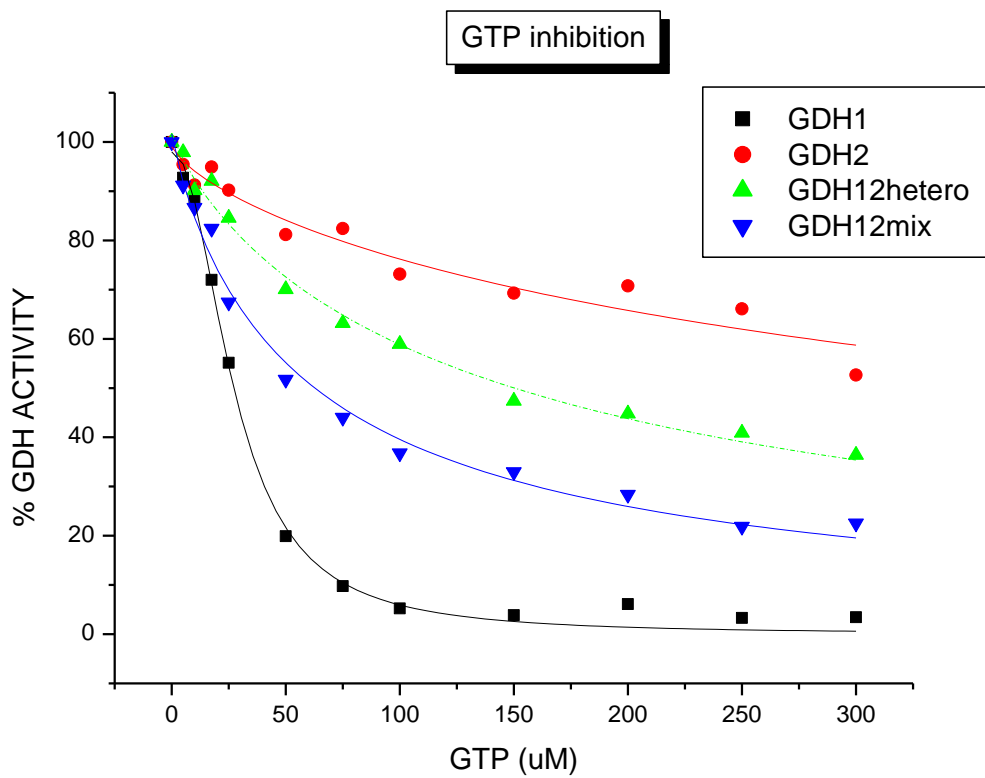
Figure 31: Comparative kinetic studies of inhibition by GTP for different GDH preparations. The possible hetero-hexamer's (GDH1/2hetero) inhibition curve displays a different regulation pattern and its characteristics, such as IC_{50} and Hill coefficient, differ significantly from the ones corresponding to a simple in vitro hGDH mix (GDH1+2mix).

Table 2: GTP inhibition curves' characteristics and statistical analyses between different GDH preparations.

GTP inhibition curves				
	hGDH1	hGDH2	hGDH1/2 hetero-hexamer	hGDH1+hGDH2 mix
V_{max}	98.01 ±1.82	99.03 ±3.00	101.75 ±2.02	101.59 ±2.80
IC_{50} (uM)	27.72 ±1.010	493.34 ±87.07*	144.33 ±9.84*, **	60.60 ±5.81 **, ***
Hill coefficient	2.18 ±0.13	0.76 ±0.144*	0.86 ±0.06*	0.90 ±0.06*

*$p<0.01$ for the comparison with the corresponding value of hGDH1,

**$p<0.01$ for the comparison with the corresponding value of hGDH2

***$p<0.01$ for the comparison with the corresponding value of hGDH1/2

The specific p values are as following:

For IC_{50} comparison between different enzymes: hGDH1-hGDH2 p=0.0017, hGDH1-hGDH1/2 p=0.0001, hGDH1-hGDH1+2 p=0.0752, hGDH2-hGDH1/2 p=0.0073, hGDH2-hGDH1+2 p=0.0026, hGDH1/2-hGDH1+2 p=0.0003

For Hill coefficient comparison between different enzymes: hGDH1-hGDH2 p=0.0004, hGDH1-hGDH1/2 p=0.0001, hGDH1-hGDH1+2 p=0.0001, hGDH2-hGDH1/2 p=0.5308, hGDH2-hGDH1+2 p=0.4047, hGDH1/2-hGDH1+2 p=0.6853

DES inhibition

Unlike GTP, DES is known to inhibit hGDH2 more potently than hGDH1 (Borompokas et al. 2010). In our studies we confirmed this finding, by showing that the two isoenzymes' IC50 for this inhibitor differ significantly (p=0.0004), with that of hGDH1 (37.12648 ±1.21816) being ~2.3-fold greater than that of hGDH2 (16.56697 ±1.48331), in the presence of 1mM ADP. Looking at the combined enzyme preparations, hGDH1/2 possible hetero-hexamer's inhibition response presented a light difference as compared to hGDHs mixture (hGDH1/2 IC_{50} 20.70142 ±1.02602, hGDH1+2 mix IC_{50} 24.13138 ±1.26916), which however did not yield statistical importance levels (p=0.1035). When looking more thoroughly at the comparative kinetics among all four enzyme preparations, both hGDH1/2 and hGDHs mixture IC50s do not differ significantly with the respective value of hGDH2, with hGDH1/2 being even closer to hGDH2's, whereas they presented a significant difference in their IC_{50} with the respective value for hGDH1 (Table 3). Inhibition curves' characteristic Hill coefficient on the other hand does not decline significantly among different enzymes, beside these

between hGDH1 and in vitro enzyme mixture, which, as seen from figure 32, displays a slightly atypical curve slope.
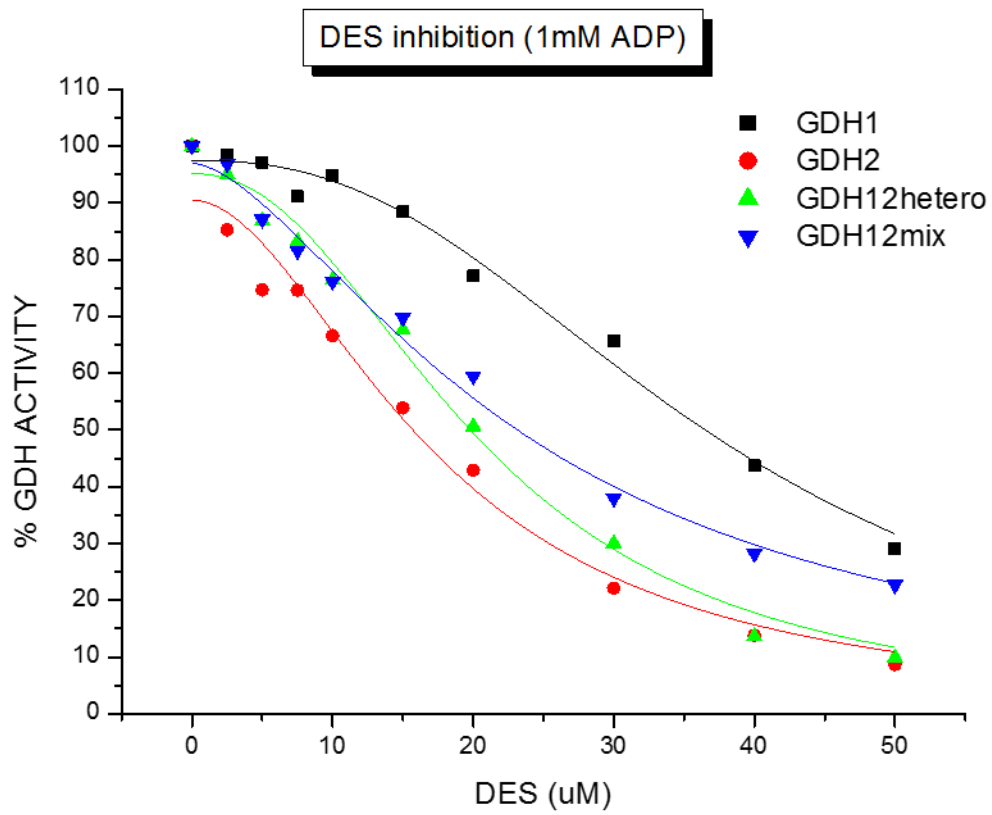
Figure 32: Comparative kinetic studies of inhibition by DES for different GDH preparations. The possible hetero-hexamer's (GDH1/2hetero) inhibition curve displays a slightly different regulation pattern with a strong tendency to differ from in vitro hGDH mix's (GDH1+2mix) curve, and to resemble to that of hGDH2.

Table 3: DES inhibition curves' characteristics and statistical analyses between different GDH preparations.

DES inhibition curves				
	hGDH1	hGDH2	hGDH1/2 hetero-hexamer	hGDH1+hGDH2 mix
V_{max}	97.59 ±1.56	92.64 ±3.93	94.16 ±2.38	96.98 ±2.26
IC_{50} (uM)	37.13 ±1.22	16.57 ±1.48*	20.70 ±1.03*	24.13 ±1.27*,**
Hill coefficient	2.51 ±0.25	1.75 ±0.22	2.31 ±0.22	1.62 ±0.13

*p<0.01 for the comparison with the corresponding value of hGDH1,

**p<0.05 for the comparison with the corresponding value of hGDH2

The specific p values are as following:

For IC_{50} comparison between different enzymes: hGDH1-hGDH2 p=0.0004, hGDH1-hGDH1/2 p=0.0005, hGDH1-hGDH1+2 p=0.0018, hGDH2-hGDH1/2 p= 0.0836, hGDH2-hGDH1+2 p=0.0179, hGDH1/2-hGDH1+2 p=0.1035

For Hill coefficient comparison between different enzymes: hGDH1-hGDH2 p=0.0837, hGDH1-hGDH1/2 p=0.5708, hGDH1-hGDH1+2 p=0.0328, hGDH2-hGDH1/2 p=0.1510, hGDH2-hGDH1+2 p=0.6338, hGDH1/2-hGDH1+2 p=0.0554

<u>Divalent ions (Mn^{2+}, Mg^{2+}, Ca^{2+}) influence</u>

Previous studies have provided evidence that regulation of GDH activity by divalent cations is observed in various organisms (LéJohn et al. 1969; Garland and Dennis 1977; Hudson and Daniel 1993). In contrast, mammalian GDHs are inhibited by rather high concentrations of Mg (Fahien et al. 1990; Kuo et al. 1994; Shashidharan et al. 1997) with Ca having no such effect (Kuo et al. 1994).

Here we initially studied the effect of Mn on purified hGDH1 and hGDH2 and for comparison, we also studied the effect of equivalent concentrations of Mg and Ca (in the presence of 0.25 and 1mM ADP), to establish the regulating impact of these cations on human GDHs. Functional assays employing the purified enzymes confirmed that Mn interacted with hGDH2 with a greater affinity than with hGDH1. Specifically, in the presence of 0.25 mM ADP, the Mn IC_{50} was 1.14 ±0.02 mM and 1.54±0.08 mM for hGDH2 and hGDH1, respectively (p=0.0001; Fig.33, Table 4). At 1 mM ADP, the Mn IC_{50} was 1.84±0.02 mM and 2.04±0.07 mM for hGDH2 and hGDH1, respectively (p=0.01; Fig.33, Table 4). These results were due to the sigmoidicity of the Mn

inhibitory curve that was more pronounced for hGDH2 than for hGDH1. Indeed, at 0.25mM ADP, the Hill coefficient value was higher for hGDH2 (3.42±0.20) than for hGDH1 (1.94±0.25; p=0.0002), indicating that the interaction of Mn with hGDH2 was substantially more co-operative than for hGDH1. Likewise, in the presence of ADP 1mM, the HC values were 3.29±0.38 and 5.12±0.27, for hGDH1 and hGDH2, respectively (p=0.001), indicating a high degree of co-operativity (approaching, in the case of hGDH2, the theoretical maximum of 6 for the hexamer). In contrast, both Ca and Mg, added at concentrations 0–3mM in the reaction mixture, did not significantly affect the activity of neither purified isoenzyme, in the presence of either 0.25mM ADP or 1mM ADP (Fig. 34, 35).

Figure 33: Mn exerts differential inhibitory effect on purified hGDH1 and hGDH2 recombinant enzymes. Assays were performed in the presence of 0.25mM ADP (up) or 1 mM ADP (down). Under both conditions, hGDH2 showed higher sensitivity to Mn inhibition (most pronounced in the presence of 0.25mMADP). Both enzymes showed significant cooperativity for this inhibition, which was higher for hGDH2.
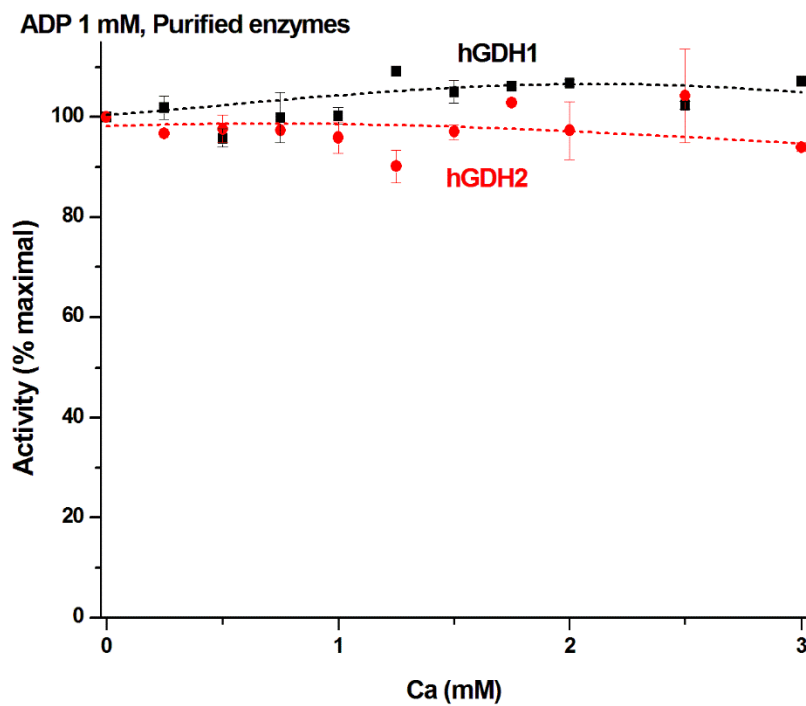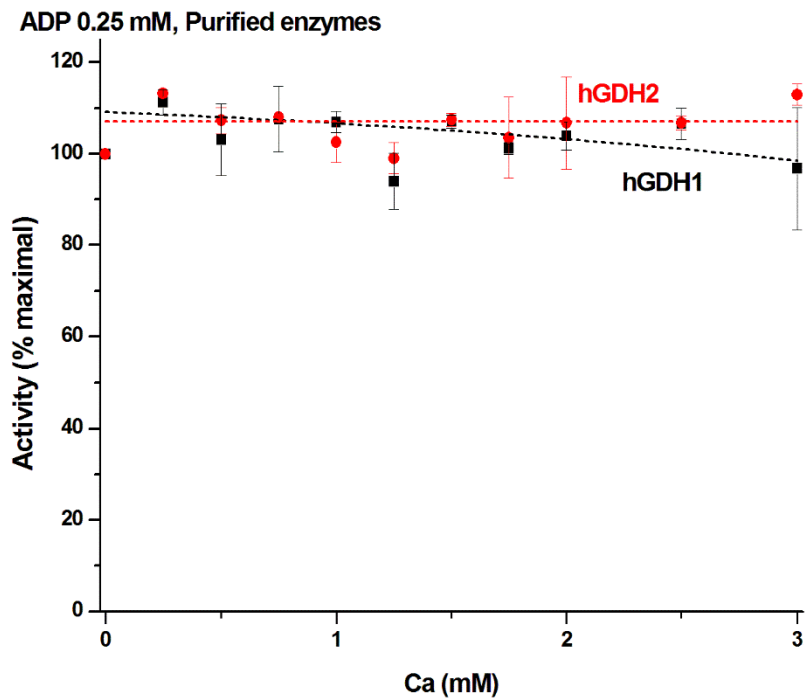
Figure 34: Ca does not exert a significant inhibitory effect on either purified hGDH1 or purified hGDH2 recombinant enzymes. Assays were performed in the presence of 0.25mM ADP (up) or 1mM ADP (down).
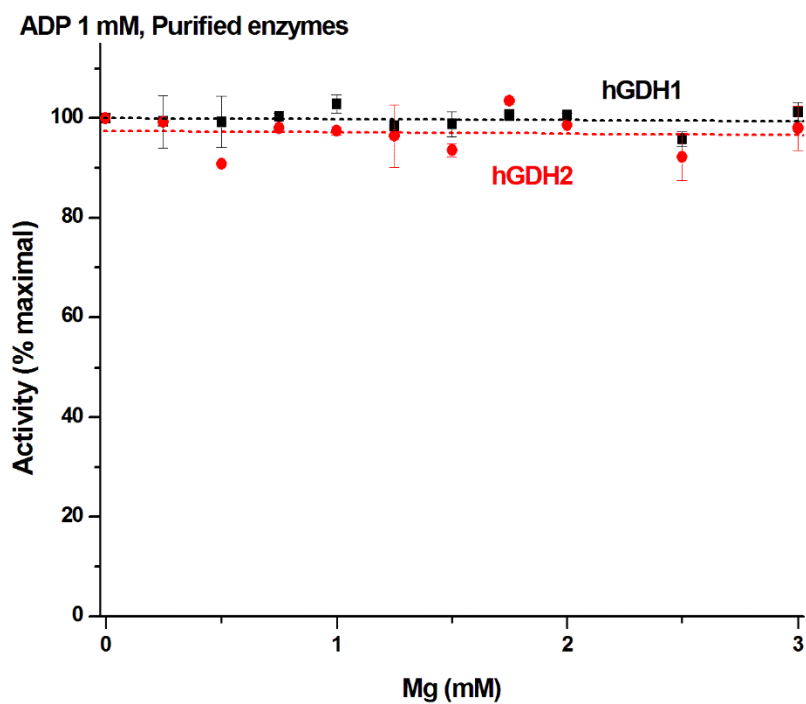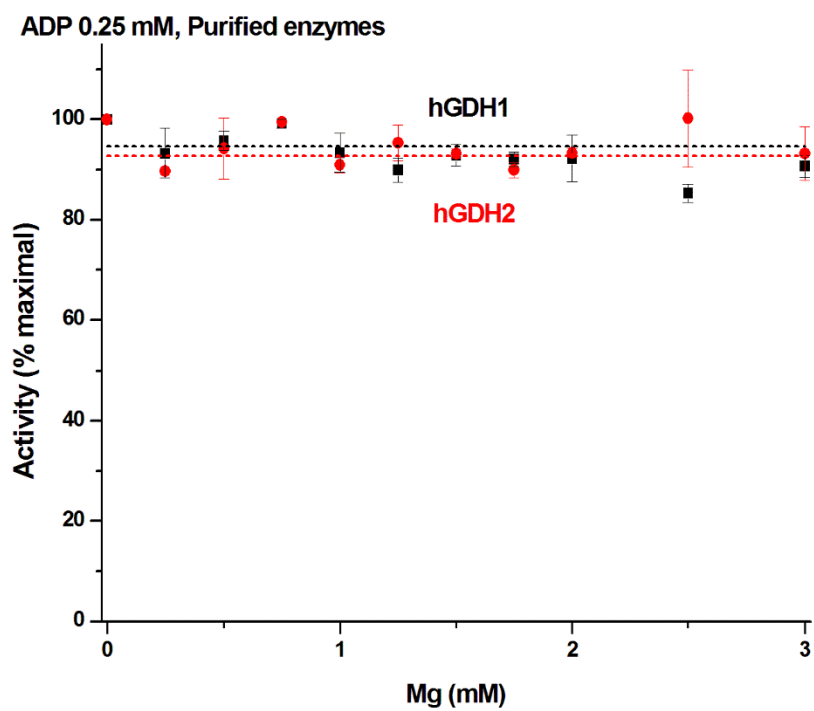
Figure 35: Mg does not exert a significant inhibitory effect on either purified hGDH1 or purified hGDH2 recombinant enzymes. Assays were performed in the presence of 0.25mM ADP (up) or 1mM ADP (down).

Table 4: Inhibition of hGDH1 and hGDH2 activity in purified enzyme preparations by Mn

Mn inhibition curves for hGDH1 and hGDH2		
ADP	0.25mM	1mM
IC$_{50}$		
hGDH1	1.54 ± 0.08	2.04 ± 0.07
hGDH2	1.14 ± 0.02	1.84 ± 0.02
P value*	0.0001	0.01
Hill Coefficient		
hGDH1	1.94 ± 0.25	3.29 ± 0.38
hGDH2	3.42 ± 0.20	5.12 ± 0.27
P value*	0.0002	0.001

In light of these results, we accordingly investigated how the possible hetero-hexamer of human GDHs or their *in vitro* mix is affected by Mn in the presence of 0.25mM ADP, that the two homo-hexamers show a profoundly different regulation pattern. Results showed that the inhibition pattern induced by Mn was comparable for the two enzymatic preparations, as their curves were lying between those of pure hGDH1 and hGDH2 (Table 5, Fig.36).
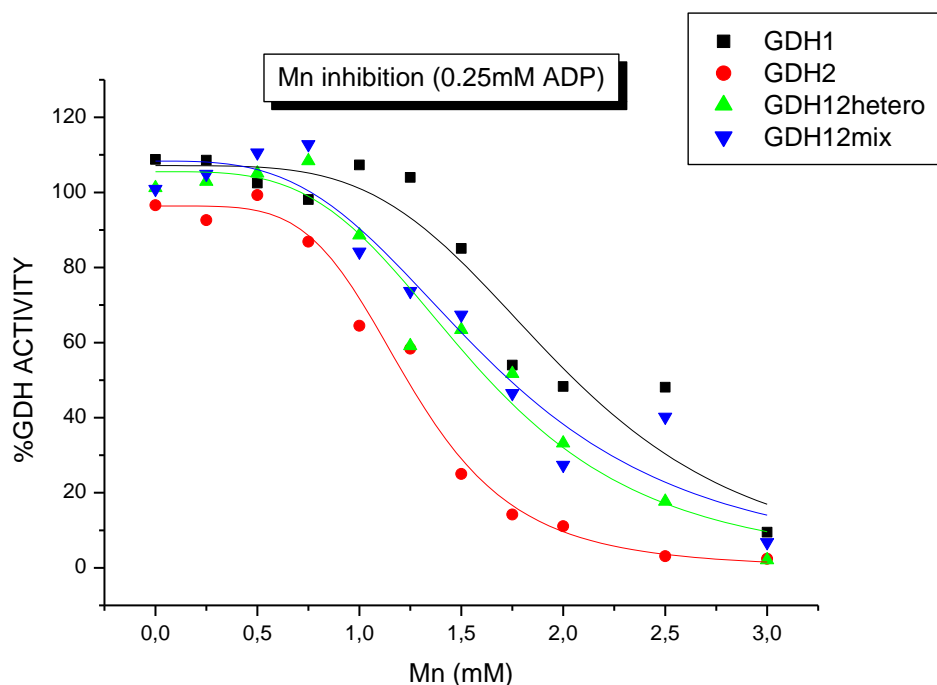
Figure 36: Comparative kinetic studies of inhibition by Mn, in the presence of 0.25 mM ADP, for different GDH preparations. The possible hetero-hexamer's (GDH1/2hetero) inhibition curve lies between the two homo-hexameric enzymes, and does not differ from in vitro hGDH mix's (GDH1+2mix) behavior at a significant level.

Table 5: Mn inhibition curves' characteristics (in the presence of 0.25mM ADP).

	hGDH1	hGDH2	hGDH1/2 hetero-hexamer	hGDH1+hGDH2 mix
	Mn inhibition curves (0.25 mM ADP)			
V_{max}	107.13 ±5.07	96.39 ±2.93	105.53 ±4.49	108.34 ±5.84
IC_{50} (uM)	1.99 ±0.11	1.26 ±0.04	1.59 ±0.08	1.66 ±0.12
Hill coefficient	4.09 ±0.94	4.72 ±0.60	3.62 ±0.03	3.21 ±0.69

L-leucine activation

hGDH2's activity is majorly depended on allosteric activators' influence. In the absence of such regulators, this enzyme is practically inactive, maintaining a very low basal activity of 4-8% of its maximal (Kanavouras et al. 2007). In addition, different activators and especially ADP and L-leucine, have been reported to act synergistically in their regulatory effect (Kanavouras et al. 2007). Here, we examined the L-leucine activation effect on our enzymatic preparations under different concentrations of ADP (0, 0.025mM, 0.05mM).

As expected, in the absence of ADP, hGDH2 presented very low basal activity and V_o, in contrast to hGDH1, whose respective characteristics where close to 50% of its maximal. hGDH1/2 possible hetero-hexamer and hGDH1 + hGDH2 mixture presented similar values which were intermediate between those of pure homo-hexameric enzymes. AC_{50} values for L-leucine activation were comparable among most of the different enzyme preparations, included those between hGDH1 and hGDH2 as well as those between hetero-hexamer and mixture. Notable statistical significance was observed in the AC_{50} values between hGDH2 and hGDH1/2 (p=0.0001), but not between the latter and hGDH1, which imply the notion that for this particular kinetic parameter the possible hetero-hexamer behaves more similarly with hGDH1. Activation curve slopes were also similar among different enzymes and no statistical significance was detected regarding Hill coefficient values (Fig.37, Table 6).

When the enzymatic behaviors in respect with L-leucine activation were assayed in the presence of 0.025 and 0.05mM ADP (Fig.38,39 and Tables 7,8), all enzymes responded alike, with no statistical significance being observed among their AC50 and Hill coefficient values. Nevertheless, the previously mentioned pattern according to which hGDH2 has the lowest V_o, followed by hGDH mixture, hGDH1/2 hetero-hexamer and hGDH1 was also apparent under the conditions studied. By increasing ADP levels, the differences are attenuated due to their reaching at a plateau of maximal activity.
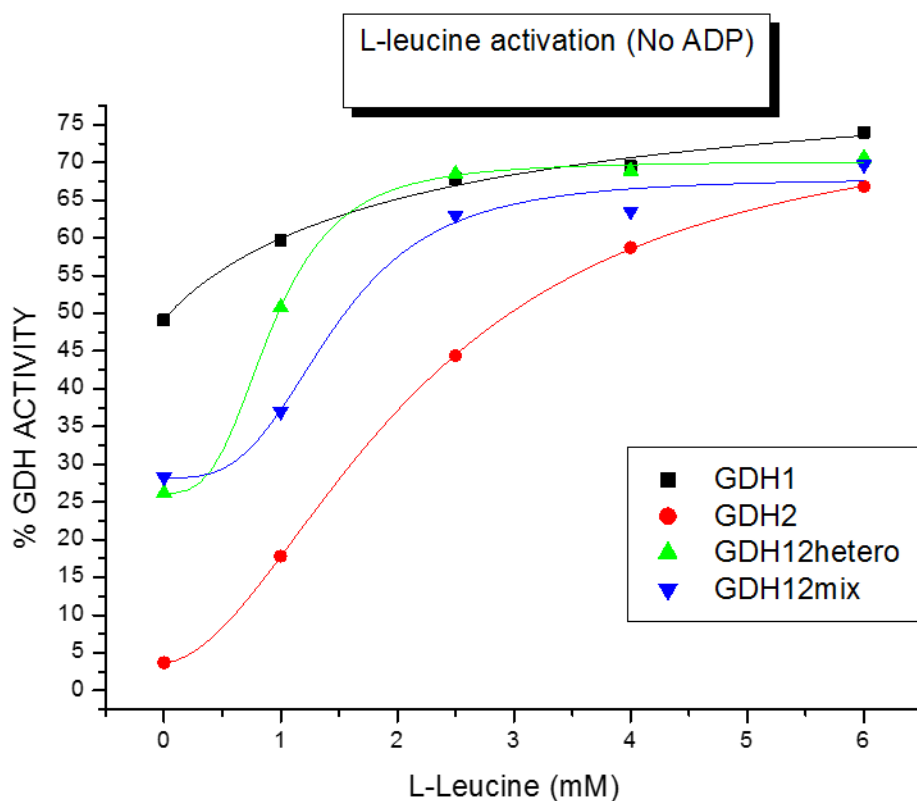
Figure 37: Comparative kinetic studies of activation by L-leucine, in the absence of ADP, for different GDH preparations. The possible hetero-hexamer's (GDH1/2hetero) activation curve displays a subtle tendency to differ from in vitro hGDH mix's (GDH1+2mix) curve, and to resemble to that of hGDH1.

Table 6: L-leucine activation curves' characteristics (in the absence of ADP) and statistical analyses between different GDH preparations.

	L-leucine activation curves (No ADP)			
	hGDH1	hGDH2	hGDH1/2 hetero-hexamer	hGDH1+hGDH2 mix
V_o	48.91 ±1.75	3.72 ±0.24	26.20 ±1.01	28.20 ±3.81
V_{max}	27.92 ±8.07	73.44 ±0.87	43.93 ±1.41	39.72 ±5.50
AC_{50} (uM)	1.46 ±0.76	2.21 ±0.03	0.93 ±0.03*	1.46 ±0.30
Hill coefficient	1.29 ±0.75	1.82 ±0.04	3.15 ±0.93	3.26 ±1.35

*$p < 0.01$ for the comparison with the corresponding value of hGDH2

The specific p values are as following:

For IC_{50} comparison between different enzymes: hGDH1-hGDH2 p=0.3838, hGDH1-hGDH1/2 p=0.5197, hGDH1-hGDH1+2 p=0.9944, hGDH2-hGDH1/2 p=0.0001, hGDH2-hGDH1+2 p=0.0664, hGDH1/2-hGDH1+2 p=0.1511

For Hill coefficient comparison between different enzymes hGDH1-hGDH2 p=0.5185, hGDH1-hGDH1/2 p=0.1950, hGDH1-hGDH1+2 p=0.2716, hGDH2-hGDH1/2 p=0.2274, hGDH2-hGDH1+2 p=0.3473, hGDH1/2-hGDH1+2 p=0.9500

Figure 38: Comparative kinetic studies of activation by L-leucine, in the presence of 25uM ADP, for different GDH preparations. The possible hetero-hexamer's (GDH1/2hetero) activation curve lies between the two homo-hexameric enzymes, and does not differ from in vitro hGDH mix's (GDH1+2mix) behavior at a significant level.

Table 7: L-leucine activation curves' characteristics (in the presence of 25uM ADP) and statistical analyses between different GDH preparations.

	hGDH1	hGDH2	hGDH1/2 hetero-hexamer	hGDH1+hGDH2 mix
	L-leucine activation curves (25uM ADP)			
V_o	81.68 ±2.57	8.92 ±3.41	61.50 ±3.21	45.29 ±2.65
V_{max}	22.72 ±3.48	78.86 ±5.32	32.66 ±4.72	39.87 ±4.14
AC_{50} (uM)	0.42 ±0.08	0.65 ±0.06	0.48 ±0.07	0.51 ±0.05
Hill coefficient	4.26 ±3.07	3.08 ±0.75	4.46 ±4.16	5.27 ±5.11

The specific p values from the comparison of the different enzymes' AC_{50} and Hill coefficient are as following:

For AC_{50} comparison between different enzymes: hGDH1-hGDH2 p=0.0889, hGDH1-hGDH1/2 p=0.6041, hGDH1-hGDH1+2 p= 0.3864, hGDH2-hGDH1/2 p= 0.1437, hGDH2-hGDH1+2 p= 0.1469, hGDH1/2-hGDH1+2 p= 0.7316

For Hill coefficient comparison between different enzymes hGDH1-hGDH2 p=0.7272, hGDH1-hGDH1/2 p=0.9711, hGDH1-hGDH1+2 p=0.8754, hGDH2-hGDH1/2 p=0.7602, hGDH2-hGDH1+2 p=0.6945, hGDH1/2-hGDH1+2 p=0.9096

Figure 39: Comparative kinetic studies of activation by L-leucine, in the presence of 50uM ADP, for different GDH preparations. The possible hetero-hexamer's (GDH1/2hetero) activation curve is strongly similar to that of in vitro hGDH mix's (GDH1+2mix), and both follow a pattern that resembles that of hGDH2 activation.

Table 8: L-leucine activation curves' characteristics (in the presence of 50uM ADP) and statistical analyses between different GDH preparations.
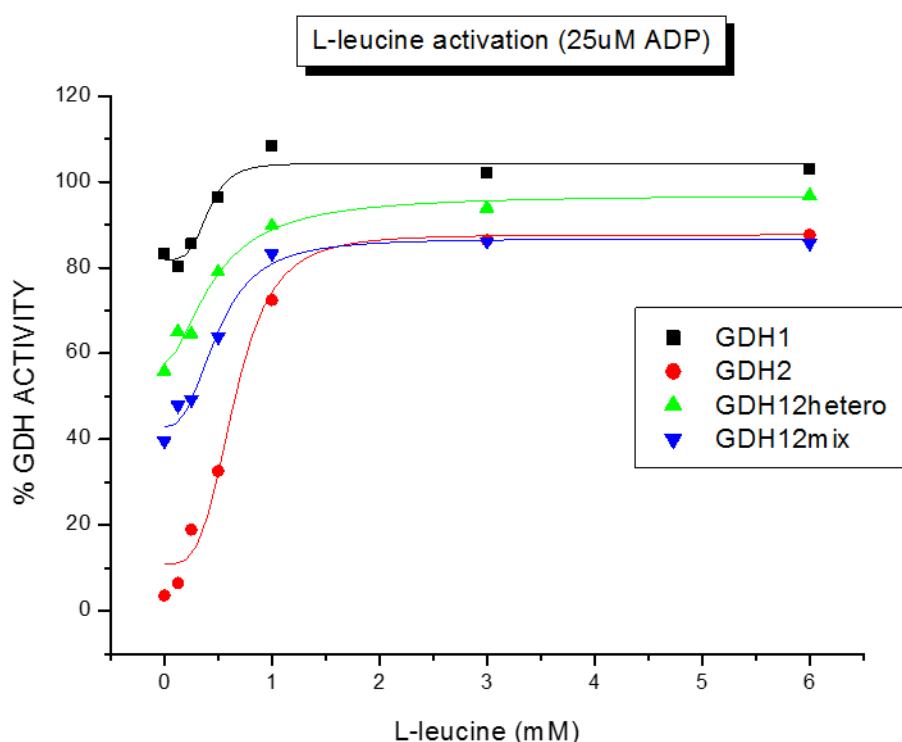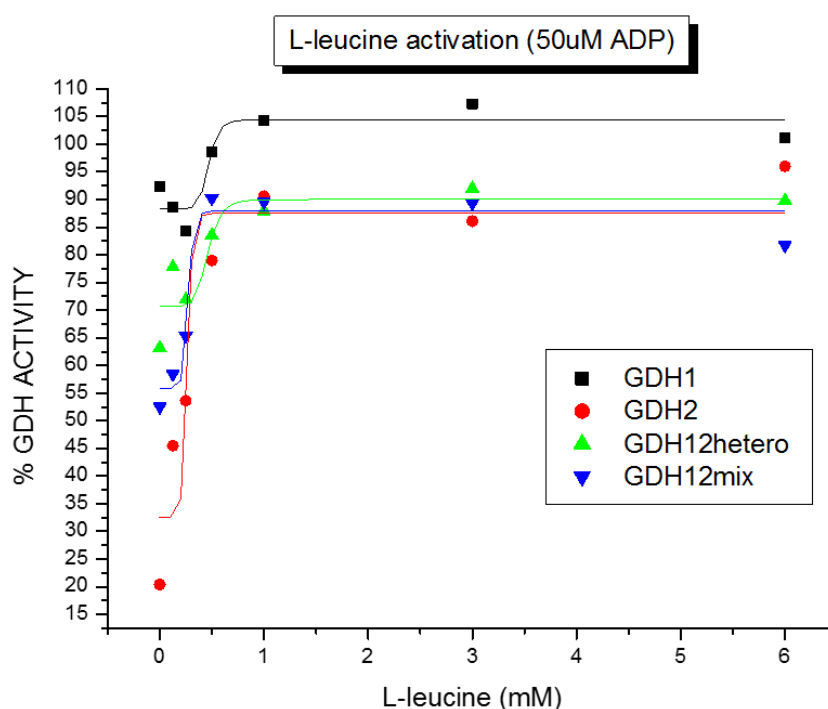
L-leucine activation curves (50uM ADP)				
	hGDH1	hGDH2	hGDH1/2 hetero-hexamer	hGDH1+hGDH2 mix
V_o	88.29 ±2.90	32.55 ±9.21	70.68 ±4.36	55.81 ±3.37
V_{max}	16.13 ±3.97	55.01 ±12.38	19.32 ±5.98	32.18 ±4.47
AC_{50} (uM)	0.47 ±0.75	0.26 ±0.47	0.46 ±0.31	0.27 ±0.32
Hill coefficient	10.04 ±243.80	10.87 ±415.88	7.60 ±57.67	10.48 ±146.90

The specific p values from the comparison of the different enzymes' AC_{50} and Hill coefficient are as following:

For AC_{50} comparison between different enzymes: hGDH1-hGDH2 p=0.8272, hGDH1-hGDH1/2 p=0.9919, hGDH1-hGDH1+2 p= 0.8207, hGDH2-hGDH1/2 p=0.7450, hGDH2-hGDH1+2 p=0.9875, hGDH1/2-hGDH1+2 p=0.6947

For Hill coefficient comparison between different enzymes hGDH1-hGDH2 p=0.9987, hGDH1-hGDH1/2 p=0.9927, hGDH1-hGDH1+2 p=0.9988, hGDH2-hGDH1/2 p=0.9942, hGDH2-hGDH1+2 p=0.9993, hGDH1/2-hGDH1+2 p=0.9863

Heat inactivation

Among their many enzymatic properties, the two human GDH enzymes have also been reported to differ in their resistance to heat inactivation, a characteristic also known as heat stability (Shashidharan et al. 1997). hGDH1 is highly stable when subjected to temperatures (47°C) higher than the physiological whereas hGDH2 is rather heat labile. In our experiments we confirmed the abovementioned observations (p=0.0005) and we further tested the possible hetero-hexamer's behavior against incubation at 47°C for a total of three hours, in comparison with the homo-hexamers' in vitro mixture. Results showed that the combined enzyme preparations both *in vivo* and *in vitro*, displayed equivalent instability pattern in this assay (p=0.2434), with their linear graphs lying in the middle ground between those of hGDH1 and hGDH2. Thus, it could be proposed that the possible hetero-hexamer resembles hGDH1 + hGDH2 mixture as far as their heat inactivation is concerned (Fig.40 and Table 9).
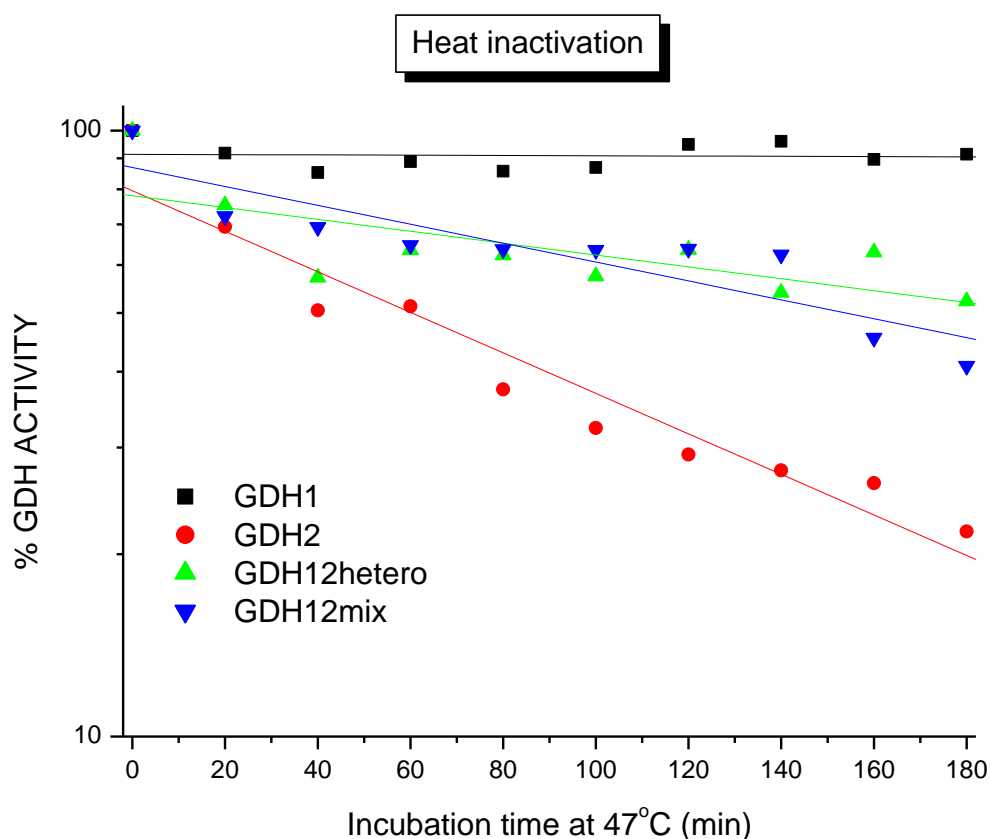
Figure 40: Comparative kinetic studies of heat inactivation at 47°C, for different GDH preparations. The possible hetero-hexamer's (GDH1/2hetero) heat sensitivity curve is almost identical to that of in vitro hGDH mix's (GDH1+2mix), and they both lie between homo-hexameric GDHs' curves.

Table 9: Heat inactivation linear fit characteristics on linearized scales [yscale(Y) = A + B * xscale(X)] and statistical analyses between different GDH preparations.

Heat inactivation curves				
	hGDH1	hGDH2	hGDH1/2 hetero-hexamer	hGDH1+hGDH2 mix
A	1.96 ±0.01	1.9 ±0.03	1.89 ±0.03	1.94 ±0.03
B (slope)	-0.00002 ±0.0001	-0.00334* ±0.0003	-0.00098*,** ±0.0003	-0.00156*,** ±0.0003

*$p < 0.05$ for the comparison with the corresponding value of hGDH1

**$p < 0.05$ for the comparison with the corresponding value of hGDH2

The specific p values are as following:

hGDH1-hGDH2 p=0.0005, hGDH1-hGDH1/2 p=0.0386, hGDH1-hGDH1+2 p=0.0082, hGDH2-hGDH1/2 p=0.0051, hGDH2-hGDH1+2 p=0.0137, hGDH1/2-hGDH1+2 p=0.2434

116

<u>Basal activity</u>

Basal activity, as defined by the enzymes' activity in the absence of allosteric enhancers, is critical for GDHs' function description and it is one of the main properties in which the two human isoenzymes present fundamental differences. As described earlier, hGDH1 maintains approximately 40% of its maximal activity in a basal state, whereas hGDH2 is barely active (4-8% of its maximal activity) under the same conditions (Shashidharan et al. 1997, Kanavouras et al. 2007). Interestingly, we observed that these differences are highly depended on the reaction temperature, as in lower temperatures hGDH2 displays an abnormally high basal activity, comparable to that of hGDH1. In contrast, when the same assays were performed at the most physiologically relevant temperature, which was 37°C, the basal activity differences were found as sharpened as previously reported. For that reason we performed comparative kinetic studies in different reaction temperatures, by incubation the reaction buffer in 20°C, 25°C, 30°C and 37°C (Fig.41). Results revealed that at 37°C, hGDH1/2 hetero-hexamer maintained a basal activity which was very similar to that of homo-hexamers' mixture, and which was taking intermediate values between the pure homo-hexameric preparations. hGDH1/2's basal activity (30,625±6,002274) was subtly higher than that of hGDH mixture (27.675±1,500767), yet that difference is not statistically significant (p=0.6504). This finding supports the implication that the two combined enzymatic preparations are comprised of equal proportions of each isoform, as they follow comparative kinetic patterns when assayed under specific conditions. Instead, each of the remaining enzymes' basal activities differed significantly from one another (Table 10).
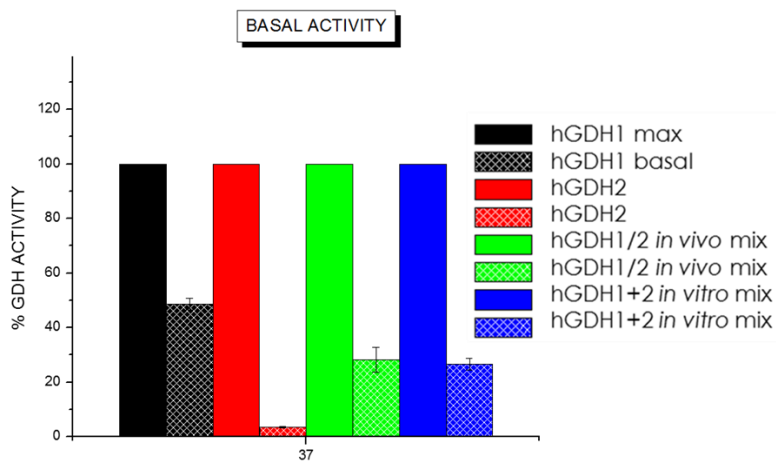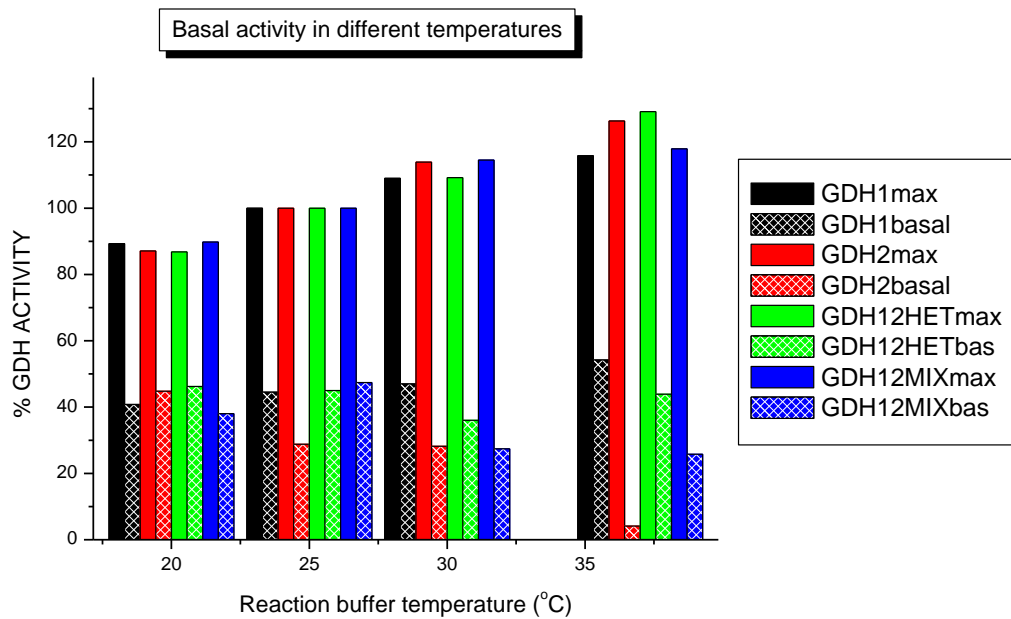
Figure 41: UP: Comparative kinetic studies of maximal and basal activity at different reaction temperatures for different GDH preparations. It is profound that basal activity of human GDHs is highly dependent on the reaction temperature, and has its lower value at 37°C, which is the most physiologically relevant. DOWN: At this temperature, the possible hetero-hexamer's (GDH1/2hetero) basal activity (as a percentage of its maximal) is similar to that of in vitro hGDH mix's (GDH1+2mix), presenting values which are intermediate between the respective homo-hexameric GDHs'.

Table 10: Basal activity characteristics at 37°C (in the absence of ADP) and statistical analyses between different GDH preparations.

Basal activity at 37°C				
	hGDH1	hGDH2	hGDH1/2 hetero-hexamer	hGDH1+hGDH2 mix
% of maximal activity	48.55 ±2.36	3.58 ±0.33*	28.15 ±5.00*,**	26.70 ±2.10*,**

*p<0.01 for the comparison with the corresponding value of hGDH1

**p<0.01 for the comparison with the corresponding value of hGDH2

The specific p values are as following:

hGDH1-hGDH2 p<0.0001, hGDH1-hGDH1/2 p=0.0093, hGDH1-hGDH1+2 p=0.0003, hGDH2-hGDH1/2 p=0.0027, hGDH2-hGDH1+2 p<0.0001, hGDH1/2-hGDH1+2 p=0.7981

<u>Reaction buffer characteristics</u>

Apart from the kinetic properties, we were interested in investigating the optimal reaction conditions, such as salt concentration and pH, of the possible hetero-hexameric GDH, in comparison with the pure homo-hexameric forms as well as their mixture.

Regarding buffer kind and salt concentration, basic 50mM TRA buffer, which is used in most kinetic assays, was replaced by Tris-HCl or $NAHPO_4$ pH 8. All enzymes showed an operation preference towards lower salt concentration environments (50mM) (Fig.42). In contrast, high concentrations hindered their function, which was more apparent for $NAHPO_4$ 250mM buffer. This possibly happens due to the instability of the respective enzymes as the solution ions might interfere with their subunits and hinder the closed conformation of the protein's structure. Statistical significance among the enzymatic activities assayed under different buffer compositions was not yielded for most enzymes except for those between hGDH1 and hGDH2 (p=0.015) and between hGDH1 and hGDH1/2 (p=0.055) at $NaHPO_4$ 50 mM, with the former being more active (Table 11). It is thus safe to assume that all enzymes operate alike as far as their ionic environment is concerned and salt levels effect apply in the same manner for human GDHs at the biochemical level.
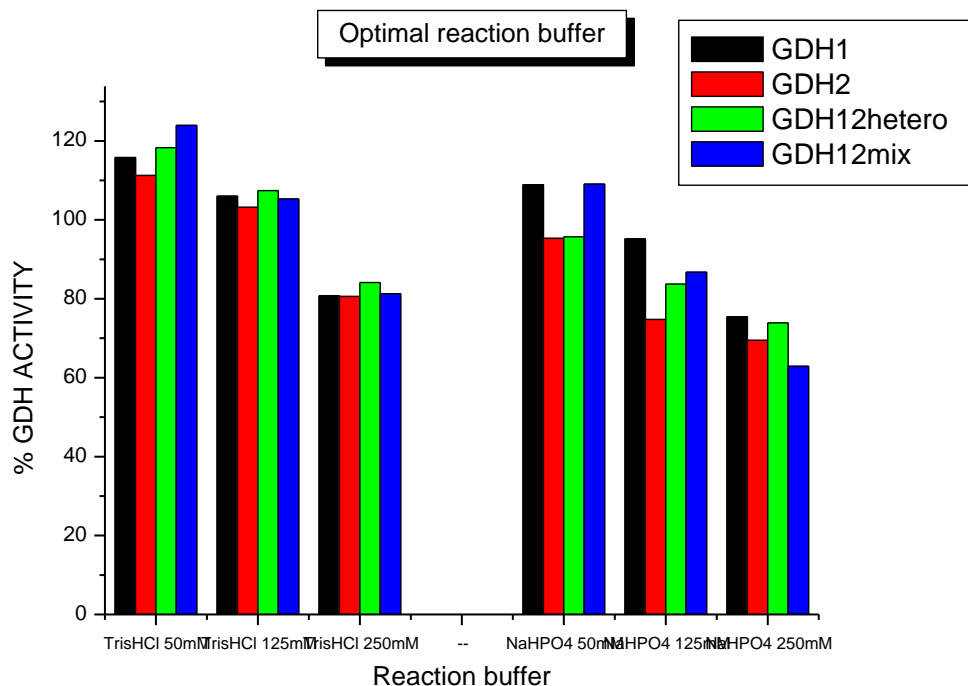
Figure 42: Comparative kinetic studies in different reaction buffers for different GDH preparations. All enzymes function optimally at low concentration (50mM) Tris-HCl environment. Most of the differences observed between the different enzyme preparations under the same conditions are not statistically significant.

Table 11: Statistical analyses between different GDH preparations under different buffer conditions.

Buffer	*P* hGDH1/2-hGDH1+2	*P* hGDH1/2-hGDH2	*P* hGDH1/2-hGDH1	*P* hGDH1+2 hGDH2	*P* hGDH1+2-hGDH1	*P* hGDH1-hGDH2
Tris-HCl 50mM	0,65562	0,491985	0,84162	0,275782	0,537152	0,665016082
Tris-HCl 125mM	0,863473	0,473115	0,858886	0,869193	0,959622	0,754160785
Tris-HCl 250mM	0,661936	0,609097	0,645989	0,832189	0,90382	0,973739202
NaHPO$_4$ 50mM	0,326133	0,938031	0,055046	0,314299	0,988793	0,015313188*
NaHPO$_4$ 125mM	0,673162	0,304527	0,328533	0,237238	0,475583	0,144625019
NaHPO$_4$ 250mM	0,097212	0,598382	0,728843	0,458735	0,728843	0,479391772

Regarding optimal pH, a rough assessment was performed on the maximal activity of the enzymatic preparations (1 mM ADP) in a wide range of pH (6-9), while a more detailed investigation was conducted at the basal activity level, at which subtle pH differences' impact (in the range of 7-8) was examined. Previous studies have revealed that hGDH2 operates optionally at more acidic environments as compared with hGDH1 (Poitry et al. 2000). In our experiments this finding was not replicated, as hGDH1 was found to operate better at pH 7.6, whereas hGDH2's activity showed a preference at pH 8, when both isoenzymes were assayed in respect with their basal activity. The possible hetero-hexamer's behavior to pH changes implied the fact that, like hGDH1+hGDH2 mixture, it presented a preference of intermediate pH values between the optimal ones for each isoform separately. Indeed, both GDH hetero-hexamer and the in vitro enzyme mixture reached a basal activity peak at pH 7.8, with the differences observed in their activities not belonging to the statistical significance spectrum (Fig.43,44 and Tables 12,13).

The most interesting kinetic features of different enzyme preparations are summarized in table 14.
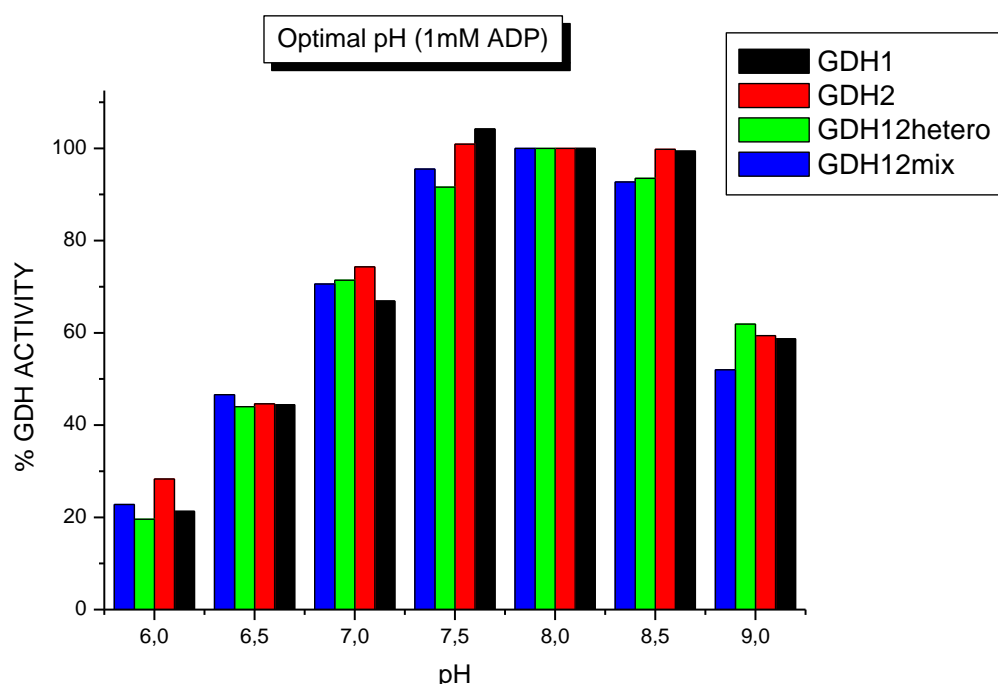
Figure 43: Comparative kinetic studies in different reaction pHs, in the presence of 1mM ADP, for different GDH preparations. The possible hetero-hexamer seems to optimally function at pH range 7.5-8.5, with a slight preference for the higher pHs. The vast majority of the differences observed between the different enzyme preparations under the same conditions are not statistically significant.

Table 12: Statistical analyses between different GDH preparations under pH conditions, in the presence of 1mM ADP.

pH	P hGDH1/2-hGDH1+2	P hGDH1/2-hGDH2	P hGDH1/2-hGDH1	P hGDH1+2 hGDH2	P hGDH1+2-hGDH1	P hGDH1-hGDH2
9	0,272932	0,550794	0,521031	0,247154	0,336129	0,890051441
8.5	0,642105	0,895871	0,932483	0,454091	0,542454	0,965764101
7.5	0,378014	0,074297	0,196334	0,312873	0,312873	0,670712564
7	0,511564	0,985017	0,294705	0,640075	0,588195	0,401795256
6.5	0,700608	0,588602	0,486232	0,759045	0,592824	0,977200157
6	0,186945	0,009551*	0,740129	0,070686	0,790784	0,282585232
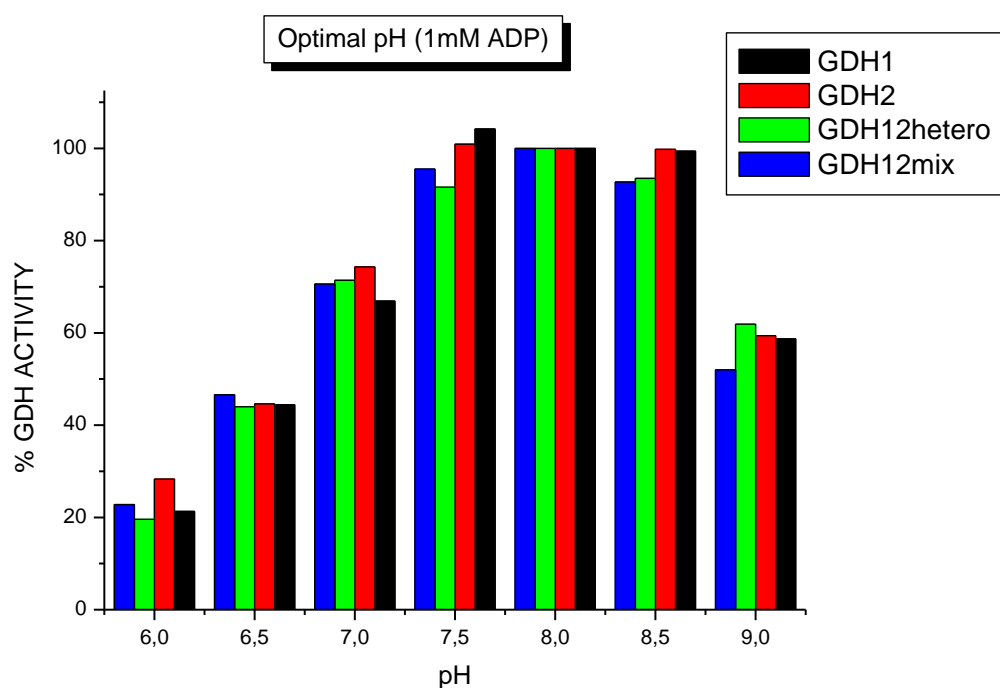
Figure 44: Comparative kinetic studies in different reaction buffers, in the absence of ADP, for different GDH preparations. The possible hetero-hexamer's optimal pH leans towards more alkaline conditions, presenting its highest activity at 7.8. Nevertheless, the differences observed between hGDH1/2 and hGDH1+2 in vitro mix, under the same conditions are not statistically significant.

Table 13: Statistical analyses between different GDH preparations under pH conditions, in the absence of ADP.

pH	P hGDH1/2-hGDH1+2	P hGDH1/2-hGDH2	P hGDH1/2-hGDH1	P hGDH1+2 hGDH2	P hGDH1+2-hGDH1	P hGDH1-hGDH2
7	0,2559	0,143416	0,071293	0,256005	0,003414*	4,06177E-05*
7.2	0,110262	0,019945*	0,056432	0,339651	0,020236*	0,000536955*
7.4	0,321988	0,116997	0,105866	0,266522	0,023182*	0,00822919*
7.6	0,234622	0,019929*	0,013153*	0,037013*	0,004372*	0,002447606*
7.8	0,585512	0,02929*	0,105333	0,020781*	0,028877*	0,00064267*
8	0,277956	0,037905*	0,177549	0,039062*	0,01892*	0,002307404*

Table 14: Summary of comparative kinetic characteristics of different human GDH preparations.

ASSAY	hGDH1	hGDH1+2 *in vitro* mix	hGDH1/2 *in vivo* mix	hGDH2
GTP inhibition IC_{50}	sensitive	Mildly sensitive	Mildly resistant	Resistant
GTP inhibition Hill Coefficient	Cooperative	Non-cooperative	Non-cooperative	Non-cooperative
Basal Activity	High	Intermediate	Intermediate	Low
DES inhibition	Resistant	Intermediate	Intermediate	Sensitive
Mn inhibition	Resistant	Intermediate	Intermediate	Sensitive
L-leucine activation	Resistant	Intermediate	Intermediate	Sensitive
Heat sensitivity	Resistant	Intermediate	Intermediate	Labile

4. STRUCTURAL STUDIES ON HUMAN GDHs

Conformations of GDHs in native form

Towards the production of high quality hGDH2 crystals (described later in this section), we seeked a way to evaluate the conformation of the enzyme in solution, since not all macromolecules behave alike. In fact, they may have a different conformation than molecular standards or exhibit unexpected column interactions. We performed SEC-MALS - the combination of Size Exclusion Chromatography with Multi-Angle Light Scattering analysis, which is an absolute technique for determining molar mass and rms radius in solution. We injected 100ul of a 5mg/ml highly purified (according to standard protocols) hGDH2 solution in 0.1M phosphate buffer pH 7. Apart from hGDH2, we also tested, with SEC/MALS, highly homogenous hGDH1 and industrially available bo-GDH, for comparison. Results showed that all enzymes behave according the expected hexameric conformation, presenting a major peak at approximately 350 kDA (Fig.45, 46). Bo-GDH is reflected by a single peak, representing a monodisperse sample (Fig.47.). On the other hand, both human GDHs reveal some minor extra peaks generated by laser detectors, which represent conformations of different molecular weights (Fig.45, 46). Most of them are products of higher molecular weight conformations, possibly representing multimers of the enzymes due to aggregation processes in the solution. For hGDH2 specifically, lower molecular weight structures are also present, whose existence could be attributed to degradation of the protein, since it is already known that it is rather prone to instability as a result of environmental factors' effect.
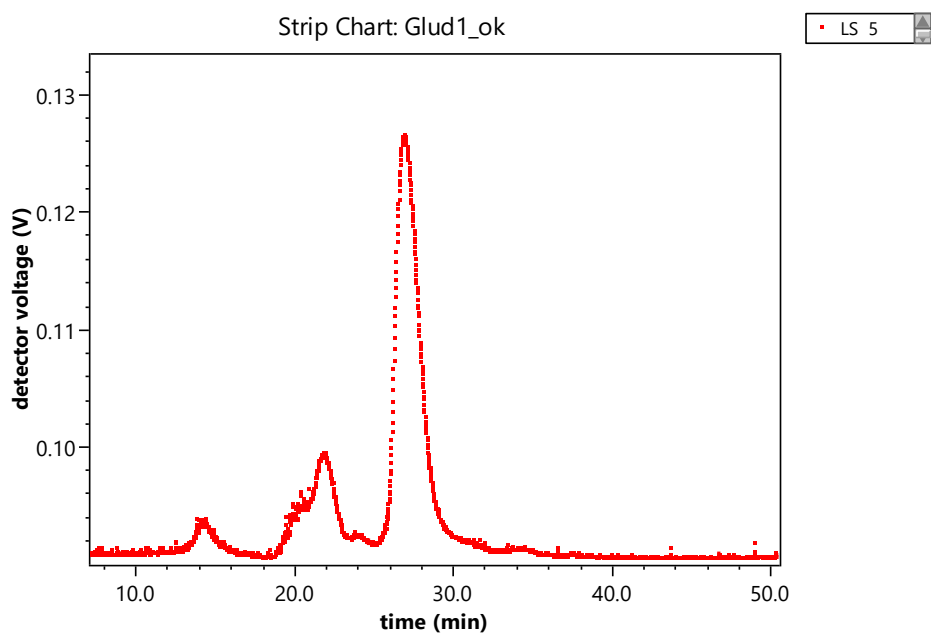
Figure 45: SEC/MALS chromatogram of hGDH1 in phosphate buffer pH 7. Native conformations of hGDH1 reveal that the sample consists of more than a monodisperse hexameric structure, as it shows multimeric macromolecular associations towards higher molecular weights.
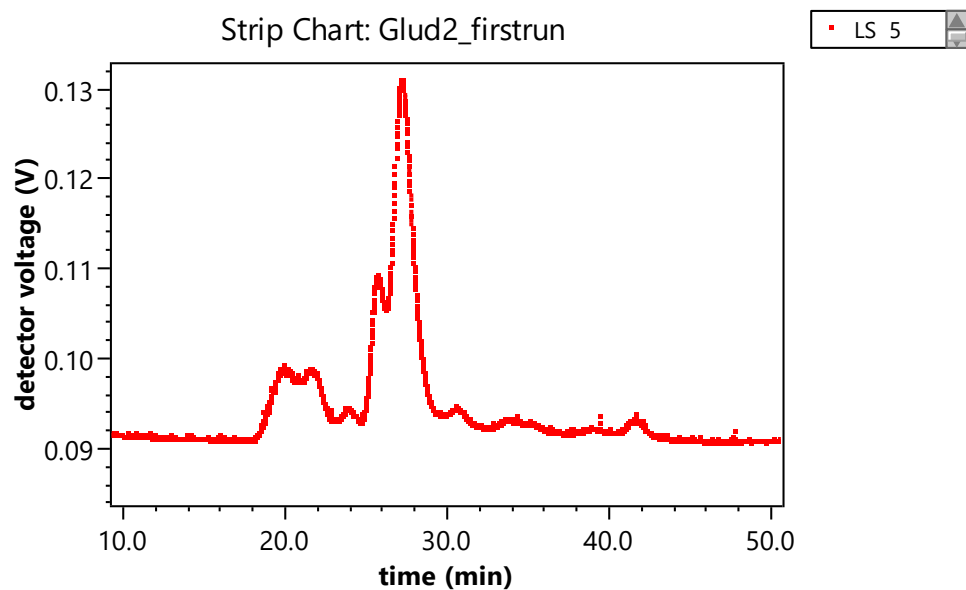
Figure 46: SEC/MALS chromatogram of hGDH2 in phosphate buffer pH 7. Native conformations of hGDH2 reveal that the sample consists of more than a monodisperse hexameric structure. Multimers and degradation products are evident from the extra minor peaks before and after the main hexameric form respectively.
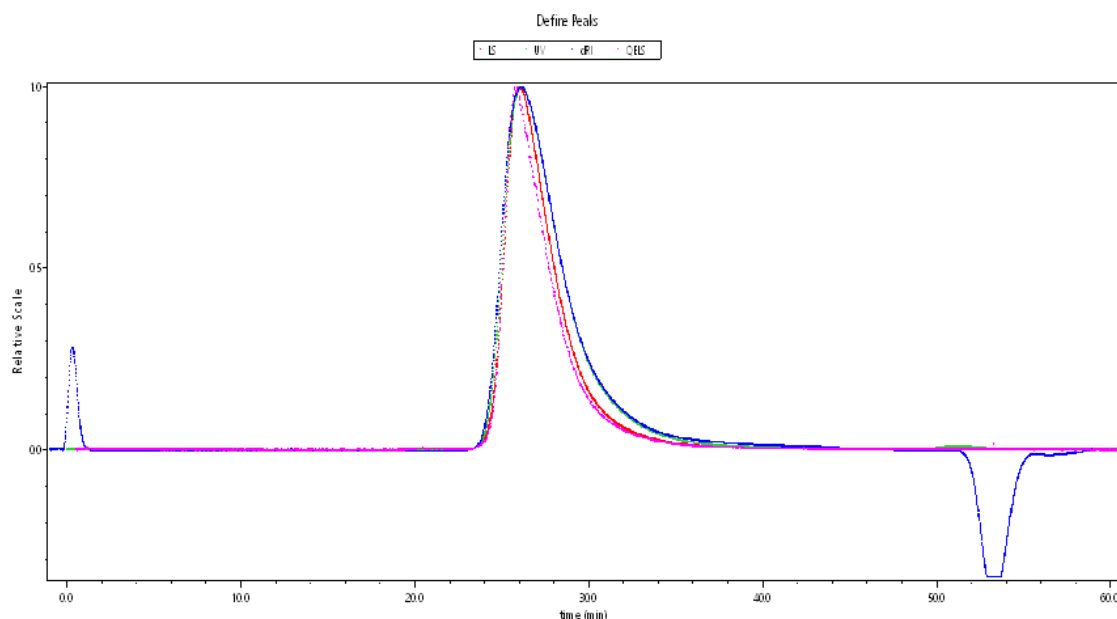
Figure 47: SEC/MALS chromatogram of boGDH in phosphate buffer pH 7. Native conformations of boGDH consist of a monodisperse hexameric structure.

In an attempt to examine whether this innovative method is also able to discriminate between the two human isoforms, and therefore whether it could be employed to study the possible hGDH1/2 hetero-hexamer, we experimented with a hGDH1 and hGDH2 in vitro mixture. As previously observed with blue native electrophoresis, hGDH1 and hGDH2 were not evidently separable by this method due to their similar molecular weight (Fig.48). The mixture produced a single hexameric peak as detected by laser beams, representing both human GDHs. The only slight difference from single enzyme runs was that this particular peak leans towards the lower molecular weights range, as if it consists of two molecules. The point at which a second arm is dimly visible could be the separation point of hGDH2 from hGDH1, with the latter being eluted hardly later from the size exclusion column. However, intermediate molecular weights as those expected for the possible hetero-hexamer would be impossible to separate from these homo-hexamers by this method.
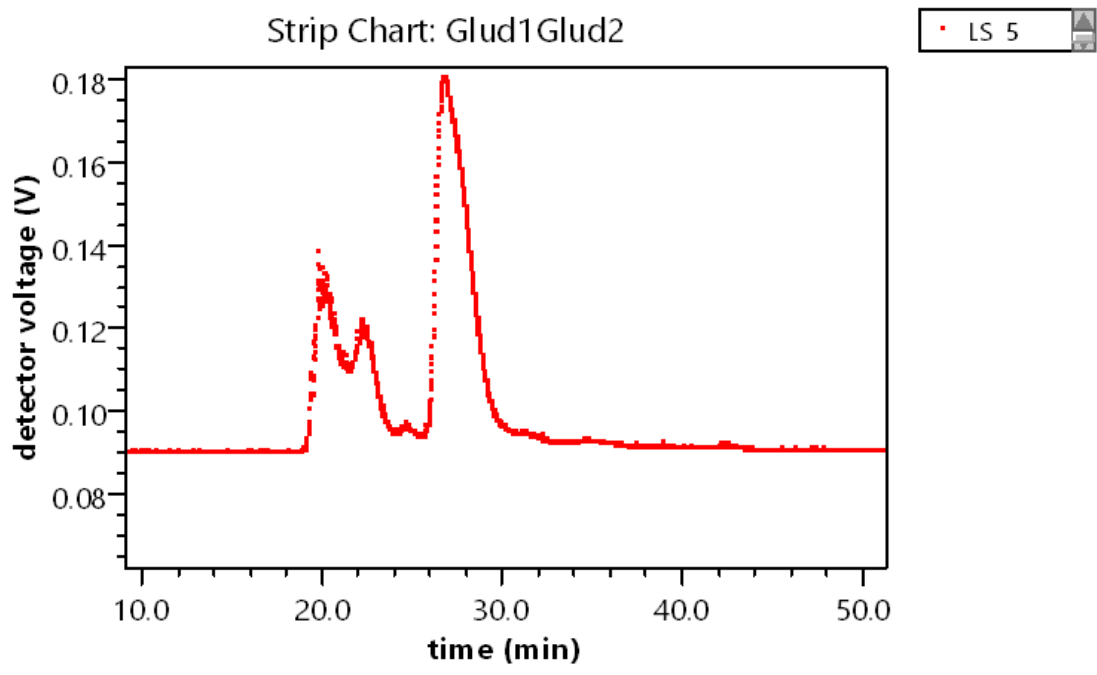
Figure 48: SEC/MALS chromatogram of hGDH1 and hGDH2 in vitro mixture, in phosphate buffer pH 7. The two isoforms do not differ adequately in their native molecular weight, and thus cannot be distinguishable with this method. Although one main hexameric peak is evident, it seems to lean towards the lower molecular weights range, as if it consists of two molecules.

Conformations of GDHs under different pH conditions

Based on previous studies, it is known that hGDH2 is sensitive to partial deactivation under changing environmental conditions including temperature, salt concentration and solution acidity. In order to whether this sensitivity is driven by structural deformations, we studied the different conformations acquired by hGDH2 and boGDH under different pH conditions, using SEC/MALS technology. We examined three different pH conditions, which were 6, 7 and 8 by dialyzing the enzymatic preparations against phosphate buffers of the respective pH values and by equilibrating the column with the same buffers each time. For boGDH we further advanced our study by dialyzing the sample back to pH 7 after it was first subjected to either pH 6 or 8. Indeed, these experiments showed significant pH dependence of GDHs' conformation, which, as previously proven, was more evident for hGDH2. Specifically, the main population in both samples was, as expected, the hexameric structures. When the pH was moving towards more acidic values, more populations consistent with lower molecular weight molecules, were present. The opposite was happening when the pH became more basic, namely bigger molecular weight populations were revealed (Fig.49). Consequently, these findings imply that acidic conditions favor procedures of GDH

127

degradation, whereas alkaline conditions seem to favor aggregation mechanisms. Another interesting finding was that when pH switched from 6->7 or from 8->7 for boGDH, the conformational effect was ameliorated, resulting in a single hexameric peak as if the structure has never been disrupted (Fig.50). This observation is of particular significance since it indicates that pH can act as a regulatory mechanism of GDHs, rendering them inactive when the physiological conditions are such that do support metabolic procedures to occur.
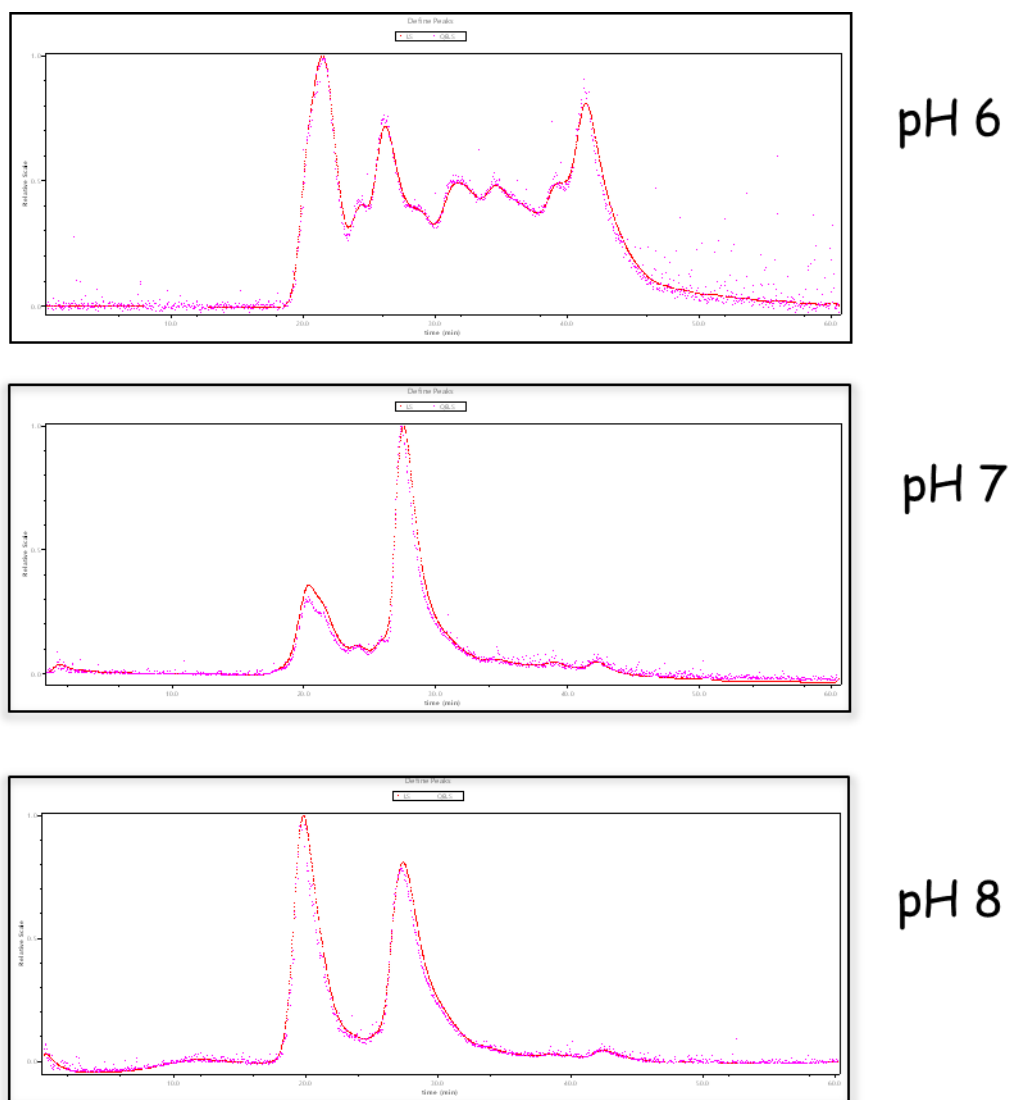
Figure 49: SEC/MALS chromatogram of hGDH2 under different phosphate buffer pH conditions. Different conformations of the same enzyme preparation are generated due to pH changes. Acidic pH magnifies the degradation effect normally observed in a purified hGDH2 preparation, whereas alkaline environment seems to favor aggregation procedures.
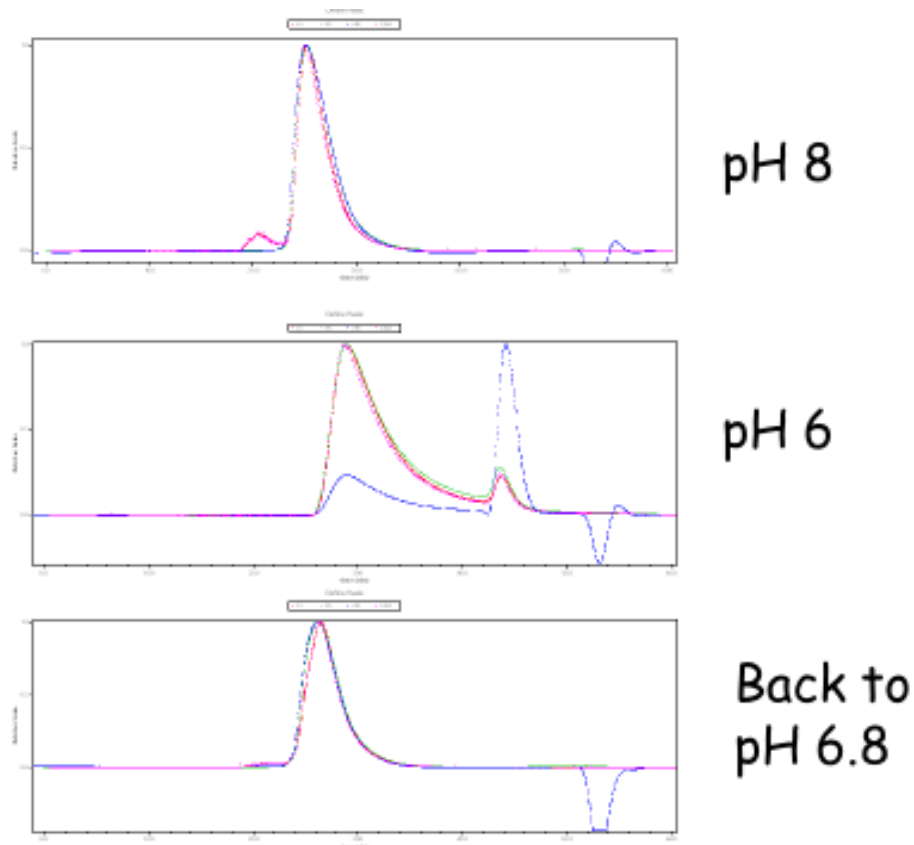
Figure 50: SEC/MALS chromatogram of boGDH2 under different phosphate buffer pH conditions. Acidic pH favors the enzyme's degradation and the production of lower molecular weight structures, whereas alkaline environment seems to favor aggregation procedures. When the enzymatic samples were returned back to pH 6.8, their physiological hexameric conformation was restored.

Crystallization of hGDH2

Crystallization of hGDH2 has been a long term aim and it has been attempted using several protein production systems and optimizations by Professor Kokkinidis' laboratory. Even though its highly homologous isoenzyme hGDH1 as well as boGDH have produced crystal structures in both apo-forms and bound with allosteric regulators (Smith et al. 2002; Peterson and Smith 1999; Smith et al. 2001; Banerjee et al. 2003; Li et al. 2011; Li et al. 2009), hGDH2 was rather resistant to crystallization. This could be partially attributed to its particular sensitivity to environmental factors, such as temperature, and to its overall instability. Another drawback was that it was laborious to produce as highly homogenous protein preparations as those required for data quality crystallization. After several unsuccessful trials, hGDH2 was eventually purified to homogeneity and it was crystallized under several conditions, similar to those under which hGDH1 has been previously crystallized (Smith et al. 2002). Specifically, initial

crystallization screening was performed using commercially available crystallization kits including Structure Screen 1 and 2, Grid screen Ammonium Sulfate, Grid screen MPD, Grid screen PEG 6000, GBS screen 3, 6, 7, 8, 9, 10, Grid screen PEG ion, MEB FAK and Natrix screen, from Molecular Dimensions. Additional screening was performed in OryXNano crystallization robot from Douglas Instruments, using the crystallization kits JBScreen JCSG++ HTS, Structure Screen 1, 2 MD1-30, 1-31, 1-32, 136 and MIDAS. Fruitful crystallization trials were obtained using

6-12% PEG 8000 (optimal at 8% and to a lesser extent at 10%)

MPD 2-15%

NaCl 200-800mM (optimal at 400mM)

Phosphate buffer 0.1 M, pH 7

Initial results presented with a difficulty in achieving high resolution structures of hGDH2, lying primarily on the generation of very thin, needle-like (Fig.51) crystals which are fragile and hard to handle, and the fact that these crystals do not consist of an adequate number of units in order to be thoroughly analyzed. It was observed that when trying to optimize the precipitants (PEG, MPD) effect, elevating PEG 8000 concentration worsened the crystals' image while elevating MPD was critical for obtaining better crystals. Data quality crystals of hGDH2 were obtained with 8% PEG 8000, 15% MPD, 0.4M NaCl and 0.1M phosphate buffer pH 7, using the hanging-drop vapour-diffusion method in 24-well Linbro cell-culture plates (Fig.52). The drops were made up of 2 ul protein solution of 9.7 mg/ml mixed with an equal volume of reservoir solution and were equilibrated against 1000 ul reservoir solution at 291 K. To establish the feasibility of crystallographic studies, there have been collected, for the first time, hGDH2 X-ray diffraction data in satisfying resolution (3.2 Å), which allowed the determination of the space group of the crystal as P2, and the first statistical analysis of the structure. This is an extremely promising ongoing analysis taking place by Professor Kokkinidis' laboratory experts, and as it is far beyond the purposes of the present thesis, will not be further discussed here.
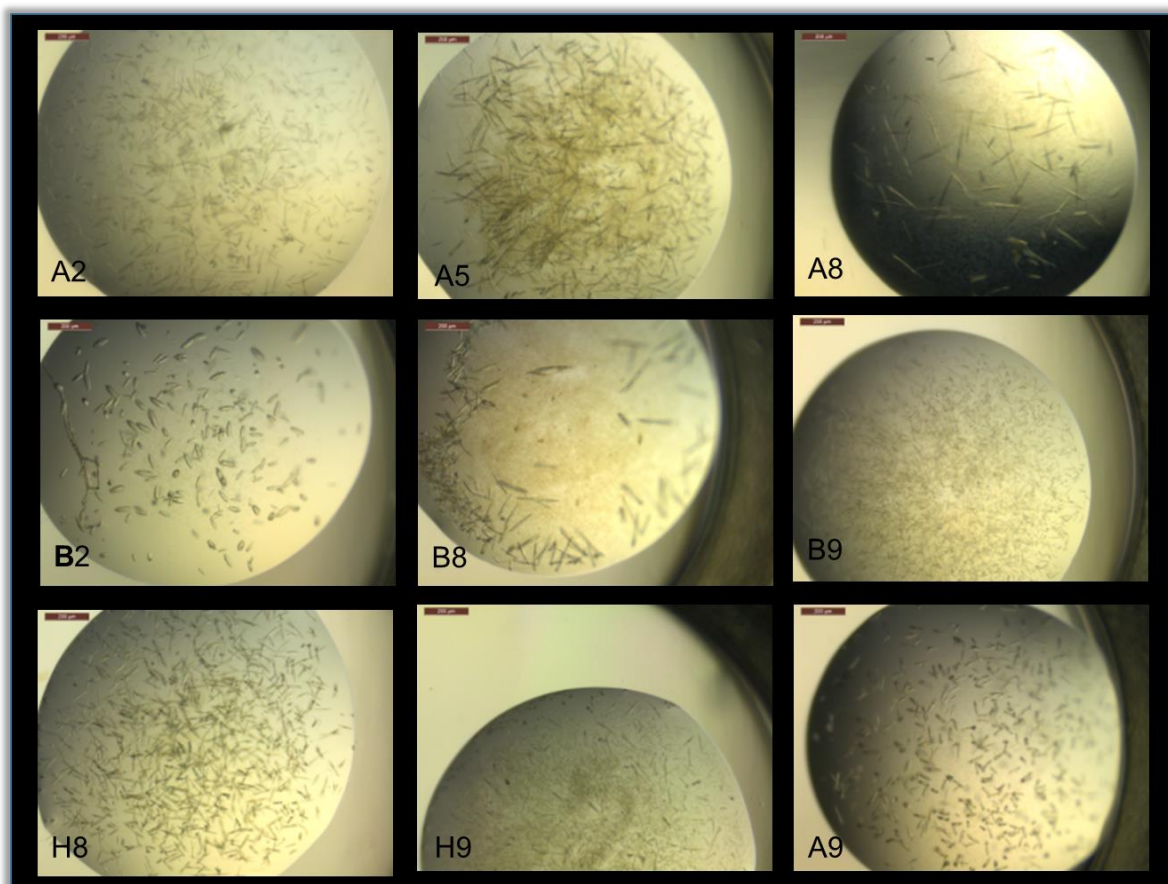
Figure 51: Initial hGDH2 crystallization screening results using JBscreen JCSG++ (200x30um). Fragile, difficult in handling, needle like crystals of hGDH2 were obtained under different conditions. Best samples were analyzed by synchrotron technology but yield 5 Å resolution, incapable of producing high quality structural data (provided by Dr. Sarrou, Dr. Kokkinidis group).
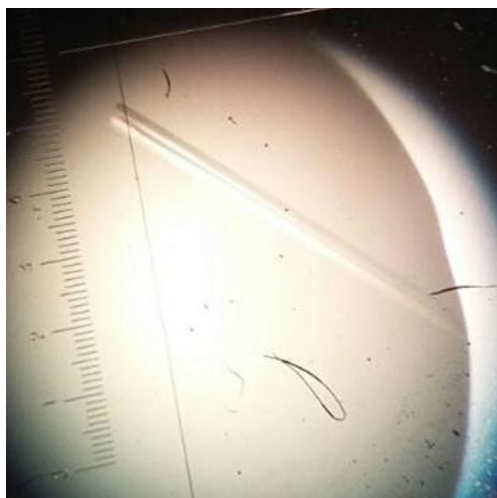
Figure 52: Needle-like crystals of hGDH2. X-ray diffraction data were collected from a single crystal using synchrotron radiation on the X06SA beamline at the Swiss Light Source, Paul Scherrer Institut, Villigen, Switzerland. The best data were in 3.2 Angstrom resolution and are consistent with space group P2 (provided by Ntina Kotsifaki, Dr. Kokkinidis group).

5. GENETIC ANALYSES OF GLUD1 AND GLUD2 AND AD-RELATED GENES IN THE CRETAN AGING COHORT

The final part of our results is dedicated to the genetic studies on human *GLUD1* and *GLUD2* genes. We were genuinely interested in unravelling the genetic variation's spectrum of these genes since each of them has been associated with pathological conditions in human. Specifically, *GLUD1* mutations are related to HI/HA syndrome manifestation (Stanley 2011) whereas a *GLUD2* variant Ser498Ala (formerly referred as Ser445Ala), confer increased risk for Parkinson disease earlier onset (Plaitakis et al. 2010).

Screening of *GLUD1* and *GLUD2* genes for variants, was performed by using 201 WES analyses, already available in Neurology laboratory, from a large scale genetic project (Thalis MNSAD). In addition, due to more powerful sample needs for valid associations between a polymorphism on *GLUD2* gene and dementia-state groups (discussed later), we extended our analyses in an additional similar cohort of 232 Cretan individuals. The characteristics of the different diagnostic groups in our sample of 433 individuals are shown in Table 15.

Table 15: Clinical and demographic characteristics of Cretan Aging genetic sub-cohort, grouped according to their diagnosis

	Dementia (n=126)	MCI (n=90)	Controls (n=217)
Females (%)	63.6	63.5	51.7
Mean age (y)	79.6 ± 6.3	70.9 ± 7.7**	67.9 ± 7.6*,**
Mean education (y)	4.9 ± 3.6	8.6 ± 4.7**	9.2 ± 4.6**
Age of onset (y)*	75.5 ± 10.2	-	-

* p<0.05 for the comparison with MCI group

**p<0.001 for the comparison with the dementia group

***Available for 104 patients

From the 201 well characterized individuals in our cohort (100 with dementia, 20 with MCI and 81 cognitively normal controls) with WES data available, 71 had a family history of dementia with at least one affected first degree relative. Specifically, 41 (41.0%) and 9 (45.0%) of the dementia and MCI patients, respectively, had at least one affected first degree relative, compared to 21 (25.9%) of controls. Both patient groups had higher frequency of positive family history for dementia in a first degree

relative compared to cognitively normal controls (25.9%; p=0.036 for the comparison with the dementia group).

On the basis of the detailed family history information on dementia-affected relatives for 187 out of the 201 participants we constructed 181 pedigrees. Of those 181 pedigrees, 35 (19.3%) had 2 or more dementia affected members. For the 100 patients with dementia, 85 pedigrees were constructed and of those, 11 (12.9%) included at least two first degree relatives of the index patient affected with dementia.

To characterize our sample, we chose first to identify putatively disease-causing variants in known AD associated genes. Regarding the three established early-onset familial AD causative genes (*APP, PSEN1* and *PSEN2*), we sought to identify genetic variants within our sample that either have already been characterized as pathogenic or are of unknown significance. Even though our cohort consists of an aging population whose age range exceeds the typical early onset AD age span, it is not unexpected for specific variants of these genes to be present in late onset AD (Gaitery et al. 2016; Van Cauwenberghe et al. 2016, Cruchaga et al. 2012). Table 16 summarizes the non-synonymous genetic variations detected within the coding region of the abovementioned genes. All genetic variants detected by WES, were subsequently validated by Sanger sequencing.

Table 16: Rare coding variants in *APP, PSEN1* and *PSEN2* and distribution to dementia, MCI and control groups.

GENE	chromosomal location	SNP nomenclature	c.DNA	Protein effect	Frequency Dementia	Frequency MCI	Frequency Controls	Algorithmic prediction (Polyphen2)	Population Frequency (ExAC)	Association with AD
APP	chr21:27354758	rs141331202	c.1123G>A	p.Val375Ile	**1/100**	0/20	0/81	Possibly damaging (0.521)	0.0000330 0	NA
APP	chr21:27269893	NA	c.2056C>G	p.Gln686Glu	0/100	**1/20**	0/81	Possibly damaging (0.623)	NA	NA
APP	chr21:27423395	NA	c.583A>G	p.Asn195Asp	0/100	0/20	**1/81**	Benign (0.000)	NA	NA
PSEN 1	chr14:73673178	rs17125721	c.953A>G	p.Glu318Gly	**3/100**	0/20	**2/81**	Benign (0.011)	0.0153	Increased risk in *APOE* ε4 carriers (Benitez et al. 2013)
PSEN 2	Ch1: 227069694	NA	c.86G>A	p.Arg29His	**3/100**	0/20	0/81	Probably damaging (0.994)	0.0000024 82	Not pathogenic/ Reported in AD&FTD mutation database
PSEN 2	chr1:227071449	rs58973334	c.185G>A	p.Arg62His	**1/100**	**1/20**	**3/81**	Benign (0.001)	0.009897	Unclear pathogenicity/ Reported in AD&FTD mutation database
PSEN 2	chr1:227081806	NA	c.1171T>C	p.Cys391Arg	0/100	**1/20**	0/81	Probably damaging (1.000)	NA	NA
APOE	chr19:45411987	rs267606664	c.434G>A	p.Gly145Asp	**1/100**	0/20	0/81	Probably damaging (1.000)	0.0003773	Co-segregation with Arg176Cys (Iron et al. 1995)

APP protein (the product of the *APP* gene) is the precursor of the Aβ peptide, that forms the amyloid plaques that are considered a hallmark of AD pathology. The Aβ peptide derives from APP through proteolytic processing by the γ-secretase, a key component of which are presenilin 1 and presenilin 2 (encoded by the *PSEN1* and *PSEN2* genes, respectively). It is not thus unexpected that the amyloidogenic pathway where the protein products of these 3 genes play a major role has occupied center-stage in the discussion about AD pathogenesis. The availability of the WES approach, as employed here, enables the probing of these genes in search for private mutations that would otherwise elude traditional genetic research approaches, such as Genome-Wide Assosciation Studies (GWAS).

Regarding the *APP* gene, 51 AD-causing mutations in 121 families have been described so far (http://www.molgen.vib-ua.be/ADMutations/; Cruts et al. 2012), in addition to a rare protective variant (p.Ala673Thr) observed in Iceland (Johnsson et al. 2012). Most of these mutations, encoded by exons 16 and 17, cluster in the part of the protein that undergoes processing during amyloidogenesis. In our cohort, the, previously non-characterized, p.Val375Ile, p.Gln686Glu and p.Asn195Asp *APP* gene variants were detected in a patient affected with dementia, a patient affected with MCI and a cognitive normal control, respectively (Table 16). According to Polyphen2 predictions, p.Val375Ile and p.Gln686Glu are classified as possibly damaging for the protein product, (Table 16). In addition, p.Gln686Glu is flanked by disease-causing *APP* mutations (http://www.alzforum.org/mutations), resides at the site of cleavage by α-secretase (Nussbaum and Ellis 2003), and is thus expected to affect amyloidogenic processing of APP. In contrast, p.Asn195Asp, found in one control subject, is predicted by Polyphen2 to be a benign polymorphism.

PSEN1 mutations are the most common cause of early-onset autosomal dominant AD, with 219 mutations in 480 families described thus far (http://www.molgen.vib-ua.be/ADMutations/; Cruts et al. 2012). These mutations show essentially complete penetrance and early disease onset (25-65 years of age; Van Cauwenberghe et al. 2016). Only the *PSEN1* p.Glu318Gly variant was present in our sample in three dementia patients and in two normal controls (Table 16). The coexistence of the *APOE* ε4 allele with the *PSEN1* p.Glu318Gly occurred in one of our dementia cases, a coexistence that has been previously characterized by Benitez et al. (2013) as associated with increased risk of developing AD. However, this finding was not replicated in a follow-up study (Hippen et al. 2016). Also, in the Finish, Italian and Australian populations, the possibility was raised that the *PSEN1* p.Glu318Gly variant

was a risk factor associated with familial AD (Helisalmi et al. 2000; Taddei et al. 2002; Albani et al. 2007). However, these findings were not verified in other populations (Mattila et al. 1998; Dermaut et al. 1999; Zekanowski et al. 2004; Jin et al. 2012). The p.Glu318Gly variant is located on exon 9 of *PSEN1*, is not evolutionary conserved and is predicted to be benign for the protein's function, according to Polyphen2.

In contrast to *PSEN1* mutations, *PSEN2* AD-causing mutations show incomplete penetrance and are associated with a significantly older disease onset (39–83 years; Van Cauwenberghe et al. 2016). Among the three autosomal dominant AD causative genes, *PSEN2* showed the most missense variants in our sample, with these variants spanning the whole length of the gene and, some of them, being detected in several individuals.

Specifically, a very rare variant of *PSEN2*, p.Arg29His, was present in three individuals with dementia, while it was absent from normal controls (Table 16). This variant has also been reported by Guerreiro et al. (2010), but it has not been studied. Being in an extremely conservative position, Polyphen2 prediction for p.Arg29His indicates that it is probably damaging for the protein product. However, AD&FTD mutation database (http://www.molgen.vib-ua.be/ADMutations/; Cruts et al. 2012) classifies it as not pathogenic, and in support of that, another variation in the same position, Arg29Cys has been also reported (http://databases.lovd.nl/whole_genome).

PSEN2 p.Arg62His was present in one subject from dementia and one from MCI groups of our cohort, whereas three normal controls were also carriers. This variant has been previously reported in the literature by different researchers (Cruts et al. 1998; Sassi et al. 2014; Sleegers et al. 2004) and AD&FTD mutation database classifies it as variant of unknown pathogenicity. Residue 62 of presenilin 2 is not conserved among different species and another variation in human *PSEN2* that occurs at the same position and causes the substitution of arginine to cysteine, has also been reported as benign (Sassi et al. 2014; Sleegers et al. 2004). Algorithmic predictions by Polyphen2 indicate that *PSEN2* p.Arg62His is a benign variant. Also, it seems not to lead to any functional effect on the protein (Walker et al. 2005). However, there is possibility that it could be a disease modifier by decreasing AD disease onset (Cruchaga et al. 2012).

Lastly, in a subject with MCI, a unique variant of *PSEN2* (p.Cys391Arg) was detected that has not been previously reported in the literature and is absent from AD&FTD

mutation database, dbSNP or ExAC browser. Polyphen2 prediction places it at a very high risk of being damaging, according to the conservativity profile of 391 amino acid positions. Its presence in the MCI subject does not necessarily excludes the scenario of probable pathogenicity, given that this individual could develop dementia in the future.

As an additional step towards validating our cohort for known genetic risk factors for AD, the frequency of the *APOE* ε4 allele (which approximately triples the risk for AD) was assessed in dementia, MCI and control subjects. Results showed that *APOE* ε4 allele was present in heterozygous state in 37 out of the 201 samples of our cohort. Of these, 25 belonged to the dementia group (25.0% of tested dementia individuals), 5 to the MCI group (25.0% of tested MCI individuals) and 7 to the control group (8.6% of tested control individuals). In accordance with previous studies (Saunders et al. 1993; Corder et al. 1993; Bettens et al. 2013) the ε4 allele was significantly more frequent in the former group (p=0.006; Fig.53). This can be considered an external validator of the genetic composition of our patient cohort, since it replicates the results of similar studies in other populations (Bertram et al. 2007). *APOE* genotyping was validated for all subjects by PCR/RFLP using HhaI restriction enzyme (Fig.54), as previously described by Kim et al. (2010).
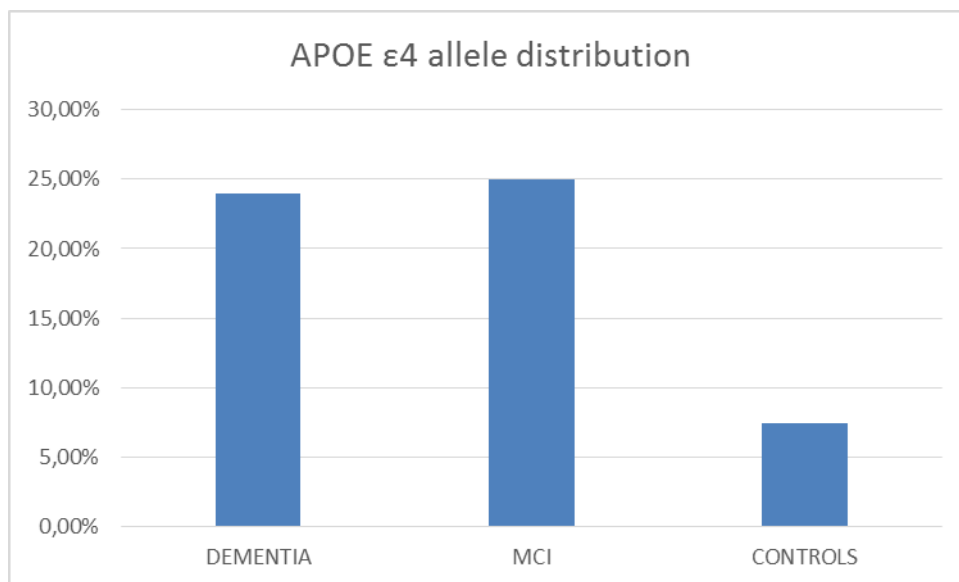
Figure 53: *APOE* ε4 allele distribution in 201 Cretan subjects (100 affected with dementia, 20 diagnosed as MCI and 81 cognitively non-impaired controls) analyzed by WES in this study. Data revealed that, as expected, dementia subjects had a higher frequency of the *APOE* ε4 allele compared to controls (p=0.006). In addition, the *APOE* ε4 allele had a tendency to be more frequent in the MCI group compared to controls (p=0.058), whereas MCI and dementia groups showed very similar ε4 allele distribution.
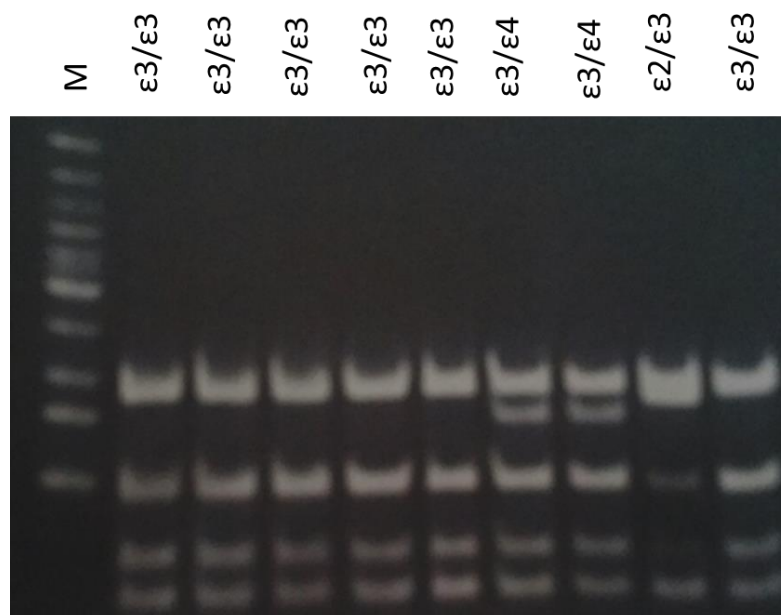
Figure 54: APOE genotyping by PCR-RFLP. APOE genotypes were determined by the patterns of restriction fragments [ε3/ε3 (91, 48, and 35 bp), ε2/ε3 (91, 83, 48, and 35 bp), and ε3/ε4 (91, 72, 48, and 35 bp)]. Lane M is Low Molecular Weight DNA Ladder (NEB, USA). The restriction fragments were identified with 13% polyacrylamide gel electrophoresis and 3X gel red staining.

In addition to ε4 genotyping, we screened the *APOE* gene for missense variants and we detected the p.Gly145Asp alteration in one individual with dementia (Table 17). *APOE* p.Gly145Asp has been previously reported by Iron et al. (1995), who have observed that it co-segregated with p.Arg176Cys (Weisgraber allele). In contrast, in the case we report here, the p.Gly145Asp carrier's genotype was ε3/ε3. Of note, Polyphen2 algorithm indicates that this is a probably damaging variant for apolipoprotein E.

Having described the AD-related genetic background of our subjects, we then proceeded to analyzing their genetic variations lying on *GLUD1* and *GLUD2* genes. In the *GLUD1* gene, only one variant (p.Asp341Gly) was present only in a normal control. This variant, even though novel, is predicted to confer a benign alteration to the protein, according to algorithmic predictions (Table 16). Also present in our cohort was a rare, not previously studied, variant of *GLUD2* (p.Asp414Gly) which was uniquely present in a patient affected with dementia and is probably a benign polymorphism, according to Polyphen2 predictions. A previously described variant in the leader peptide of

GLUD2 (p.Gly35Arg) was as common in dementia patients as in controls (Table 17). This variant has also been found in the past not to affect the frequency or the age at onset of Parkinson's disease (Plaitakis et al. 2010). In addition, this polymorphism has been shown recently not to affect the targeting efficiency of the mitochondrial peptide of hGDH2 (Kalef-Ezra et al. 2016). Also common in our cohort was the *GLUD2* p.Ser498Ala, which has been previously described by Plaitakis et al. (2010) as a modifier of PD age of onset for hemizygous males. p.Ser498Ala was also confirmed by PCR/RFLP (Fig.55) using AciI restriction enzyme (described by Plaitakis et al. 2010).

Regarding common variants that were detected on human *GLUD* exons (*GLUD2* c.1492T>G, GLUD2 c.103G>A), we investigated whether any of them tend to associate with clinical parameters in which GDH is suspected to play a role. Based on literature indications that GDH is indirectly related to neurodegeneration, we initially examined the variants distribution between the groups of affected with dementia, MCI and non-affected individuals of our cohort.

Interestingly, the *GLUD2* Ser498Ala variant, which has been previously described as an accelerating factor for Parkinson's disease in hemizygous males (Plaitakis et al. 2010), was more frequent in cognitively normal individuals in our cohort (Table 17). Specifically, it was present in 3 (3.0%) dementia patients, 3 (15.0%) MCI patients and 13 (16.05%) controls (p=0.03 for the comparison between the dementia and control groups).

In light of these results, we then expanded the *GLUD2* Ser498Ala genotype analysis on a second well-characterized cohort of 232 aged adults (26 with dementia, 70 MCI and 136 cognitively normal controls), also residing in the prefecture of Heraklion, Crete and characterized in a manner similar to the Thalis/MNSAD cohort (Simos et al. in preparation). The Ser498Ala *GLUD2* genotype in the combined cohort of 433 individuals was in Hardy-Weinberg equilibrium (data not shown). In this combined cohort, Ser498Ala was present in 6 (3.8%) of the 206 dementia X chromosomes, in 7 (5.1%) of the 136 chromosomes of the MCI group and in 25 (7.0%) of the 355 chromosomes of the cognitive normal controls (Fig.56; p=0.053 for the comparison between dementia and controls). The difference in Ser498Ala genotype was significant only in males and not in females (Fig.56). Specifically, none (0%) of the 46 males affected with dementia X chromosomes had the Ser498Ala *GLUD2* genotype, compared to 7 (8.9%) of the 79 male control individuals' chromosomes (p=0.046;

Fig.56). It should be noted that, due to the need for larger population associations, this is an on-going project. We aim to genotype additional Cretan Aging individuals from Thalis cohort, whose blood sample is already available in our laboratory, in order to increase our power analysis.

Table 17: *GLUD1* and *GLUD2* variant spectrum in 201 Cretan individuals from the CAC/genetic sub-cohort. One novel genetic variant (Asp341Gly) was detected on *GLUD1*, while *GLUD2* carried two previously described SNPs (Ser498Ala, which has been associated with Parkinson's disease onset; Plaitakis et al. 2010, and Gly35Arg) and one (Asp414Gly) not yet characterized.

GENE	Chromosomal Location	SNP rs	c.DNA	Protein effect	ExAC Frequency	Frequency Dementia	Frequency MCI	Frequency Controls
GLUD1	10: 88820709	NA	c.1022A>G	p.Asp341Gly	NA	0/100	0/20	1/81
GLUD2	X: 120181641	rs191769566	c.103G>A	p.Gly35Arg	0.1209	14/100	6/20	7/81
	X: 120183030	rs9697983	c.1492T>G	p.Ser498Ala	0.0276	**3/100**	**3/20**	**13/81***
	X: 120182779	rs62623672	c.1241A>G	p.Asp414Gly	0.0022	1/100	0/20	0/81
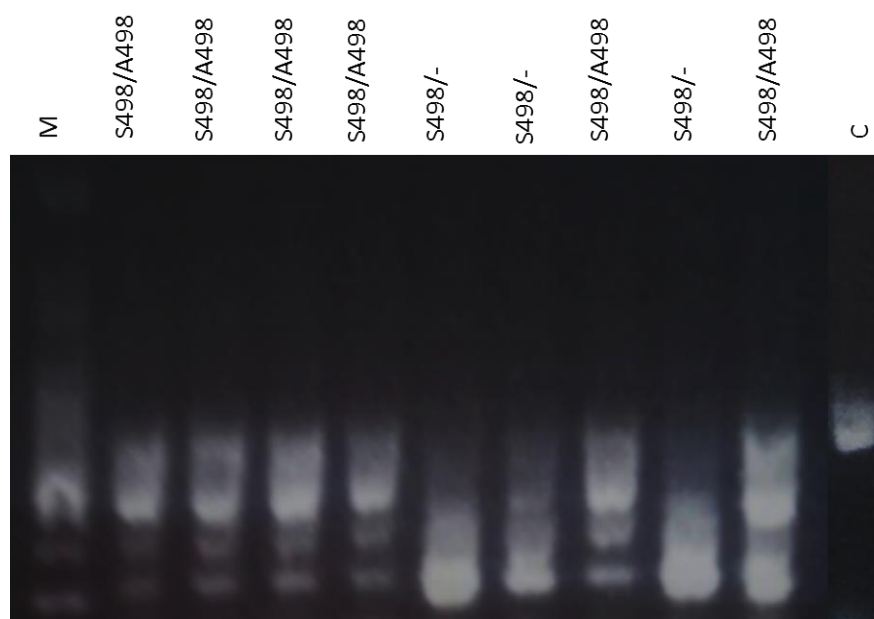
Figure 55: *GLUD2* p.Ser498Ala genotyping by PCR-RFLP. Genotypes were determined by the patterns of restriction fragments produced by AciI. [Ser498/Ala498 (527, 204 and 323 bp), Ala498 hemizygous (204 and 323 bp), and Ser498/Ser498 or Ser498 hemizygous (527 bp)]. All women carrying the polymorphism were heterozygotes. Lane M is 100bp DNA ladder (Nippon Genetics, Germany). Lane C is added for restriction pattern comparison with a non-carrier. The restriction fragments were identified with 1% agarose gel electrophoresis.
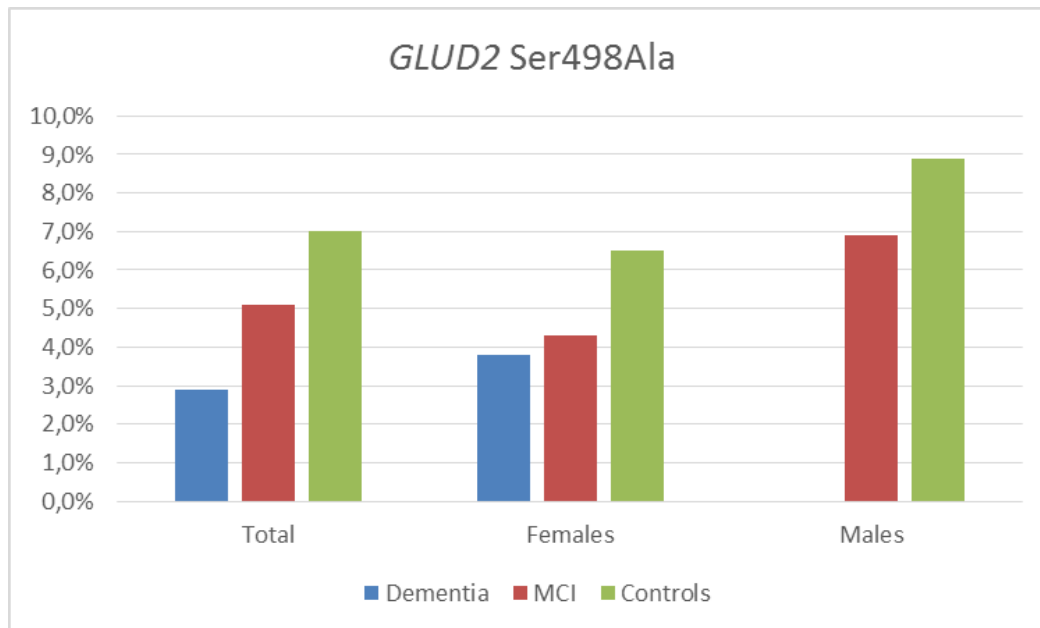
Figure 56: Genotyping analyses of 433 individuals (126 dementia patients, 90 diagnosed with MCI and 217 controls) from both the Thalis/MNSAD and Interreg «ΣΚΕΨΗ» cohorts revealed that the *GLUD2* Ser498Ala polymorphism showed a tendency to be more frequent in cognitively non-impaired participants' chromosomes compared to dementia affected individuals' chromosomes (p=0.053). In contrast, when participants diagnosed with MCI's chromosomes were compared with either dementia patients' or controls' chromosomes, they did not show significant differences in respect to their Ser498Ala genotype. When the results were analyzed by gender, the difference in Ser498Ala *GLUD2* frequency was significant in males but not in females (in males, 0% of dementia patients and 8.9% of controls had this variant, p=0.046). The total sample of 433 participants contains 10 male hemizygotes (G- genotype), 2 female homozygotes (GG genotype), and 24 female heterozygotes (GT genotype).

In addition, we investigated whether p.Ser498Ala can also affect the age of dementia onset in our cohort. Results showed that there were no statistically significant differences between the mean ages of onset of polymorphism carriers versus those who did do have it (mean age of dementia onset for Ser498Ala carriers= 76.2 ± 7.0 years, mean age of onset for non-carriers= 75.3 ± 4.0 years, p=0.8296).

GLUD2 c.103G>A on the other hand seem to have a very similar distribution between affected and non-affected individuals (p=1).

This work is dedicated to a thorough investigation of the structural, functional and genetic properties of human GDHs. Advances from this research aimed in contributing to a better understanding of mitochondrial function in respect to metabolic processes in which this system is involved. We specifically addressed the question whether hGDH1 and hGDH2 are in the form of homo- or hetero- hexamers when they are co-expressed and what advantageous enzymatic characteristics they may acquire by forming macromolecular hetero-complexes. Also, the structural basis of the two isoforms' diversity was approached by crystallization of hGDH2, which in comparison with hGDH1 structure is expected to provide definite answers to the question why such homologous enzymes present so different regulation properties. Finally, we addressed the question whether the GDH system is involved in the pathogenesis of major human disorders such as AD. Establishing GDH malfunction in AD could open a new field in the research towards a better understanding of the disease.

To our knowledge so far, humans possess two enzyme isoforms with glutamate dehydrogenase activity, named hGDH1 and hGDH2 (Shashidharan et al. 1997). The two isoforms display distinct regulation properties, optimal functioning conditions as well as tissue expression patterns (Zaganas et al. 2014). Previous studies using a specific anti-GDH2 antibody have revealed that GDH2 is expressed endogenously in human neural and testicular tissues. In fact, for testis a 1:1 ratio of the two isoforms was reported from both crude extracts and from mitochondrial fractions (Spanaki et al. 2010). In this study we provide evidence on the existence of hetero-hexameric forms of human GDHs isoenzymes, after their 1:1 co-expression, with possibly unique enzymatic properties.

The rationale behind the investigation of hGDH1/2 hetero-hexamers existence was that on one hand both isoforms are available in the mitochondrial milieu of some tissues, and on the other hand such structures between highly homologous enzymes are theoretically expected to occur. Given that GDH acquires its hexameric functional form in the mitochondrial matrix, it can be postulated that when both monomeric isoforms are available, the physical rules governing protein-protein interactions can

possibly lead the interwining of different subunits towards the formation of a hetero-hexameric holo-enzyme. If we consider that hGDH1 and hGDH2 monomers, due to their homology, should be characterized by similar site-specific hydrophobicity, size, and H-bonds' location (Zhanhua et al. 2005), which are fundamental factors for subunit interaction to form a fully functional quaternary protein structure, it can be predicted that there should be no major obstacles in the generation of both homo- and hetero-hexamers of GDH, in the cell types where both are present.

For our experiments' purposes, we initially achieved a 1:1 co-expression of hGDH1/hGDH2 enzymes in the Sf21 culture system, using a dual vector (pFastBacDual) carrying both *GLUD1* and *GLUD2* cDNAs. Subsequently, we approached the investigation of GDH hetero-hexamers existence by employing two different methods, both relying on affinity properties of the two different homo-hexamers, in order to strengthen our experimental results. The affinity properties were chosen carefully and were such that they would differ between the two separate isoenzymes, so that we would be accordingly able to discriminate between the possible hetero-hexamers and the in vitro mixture of separately expressed GDH isoforms.

Co-IP experiments, revealed that hGDH1/2 possible hetero-hexamer was able to precipitate along with anti-GDH2 specific antibody, rendering hGDH1 subunits participating in its structure visible, when subjected to western blot with a non-specific hGDH antibody. In contrast, a simple in vitro mixture of the homo-hexameric enzymes was not respectively precipitated, as only hGDH2 was detected in the IP pellet, whereas hGDH1 remained in the supernatant. This finding implies that the bonds developed between the subunits of the possible hetero-hexamer were such that drawn hGDH1 parts in the IP pellet, even though they are not recognized by anti-GDH2 antibody. Therefore, it could be postulated that this enzymatic sample represents a holoenzyme comprising of two different types of subunits. In the case of the in vitro mixture of homo-hexamers, hGDH1 and hGDH2 represented two distinct holoenzymes, thus the enzyme subunits were not as strongly associated so that they would precipitate together by the IP with anti-GDH2 antibody.

GTP affinity chromatography experiments provided further support for the existence of hetero-hexamers of the hGDH1 and hGDH2 isoenzymes. GTP sepharose resin was used for this set of experiments, due to the selective affinity of GTP for hGDH1, as implied by several studies which report that hGDH1 is particularly sensitive to this molecule (Zaganas and Plaitakis 2002). When subjected to this assay, each enzyme

preparation displayed a different elution pattern, characteristic for the respective sample constitution. In particular, hGDH1, being highly GTP associated, was bound potently on GTP resin and was eluted after the application of a KCl gradient solution. hGDH2 was immediately eluted in the flow through, being only marginally bound on GTP. Hetero-hexameric GDH was also eluted in the flow through, presenting low affinity for GTP. In contrast, hGDH1 and hGDH2 *in vitro* mix was eluted in two separate peaks, one detected in the flow through, following hGDH2's pattern, and the other was eluted after the application of KCl gradient buffer, following hGDH1's pattern. This outcome supports the findings obtained from Co-IP experiments that the hetero-hexameric GDH behaves as a separate holoenzyme with distinct affinity and accordingly structural properties as compared with a simple *in vitro* mixture. It is therefore reasonable to assume that hGDH1/2 sample resulting from the co-expression of *GLUD1* and *GLUD2* cDNAs, mainly (if not exclusively) consists of a single enzyme composed of two different subunit types, some corresponding to hGDH1 and others to hGDH2.

Having confirmed the abovementioned implications about hGDH1/2 hetero-hexamer existence, we proceeded to characterization of the enzymatic properties that this macromolecule possesses. For this purpose, we performed a series of kinetic studies, employing factors (biochemical or related to the reaction's environment) that have been previously reported to differentially affect hGDH1 and hGDH2.

It is already known that ADP and GTP are the main activity modulators of GDH (Hudson and Daniel 1993). This leads to the conclusion that GDH is essentially controlled by the cell energy demands. hGDH2's unique enzymatic properties seem to have favored its adaptation to the high-energy demanding neural and testicular tissues. GTP resistance for instance is one of the advantageous characteristics that hGDH2 has acquired during evolution (Shashidharan et al. 1994). GTP levels are higher in brain than in other tissues and could hinder GDH action, which is true for hGDH1. However, hGDH2 remains active even under conditions of intense TCA cycle operation, which generate GTP levels sufficient to inactivate hGDH1. On the other hand, dependence of hGDH2 activity on ADP facilitates this enzyme's function under increased energy demands, like these occurring in the respective cell types where it is expressed. In addition, L-leucine which also acts as an energy index and a GDH stimulator, permits hGDH2 to sense even subtle changes in ADP concentration, even in the absence of an energy deficit (Kanavouras et al. 2007). This could be beneficial for Sertoli cells and astrocytes, where the two hGDH isoforms are co-expressed, as it

could act as a protective mechanism against energy insufficiency which would be detrimental for the synchronized function of these supporting cells.

It is thus evident that by possessing only two GDH isoforms which are distinctly regulated, Sertoli cells and astrocytes are endowed with a fine tuning energy sensing mechanism which is directly bound to TCA cycle and ATP production, and is capable of responding to different energy demands. As suggested in this study, the presence of even more than two GDH isoenzymes by forming hetero-hexamers in the tissues where they are co-expressed, could be an even more sensitive mechanism that would permit GDH operation under almost any micro-environmental conditions occurring in the mitochondrion. We could even make the assumption that according to its energy status and environmental conditions prevailing at a given time, the cell machinery is able to generate either hGDH1, hGDH2, or hGDH1/2 hetero-hexamers and the molecules that can address optimally the cell needs will be exploited.

Specifically, hGDH1/2 possible hetero-hexamer is less resistant to GTP than hGDH2, but its inhibition pattern resembles more that of hGDH2 than a simple combination of the two homo-hexamers. Regarding ADP activation, hGDH1/2 is able to function equally well under baseline conditions with a mixture of the two iso-enzymes, with its basal activity lying between those of homo-hexamers. L-leucine activation pattern presents intermediate values which are comparable to those of a simple hGDH1 and hGDH2 combination. Steroid hormones' impact on hGDH1/2's activity, and DES in particular, was somewhat similar to that of hGDH2, presenting higher sensitivity than that of hGDH1 and hGDH2 mixture. The possible hetero-hexamer displays optimal operation at pH 7.8 and low ionic concentrations, while it is moderately heat labile.

In summary, enzymatic assays have shed some light on the properties that the possible hetero-hexamer possesses. hGDH1/2, although presenting a similar behavior with hGDH1 + hGDH2 *in vitro* mix under some conditions, it also displayed a unique functioning pattern under some other conditions, such as GTP inhibition and, although not as profoundly, DES inhibition. On the one hand, the finding that hGDH1/2 and hGDH1+2 share common kinetic behaviors under some conditions is a quality control enhancing earlier estimations that hGDH1 and hGDH2 are indeed equally co-expressed in Sf21 cultures. On the other hand, the different kinetic behaviors that the possible hetero-hexamer hGDH1/2 displays, which in fact render it more similar to hGDH2 than hGDH1, imply that this might be a new molecule, that can function differently than each isoform separately and their combination (mix) as well.

The presence of hGDH1/2 hetero-hexamers, with properties distinct to those of the homo-hexamers, may provide flexibility to human cells, by equipping them with more than two isoenzymes. hGDH1/2 seems to be a unique enzyme with its own regulation properties and optimal functioning conditions, that is active under infinitesimally changing conditions that constantly happen within the cell, where the homo-hexamers are not able to function as efficiently. Sertoli cells and astrocytes where both isoenzymes are expressed, and thus probably their hetero-hexameric complex is also expressed, could be able to exploit this fine tuning in order to reciprocate the demanding energy consuming environment they neighbor, which consists of developing sperm cells and neurons respectively.

In order to verify whether the possible hetero-hexamer is also formed in the human tissues where both hGDH1 and hGDH2 are expressed, future work involves the repetition of GTP affinity chromatography and co-IP experiments on testis and possibly on brain. Further exploration of hGDH1/2's enzymatic properties is needed in order to better understand what advantageous profile those cells possess and how this can be physiologically significant. A more precise image regarding hGDH1/2 expressing cells profits would be obtained by recombinantly expressing the possible hetero-hexamers in various cell-lines, among which neural cells and accompanying astrocytes, and compare their metabolic profile with wild type cells.

Structure analysis of hGDH2 by crystallization and SEC/MALS is a major achievement towards the understanding of its structural properties and the basis of its functional diversity from hGDH1. In this study we established the conditions for crystallization of hGDH2. The crystallographic X-ray structure of hGDH2 at atomic resolution was successful after a series of labor trials and fails, and for the first time we managed to collect crystallographic data at 3.2Å (Dr. Kokkinidis lab). We have in our disposal the first statistical analyses on the structure of hGDH2 and we are in the process of analyzing its, so far unsolved, crystal structure. Since protein structure and function are directly related, hGDH2 special features can be presumably narrowed down to its structural particularities. This achievement will help us draw conclusions on the enzyme's actual function and maybe even the needs that forced its evolution. Also, studying its amino-acid differences from hGDH1 is expected to reveal what particular characteristics hGDH2 possesses that enable it to have augmented sensitivity to some regulators (i.e. ADP, L-leucine, steroid hormones, neuroleptic drugs etc.) while it presents low affinity for others (i.e. GTP). Having established the conditions under

which hGDH2 is ultimately crystallized, prospective studies could include its crystallization in bound form with some major regulators.

As SEC/MALS is increasingly emerging as a powerful technique to study the conformation of proteins in solution, we thought that this would be an ideal technique to study hGDH2 in comparison with its extensively studied iso-enzyme hGDH1. More specifically, we performed SEC/MALS to study and compare the conformation of hGDH1 and hGDH2 under different conditions (i.e. to characterize via MALS the various folding and assembly/association states of hGDH1 and hGDH2). Moreover, we studied the conformational changes induced to the hGDH1 and hGDH2 enzymes upon change in their biochemical environment, i.e. alterations in the pH of the reaction buffer. To investigate this, we performed SEC/MALS experiments on purified enzymes. Indeed, these experiments showed remarkable pH dependence of the conformation of GDHs, both from human and bovine origin, which were more profound for hGDH2.

The genetics of *GLUD1* and *GLUD2* genes belonged to the scopes of this work for a number of reasons. *GLUD1* and *GLUD2* genes are among the genetic candidates possibly implicated in dementia pathophysiology. Variants in these two genes have been previously described in neurological conditions, such as epilepsy (in the context of the hyperinsulinism/ hypermammonemia syndrome associated with activating *GLUD1* mutations; Stanley et al. 1998; Raizen et al. 2005) and Parkinson's disease (with the Ser498Ala *GLUD2* variant conferring risk for earlier disease onset in hemizygous males; Plaitakis et al. 2010). More importantly, selective overexpression of *GLUD1* in mice brains resulted in upregulation of glutamate release and consequently, excitotoxicity. The mice were exhibiting a phenotype compatible with progressive neurodegeneration, and more specifically age-dependent degenerative changes in the CA1 region of the hippocampus (Bao et al. 2009). We were interested to uncover the genetic variations' spectrum within an aging Cretan population, which can represent a mirror of the *GLUDs* variants' frequencies within Cretan population in general. Detecting common variants is of particular significance because on the one hand, those are excluded from causative candidates for major diseases while, on the other hand, they can be investigated through the prism of risk factors for a pathogenic phenotype or they could even serve as haplotype indexes. Also, we were particularly interested in deciphering whether there are any unique variants of *GLUD1* and *GLUD2* genes, and which of those present a damaging profile according to their nature and *in silico* predictions. Deleterious genetic alterations that are uniquely present in dementia

cases might worth a thorough functional characterization, in respect to their contribution in neurodegeneration processes.

In the *GLUD1* gene, only one variant (p.Asp341Gly) was present only in a normal control. This variant, even though novel, is predicted to confer a benign alteration to the protein, according to algorithmic predictions. Also present in our cohort was a rare, not previously studied, variant of *GLUD2* (p.Asp414Gly) which was uniquely present in a patient affected with dementia and is probably a benign polymorphism, according to Polyphen2 predictions. A previously described variant in the leader peptide of *GLUD2* (p.Gly35Arg) was as common in dementia patients as in controls. This variant has also been found in the past not to affect the frequency or the age at onset of Parkinson's disease (Plaitakis et al. 2010). Also, this polymorphism has been shown recently not to affect the targeting efficiency of the mitochondrial peptide of hGDH2 (Kalef-Ezra et al. 2016).

To our surprise, the *GLUD2* - p.Ser498Ala variant, which has been previously described as an accelerating factor for Parkinson's disease associated neurodegeneration (Plaitakis et al. 2010), was more frequent in cognitively normal individuals in our cohort compared to patients with dementia. This p.Ser498Ala *GLUD2* variant (denoted Ser445Ala in Plaitakis et al. 2010) accelerates PD onset in male hemizygotes but not in female heterozygotes (Plaitakis et al. 2010). Functional characterization of this variant showed that it results in gain of function, as it shows a basal activity higher than that of the wild-type Ala498-hGDH2 (Plaitakis et al. 2010). Furthermore, it can be argued that its location on the small α-helix of the antenna of the hGDH2 enzyme that undergoes major changes during the catalytic cycle could affect enzymatic function.

We can only speculate about the mechanism that the hGDH2-Ala498 gain-of-function variant protects from AD. However, it is tempting to hypothesize that the increased activity of the Ala498-hGDH2 protein (Plaitakis et al. 2010) degrades excess glutamate and delays the onset of neurodegeneration in selected brain areas such as the hippocampus. Compatible with this view is the fact that glutamate neurotoxicity is a prevailing theory for AD pathogenesis and that memantine, which is used as a treatment for AD, acts by negating the detrimental effect of glutamate over-excitation (Chen et al. 1992). The fact that the protective effect was seen only in males and not in females, given that the sensitivity of the Ser498Ala variant to estrogens is the same as that of the wild type hGDH2 (Plaitakis et al. 2010), could relate simply to the fact

that females possess an additional wild-type allele that could prohibit expression of the protective phenotype conferred by this variant.

Is this compatible with the detrimental effect of the same *GLUD2* Ser498Ala variant observed in PD? One can think that this could be attributed to the existence of different glutamate pools in human brain, that are differentially affected by the Ser498Ala *GLUD2* change. Also, the differential localization of the hGDH2 enzyme in different brain structures, such as the medial temporal lobes, and the hippocampus, involved primary in AD pathogenesis, compared to the striatum and substantia nigra, mainly affected during PD onset, could account for the inverse effects of this *GLUD2* variant in neurodegeneration in these two disorders.

In conclusion, this work advanced further our knowledge on the structural and functional properties of human GDHs, as well as on the implications of genetic variants of their genes. We hope that advances from this research will contribute to a better understanding of mitochondrial metabolism, given that we have shown that hGDH1 and hGDH2 in the form of hetero- hexamers when they are co-expressed have advantageous enzymatic characteristics that equip the cell with remarkable versatility. Crystallization of hGDH2 will, through comparison with hGDH1 structure, shed light on the structural basis of the different regulatory properties of the two isoenzymes. Finally, our finding that a *GLUD2* variant can offer neuroprotection in dementia, could open a new field of research towards a better understanding of the disease.

References

Adeva, M. M., G. Souto, et al. (2012). "Ammonium metabolism in humans." Metabolism 61(11): 1495-1511.

Albani, D., I. Roiter, et al. (2007). "Presenilin-1 mutation E318G and familial Alzheimer's disease in the Italian population." Neurobiol Aging 28(11): 1682-1688.

Allen, A., J. Kwagh, et al. (2004). "Evolution of glutamate dehydrogenase regulation of insulin homeostasis is an example of molecular exaptation." Biochemistry 43(45): 14431-14443.

American Psychiatric Association (1994). "Diagnostic and Statistical Manual of Mental Disorders", Fourth Edition. Washington, DC American Psychiatric Association

Anagnou, N. P., H. Seuanez, et al. (1993). "Chromosomal mapping of two members of the human glutamate dehydrogenase (GLUD) gene family to chromosomes 10q22.3-q23 and Xq22-q23." Hum Hered 43(6): 351-356.

Andersson, J. O. and A. J. Roger (2003). "Evolution of glutamate dehydrogenase genes: evidence for lateral gene transfer within and between prokaryotes and eukaryotes." BMC Evol Biol 3: 14.

Aoki, C., T. A. Milner, et al. (1987). "Glial glutamate dehydrogenase: ultrastructural localization and regional distribution in relation to the mitochondrial enzyme, cytochrome oxidase." J Neurosci Res 18(2): 305-318.

Aso, K., Y. Okano, et al. (2011). "Spectrum of glutamate dehydrogenase mutations in Japanese patients with congenital hyperinsulinism and hyperammonemia syndrome." Osaka City Med J 57(1): 1-9.

Attwell, D. and S. B. Laughlin (2001). "An energy budget for signaling in the grey matter of the brain." J Cereb Blood Flow Metab 21(10): 1133-1145.

Bailey, J., E. T. Bell, et al. (1982). "Regulation of bovine glutamate dehydrogenase. The effects of pH and ADP." J Biol Chem 257(10): 5579-5583.

Banerjee, S., T. Schmidt, et al. (2003). "Structural studies on ADP activation of mammalian glutamate dehydrogenase and the evolution of regulation." Biochemistry 42(12): 3446-3456.

Bao, X., R. Pal, et al. (2009). "Transgenic expression of Glud1 (glutamate dehydrogenase 1) in neurons: in vivo model of enhanced glutamate release, altered synaptic plasticity, and selective neuronal vulnerability." J Neurosci 29(44): 13929-13944.

Barderi, P., O. Campetella, et al. (1998). "The NADP+-linked glutamate dehydrogenase from Trypanosoma cruzi: sequence, genomic organization and expression." Biochem J 330 (Pt 2): 951-958.

Belanger, M., I. Allaman, et al. (2011). "Brain energy metabolism: focus on astrocyte-neuron metabolic cooperation." Cell Metab 14(6): 724-738.

Benitez, B. A., C. M. Karch, et al. (2013). "The PSEN1, p.E318G variant increases the risk of Alzheimer's disease in APOE-epsilon4 carriers." PLoS Genet 9(8): e1003685.

Bertram, L., M. B. McQueen, et al. (2007). "Systematic meta-analyses of Alzheimer disease genetic association studies: the AlzGene database." Nat Genet 39(1): 17-23.

Bettens, K., K. Sleegers, et al. (2013). "Genetic insights in Alzheimer's disease." Lancet Neurol 12(1): 92-104.

Blumenthal, K. M., K. Moon, et al. (1975). "Nicotinamide adenine dinucleotide phosphate-specific glutamate dehydrogenase of Neurospora." J Biol Chem 250(10): 3644-3654.

Borompokas, N., M. M. Papachatzaki, et al. (2010). "Estrogen modification of human glutamate dehydrogenases is linked to enzyme activation state." J Biol Chem 285(41): 31380-31387.

Bouvier, M., M. Szatkowski, et al. (1992). "The glial cell glutamate uptake carrier countertransports pH-changing anions." Nature 360(6403): 471-474.

Burki, F. and H. Kaessmann (2004). "Birth and adaptive evolution of a hominoid gene that supports high neurotransmitter flux." Nat Genet 36(10): 1061-1063.

Butterworth, R. F. (2002). "Pathophysiology of hepatic encephalopathy: a new look at ammonia." Metab Brain Dis 17(4): 221-227.

Carneiro, V. T. and R. A. Caldas (1983). "Regulatory studies of L-glutamate dehydrogenase from Trypanosoma cruzi epimastigotes." Comp Biochem Physiol B 75(1): 61-64.

Carobbio, S., F. Frigerio, et al. (2009). "Deletion of glutamate dehydrogenase in beta-cells abolishes part of the insulin secretory response not required for glucose homeostasis." J Biol Chem 284(2): 921-929.

Caughey, W. S., L. Hellerman, et al. (1957). "L-glutamic acid dehydrogenase

Chen, H. S., J. W. Pellegrini, et al. (1992). "Open-channel block of N-methyl-D-aspartate (NMDA) responses by memantine: therapeutic advantage against NMDA receptor-mediated neurotoxicity." J Neurosci 12(11): 4427-4436.

Chen, R., M. C. Nishimura, et al. (2014). "Hominoid-specific enzyme GLUD2 promotes growth of IDH1R132H glioma." Proc Natl Acad Sci U S A 111(39): 14217-14222.

Choi, M. M., E. A. Kim, et al. (2007). "Amino acid changes within antenna helix are responsible for different regulatory preferences of human glutamate dehydrogenase isozymes." J Biol Chem 282(27): 19510-19517.

Colon, A. D., A. Plaitakis, et al. (1986). "Purification and characterization of a soluble and a particulate glutamate dehydrogenase from rat brain." J Neurochem 46(6): 1811-1819.

Cooper, A. J. (2011). "13N as a tracer for studying glutamate metabolism." Neurochem Int 59(4): 456-464.

Cooper, A. J., J. M. McDonald, et al. (1979). "The metabolic fate of 13N-labeled ammonia in rat brain." J Biol Chem 254(12): 4982-4992.

Corder, E. H., A. M. Saunders, et al. (1993). "Gene dose of apolipoprotein E type 4 allele and the risk of Alzheimer's disease in late onset families." Science 261(5123): 921-923.

Couee, I. and K. F. Tipton (1990). "The inhibition of glutamate dehydrogenase by some antipsychotic drugs." Biochem Pharmacol 39(5): 827-832.

Couee, I. and K. F. Tipton (1990). "Inhibition of ox brain glutamate dehydrogenase by perphenazine." Biochem Pharmacol 39(7): 1167-1173.

Cruchaga, C., G. Haller, et al. (2012). "Rare variants in APP, PSEN1 and PSEN2 increase risk for AD in late-onset Alzheimer's disease families." PLoS One 7(2): e31039.

Cruts, M., J. Theuns, et al. (2012). "Locus-specific mutation databases for neurodegenerative brain diseases." Hum Mutat 33(9): 1340-1344.

Cruts, M., C. M. van Duijn, et al. (1998). "Estimation of the genetic contribution of presenilin-1 and -2 mutations in a population-based study of presenile Alzheimer disease." Hum Mol Genet 7(1): 43-51.

Daikhin, Y. and M. Yudkoff (2000). "Compartmentation of brain glutamate metabolism in neurons and glia." J Nutr 130(4S Suppl): 1026S-1031S.

Dalziel, K. and P. C. Engel (1968). "Antagonistic homotropic interactions as a possible explanation of coenzyme activation of glutamate dehydrogenase." FEBS Lett 1(5): 349-352.

De Lonlay, P., C. Benelli, et al. (2001). "Hyperinsulinism and hyperammonemia syndrome: report of twelve unrelated patients." Pediatr Res 50(3): 353-357.

Deloukas, P., J. G. Dauwerse, et al. (1993). "Three human glutamate dehydrogenase genes (GLUD1, GLUDP2, and GLUDP3) are located on chromosome 10q, but are not closely physically linked." Genomics 17(3): 676-681.

Dermaut, B., M. Cruts, et al. (1999). "The Glu318Gly substitution in presenilin 1 is not causally related to Alzheimer disease." Am J Hum Genet 64(1): 290-292.

Di Prisco, G. and H. J. Strecker (1969). "Effects of phosphate and other ionic compounds on the activity of crystalline beef liver glutamate dehydrogenase." Eur J Biochem 9(4): 507-511.

Diprisco, G., S. M. Arfin, et al. (1965). "Studies on the Nature of the Inhibition of Glutamic Dehydrogenase by N-2-Fluorenylacetamide and Other Compounds." J Biol Chem 240: 1611-1615.

Duran, R. V., W. Oppliger, et al. (2012). "Glutaminolysis activates Rag-mTORC1 signaling." Mol Cell 47(3): 349-358.

Engel, P. C. and K. Dalziel (1969). "Kinetic studies of glutamate dehydrogenase with glutamate and norvaline as substrates. Coenzyme activation and negative homotropic interactions in allosteric enzymes." Biochem J 115(4): 621-631.

Fahien, L. A. and E. Kmiotek (1981). "Regulation of glutamate dehydrogenase by palmitoyl-coenzyme A." Arch Biochem Biophys 212(1): 247-253.

Fahien, L. A., E. H. Kmiotek, et al. (1985). "Regulation of aminotransferase-glutamate dehydrogenase interactions by carbamyl phosphate synthase-I, Mg2+ plus leucine versus citrate and malate." J Biol Chem 260(10): 6069-6079.

Fahien, L. A., M. J. MacDonald, et al. (1988). "Regulation of insulin release by factors that also modify glutamate dehydrogenase." J Biol Chem 263(27): 13610-13614.

Fahien, L. A., J. K. Teller, et al. (1990). "Regulation of glutamate dehydrogenase by Mg2+ and magnification of leucine activation by Mg2+." Mol Pharmacol 37(6): 943-949.

Frieden, C. (1959). "Glutamic dehydrogenase. II. The effect of various nucleotides on the association-dissociation and kinetic properties." J Biol Chem 234(4): 815-820.

Frieden, C. (1962). "The unusual inhibition of glutamate dehydrogenase by guanosine di- and triphosphate." Biochim Biophys Acta 59: 484-486.

Frigerio, F., M. Karaca, et al. (2012). "Deletion of glutamate dehydrogenase 1 (Glud1) in the central nervous system affects glutamate handling without altering synaptic transmission." J Neurochem 123(3): 342-348.

Fujioka, H., Y. Okano, et al. (2001). "Molecular characterisation of glutamate dehydrogenase gene defects in Japanese patients with congenital hyperinsulinism/hyperammonaemia." Eur J Hum Genet 9(12): 931-937.

Gaiteri, C., S. Mostafavi, et al. (2016). "Genetic variants in Alzheimer disease - molecular and brain network approaches." Nat Rev Neurol 12(7): 413-427.

Garland, W. J. and D. T. Dennis (1977). "Steady-state kinetics of glutamate dehydrogenase from Pisum sativum L. mitochondria." Arch Biochem Biophys 182(2): 614-625.

Gozes, I. (2010). "Tau pathology: predictive diagnostics, targeted preventive and personalized medicine and application of advanced research in medical practice." EPMA J 1(2): 305-316.

Guerreiro, R. J., M. Baquero, et al. (2010). "Genetic screening of Alzheimer's disease genes in Iberian and African samples yields novel mutations in presenilins and APP." Neurobiol Aging 31(5): 725-731.

Helisalmi, S., M. Hiltunen, et al. (2000). "Is the presenilin-1 E318G missense mutation a risk factor for Alzheimer's disease?" Neurosci Lett 278(1-2): 65-68.

Hellerman, L., K. A. Schellenberg, et al. (1958). "L-glutamic acid dehydrogenase. II. Role of enzyme sulfhydryl groups." J Biol Chem 233(6): 1468-1478.

Hippen, A. A., M. T. Ebbert, et al. (2016). "Presenilin E318G variant and Alzheimer's disease risk: the Cache County study." BMC Genomics 17 Suppl 3: 438.

Hudson, R. C. and R. M. Daniel (1993). "L-glutamate dehydrogenases: distribution, properties and mechanism." Comp Biochem Physiol B 106(4): 767-792.

Hussain, M. M., V. I. Zannis, et al. (1989). "Characterization of glutamate dehydrogenase isoproteins purified from the cerebellum of normal subjects and patients with degenerative neurological disorders, and from human neoplastic cell lines." J Biol Chem 264(34): 20730-20735.

Hutson, S. M., M. M. Islam, et al. (2011). "Interaction between glutamate dehydrogenase (GDH) and L-leucine catabolic enzymes: intersecting metabolic pathways." Neurochem Int 59(4): 518-524.

Islam, M. M., M. Nautiyal, et al. (2010). "Branched-chain amino acid metabolon: interaction of glutamate dehydrogenase with the mitochondrial branched-chain aminotransferase (BCATm)." J Biol Chem 285(1): 265-276.

Jayadev, S., J. B. Leverenz, et al. (2010). "Alzheimer's disease phenotypes and genotypes associated with mutations in presenilin 2." Brain 133(Pt 4): 1143-1154.

Jin, S. C., P. Pastor, et al. (2012). "Pooled-DNA sequencing identifies novel causative variants in PSEN1, GRN and MAPT in a clinical early-onset and familial Alzheimer's disease Ibero-American cohort." Alzheimers Res Ther 4(4): 34.

Jonsson, T., J. K. Atwal, et al. (2012). "A mutation in APP protects against Alzheimer's disease and age-related cognitive decline." Nature 488(7409): 96-99.

Kahn, C. R. (1994). "Banting Lecture. Insulin action, diabetogenes, and the cause of type II diabetes." Diabetes 43(8): 1066-1084.

Kalef-Ezra, E., D. Kotzamani, et al. (2016). "Import of a major mitochondrial enzyme depends on synergy between two distinct helices of its presequence." Biochem J.

Kanavouras, K., N. Borompokas, et al. (2009). "Mutations in human GLUD2 glutamate dehydrogenase affecting basal activity and regulation." J Neurochem 109 Suppl 1: 167-173.

Kanavouras, K., V. Mastorodemos, et al. (2007). "Properties and molecular evolution of human GLUD2 (neural and testicular tissue-specific) glutamate dehydrogenase." J Neurosci Res 85(15): 3398-3406.

Kapoor, R. R., S. E. Flanagan, et al. (2009). "Hyperinsulinism-hyperammonaemia syndrome: novel mutations in the GLUD1 gene and genotype-phenotype correlations." Eur J Endocrinol 161(5): 731-735.

Kawaguchi, A. and K. Bloch (1976). "Inhibition of glutamate dehydrogenase and malate dehydrogenases by palmitoyl coenzyme A." J Biol Chem 251(5): 1406-1412.

Kelly, A. and C. A. Stanley (2001). "Disorders of glutamate metabolism." Ment Retard Dev Disabil Res Rev 7(4): 287-295.

Kim, S. W., J. H. Heo, et al. (2010). "Rapid and direct detection of apolipoprotein E genotypes using whole blood from humans." J Toxicol Environ Health A 73(21-22): 1502-1510.

Kotzamani, D. and A. Plaitakis (2012). "Alpha helical structures in the leader sequence of human GLUD2 glutamate dehydrogenase responsible for mitochondrial import." Neurochem Int 61(4): 463-469.

Kulijewicz-Nawrot, M., E. Sykova, et al. (2013). "Astrocytes and glutamate homoeostasis in Alzheimer's disease: a decrease in glutamine synthetase, but not in glutamate transporter-1, in the prefrontal cortex." ASN Neuro 5(4): 273-282.

Kuo, N., M. Michalik, et al. (1994). "Inhibition of glutamate dehydrogenase in brain mitochondria and synaptosomes by Mg2+ and polyamines: a possible cause for its low in vivo activity." J Neurochem 63(2): 751-757.

LeJohn, H. B., S. G. Jackson, et al. (1969). "Regulation of mitochondrial glutamic dehydrogenase by divalent metals, nucleotides, and alpha-ketoglutarate. Correlations between the molecular and kinetic mechanisms, and the physiological implications." J Biol Chem 244(19): 5346-5356.

Li, C., A. Allen, et al. (2006). "Green tea polyphenols modulate insulin secretion by inhibiting glutamate dehydrogenase." J Biol Chem 281(15): 10214-10221.

Li, M., A. Allen, et al. (2007). "High throughput screening reveals several new classes of glutamate dehydrogenase inhibitors." Biochemistry 46(51): 15089-15102.

Li, M., C. Li, et al. (2011). "The structure and allosteric regulation of glutamate dehydrogenase." Neurochem Int 59(4): 445-455.

Li, M., C. Li, et al. (2012). "The structure and allosteric regulation of mammalian glutamate dehydrogenase." Arch Biochem Biophys 519(2): 69-80.

Li, M., C. J. Smith, et al. (2009). "Novel inhibitors complexed with glutamate dehydrogenase: allosteric regulation by control of protein dynamics." J Biol Chem 284(34): 22988-23000.

Lin, M. T. and M. F. Beal (2006). "Mitochondrial dysfunction and oxidative stress in neurodegenerative diseases." Nature 443(7113): 787-795.

Liu, C. C., T. Kanekiyo, et al. (2013). "Apolipoprotein E and Alzheimer disease: risk, mechanisms and therapy." Nat Rev Neurol 9(2): 106-118.

Lu, C. D. and A. T. Abdelal (2001). "The gdhB gene of Pseudomonas aeruginosa encodes an arginine-inducible NAD(+)-dependent glutamate dehydrogenase which is subject to allosteric regulation." J Bacteriol 183(2): 490-499.

MacMullen, C., J. Fang, et al. (2001). "Hyperinsulinism/hyperammonemia syndrome in children with regulatory mutations in the inhibitory guanosine triphosphate-binding domain of glutamate dehydrogenase." J Clin Endocrinol Metab 86(4): 1782-1787.

Mastorodemos, V., D. Kotzamani, et al. (2009). "Human GLUD1 and GLUD2 glutamate dehydrogenase localize to mitochondria and endoplasmic reticulum." Biochem Cell Biol 87(3): 505-516.

Mastorodemos, V., I. Zaganas, et al. (2005). "Molecular basis of human glutamate dehydrogenase regulation under changing energy demands." J Neurosci Res 79(1-2): 65-73.

Mattila, K. M., C. Forsell, et al. (1998). "The Glu318Gly mutation of the presenilin-1 gene does not necessarily cause Alzheimer's disease." Ann Neurol 44(6): 965-967.

Mavrothalassitis, G., G. Tzimagiorgis, et al. (1988). "Isolation and characterization of cDNA clones encoding human liver glutamate dehydrogenase: evidence for a small gene family." Proc Natl Acad Sci U S A 85(10): 3494-3498.

McKenna, M. C. (2007). "The glutamate-glutamine cycle is not stoichiometric: fates of glutamate in brain." J Neurosci Res 85(15): 3347-3358.

McKenna, M. C., U. Sonnewald, et al. (1996). "Exogenous glutamate concentration regulates the metabolic fate of glutamate in astrocytes." J Neurochem 66(1): 386-393.

Michaelidis, T. M., G. Tzimagiorgis, et al. (1993). "The human glutamate dehydrogenase gene family: gene organization and structural characterization." Genomics 16(1): 150-160.

Miki, Y., T. Taki, et al. (2000). "Novel missense mutations in the glutamate dehydrogenase gene in the congenital hyperinsulinism-hyperammonemia syndrome." J Pediatr 136(1): 69-72.

Nussbaum, R. L. and C. E. Ellis (2003). "Alzheimer's disease and Parkinson's disease." N Engl J Med 348(14): 1356-1364.

Olabarria, M., H. N. Noristani, et al. (2011). "Age-dependent decrease in glutamine synthetase expression in the hippocampal astroglia of the triple transgenic Alzheimer's disease mouse model: mechanism for deficient glutamatergic transmission?" Mol Neurodegener 6: 55.

Pellerin, L. and P. J. Magistretti (1994). "Glutamate uptake into astrocytes stimulates aerobic glycolysis: a mechanism coupling neuronal activity to glucose utilization." Proc Natl Acad Sci U S A 91(22): 10625-10629.

Peterson, P. E. and T. J. Smith (1999). "The structure of bovine glutamate dehydrogenase provides insights into the mechanism of allostery." Structure 7(7): 769-782.

Plaitakis, A., S. Berl, et al. (1984). "Neurological disorders associated with deficiency of glutamate dehydrogenase." Ann Neurol 15(2): 144-153.

Plaitakis, A., H. Latsoudis, et al. (2010). "Gain-of-function variant in GLUD2 glutamate dehydrogenase modifies Parkinson's disease onset." Eur J Hum Genet 18(3): 336-341.

Plaitakis, A., H. Latsoudis, et al. (2011). "The human GLUD2 glutamate dehydrogenase and its regulation in health and disease." Neurochem Int 59(4): 495-509.

Plaitakis, A., M. Metaxari, et al. (2000). "Nerve tissue-specific (GLUD2) and housekeeping (GLUD1) human glutamate dehydrogenases are regulated by distinct allosteric mechanisms: implications for biologic function." J Neurochem 75(5): 1862-1869.

Plaitakis, A., C. Spanaki, et al. (2003). "Study of structure-function relationships in human glutamate dehydrogenases reveals novel molecular mechanisms for the regulation of the nerve tissue-specific (GLUD2) isoenzyme." Neurochem Int 43(4-5): 401-410.

Plaitakis, A. and I. Zaganas (2001). "Regulation of human glutamate dehydrogenases: implications for glutamate, ammonia and energy metabolism in brain." J Neurosci Res 66(5): 899-908.

Plaitakis, A., I. Zaganas, et al. (2013). "Deregulation of glutamate dehydrogenase in human neurologic disorders." J Neurosci Res 91(8): 1007-1017.

Poitry, S., C. Poitry-Yamate, et al. (2000). "Mechanisms of glutamate metabolic signaling in retinal glial (Muller) cells." J Neurosci 20(5): 1809-1821.

Raizen, D. M., A. Brooks-Kayal, et al. (2005). "Central nervous system hyperexcitability associated with glutamate dehydrogenase gain of function mutations." J Pediatr 146(3): 388-394.

Richards, S., N. Aziz, et al. (2015). "Standards and guidelines for the interpretation of sequence variants: a joint consensus recommendation of the American College of Medical Genetics and Genomics and the Association for Molecular Pathology." Genet Med 17(5): 405-424.

Rosso, L., A. C. Marques, et al. (2008). "Mitochondrial targeting adaptation of the hominoid-specific glutamate dehydrogenase driven by positive Darwinian selection." PLoS Genet 4(8): e1000150.

Rothe, F., M. Brosz, et al. (1994). "Quantitative ultrastructural localization of glutamate dehydrogenase in the rat cerebellar cortex." Neuroscience 62(4): 1133-1146.

Santer, R., M. Kinner, et al. (2001). "Novel missense mutations outside the allosteric domain of glutamate dehydrogenase are prevalent in European patients with the congenital hyperinsulinism-hyperammonemia syndrome." Hum Genet 108(1): 66-71.

Sassi, C., R. Guerreiro, et al. (2014). "Investigating the role of rare coding variability in Mendelian dementia genes (APP, PSEN1, PSEN2, GRN, MAPT, and PRNP) in late-onset Alzheimer's disease." Neurobiol Aging 35(12): 2881 e2881-2886.

Saunders, A. M., W. J. Strittmatter, et al. (1993). "Association of apolipoprotein E allele epsilon 4 with late-onset familial and sporadic Alzheimer's disease." Neurology 43(8): 1467-1472.

Schousboe, A., L. K. Bak, et al. (2013). "Astrocytic Control of Biosynthesis and Turnover of the Neurotransmitters Glutamate and GABA." Front Endocrinol (Lausanne) 4: 102.

Schousboe, A., H. M. Sickmann, et al. (2011). "Neuron-glia interactions in glutamatergic neurotransmission: roles of oxidative and glycolytic adenosine triphosphate as energy source." J Neurosci Res 89(12): 1926-1934.

Shashidharan, P., D. D. Clarke, et al. (1997). "Nerve tissue-specific human glutamate dehydrogenase that is thermolabile and highly regulated by ADP." J Neurochem 68(5): 1804-1811.

Shashidharan, P., T. M. Michaelidis, et al. (1994). "Novel human glutamate dehydrogenase expressed in neural and testicular tissues and encoded by an X-linked intronless gene." J Biol Chem 269(24): 16971-16976.

Shashidharan, P. and A. Plaitakis (2014). "The discovery of human of GLUD2 glutamate dehydrogenase and its implications for cell function in health and disease." Neurochem Res 39(3): 460-470.

Shemisa, O. A. and L. A. Fahien (1971). "Modifications of glutamate dehydrogenase by various drugs which affect behavior." Mol Pharmacol 7(1): 8-25.

Shen, J. (2005). "In vivo carbon-13 magnetization transfer effect. Detection of aspartate aminotransferase reaction." Magn Reson Med 54(6): 1321-1326.

Sleegers, K., G. Roks, et al. (2004). "Familial clustering and genetic risk for dementia in a genetically isolated Dutch population." Brain 127(Pt 7): 1641-1649.

Smith, E. L. and D. Pisziewicz (1973). "Bovine glutamate dehydrogenase. The pH dependence of native and nitrated enzyme in the presence of allosteric modifiers." J Biol Chem 248(9): 3089-3092.

Smith, T. J., P. E. Peterson, et al. (2001). "Structures of bovine glutamate dehydrogenase complexes elucidate the mechanism of purine regulation." J Mol Biol 307(2): 707-720.

Smith, T. J., T. Schmidt, et al. (2002). "The structure of apo human glutamate dehydrogenase details subunit communication and allostery." J Mol Biol 318(3): 765-777.

Smith, T. J. and C. A. Stanley (2008). "Untangling the glutamate dehydrogenase allosteric nightmare." Trends Biochem Sci 33(11): 557-564.

Smits, R. A., F. R. Pieper, et al. (1984). "Purification of NADP-dependent glutamate dehydrogenase from Pseudomonas aeruginosa and immunochemical characterization of its in vivo inactivation." Biochim Biophys Acta 801(1): 32-39.

Sonnewald, U., N. Westergaard, et al. (1997). "Glutamate transport and metabolism in astrocytes." Glia 21(1): 56-63.

Spanaki, C., D. Kotzamani, et al. (2014). "Heterogeneous cellular distribution of glutamate dehydrogenase in brain and in non-neural tissues." Neurochem Res 39(3): 500-515.

Spanaki, C., D. Kotzamani, et al. (2015). "Expression of human GLUD1 and GLUD2 glutamate dehydrogenases in steroid producing tissues." Mol Cell Endocrinol 415: 1-11.

Spanaki, C. and A. Plaitakis (2012). "The role of glutamate dehydrogenase in mammalian ammonia metabolism." Neurotox Res 21(1): 117-127.

Spanaki, C., I. Zaganas, et al. (2010). "Human GLUD2 glutamate dehydrogenase is expressed in neural and testicular supporting cells." J Biol Chem 285(22): 16748-16756.

Spanaki, C., I. Zaganas, et al. (2012). "The complex regulation of human glud1 and glud2 glutamate dehydrogenases and its implications in nerve tissue biology." Neurochem Int 61(4): 470-481.

Srere, P. A. (2000). "Macromolecular interactions: tracing the roots." Trends Biochem Sci 25(3): 150-153.

Stanley, C. A. (2011). "Two genetic forms of hyperinsulinemic hypoglycemia caused by dysregulation of glutamate dehydrogenase." Neurochem Int 59(4): 465-472.

Stanley, C. A., J. Fang, et al. (2000). "Molecular basis and characterization of the hyperinsulinism/hyperammonemia syndrome: predominance of mutations in exons 11 and 12 of the glutamate dehydrogenase gene. HI/HA Contributing Investigators." Diabetes 49(4): 667-673.

Stanley, C. A., Y. K. Lieu, et al. (1998). "Hyperinsulinism and hyperammonemia in infants with regulatory mutations of the glutamate dehydrogenase gene." N Engl J Med 338(19): 1352-1357.

Stillman, T. J., P. J. Baker, et al. (1993). "Conformational flexibility in glutamate dehydrogenase. Role of water in substrate recognition and catalysis." J Mol Biol 234(4): 1131-1139.

Stillman, T. J., A. M. Migueis, et al. (1999). "Insights into the mechanism of domain closure and substrate specificity of glutamate dehydrogenase from Clostridium symbiosum." J Mol Biol 285(2): 875-885.

Subbalakshmi, G. Y. and C. R. Murthy (1985). "Isolation of astrocytes, neurons, and synaptosomes of rat brain cortex: distribution of enzymes of glutamate metabolism." Neurochem Res 10(2): 239-250.

Taddei, K., C. Fisher, et al. (2002). "Association between presenilin-1 Glu318Gly mutation and familial Alzheimer's disease in the Australian population." Mol Psychiatry 7(7): 776-781.

Tamir, A., M. Rigbi, et al. (1981). "The interaction of chlorpromazine and butyrophenones with glutamate dehydrogenase." Biochem Pharmacol 30(12): 1469-1473.

Tanizawa, Y., K. Nakai, et al. (2002). "Unregulated elevation of glutamate dehydrogenase activity induces glutamine-stimulated insulin secretion: identification and characterization of a

GLUD1 gene mutation and insulin secretion studies with MIN6 cells overexpressing the mutant glutamate dehydrogenase." Diabetes 51(3): 712-717.

Tomita, T., T. Kuzuyama, et al. (2011). "Structural basis for leucine-induced allosteric activation of glutamate dehydrogenase." J Biol Chem 286(43): 37406-37413.

Tomita, T., T. Miyazaki, et al. (2010). "Hetero-oligomeric glutamate dehydrogenase from Thermus thermophilus." Microbiology 156(Pt 12): 3801-3813.

Traut, T. W. (1994). "Physiological concentrations of purines and pyrimidines." Mol Cell Biochem 140(1): 1-22.

Vallender, E. J., N. Mekel-Bobrov, et al. (2008). "Genetic basis of human brain evolution." Trends Neurosci 31(12): 637-644.

Van Cauwenberghe, C., C. Van Broeckhoven, et al. (2016). "The genetic landscape of Alzheimer disease: clinical implications and perspectives." Genet Med 18(5): 421-430.

Veronese, F. M., J. F. Nyc, et al. (1974). "Nicotinamide adenine dinucleotide-specific glutamate dehydrogenase of Neurospora. I. Purification and molecular properties." J Biol Chem 249(24): 7922-7928.

Walker, E. S., M. Martinez, et al. (2005). "Presenilin 2 familial Alzheimer's disease mutations result in partial loss of function and dramatic changes in Abeta 42/40 ratios." J Neurochem 92(2): 294-301.

Wang, X., N. D. Patel, et al. (2014). "Gene expression patterns in the hippocampus during the development and aging of Glud1 (Glutamate Dehydrogenase 1) transgenic and wild type mice." BMC Neurosci 15: 37.

Westergaard, N., J. Drejer, et al. (1996). "Evaluation of the importance of transamination versus deamination in astrocytic metabolism of [U-13C]glutamate." Glia 17(2): 160-168.

Wheeler, L. J. and C. K. Mathews (2011). "Nucleoside triphosphate pool asymmetry in mammalian mitochondria." J Biol Chem 286(19): 16992-16996.

Winblad, B., K. Palmer, et al. (2004). "Mild cognitive impairment--beyond controversies, towards a consensus: report of the International Working Group on Mild Cognitive Impairment." J Intern Med 256(3): 240-246.

Yang, S. J., J. W. Huh, et al. (2004). "Important role of Ser443 in different thermal stability of human glutamate dehydrogenase isozymes." FEBS Lett 562(1-3): 59-64.

Yang, S. J., J. W. Huh, et al. (2003). "Inactivation of human glutamate dehydrogenase by aluminum." Cell Mol Life Sci 60(11): 2538-2546.

Yasuda, K., N. Koda, et al. (2001). "A Japanese case of congenital hyperinsulinism with hyperammonemia due to a mutation in glutamate dehydrogenase (GLUD1) gene." Intern Med 40(1): 32-37.

Yielding, K. L. and G. M. Tomkins (1960). "Structural Alterations in Crystalline Glutamic Dehydrogenase Induced by Steroid Hormones." Proc Natl Acad Sci U S A 46(11): 1483-1488.

Yielding, K. L. and G. M. Tomkins (1961). "An effect of L-leucine and other essential amino acids on the structure and activity of glutamic dehydrogenase." Proc Natl Acad Sci U S A 47: 983-989.

Yorifuji, T., J. Muroi, et al. (1999). "Hyperinsulinism-hyperammonemia syndrome caused by mutant glutamate dehydrogenase accompanied by novel enzyme kinetics." Hum Genet 104(6): 476-479.

Zaganas, I., K. Kanavouras, et al. (2009). "The human GLUD2 glutamate dehydrogenase: localization and functional aspects." Neurochem Int 55(1-3): 52-63.

Zaganas, I. and A. Plaitakis (2002). "Single amino acid substitution (G456A) in the vicinity of the GTP binding domain of human housekeeping glutamate dehydrogenase markedly attenuates GTP inhibition and abolishes the cooperative behavior of the enzyme." J Biol Chem 277(29): 26422-26428.

Zaganas, I., C. Spanaki, et al. (2002). "Substitution of Ser for Arg-443 in the regulatory domain of human housekeeping (GLUD1) glutamate dehydrogenase virtually abolishes basal activity and markedly alters the activation of the enzyme by ADP and L-leucine." J Biol Chem 277(48): 46552-46558.

Zaganas, I., C. Spanaki, et al. (2012). "Expression of human GLUD2 glutamate dehydrogenase in human tissues: functional implications." Neurochem Int 61(4): 455-462.

Zaganas, I. V., K. Kanavouras, et al. (2014). "The odyssey of a young gene: structure-function studies in human glutamate dehydrogenases reveal evolutionary-acquired complex allosteric regulation mechanisms." Neurochem Res 39(3): 471-486.

Zatta, P., E. Lain, et al. (2000). "Effects of aluminum on activity of krebs cycle enzymes and glutamate dehydrogenase in rat brain homogenate." Eur J Biochem 267(10): 3049-3055.

Zekanowski, C., B. Peplonska, et al. (2004). "The E318G substitution in PSEN1 gene is not connected with Alzheimer's disease in a large Polish cohort." Neurosci Lett 357(3): 167-170.

Zhanhua, C., J. G. Gan, et al. (2005). "Protein subunit interfaces: heterodimers versus homodimers." Bioinformation 1(2): 28-39.

Alzforum http://www.alzforum.org/mutations

Alzheimer Disease & Frontotemporal Dementia Mutation Database http://www.molgen.vib-ua.be/ADMutations/

Biology http://biology.reachingfordreams.com/cellular-energy/cellular-respiration/glycolysis.html

Biochemistry lectures https://www3.nd.edu/~aseriann/tcacfates.html

Chem. Uwec. http://www.chem.uwec.edu/Webpapers2005/mintermm/pages/GDH.html

Ensembl http://www.ensembl.org/index.html

LOVD Whole Genome Datasets http://databases.lovd.nl/whole_genome

OligoEvaluator (http://www.oligoevaluator.com/OligoCalcServlet

Primer3 http://bioinfo.ut.ee/primer3-0.4.0/

Polyphen 2 (http://genetics.bwh.harvard.edu/cgi-bin/ggi/ggi2.cgi
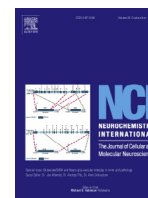
Differential interaction of hGDH1 and hGDH2 with manganese: Implications for metabolism and toxicity

Christina Dimovasili [a], Michael Aschner [b], Andreas Plaitakis [a], Ioannis Zaganas [a,*]

[a] Neurology Laboratory, School of Health Sciences, Faculty of Medicine, University of Crete, Heraklion, Crete, Greece
[b] Department of Molecular Pharmacology, Albert Einstein College of Medicine, Bronx, New York, USA

ARTICLE INFO

ABSTRACT

Manganese (Mn) is an essential trace element that serves as co-factor for many important mammalian enzymes. In humans, the importance of this cation is highlighted by the fact that low levels of Mn cause developmental and metabolic abnormalities and, on the other hand, chronic exposure to excessive amounts of Mn is characterized by neurotoxicity, possibly mediated by perturbation of astrocytic mitochondrial energy metabolism. Here we sought to study the effect of Mn on the two human glutamate dehydrogenases (hGDH1 and hGDH2, respectively), key mitochondrial enzymes involved in numerous cellular processes, including mitochondrial metabolism, glutamate homeostasis and neurotransmission, and cell signaling. Our studies showed that, compared to magnesium (Mg) and calcium (Ca), Mn exerted a significant inhibitory effect on both human isoenzymes with hGDH2 being more sensitive than hGDH1, especially under conditions of low ADP levels. Specifically, in the presence of 0.25 mM ADP, the Mn IC_{50} was 1.14 ± 0.02 mM and 1.54 ± 0.08 mM for hGDH2 and for hGDH1, respectively (p = 0.0001). Increasing Mn levels potentiated this differential effect, with 3 mM Mn inhibiting hGDH2 by 96.5% and hGDH1 by 70.2%. At 1 mM ADP, the Mn IC_{50} was 1.84 ± 0.02 mM and 2.04 ± 0.07 mM (p = 0.01) for hGDH2 and hGDH1, respectively, with 3 mM Mn inhibiting hGDH2 by 93.6% and hGDH1 by 70.9%. These results were due to the sigmoidal inhibitory curve of Mn that was more pronounced for hGDH2 than for hGDH1. Indeed, at 0.25 mM, the Hill coefficient value was higher for hGDH2 (3.42 ± 0.20) than for hGDH1 (1.94 ± 0.25; p = 0.0002) indicating that interaction of Mn with hGDH2 was substantially more co-operative than for hGDH1. These findings, showing an enhanced sensitivity of the hGDH2 isoenzyme to Mn, especially at low ADP levels, might be of pathophysiological relevance under conditions of Mn neurotoxicity.

© 2015 Elsevier Ltd. All rights reserved.

1. Introduction

Manganese (Mn), an essential trace element, is a key component of several important enzymes (Takeda, 2003), including glutamine synthetase (GS) (Wedler and Denman, 1984; Wedler et al., 1982) and superoxide dismutase (MnSOD) (Keele et al., 1970) (Miriyala et al., 2012; Stallings et al., 1991). The importance of this cation is highlighted by the fact that low levels of Mn cause developmental and metabolic abnormalities (Aschner and Aschner, 2005). On the other hand, chronic exposure to excessive amounts of Mn leads to neurotoxicity, referred to as manganism (Chen et al., 2014), a syndrome characterized by neurological abnormalities that resemble parkinsonism (Huang et al., 1989; Mena et al., 1967).

The pathogenesis underlying Mn neurotoxicity remains unclear, but the sequestration of the metal by astrocytes (Aschner et al., 1992; Wedler et al., 1989) and its subsequent accumulation in mitochondria (Wedler et al., 1989) may lead to perturbation of astrocytic mitochondrial energy metabolism and glutamate homeostasis (Crooks et al., 2007; Zwingmann et al., 2003). Specifically, it has been shown that Mn treatment leads to decreased glutamate transport by astrocytes (Hazell and Norenberg, 1997), a process crucial for the removal of transmitter glutamate from the synaptic cleft. This disturbance of glutamate transport may contribute to the excitotoxic-type neuropathology observed in manganism. In addition, Mn could affect astrocytic metabolism by inhibiting GS (Joseph et al., 1979; Tholey et al., 1987) and pyruvate carboxylase (PC) (Wimhurst and Manchester, 1970), which are vital for astrocytic glucose oxidation and brain energy metabolism. Concerning the specific effects of Mn on mitochondrial function, Mn was shown to exert inhibitory effects on oxidative phosphorylation (Gavin et al., 1992). When injected intrastriatally, Mn leads to decreased ATP levels (Brouillet et al., 1993). Mn-induced mitochondrial neurotoxicity could be also associated with production of reactive oxygen species, disturbance of mitochondrial dynamics and disruption of nitric oxide synthase (iNOS) expression and function (Barhoumi et al., 2004; Martinez-Finley et al., 2013).

* Corresponding author. Neurology Laboratory, Medical School, University of Crete, Voutes, 71003 Heraklion, Crete, Greece. Tel.: +30 2810 394643; fax: +30 2810 394839.
E-mail address: johnzag@yahoo.com (I. Zaganas).

In mammalian mitochondria, the reversible inter-conversion of glutamate to α-ketoglutarate and ammonia is catalyzed by glutamate dehydrogenase (GDH) (Hudson and Daniel, 1993), which lies at the crossroads of several astrocytic metabolic pathways. The functional role of this enzyme includes, among others, interconnection of the Krebs cycle with amino-acid metabolism and possibly regulation of synaptic glutamate levels (Plaitakis and Zaganas, 2001). Indeed, the levels of the main allosteric effectors of GDH (ADP, GTP, and L-leucine) depend on the cellular energy charge, suggesting that the activity of this enzyme is tightly associated with energy metabolism (Plaitakis and Zaganas, 2001). In humans and other primates, GDH exists in two isoforms, named hGDH1 and hGDH2, respectively (Shashidharan et al., 1994). Despite their high amino-acid sequence similarity, the two isoenzymes differ significantly in their enzymatic properties (Zaganas et al., 2009). Specifically, hGDH2's function is strongly dependent on ADP activation and is practically insensitive to GTP inhibition, while hGDH1 is potently inhibited by GTP and shows significant baseline activity in the absence of ADP (Zaganas and Plaitakis, 2002; Zaganas et al., 2002). In addition to the allosteric regulators mentioned above, there is preliminary evidence that divalent cations, such as Mn, magnesium (Mg) and calcium (Ca), exert a regulatory effect on GDH in various species (Fahien et al., 1990; Shashidharan et al., 1997).

Given the importance of GDH for mitochondrial metabolism and the possibility that Mn neurotoxicity is mediated through disruption of mitochondrial function, we studied the effect of Mn on hGDHs. For comparison, we also studied the effect of equivalent concentrations of Mg and Ca, two other divalent cations involved in a variety of biological processes. Results showing that Mn interacted with hGDH2 with a greater affinity than with hGDH1 are described below.

2. Materials and methods

2.1. Protein expression

Recombinant hGDH1 and hGDH2 proteins were produced in Sf21 (*Spodoptera frugiperda*) cells using the Baculovirus expression system, as previously described (Shashidharan et al., 1994). pVL1393 and pVL1392 plasmid vectors, carrying hGDH1 and hGDH2 cDNAs, respectively (Shashidharan et al., 1994), have been combined with linearized baculovirus DNA (Baculogold, BD, Pharmingen) (Zaganas and Plaitakis, 2002). For the Sf21 cell culture, Grace's Insect medium supplemented with 10% fetal bovine serum (FBS), 0.1% pluronic surfactant and gentamicin were used. Erlenmeyer or spinner flasks were kept in a 27 °C incubator, for large-scale protein production. For cell lysis and homogenization, the cell pellets were resuspended in a lysis buffer containing 10 mM Tris–HCl, 0.5M NaCl, 0.5 mM ethylenediamine tetraacetic acid (EDTA) (pH 7.4), Triton 1% and protease inhibitors. The obtained crude cell extracts were subsequently used for enzymatic assays or for protein purification.

2.2. Protein purification

Following standard protocols in our laboratory, GDH purification was performed in a four-step procedure that included two ammonium sulfate precipitation cuts (30% and 65%), hydrophobic interaction chromatography and, finally, hydroxyapatite chromatography (Zaganas and Plaitakis, 2002). The pellet from the last ammonium sulfate cut was re-suspended in a 15% ammonium sulfate solution (in Tris–HCl, pH 6) and loaded on a phenyl-sepharose column pre-equilibrated with the same solution. Elution was performed by a 15% ammonium sulfate –90% ethylene-glycol gradient. The fractions from hydrophobic interaction chromatography containing GDH activity were pooled together and dialyzed against a 200 mM KCl solution using a dialysis membrane with MWCO 7000.

The post-dialysis sample was then subjected to hydroxyapatite chromatography. The hydroxyapatite column was equilibrated with 50 mM sodium phosphate pH 6.8, before sample loading. The GDH enzymes were finally eluted with a 50–400 mM sodium phosphate, pH 6.8 gradient. The desired fractions containing the purified proteins were used for enzymatic assays.

2.3. Enzymatic assays

Enzymatic assays of human GDHs were performed spectrophotometrically at 340 nm in the reductive amination direction. The reaction mixture, of 1 ml final volume, contained 50 mM triethanolamine pH 8, 100 mM ammonium acetate and 100 μM NADPH. Enzyme reaction was initiated with the addition of α-ketoglutarate to obtain a final concentration of 10 mM. ADP was added in the reaction, either at 0.25 mM or, for maximal activity, at 1 mM, since hGDH2 shows very little activity in the absence of ADP. For the kinetic studies with Mn, 0.25–3 mM of $MnCl_2$ (M3634, Sigma, St. Louis, MO, USA) was added to the reaction mixture. Similar concentrations $CaCl_2$ (C5080, Sigma, St. Louis, MO, USA) and $MgCl_2$ (#5833, Merck, Darmstadt, Germany) were used for studying the effect of Ca and Mg, respectively. As a control, EDTA was added in the reaction buffer (at a concentration of 2.6 mM) and the Mn kinetic studies were repeated for both iso-enzymes.

2.4. Statistical analysis

All findings presented were replicated in at least 3 independent experiments and were plotted as % of the maximal activity (activity obtained in the absence of the cation under study) versus the cation concentration. T-test was used to compare the variables (IC_{50}, slope of the regression line) of the transformed linear regression curves. $p < 0.05$ was considered significant.

3. Results

3.1. Manganese inhibits hGDH2 more potently than hGDH1

Cell extracts from baculovirus-infected Sf21 cells displayed measurable GDH activity when assayed in the presence of either NADH or NADPH. Since the insect's endogenous GDH is NADH specific, activity measured in the presence of NADPH originated only from the exogenous (recombinantly expressed) hGDH1 and hGDH2, respectively. Thus, all assays described below were performed with NADPH as previously described (Shashidharan et al., 1994). In addition, in accordance with previous findings (Shashidharan et al., 1997), hGDH2 showed, in the absence of allosteric activators (ADP and L-leucine), very low basal activity compared to hGDH1; this activity was fully restored, as expected, by the addition of 1 mM ADP.

Initial studies that explored the effect of the three metals (Mn, Ca and Mg) on human GDHs were performed in crude cell extracts at 0.25 mM and 1.0 mM ADP. These assays revealed that Mn exerts significant inhibitory effect on both hGDHs in a concentration-dependent manner, and this inhibition was more potent for hGDH2 compared to hGDH1 (Suppl. Fig. S1). Specifically, in the presence of 0.25 mM ADP, the Mn IC_{50} (Inhibitory Concentration 50: concentration of inhibitor which lowers enzyme activity to 50% of its maximal) was 1.36 ± 0.13 mM for hGDH2 and 2.61 ± 0.07 mM for hGDH1 ($P < 0.0001$; Suppl. Fig. S1A; Suppl. Table S1). The inhibition effect of Mn was less pronounced when the reaction was performed in the presence of 1 mM ADP, with hGDH2 proving again to be more sensitive to Mn than hGDH1 (Suppl. Fig. S1B). On the other hand, in crude cell extracts, Mg and Ca exerted lesser effects on hGDH1 and hGDH2. Specifically, in the presence of ADP 0.25 mM, 3.0 mM of Ca decreased hGDH1 and hGDH2 activity by 10.6% and 33.4%, respectively (Suppl. Fig. S2A). Likewise, 3.0 mM of Mg de-

creased hGDH1 and hGDH2 activity by 29.5% and 39.7%, respectively (Suppl. Fig. S3A). When the concentration of ADP was increased to 1 mM, neither Ca nor Mg exerted a significant inhibitory effect on hGDH1 and hGDH2 (Suppl. Figs. S2B, S3B). As an additional control for our studies, we performed the same experiment in the presence of EDTA (2.6 mM), a Mn chelator. Results showed that, under these conditions, neither hGDH1 nor hGDH2 was inhibited by Mn (Suppl. Fig. S4). As shown in Suppl. Fig. S4, the linear regression line of activity versus Mn concentration was almost parallel to the x-axis.

In light of the results obtained with the use of crude cells extracts, we then tested that effect of the three cations on highly purified recombinant hGDH1 and hGDH2, obtained as described in Materials and Methods. Functional assays employing the purified enzymes confirmed that Mn interacted with hGDH2 with a greater affinity than with hGDH1. However, under the same conditions, Ca and Mg essentially had no inhibitory effect on either purified human isoenzyme (Figs. 1–3). Specifically, in the presence of 0.25 mM ADP, the Mn IC_{50} was 1.14 ± 0.02 mM and 1.54 ± 0.08 mM for hGDH2 and hGDH1, respectively ($p = 0.0001$; Fig. 1A, Table 1). Increasing Mn levels potentiated this differential effect, with 3 mM Mn inhibiting hGDH2 by 96.5% and hGDH1 by 70.2%. At 1 mM ADP, the Mn IC_{50} was 1.84 ± 0.02 mM and 2.04 ± 0.07 mM for hGDH2 and hGDH1, respectively ($p = 0.01$; Fig. 1B, Table 1), with 3 mM Mn inhibiting hGDH2 by 93.6% and hGDH1 by 70.9%. These results were due to the sigmoidicity of the Mn inhibitory curve that was more pronounced for hGDH2 than for hGDH1. Indeed, at 0.25 mM ADP, the Hill coefficient value was higher for hGDH2 (3.42 ± 0.20) than for hGDH1 (1.94 ± 0.25; $p = 0.0002$), indicating that the interaction of Mn with hGDH2 was substantially more co-operative than for hGDH1. Likewise, in the presence of ADP 1 mM, the HC values were 3.29 ± 0.38 and 5.12 ± 0.27, for hGDH1 and hGDH2, respectively ($p = 0.001$), indicating a high degree of co-operativity (approaching, in the case of hGDH2, the theoretical maximum of 6 for the hexamer).

In contrast, both Ca and Mg, added at concentrations 0–3 mM in the reaction mixture, did not significantly affect the activity of neither purified isoenzyme, in the presence of either 0.25 mM ADP or 1 mM ADP (Figs. 2 and 3). Interestingly, even in the presence of 0.25 mM ADP, Ca and Mg did not exert on purified hGDH1 and hGDH2 the small inhibitory effect observed in crude extracts (Figs. 2A, 3A, Suppl. Figs. S2A, S3A), indicating that a component of the crude extracts could possibly affect the interaction of Ca and Mg with the human GDH isoenzymes.

4. Discussion

Here we report that Mn has the capacity to inhibit hGDH1 and hGDH2 activity measured in the direction of reductive amination of α-ketoglutarate to glutamate, in the presence of either 0.25 or 1 mM ADP (with the strongest inhibitory effect seen in the presence of 0.25 mM ADP). Previous studies have provided evidence that regulation of GDH activity by Mn is observed in various organisms. For example, it was shown that GDH activity (studied in the direction of oxidative deamination of glutamate) from *Blastocladiella emersonii* was activated by Mn (LéJohn et al., 1969). Likewise, GDH activity (in the direction of reductive amination) of pea seeds (*Pisum sativum L.*) was activated by Ca and Mn (Garland and Dennis, 1977), and that of the extremely thermophilic archaebacterial isolate AN1 was activated by Ca, Mg and Mn (Hudson and Daniel, 1993; Hudson et al., 1993). In contrast, mammalian GDHs are inhibited by rather high concentrations of Mg (Fahien et al., 1990; Kuo et al., 1994; Shashidharan et al., 1997) with Ca having no such effect (Kuo et al., 1994). However, there are several controversies regarding the effect of Mg, Ca and Mn on mammalian GDHs, indicating that the exact effect of these cations depends on the biochemical environment where the GDH reaction takes place (Bailey et al., 1982; Fahien et al., 1990; Kuo et al., 1994; Shashidharan et al., 1997).


(A)

ADP 0.25mM, Purified enzymes
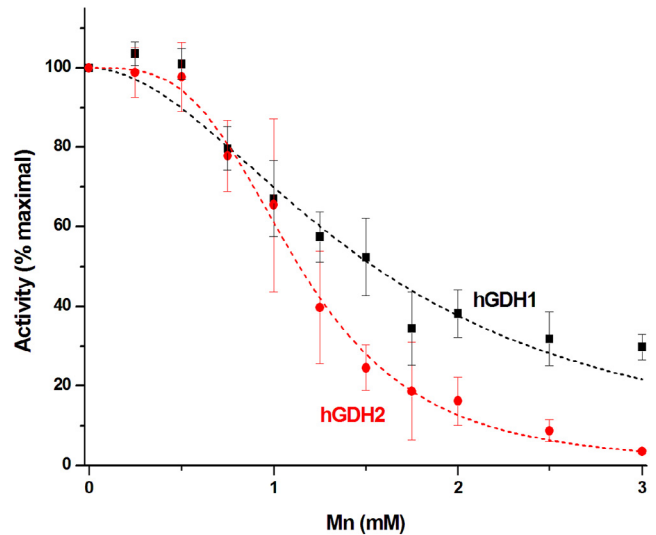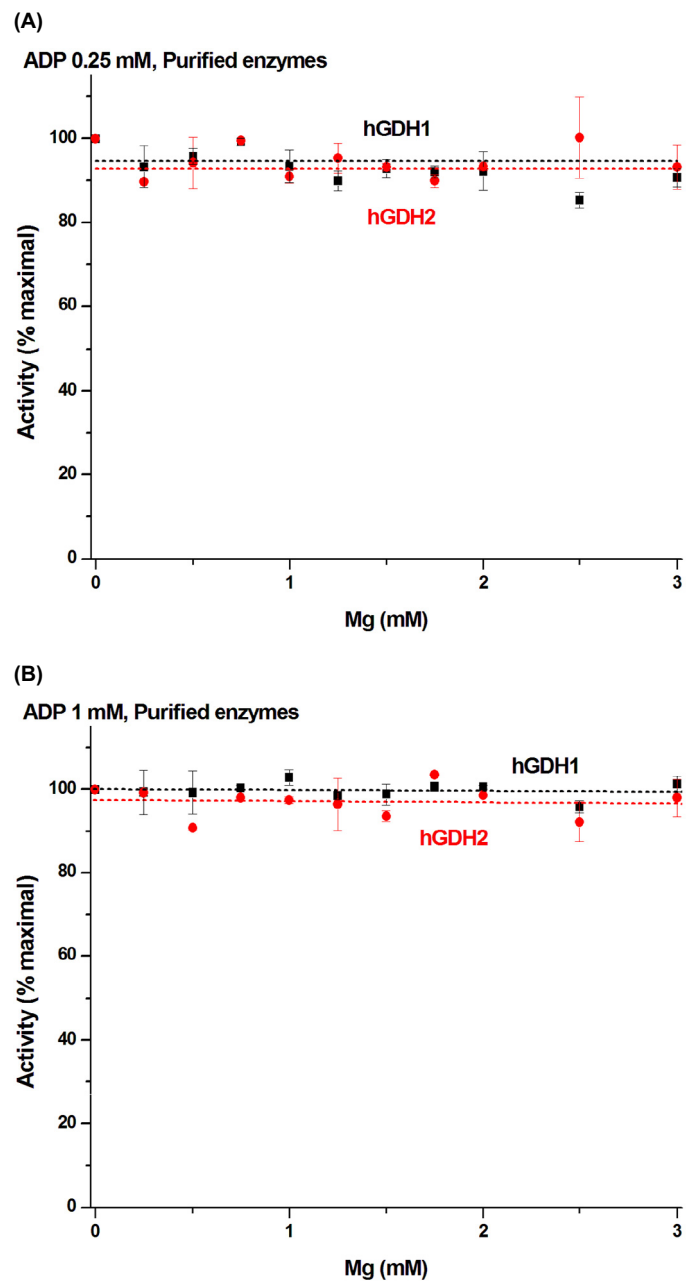
(B)

ADP 1mM, Purified Enzymes
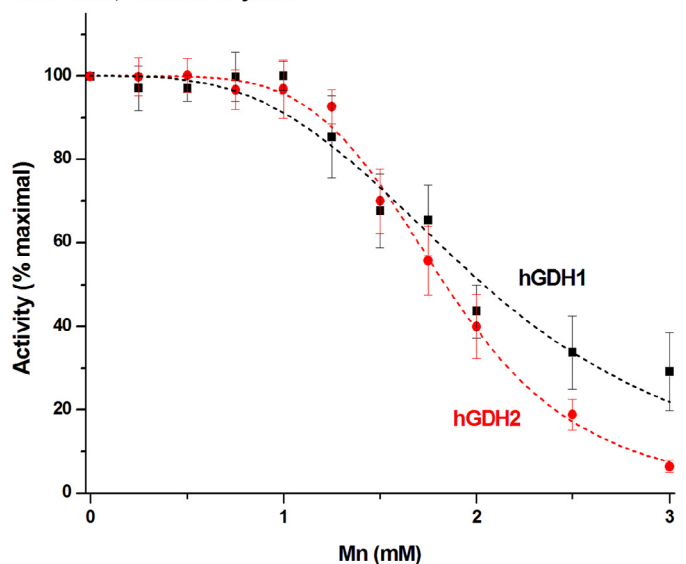
Fig. 1. Mn exerts differential inhibitory effect on purified hGDH1 and hGDH2 recombinant enzymes. Assays were performed in the presence of 0.25 mM ADP (A) or 1 mM ADP (B). Kinetic studies were performed as described in Materials and Methods. Data points represent the mean of at least 3 independent determinations and error bars the SEM. Under both conditions, hGDH2 showed higher sensitivity to Mn inhibition (most pronounced in the presence of 0.25 mM ADP). Both enzymes showed significant cooperativity for this inhibition, which was higher for hGDH2 (Table 1).

The inhibitory effect of Mn on both hGDH1 and hGDH2 was evident when the concentration of Mn was increased to >1.0 mM in the reaction buffer. It is reported that glial cells possess a highly efficient transport mechanism for Mn (Aschner et al., 1992), and have the capacity to accumulate Mn in intracellular levels of at least 50–75 μM (Tholey et al., 1987). More recently Bowman and Aschner (2014) have calculated astrocytic intracellular Mn concentrations, estimating the normal human brain Mn concentrations at 5.32–14.03 ng Mn/mg protein (corresponding to 20.0–52.8 μM Mn). Given that general toxic responses occur when Mn brain concentrations are elevated by ~3 fold (Erikson et al., 2007; Molina et al., 2011),
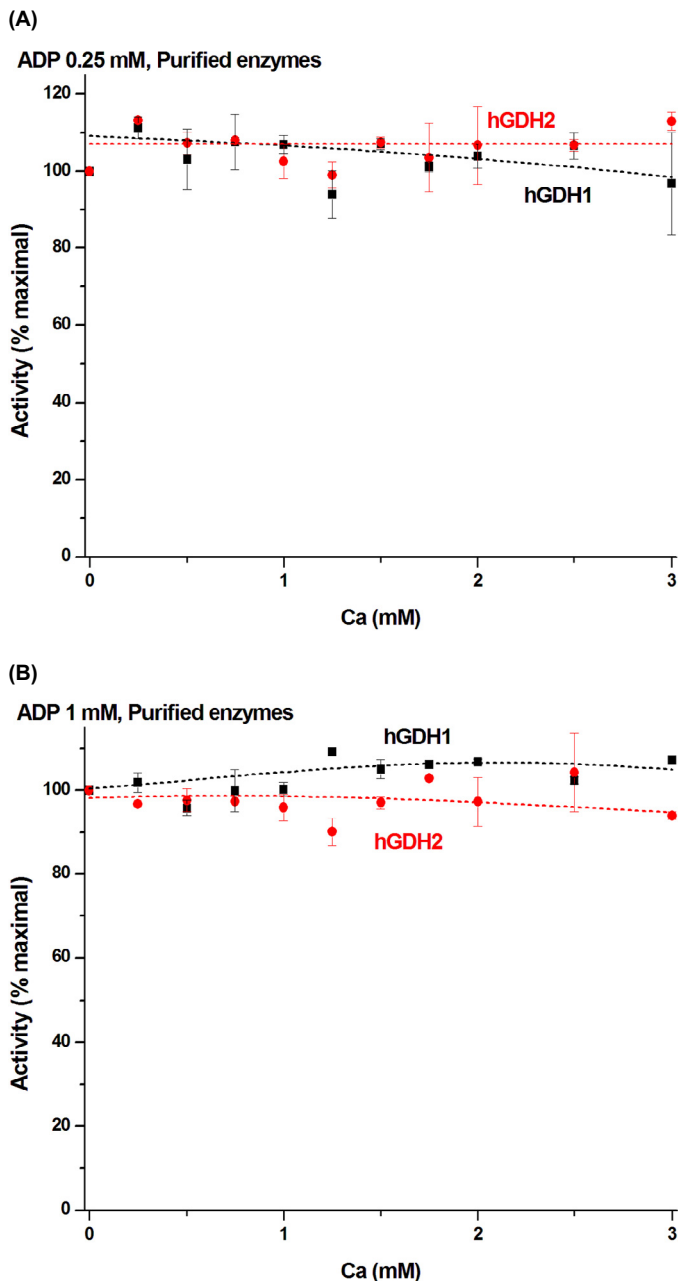
Fig. 2. Ca does not exert a significant inhibitory effect on either purified hGDH1 or purified hGDH2 recombinant enzymes. Assays were performed in the presence of 0.25 mM ADP (A) or 1 mM ADP (B). Kinetic studies were performed as described in Materials and Methods. Data points represent the mean of at least 2 independent determinations and error bars the SEM. Under both ADP conditions, neither hGDH1 nor hGDH2 is sensitive to Ca inhibition.

Fig. 3. Mg does not exert a significant inhibitory effect on either purified hGDH1 or purified hGDH2 recombinant enzymes. Assays were performed in the presence of 0.25 mM ADP (A) or 1 mM ADP (B). Kinetic studies were performed as described in Materials and Methods. Data points represent the mean of at least 2 independent determinations and error bars the SEM. Under both ADP conditions, neither hGDH1 nor hGDH2 is sensitive to Mg inhibition.

aberrant function would be expected to occur at Mn brain concentrations of 60.1–158.4 µM Mn, below the range ascertained herein for the Mn-induced inhibition of hGDH2 (>1 mM Mn). Nevertheless, taking into account that 60–70% of Mn is sequestered in mitochondria (Wedler et al., 1989), it is postulated that the microenvironment conditions prevailing in these organelles may favor Mn concentrations in excess of 1 mM. Additionally, even though concentrations lower than 1 mM may not significantly affect the enzyme's activity, given that the enzyme functions at equilibrium, even slight effects (brought about by rather low Mn concentrations) may affect the way GDH regulates intra-mitochondrial metabolite levels.

Although the Mn inhibition effect was observed for both human GDHs, this cation preferentially inhibited hGDH2. Given the high sequence similarity between the two human GDHs (Shashidharan et al., 1994), one would expect them to have a similar pattern of inhibition. Nevertheless, as observed with a range of other inhibitors/activators, the two isoenzymes display different regulatory properties, which are mainly due to two of the amino acid substitutions acquired by hGDH2 during its evolution, namely Arg443Ser and Gly456Ala (Mastorodemos et al., 2015; Zaganas et al., 2009). Of note, hGDH2 showed a highly cooperative behavior during Mn inhibition, as indicated by the sigmoidicity of the inhibitory curve, and the high HC values, approaching the theoretical maximum of 6 for

Table 1
Inhibition of hGDH1 and hGDH2 activity in purified enzyme preparations by Mn.

ADP	Mn (purified enzymes)	
	0.25 mM	1 mM
IC_{50} (mM)		
hGDH1	1.54 ± 0.08	2.04 ± 0.07
hGDH2	1.14 ± 0.02	1.84 ± 0.02
P value*	0.0001	0.01
Hill coefficient		
hGDH1	1.94 ± 0.25	3.29 ± 0.38
hGDH2	3.42 ± 0.20	5.12 ± 0.27
P value*	0.0002	0.001

* *P* values refer to the comparison of hGDH1 and hGDH2 under the same conditions.
Values derive from the composite linear curves presented in Fig. 1A and B.

the hGDH2 hexamer. This contrasts the non-cooperative behavior of the hGDH2 isoenzyme toward several allosteric effectors (including GTP and steroids), but is in accordance with the highly cooperative behavior shown by hGDH2 during inhibition by spermidine (Spanaki et al., 2012). While differences in the degree of inhibition of hGDH1 and hGDH2 by Mn were rather small (as reflected in the IC_{50}), interaction of Mn with the two isoenzymes was substantially different (as revealed by the study of their inhibitory curves), indicating that the molecular mechanisms involved are distinct. In fact the high degree of co-operativity, obtained with hGDH2 inhibition, suggests that initial binding of Mn to hGDH2 induces a chain of subunit interactions that markedly facilitates the binding of the cation to the remaining subunits. Additional studies may shed light on these important molecular mechanisms of this differential inhibition by Mn, which may be relevant to enzyme function in health and disease.

Our results may imply that the hGDH2 isoenzyme is preferentially affected (compared to hGDH1) by Mn under toxic conditions. A careful analysis of the inhibitory curves of the purified recombinant hGDHs revealed that Mn at 3.0 mM is capable of inhibiting hGDH2 by about 95% and hGDH1 by about 70%. As GDH is shown to attain very high levels in astrocytic mitochondria (up to 10 mg/ml mitochondrial matrix), a near complete inhibition of enzyme activity may be needed to prevent glutamate flux through the GDH pathway. As such, our data suggest that this may be possible for hGDH2 but not for hGDH1 given the presence of these proteins in excess in the mitochondrial matrix. Given the differential distribution of the two isoenzymes (Zaganas et al., 2012), this could result in differential vulnerability of different tissues to Mn. This is also consistent with the fact that mitochondrial function is differentially affected by Mn in various tissues (Gunter et al., 2010).

The ADP levels in the mitochondrial matrix fluctuate, dependent upon the energy status of the cell, and have been shown to be in the mM range (Metelkin et al., 2009). In our studies, lowering the ADP concentration from 1 to 0.25 mM led to an increase in the Mn-induced inhibition of both the hGDH1 and the hGDH2 isoenzyme. Since the ADP levels at this range of concentrations directly affect the activity of the latter, this could also indicate that this Mn-induced inhibition is inversely correlated to the hGDH2 enzymes' activation state. In other words, at low ADP levels, the vulnerability of the hGDH2 isoenzyme to Mn inhibition becomes highest. This could be physiologically relevant, since it has been shown that under intense glutamatergic neurotransmission there is significant energy expenditure, leading to high ADP levels. Inversely, this could also signify increased vulnerability of the hGDH2 isoenzyme of non-actively transmitting neurons (and surrounding astrocytes) to the toxic effect of Mn, due to low ADP levels.

It is of interest that the clinical effects of Mn neurotoxicity resemble Parkinson's disease (Aschner et al., 2009). In this respect, it has been shown that a rare variant of the hGDH2 gene leads to earlier age of onset in Parkinson's disease patients (Plaitakis et al., 2010). Since Mn preferentially inhibits hGDH2 (as shown in this study), and hGDH2 variants could be involved in the phenotype of Parkinson's disease, it is tempting to speculate that in both cases, part of the parkinsonian phenotype is due to disruption of hGDH2 function in basal ganglia. Furthermore, our findings on the ability of EDTA to reverse the Mn-induced inhibition of both hGDH1 and hGDH2 are consistent with earlier observations establishing EDTA's efficacy in attenuating symptoms associated with Mn-induced parkinsonism (Herrero Hernandez et al., 2006).

In summary, we have shown that Mn preferentially inhibits hGDH2 (particularly at low ADP concentrations) with other divalent cations, such as Mg and Ca, having little effect on this enzyme. Our findings on hGDH2 inhibition by Mn could be of pathophysiological relevance for the neurotoxicity observed in manganism and, even though less likely, for the pathogenesis of Parkinson's disease.

Appendix: Supplementary material

Supplementary data to this article can be found online at doi:10.1016/j.neuint.2015.03.004.

References

Aschner, J.L., Aschner, M., 2005. Nutritional aspects of manganese homeostasis. Mol. Aspects Med. 26, 353–362.

Aschner, M., Gannon, M., Kimelberg, H.K., 1992. Manganese uptake and efflux in cultured rat astrocytes. J. Neurochem. 58, 730–735.

Aschner, M., Erikson, K., Hernández, E., Tjalkens, R., 2009. Manganese and its role in Parkinson's disease: from transport to neuropathology. Neuromolecular Med. 11, 252–266.

Bailey, J., Bell, E.T., Bell, J.E., 1982. Regulation of bovine glutamate dehydrogenase. The effects of pH and ADP. J. Biol. Chem. 257, 5579–5583.

Barhoumi, R., Faske, J., Liu, X., Tjalkens, R.B., 2004. Manganese potentiates lipopolysaccharide-induced expression of NOS2 in C6 glioma cells through mitochondrial-dependent activation of nuclear factor kappaB. Molecular Brain Research 122, 167–179.

Bowman, A.B., Aschner, M., 2014. Considerations on manganese (Mn) treatments for in vitro studies. Neurotoxicology 41, 141–142.

Brouillet, E.P., Shinobu, L., McGarvey, U., Hochberg, F., Beal, M.F., 1993. Manganese injection into the rat striatum produces excitotoxic lesions by impairing energy metabolism. Exp. Neurol. 120, 89–94.

Chen, P., Parmalee, N., Aschner, M., 2014. Genetic factors and manganese-induced neurotoxicity. Front. Gen. 5.

Crooks, D.R., Welch, N., Smith, D.R., 2007. Low-level manganese exposure alters glutamate metabolism in GABAergic AF5 cells. Neurotoxicology 28, 548–554.

Erikson, K.M., Thompson, K., Aschner, J., Aschner, M., 2007. Manganese neurotoxicity: a focus on the neonate. Pharmacol. Ther. 113, 369–377.

Fahien, L.A., Teller, J.K., Macdonald, M.J., Fahien, C.M., 1990. Regulation of glutamate dehydrogenase by Mg^{2+} and magnification of leucine activation by Mg^{2+}. Mol. Pharmacol. 37, 943–949.

Garland, W.J., Dennis, D.T., 1977. Steady-state kinetics of glutamate dehydrogenase from Pisum sativum *L. mitochondria*. Arch. Biochem. Biophys. 182, 614–625.

Gavin, C.E., Gunter, K.K., Gunter, T.E., 1992. Mn^{2+} sequestration by mitochondria and inhibition of oxidative phosphorylation. Toxicol. Appl. Pharmacol. 115, 1–5.

Gunter, T.E., Gerstner, B., Lester, T., Wojtovich, A.P., Malecki, J., Swarts, S.G., et al., 2010. An analysis of the effects of Mn^{2+} on oxidative phosphorylation in liver, brain, and heart mitochondria using state 3 oxidation rate assays. Toxicol. Appl. Pharmacol. 249, 65–75.

Hazell, A., Norenberg, M., 1997. Manganese decreases glutamate uptake in cultured astrocytes. Neurochem. Res. 22, 1443–1447.

Herrero Hernandez, E., Discalzi, G., Valentini, C., Venturi, F., Chiò, A., Carmellino, C., et al., 2006. Follow-up of patients affected by manganese-induced Parkinsonism after treatment with CaNa2EDTA. Neurotoxicology 27, 333–339.

Huang, C.C., Chu, N.S., Lu, C.S., Wang, J.D., Tsai, J.L., Tzeng, J.L., et al., 1989. Chronic manganese intoxication. Arch. Neurol. 46, 1104–1106.

Hudson, R., Daniel, R., 1993. L-glutamate dehydrogenases: distribution, properties and mechanism. Comp. Biochem. Physiol. B. 106, 767–792.

Hudson, R., Ruttersmith, L., Daniel, R., 1993. Glutamate dehydrogenase from the extremely thermophilic archaebacterial isolate AN1. Biochim. Biophys. Acta 1202, 244–250.

Joseph, S., Bradford, N., McGivan, J., 1979. Inhibition of glutamine synthetase activity by manganous ions in a cytosol extract of rat liver. Biochem. J. 184, 477–480.

Keele, B.B., McCord, J.M., Fridovich, I., 1970. Superoxide dismutase from Escherichia coli B: a new manganese-containing enzyme. J. Biol. Chem. 245, 6176–6181.

Kuo, N., Michalik, M., Erecinska, M., 1994. Inhibition of glutamate dehydrogenase in brain mitochondria and synaptosomes by Mg^{2+} and polyamines: a possible cause for its low in vivo activity. J. Neurochem. 63, 751–757.

LéJohn, H.B., Jackson, S.G., Klassen, G.R., Sawula, R.V., 1969. Regulation of mitochondrial glutamic dehydrogenase by divalent metals, nucleotides, and α-ketoglutarate: correlations between the molecular and kinetic mechanisms, and the physiological implications. J. Biol. Chem. 244, 5346–5356.

Martinez-Finley, E.J., Gavin, C.E., Aschner, M., Gunter, T.E., 2013. Manganese neurotoxicity and the role of reactive oxygen species. Free Radic. Biol. Med. 62, 65–75.

Mastorodemos, V., Kanavouras, K., Sundaram, S., Providaki, M., Petraki, Z., Kokkinidis, M., et al., 2015. Side-chain interactions in the regulatory domain of human glutamate dehydrogenase determine basal activity and regulation. J. Neurochem. In press.

Mena, I., Marin, O., Fuenzalida, S., Cotzias, G.C., 1967. Chronic manganese poisoning. Clinical picture and manganese turnover. Neurology 17, 128–136.

Metelkin, E., Demin, O., Kovács, Z., Chinopoulos, C., 2009. Modeling of ATP–ADP steady-state exchange rate mediated by the adenine nucleotide translocase in isolated mitochondria. FEBS J. 276, 6942–6955.

Miriyala, S., Spasojevic, I., Tovmasyan, A., Salvemini, D., Vujaskovic, Z., StClair, D., et al., 2012. Manganese superoxide dismutase, MnSOD and its mimics. Biochim. Biophys. Acta 1822, 794–814.

Molina, R.M., Phattanarudee, S., Kim, J., Thompson, K., Wessling-Resnick, M., Maher, T.J., et al., 2011. Ingestion of Mn and Pb by rats during and after pregnancy alters iron metabolism and behavior in offspring. Neurotoxicology 32, 413–422.

Plaitakis, A., Zaganas, I., 2001. Regulation of human glutamate dehydrogenases: implications for glutamate, ammonia and energy metabolism in brain. J. Neurosci. Res. 66, 899–908.

Plaitakis, A., Latsoudis, H., Kanavouras, K., Ritz, B., Bronstein, J.M., Skoula, I., et al., 2010. Gain-of-function variant in GLUD2 glutamate dehydrogenase modifies Parkinson's disease onset. Eur. J. Hum. Genet. 18, 336–341.

Shashidharan, P., Michaelidis, T.M., Robakis, N.K., Kresovali, A., Papamatheakis, J., Plaitakis, A., 1994. Novel human glutamate dehydrogenase expressed in neural and testicular tissues and encoded by an X-linked intronless gene. J. Biol. Chem. 269, 16971–16976.

Shashidharan, P., Clarke, D.D., Ahmed, N., Moschonas, N., Plaitakis, A., 1997. Nerve tissue-specific human glutamate dehydrogenase that is thermolabile and highly regulated by ADP. J. Neurochem. 68, 1804–1811.

Spanaki, C., Zaganas, I., Kounoupa, Z., Plaitakis, A., 2012. The complex regulation of human glud1 and glud2 glutamate dehydrogenases and its implications in nerve tissue biology. Neurochem. Int. 61, 470–481.

Stallings, W.C., Metzger, A.L., Pattridge, K.A., Fee, J.A., Ludwig, M.L., 1991. Structure-function relationships in iron and manganese superoxide dismutases. Free Radic. Res. Commun. 12–13 (1), 259–268.

Takeda, A., 2003. Manganese action in brain function. Brain Res. Rev. 41, 79–87.

Tholey, G., Bloch, S., Ledig, M., Mandel, P., Wedler, F., 1987. Chick brain glutamine synthetase and Mn^{2+}–Mg^{2+} interactions. Neurochem. Res. 12, 1041–1047.

Wedler, F., Denman, R., 1984. Glutamine synthetase: the major Mn(II) enzyme in mammalian brain. Curr. Top. Cell. Regul. 24, 153–169.

Wedler, F., Denman, R., Roby, W., 1982. Glutamine synthetase from ovine brain is a manganese(II) enzyme. Biochemistry 21, 6389–6396.

Wedler, F., Ley, B., Grippo, A., 1989. Manganese(II) dynamics and distribution in glial cells cultured from chick cerebral cortex. Neurochem. Res. 14, 1129–1135.

Wimhurst, J., Manchester, K., 1970. Some aspects of the kinetics of rat liver pyruvate carboxylase. Biochem. J. 120, 79–93.

Zaganas, I., Plaitakis, A., 2002. Single amino acid substitution (G456A) in the vicinity of the GTP binding domain of human housekeeping glutamate dehydrogenase markedly attenuates GTP inhibition and abolishes the cooperative behavior of the enzyme. J. Biol. Chem. 277, 26422–26428.

Zaganas, I., Spanaki, C., Karpusas, M., Plaitakis, A., 2002. Substitution of ser for arg-443 in the regulatory domain of human housekeeping (GLUD1) glutamate dehydrogenase virtually abolishes basal activity and markedly alters the activation of the enzyme by ADP and l-leucine. J. Biol. Chem. 277, 46552–46558.

Zaganas, I., Kanavouras, K., Mastorodemos, V., Latsoudis, H., Spanaki, C., Plaitakis, A., 2009. The human GLUD2 glutamate dehydrogenase: localization and functional aspects. Neurochem. Int. 55, 52–63.

Zaganas, I., Spanaki, C., Plaitakis, A., 2012. Expression of human GLUD2 glutamate dehydrogenase in human tissues: functional implications. Neurochem. Int. 61, 455–462.

Zwingmann, C., Leibfritz, D., Hazell, A.S., 2003. Energy metabolism in astrocytes and neurons treated with manganese; relation among cell-specific energy failure, glucose metabolism, and intercellular trafficking using multinuclear NMR-spectroscopic analysis. J. Cereb. Blood Flow Metab. 23, 756–771.

OVERVIEW

The Odyssey of a Young Gene: Structure–Function Studies in Human Glutamate Dehydrogenases Reveal Evolutionary-Acquired Complex Allosteric Regulation Mechanisms

**Ioannis V. Zaganas · Konstantinos Kanavouras · Nikolas Borompokas ·
Giovanna Arianoglou · Christina Dimovasili · Helen Latsoudis ·
Metaxia Vlassi · Vasileios Mastorodemos**

Abstract Mammalian glutamate dehydrogenase (GDH) catalyzes the reversible inter-conversion of glutamate to α-ketoglutarate and ammonia, interconnecting carbon skeleton and nitrogen metabolism. In addition, it functions as an energy switch by its ability to fuel the Krebs cycle depending on the energy status of the cell. As GDH lies at the inter-section of several metabolic pathways, its activity is tightly regulated by several allosteric compounds that are metabolic intermediates. In contrast to other mammals that have a single GDH-encoding gene, humans and great apes possess two isoforms of GDH (hGDH1 and hGDH2, encoded by the *GLUD1* and *GLUD2* genes, respectively) with distinct reg-ulation pattern, but remarkable sequence similarity (they differ, in their mature form, in only 15 of their 505 amino-acids). The *GLUD2* gene is considered a very young gene, emerging from the *GLUD1* gene through retro-position only recently (<23 million years ago). The new hGDH2 iso-enzyme, through random mutations and natural selection, is thought to have conferred an evolutionary advantage that helped its persistence through primate evolution. The prop-erties of the two highly homologous human GDHs have been studied using purified recombinant hGDH1 and hGDH2 proteins obtained by expression of the corresponding cDNAs in Sf21 cells. According to these studies, in contrast to hGDH1 that maintains basal activity at 35–40 % of its maximal, hGDH2 displays low basal activity that is highly responsive to activation by rising levels of ADP and/or L-leucine which can also act synergistically. While hGDH1 is inhibited potently by GTP, hGDH2 shows remarkable GTP resistance. Furthermore, the two iso-enzymes are differen-tially inhibited by estrogens, polyamines and neuroleptics, and also differ in heat-lability. To elucidate the molecular mechanisms that underlie these different regulation patterns of the two iso-enzymes (and consequently the evolutionary adaptation of hGDH2 to a new functional role), we have performed mutagenesis at sites of difference in their amino acid sequence. Results showed that the low basal activity, heat-lability and estrogen sensitivity of hGDH2 could be, at least partially, ascribed to the Arg443Ser evolutionary change, whereas resistance to GTP inhibition has been attributed to the Gly456Ala change. Other amino acid sub-stitutions studied thus far cannot explain all the remaining functional differences between the two iso-enzymes. Also, the Arg443Ser/Gly456Ala double mutation in hGDH1 approached the properties of wild-type hGDH2, without being identical to it. The insights into the structural mecha-nism of enzymatic regulation and the implications in cell biology provided by these findings are discussed.

I. V. Zaganas (✉) · K. Kanavouras · N. Borompokas ·
G. Arianoglou · C. Dimovasili · H. Latsoudis ·
V. Mastorodemos
Neurology Laboratory, Medical School, University of Crete,
Voutes, 71003 Heraklion, Crete, Greece
e-mail: johnzag@med.uoc.gr; johnzag@yahoo.com

M. Vlassi
Institute of Biosciences and Applications, National Center for
Scientific Research "Demokritos",
15310 Ag. Paraskevi, Athens, Greece

Introduction
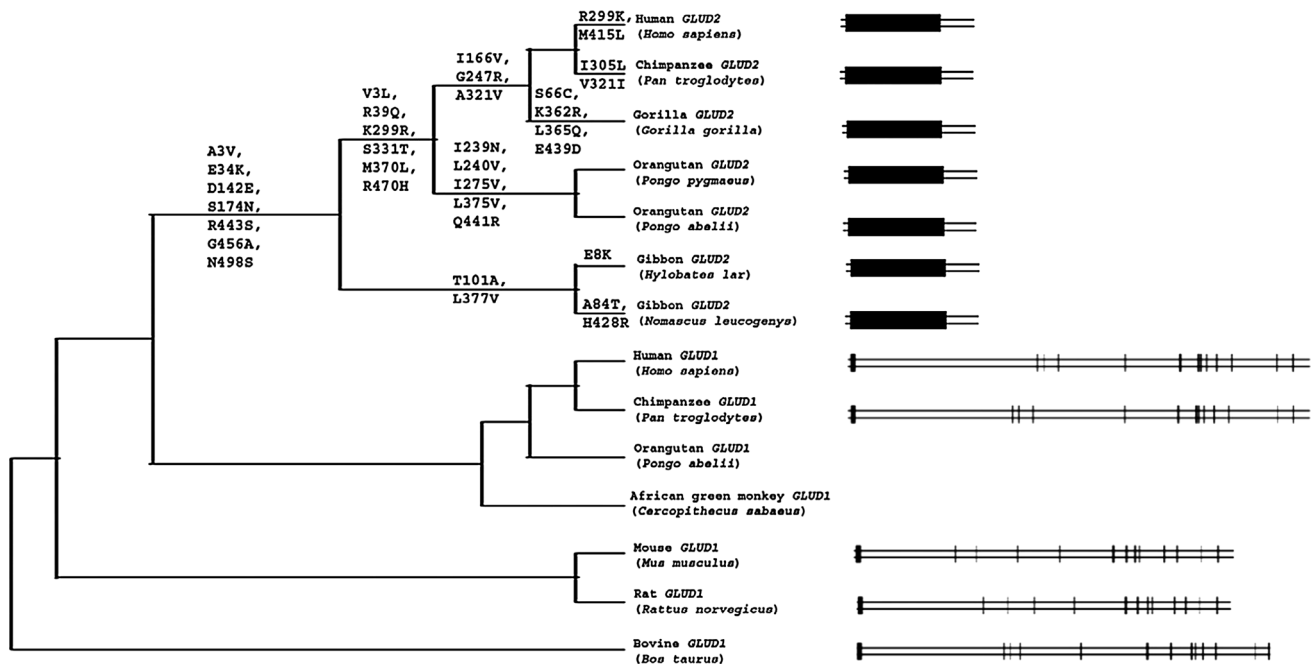
Mammalian glutamate dehydrogenase (GDH; Fig. 1) cat-alyzes the reversible inter-conversion of glutamate to α-ketoglutarate and ammonia employing NADP(H) and

Fig. 1 Evolution of mammalian *GLUD* genes. Shown is a phylogenetic tree diagram based on publicly available mammalian *GLUD* sequences encoding for a mature GDH protein. The phylogenetic tree was drawn using the ClustalW [76] and TreeView [77] programs. The bovine *GLUD1* sequence was used as outgroup. Amino acid substitutions that led to the emergence of the current sequence of GDH2 proteins in modern primates ([17]; primate genome sequencing projects) are shown on the corresponding branches. On the *right hand side*, we present the exon–intron organization of genes for which the entire sequence is currently known (with vertical bands representing exons). All *GLUD1* genes depicted contain 13 exons and are autosomal, whereas the X-linked *GLUD2* genes from primates are organized in a single exon. *GLUD1* and *GLUD2* genes are drawn to scale to each other, respectively. Reproduced from [21], with permission

NAD(H) as cofactors [1]. Although GDH is abundant in most cell types, the exact role of the enzyme in cell biology remains far from being fully understood. However, it is evident that it lies at the crossroads of several intersecting metabolic pathways and connects carbon skeleton and nitrogen metabolism. Given its nodal position, this enzyme has acquired a sophisticated control of its activity [1, 2]. In mammals, GDH is thought to function mainly in the oxidative deamination direction, permitting glutamate to fuel the Krebs cycle for energy production. This is expected to occur under certain intracellular and extracellular conditions that favor entry of glutamate in the Krebs cycle via the GDH reaction rather than via the action of transaminases [3, 4].

Thus, one can assume that much of the allosteric regulation of the GDH enzyme may have evolved to control influx (in the form of acetyl-CoA) and efflux (mainly in the form of CO_2 and NADH) of carbon atoms and energy to the Krebs cycle, through adjusting levels of α-ketoglutarate. This hypothesis is corroborated by in vitro functional studies which show that mammalian GDH is allosterically regulated by various compounds related to energy homeostasis and cell metabolism. The list of these compounds is extensive and includes, among others, purine nucleotides (ADP, ATP, GTP

and NADH), L-leucine, palmitoyl-CoA and steroid hormones [1]. Of these, GTP and ADP are thought to act as energy switches, inactivating and activating the enzyme, respectively, depending on their levels that in turn reflect the energy status of the cell. Specifically, under high energy conditions (and thus high GTP levels), GDH is inactivated and stops feeding the Krebs cycle. This effect is rather immediate, as GTP is produced in the second next step in the TCA cycle, specifically when succinyl-CoA (deriving from α-ketoglutarate) is converted to succinate via the action of succinyl-CoA synthetase (SCS) [5]. Of note, there are two isoforms of SCS, one that produces ATP and one that produces GTP [6]. Most tissues express both isoforms, even though the former is mainly expressed in high energy-consuming tissues (such as brain and muscle). To complicate things further, there is a possibility that GTP transphosphorylates with ADP through the action of nucleoside diphosphate kinase [6]. However, ATP and GTP are not readily interchangeable and may maintain different phosphorylation potentials to serve different cellular functions. Moreover, as most cells express both isoforms of SCS, it is possible that there is functional compartmentalization achieved though formation of macromolecular complexes [6]. It is possible that the GTP-producing SCS is mostly involved in GDH regulation.

When energy is depleted (and thus ADP levels increase), GDH is activated to feed glutamate to the Krebs cycle and convert more ADP to ATP, through oxidation of Kreb's cycle-derived NADH and FADH$_2$ in the respiratory chain. In turn, ATP produced from the respiratory chain can also inhibit mammalian GDH (although with much lower affinity than GTP). In addition, L-leucine activates GDH, showing a synergistic effect when used with ADP [7]. This could imply that under high protein load (e.g. after a protein meal), GDH is activated by L-leucine and feeds the Krebs cycle with the excess glutamate (direct effect) or the excess amount of other related amino acids (indirect effect; through conversion of these amino acids to glutamate; [8]), especially under conditions of energy deficit (low ADP levels). Regulating the flux of glutamate from/to the Krebs cycle and normalizing the levels of amino acids after a protein load are only two of the possible roles of GDH in cellular homeostasis. Additional roles have been investigated, including its role in ammonia management, insulin secretion and neurotransmitter production and degradation [9–12].

Structure of Mammalian Glutamate Dehydrogenase

Crystallographic studies of bovine GDH and subsequently of the human *GLUD1*-gene derived enzyme [13, 14] have elucidated in great extent the molecular mechanisms of enzyme catalysis and regulation. According to these studies, mammalian GDH is a hexameric molecule composed of six identical subunits (Fig. 2). Each subunit has three distinct domains: the NAD$^+$ binding domain, the glutamate binding domain and the regulatory domain, with the latter consisting of the antenna and the pivot helix (Figs. 2, 3).

The antenna is a protruding part of each subunit that consists of an ascending helix and a descending random coil strand that contains a small α-helix (Fig. 3). In each of the two trimers that compose the GDH hexamer, the antennae of three adjacent subunits are intertwined (Fig. 2). This interaction mediates inter-subunit communication that is thought to be essential for allosteric regulation [15].

These crystallographic studies on bovine and human GDH have shown that the NAD$^+$ domain pivots about the long axis of a long α-helix (pivot helix) connected to the descending strand of the antenna. It has been also suggested that during opening and closure of the catalytic cleft, the NAD$^+$ domain, in addition to rotating along the long axis of the pivot helix, at the same time twists about the antenna [14]. Specifically, upon substrate binding, the NAD$^+$ binding domain rotates along the pivot helix and towards the glutamate binding domain to close that catalytic cleft, while the inverse rotation occurs during opening of the catalytic cleft.
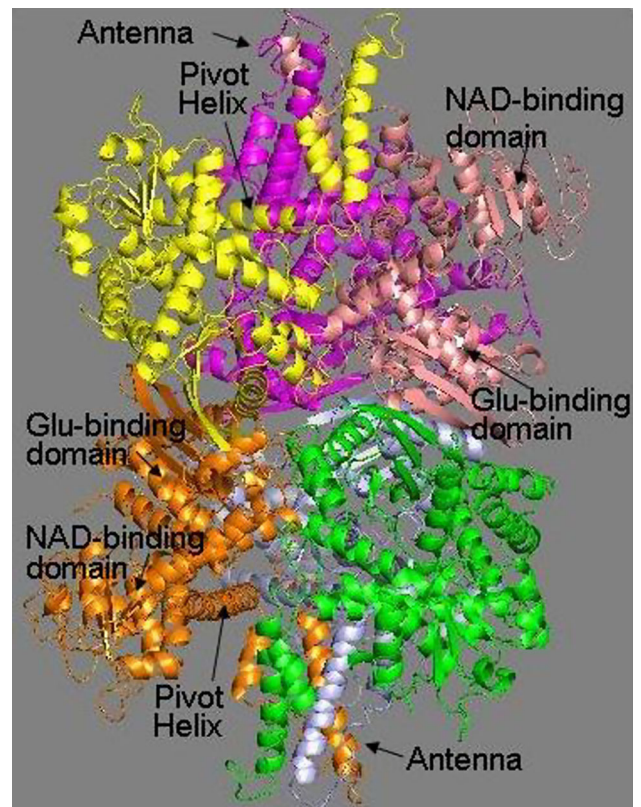
Fig. 2 Cartoon representation of the 3D-structure of the hGDH1 hexamer (apo-form; coordinates are taken from the hGDH1 crystal structure with PDB code: 1L1F; [14]). *Different coloring* is used for each monomer and only some sub-domains in different monomers are indicated, for clarity. The figure was rendered using PyMOL Molecular Graphics System, Version 1.4, Schrödinger, LLC (Color figure online)

Multiplicity of GDH in the Human and the Great Apes

Most mammals have a single functional *GLUD1* gene that is widely expressed and encodes the housekeeping GDH (hGDH1 in the human). However, less than 23 million years ago, in the common ancestor of modern-day hominoids, a retroposition event led to the emergence of a second GDH-encoding gene, termed *GLUD2* gene [16, 17] (Fig. 1). This new gene encodes an iso-enzyme (hGDH2) that is highly homologous to hGDH1 (they differ in only 15 of their 505 amino acids in their mature form), but possesses distinct enzymatic properties and tissue expression pattern. Following the cloning of the human *GLUD1* gene by Mavrothalassitis et al. [18], screening of a human retina cDNA library by Plaitakis group in Mount Sinai, New York [16] led to the cloning of the human *GLUD2* gene. *GLUD2* lacks introns and maps to the human X chromosome (see also contribution by Shashidharan and Plaitakis in this issue). The intronless nature of *GLUD2* and its high amino-acid homology to *GLUD1* have led Shashidharan et al. [16] to propose that *GLUD2* is a processed gene resulting from retro-position of the *GLUD1* gene to the X chromosome.
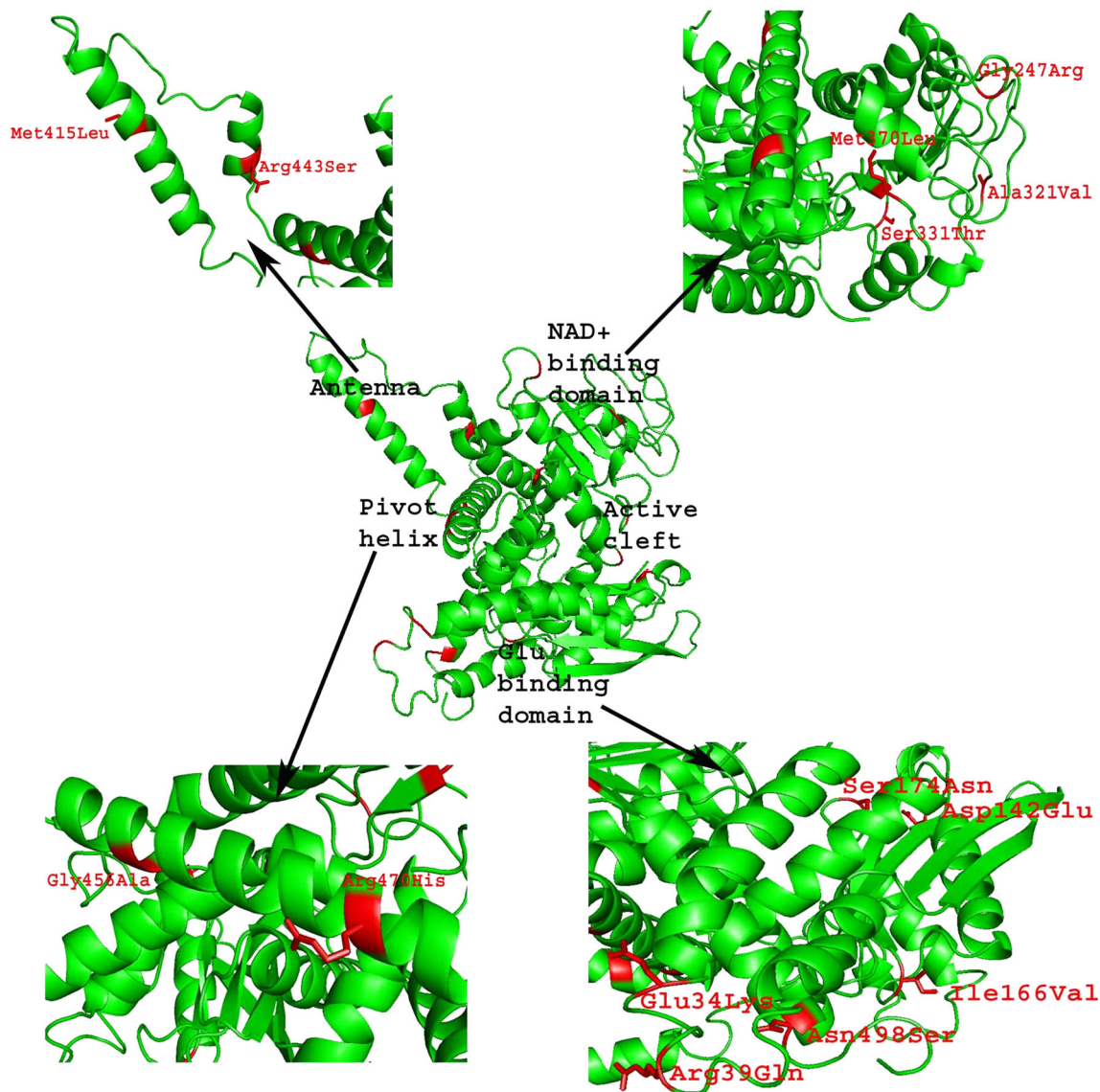
Fig. 3 Comparison of hGDH1 and hGDH2 sequences. Shown is a cartoon representation of the hGDH1 structure (apo-form; PDB code: 1L1F; [14]). For simplicity, only one of the six subunits that compose the hGDH1 hexamer is shown (in *green*). Residues at sites of difference between hGDH1 and hGDH2 are shown in *red*. The main functional parts of the subunit (NAD$^+$ binding domain, glutamate binding domain, pivot helix and antenna) are also shown. The amino acid differences between hGDH1 and hGDH2 are named separately for each of these four main functional parts, as *insets*. This diagram was produced using PyMOL (Color figure online)

This was later verified by Burki and Kaessmann [17], who provided evidence that this retro-position event occurred very recently (<23 million years ago). Following its insertion into the X chromosome, the *GLUD2* gene evolved through random mutations and subsequent natural selection.

Despite concerns that this intronless gene could simply represent a pseudogenized and subsequently decayed duplicate of the parental gene, its persistence through evolution in modern day primates (including humans) and expression data at the RNA and the protein level [16, 19–21] show that this is a fully functional gene. It is also widely accepted that retrogenes which evolve into functional genes

as a result of a natural selection pressure are most commonly species specific and are, thus, associated with interspecies differences [22]. Furthermore its importance for nervous tissue biology is underscored by the fact that a gain of function mutant of hGDH2 could relate to accelerated neurodegeneration in Parkinson's disease patients [23].

Functional Differences of hGDH1 and hGDH2

Following the cloning of the *GLUD2* gene, Plaitakis and Shashidharan expressed *GLUD1* and *GLUD2* cDNAs using

the Baculovirus/Sf cell system [16]. This permitted the production of the two human iso-enzymes (that possess dual-coenzyme specificity, i.e. can use either NADP(H) and NAD(H) with comparable efficacy) in a system with essentially zero background activity when assays were performed using NADP(H), given that the endogenous insect enzyme of Sf cells is NAD(H) specific. Furthermore, using a combination of ammonium sulfate precipitation, hydrophobic interaction chromatography and hydroxyapatite chromatography [24], the recombinant human iso-enzymes were separated from other insect proteins (including the insect GDH, data not shown) and obtained in pure form.

An issue of concern at the time was if the recombinant iso-enzymes expressed in insect (Sf) cells displayed the same enzymatic properties as the iso-enzymes from human tissues. Studies by Shashidharan et al. [16] in New York showed that the kinetic properties of the expressed hGDH2 were comparable to the kinetic properties of the particulate and the soluble GDH activity purified from human brain (with the exception of Km for NADPH in the case of the soluble GDH activity). Later on in Crete, we showed that the expressed wild-type hGDH1 enzyme behaves in a manner comparable to the endogenous human enzyme purified from human liver (known at the time to express the *GLUD1* gene only) [25]. The GDH-specific activity (measured in the presence of 1 mM ADP) of the recombinant expressed wild type hGDH1 was comparable to that of the endogenous human liver GDH (in the order of 120–130 μmol of NADPH oxidized/min/mg protein). Kinetic analyses revealed that the Km values for α-keto-glutarate and for NADPH of the purified recombinant wild type hGDH1 were similar to those of the purified endogenous human liver enzyme [25]. In addition, the maximum velocities (*V*max) of the two purified human GDHs were comparable [25]. GTP inhibition studies showed that the endogenous human liver GDH was as sensitive to GTP inhibition as the recombinant wild-type hGDH1 enzyme, and the two enzymes showed similar co-operativity for this inhibition [25]. Also, the ADP and L-leucine activation patterns of the two hGDH1 enzymes (recombinant and endogenous) were very similar [25].

As expected in the case of the eukaryotic Sf cell system, the recombinant hGDHs are processed in the cultured insect cells in a manner similar to that of the mammalian GDH, which involves removal of the 53-amino acid-long leader sequence predicted by the *GLUD1* cDNA [7, 25, 26]. Expressed recombinant hGDH1 purified from insect cell extracts shows the same molecular mass as the mature human protein purified from human liver [25] and an N-terminal amino acid sequence (Ser–Glu–Ala–Val–Ala…) identical to that obtained by sequencing of GDH purified from human liver [7]. Also, the purified hGDH1 (either expressed or purified from human liver) is slightly

larger than the commercially available bovine liver GDH [25]. This is consistent with sequencing data showing that the commercially available bovine liver enzyme is four amino acids shorter than hGDH1, probably due to proteolytic degradation during purification [27]. Of note, the expressed recombinant hGDH2 runs on SDS-PAGE at 58 kDa, which is 2 kDa higher than the hGDH1 enzyme, either the expressed recombinant or the one purified from human liver [16, 19, 28, 29].

Functional analyses of these expressed recombinant human iso-enzymes revealed that, while hGDH1 and hGDH2 are highly homologous in their amino acid sequence (Fig. 1), they differ markedly in their basal catalytic activity (activity measured in the absence of ADP or other effectors and expressed as percent of activity measured in the presence of ADP 1 mM), regulatory properties, optimal pH and relative resistance to heat inactivation [7, 30–32]. In contrast to the wild-type hGDH1, which maintains about 35–40 % of its maximal activity at baseline, hGDH2 shows very little basal catalytic activity (2–8 % of its maximal; Table 1). This basal activity seems to be enhanced at increasing enzyme concentrations in vitro, but still remains significantly lower than that of hGDH1 [23, 29]. Despite this low basal activity, hGDH2 is remarkably responsive to activation by ADP and/or L-leucine [7]. Given that the two iso-enzymes show comparable maximal activity (in the presence of 1 mM ADP) and hGDH2 has much lower basal activity than hGDH1, the proportional activation of hGDH2 by 1 mM ADP is significantly higher. However, the affinity of ADP for hGDH2 (as measured by the SC$_{50}$ values, i.e. the ADP concentration at which ADP activation is 50 % of the maximal activation) is lower than that for hGDH1 (Table 1). L-leucine also induces activation of hGDH2 that is proportionally greater compared to that of hGDH1, but the two iso-enzymes show comparable affinity for this amino-acid [29] (Table 1). Concerning inhibition by GTP, hGDH2 is remarkably resistant to this compound, either in the presence (Table 1) or the absence of ADP [30, 31]. Furthermore, hGDH1 shows a co-operative behavior for this GTP inhibition, whereas the behavior of hGDH2 is largely un-cooperative [30]. In contrast to GTP, palmitoyl-CoA, spermidine (a polyamine), ECGC (epigallocatechin gallate, a green tea polyphenol) and neuroleptics (haloperidol and perphenazine) inhibit hGDH2 more potently than hGDH1 [33–35]. In addition, the two iso-enzymes show a difference in their pH optimum, with that of hGDH2 being slightly lower than that of hGDH1 (7.5 and 8.0, respectively) [7, 29]. Finally, the hGDH2 iso-enzyme is markedly more thermo-labile than the hGDH1 iso-enzyme, especially in the absence of activators [7, 28, 29] (Table 1).

In contrast with the above significant differences in the allosteric regulation, pH dependence and thermostability of these iso-enzymes, kinetic analyses showed that the

Table 1 Properties of the wild-type hGDH1 and hGDH2, as well as of various hGDH1 and hGDH2 mutants [23, 25, 29, 31, 32, 34, 36, 40]

Property	GTP IC$_{50}$ in μM (at ADP 1 mM)	GTP Hill c. (at ADP 1 mM)	ADP SC$_{50}$ (μM)	L-Leucine SC$_{50}$ (mM)	App. basal activity (% maximal)	DES IC$_{50}$ (μM)	T$_{50}$ (min)	Haloperidol IC$_{50}$ in μM (at 0.1 mM ADP)
WT-hGDH1	12.2	2.5	24.3	1.0	35.0–40.0	32.4	348.0	121.6
WT-hGDH2	166.8	0.71	68.5	1.1	2.0–8.0	10.1	38.0	25.6
R443S-1	16.2	2.0	405.6	–	0.0–0.5	1.9	5.0	12.3
G456A-1	79.5	1.1	25.4	–	36.0–38.0	60.7	–	141.8
R443S/G456A-1	139.4	0.64	188.4	–	1.0–2.0	6.3	16.5	–
E34 K-1	–	–	–	–	–	24.2	–	71.7
R39Q-1	–	–	–	–	–	51.5	–	160.0
D142E-1	–	–	–	–	–	29.8	–	82.6
I166V-1	–	–	–	–	–	40.9	–	129.7
S174N-1	–	–	–	–	–	61.4	–	180.5
G247R-1	–	–	–	–	–	41.9	–	112.5
A321V-1	–	–	–	–	–	44.1	–	124.1
S331T-1	10.8	2.4	34.6	–	–	34.8	–	118.3
M370L-1	11.3	2.1	21.0	–	–	52.9	–	148.4
M415L-1	14.7	2.3	28.1	–	–	24.3	–	97.5
R470H-1	10.5	2.6	24.7	–	–	39.0	–	90.2
N498S-1	11.8	2.4	23.4	–	–	26.5	–	93.3
Q41R-2	227.4	0.9	72.1	–	17.9	–	78.0	–
S445L-2	317.6	0.6	58.1	–	19.0	–	158.0	–
S445A-2	257.7	–	58.2	1.0	–	–	–	–
S448P-2	186.8	0.6	62.0	–	2.9	–	–	–
K450E-2	1.8×10^5	0.4	458.4	–	1.7	–	1.5	–
H454Y-2	2,921.4	0.5	468.6	–	2.5	–	3.1	–

IC$_{50}$: half maximal inhibitory concentration

SC$_{50}$: half maximal stimulatory concentration

T$_{50}$: half life (min) at (1) 47.5 °C for the first four enzymes (in 100 mM sodium phosphate buffer 6.8; [29]) and (2) 49.5 °C for the last four enzymes (in 100 mM sodium phosphate buffer 7.4; [45])

DES diethylstilbestrol

catalytic properties of hGDH2 (Vmax and Km for substrates) were quite similar to those of the housekeeping hGDH1 [29–32].

Structural Basis of the Different Regulatory Properties of hGDH1 and hGDH2

In view of the impressively distinct allosteric regulation properties of the two hGDH iso-enzymes, we asked which of the only 15 amino acid differences (Fig. 3) could account for their functional diversity. To answer this, we systematically mutagenized the *GLUD1* cDNA, by replacing each of the 15 amino acid residues at positions of difference between the two iso-enzymes, with the amino acid residue encoded at this position by the *GLUD2* cDNA. Indeed, structure–function analyses of the mutant hGDH1s in our laboratory in Crete led to the identification of the point mutations that equipped hGDH2 with most of its unique properties [25, 29, 31, 32, 36, 37]. These analyses are presented below grouped by the region of the hGDH1 subunit where each mutated amino acid residue resides.

Mutagenesis Studies in the Pivot Helix of hGDH1

Previous structural studies had shown that the pivot helix of the mammalian GDH is important for its catalytic function and allosteric regulation, since it participates in the significant conformational changes occurring during catalysis and forms part of the cavity where GTP binds [15]. Also, Stanley et al. [38] had shown that pivot helix amino-acid substitutions, associated with the hyperinsulinism–hyperammonemia (HI/HA) syndrome, produce a mutant hGDH1 enzyme that was highly resistant to GTP. Following this, Lee et al. [39] had used mutagenesis and a bacterial expression system to identify K450 (that belongs to the pivot helix and is found mutated in some children with the HI/HA syndrome) as a site for GTP binding.

Thus, we hypothesized that the marked difference in the GTP inhibition of the two iso-enzymes could be due to mutations in the pivot helix. To test this, we replaced the two amino acid residues in the pivot helix of hGDH1 at positions of difference between the two human iso-enzymes (G456 and R470) with the corresponding hGDH2 residues, A and H, respectively [25] (Fig. 3).

Results showed that the hGDH1 iso-enzyme harboring the G456A-1 mutation was markedly resistant to GTP [25]. Under baseline conditions the IC$_{50}$ for GTP was about 10–15 times higher for the G456A-1 mutant protein than for the wild type hGDH1. These differences in GTP sensitivity were also noted when GTP inhibition was studied in the presence of ADP (Table 1). In addition, Hill plot

analyses showed that the G456A-1 mutation abolished the cooperative behavior of the enzyme [25] (Table 1). The G456A-1 substitution in hGDH1 rendered the enzyme somewhat less sensitive to estrogens, which is in the opposite direction than expected, since hGDH2 is more sensitive to estrogens than hGDH1 [40] (Table 1). However, the ADP activation pattern (Table 1), the GDH-specific activity (measured in the presence of 1 mM ADP), the maximum velocities (Vmax) and the Km values for α-ketoglutarate and NADPH of the purified G456A-1 mutant were comparable to those of the recombinant wild type hGDH1 [25]. Interestingly, while the G456A-1 mutation in hGDH1 gave the enzyme GTP inhibition properties similar to those of hGDH2 [25], the inverse change in hGDH2 is claimed to not fully revert these properties to hGDH1 properties [41].

G456 in hGDH1 lies in a tightly packed area at the interface between two GDH subunits and more precisely, it is located on the pivot helix and at a point where the pivot helix of one subunit comes in contact with the antenna of an adjacent subunit [25] (Fig. 4). The introduced A456 side chain in the G456A-1 mutant may induce a steric clash with the side chain of F387 from the same subunit and L401 side chain from the adjacent subunit [25] (Fig. 4). Furthermore, the side of the pivot helix opposite to G456 makes contact with GTP [15] (Fig. 4) and this GTP-binding pivot helix, through its interaction with the "antenna-like" region of GDH, is thought to be important for the communication between the catalytic subunits [15]. The disturbances elicited by the introduction of Ala instead of Gly at position 456 may impair the ability of the antenna to participate in inter-subunit communication, a process that may be essential for the intensity and co-operativity of GTP inhibition.

In contrast to the G456A-1 mutation, substitution of H for R470 did not affect the allosteric regulation of the enzyme by GTP, ADP or estrogens [25, 40] (Table 1). Analysis of the R470H-1 enzyme and its parental enzyme (wild-type hGDH1) gave comparable IC$_{50}$ values for GTP inhibition and SC$_{50}$ values for ADP activation [25]. In addition, the GTP inhibitory curve for R470H-1 mutant was as sigmoidal as that of the wild type hGDH1, indicating cooperative GTP binding (Table 1). R470 in hGDH1 is located on the surface of the protein (Fig. 4), with apparently no significant interactions with ligands or other amino acids.

Mutagenesis Studies in the Pivot Helix of hGDH2

The HI/HA-associated pivot helix mutations of hGDH1 (K450E-1, H454Y-1) render the enzyme GTP resistant without significantly affecting its basal activity, although
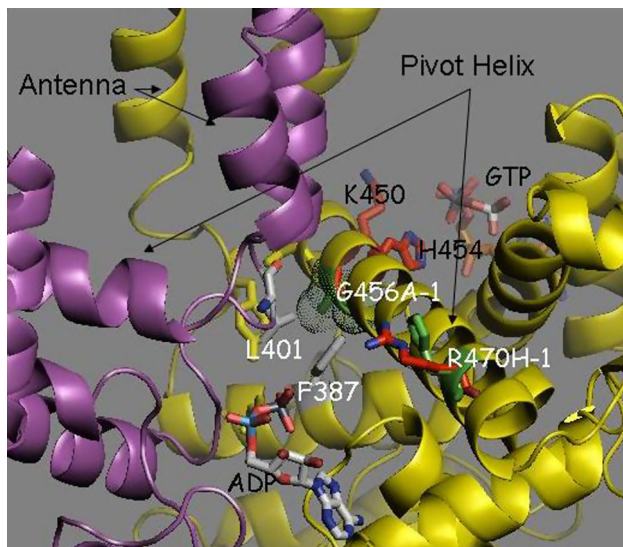
Fig. 4 Close-up of the hGDH1 3D-structure in the G456 region (open form; as in Fig. 2). Only two monomers are shown, for clarity. Important residues discussed in the text are shown as stick-models and are labeled. Residues on the pivot α-helix of hGDH1 mutated in hGDH2 and in HI/HA syndrome, are colored in *red*. Equivalent hGDH2 residues (modeled by in silico mutagenesis based on the 1L1F crystal structure) are colored in *green* and common residues in both hGDHs are colored in *silver*. The atoms of the mutated G456A in hGDH2 are depicted as *dotted spheres*. Coordinates for the GTP and ADP molecules are obtained from the crystal structures of bovine GDH1 complexes in the closed (PDB code: 3MW9; [15]) and open forms (PDB code: 1NQT; [46]), respectively. Replacement of G456 by A is thought to lead to local steric clashes (with the side-chains of F387 and L401 from the same and adjacent subunits, respectively), affecting intra-trimer communication that mediates allostery [25]. The figure was rendered using PyMOL (Color figure online)

the H454Y-1 mutation may increase the Km for NADH and α-ketoglutarate [42–44]. The functional consequences of these mutations in the same residues of hGDH2 seemed interesting to look at, as hGDH2 is already very resistant to GTP due to the G456A-1 evolutionary change discussed above. Thus, we mutagenized residues located in the pivot helix of hGDH2, essentially introducing these hGDH1 HI/HA mutations into hGDH2 [45].

Replacing either K450 with E or H454 with Y in hGDH2 significantly diminished basal activity to <2.5 % of the maximal activity [45] (Table 1). ADP restored the activity of the K450E-2 and H454Y-2 mutants, even though at substantially greater ADP concentrations than those required to activate the parental wild-type hGDH2 [45] (Table 1). In addition, the K450E-2 and the H454Y-2 mutations further increased GTP resistance (Table 1) and impaired activation by L-leucine [45]. Hill coefficient analyses of the GTP inhibition showed that both these pivot helix mutants displayed negative co-operativity [45] (Table 1). These observations showed that residues K450 and H454 (mutated in the HI/HA syndrome in hGDH1),

apart from being important for GTP inhibition, also have a role in catalytic function, at least in hGDH2.

At the structural level, it may not be surprising that these two pivot helix mutants (K450E-2 and H445Y-2) desensitized the hGDH2 enzyme to ADP activation, as ADP binds in part to the pivot helix [46] (Fig. 4). Due to their location, these amino acid substitutions in hGDH2 may prevent the NAD$^+$ domain from revolving about the pivot helix during opening and closure of the catalytic cleft. This could lead to hyper-closure of the active site of hGDH2 (thus diminishing basal catalytic activity) and prevent ADP from inducing activation. The K450E-1 and H454Y-1 mutations in hGDH1 do not have such profound functional consequences, besides increasing GTP resistance (due to the fact that K450 and H454 form part of the GTP binding pocket, coming in contact with the β-phosphate of GTP) [15] (Fig. 4). One possible explanation is that, in hGDH2, the presence of S instead of R at position 443 leads to a closed catalytic cleft conformation that is further reinforced by the introduced K450E-2 and H445Y-2 mutations [45].

Mutagenesis Studies in the Antenna of hGDH1

Previous structural studies have shown the importance of the antenna region for the enzymatic properties of GDH, since this region undergoes significant conformational changes during catalysis and allosteric regulation [15]. Stanley et al. [38] had shown that HI–HA syndrome-associated amino-acid substitutions in the antenna produce a highly GTP-resistant hGDH1 enzyme. Also, one of these antenna substitutions (S448P-1) produced a mutant hGDH1 enzyme that, in addition to GTP resistance, showed low basal activity [38]. Thus, the amino acid substitutions in the antenna region seemed attractive candidates for explaining the functional differences between hGDH1 and hGDH2 that could not be attributed to the G456A-1 change.

Indeed, site-directed mutagenesis studies showed that the low basal activity of hGDH2 relates to the evolutionary R443S-1 amino acid change [36]. The R443S-1 mutant was essentially inactive under base-line conditions (in the absence of activators) and the amount of the enzyme added to the reaction needed to be at least ten times the amount used under regular assay conditions to reach measurable activity (Table 1).

Also, the R443S-1 substitution seemed to, at least partially, account for the differences between the two wild-type human iso-enzymes in pH optimum. Although the basal activity of the wild-type hGDH1 enzyme decreased when lowering the pH from 8.0 to 7.0, that of the R443S-1 mutant increased [36]. In this respect, the hGDH2 enzyme performs equally well at pH 7.0 and 8.0 [31].

The addition of 1 mM ADP resulted in full activation of the (basally inactive) R443S-1 mutant, with its maximal specific activity approaching that of the parental wild-type hGDH1 enzyme [36]. However, the R443S-1 mutant required much higher concentrations of ADP for its activation than the wild-type hGDH1, as reflected by 10–20-fold difference in SC_{50} values of the two enzymes [36] (Table 1).

L-Leucine failed to activate the R443S-1 mutant on its own and required the presence of at least low concentrations of ADP to be able to further activate the enzyme [36]. This indicated a synergistic effect between the two activators, as occurs in the case of the hGDH2 iso-enzyme [30, 36]. On the other hand, in the presence of 1 mM ADP, the GTP inhibition (Table 1) and kinetic properties (Km and Vmax for α-ketoglutarate) of the R443S-1 mutant were similar to those of the wild-type hGDH1 [36].

Substitution of S for R443 conferred a marked sensitivity to estrogens, exceeding even that of the wild-type hGDH2 [40] (Table 1). Further studies showed that this was counter-balanced by four other amino acid substitutions (including the G456A-1 change described above) that had a moderate opposite effect, rendering hGDH2 somewhat less sensitive to estrogens than did the R443S-1 change [40]. Likewise, the R443S-1 change seemed to be responsible for the increased sensitivity of hGDH2 to inhibition by haloperidol [34] (Table 1).

R443 lies in the "antenna-like" region of the hGDH1 enzyme, near the junction of the antenna with the pivot helix (Fig. 5). Introduction of S443 side chain is thought to disrupt hydrogen bonds that exist between R443 of one subunit and S409 (part of the ascending strand of the antenna) of a neighboring subunit [36] (Fig. 5). In addition, substitution of S for R443 is expected to abrogate a cation-π like interaction between the guanidinium group of R443 and the aromatic ring of Y405 from a neighboring subunit (Fig. 5). Substitution of S for R443 could result in loss of these intra-trimer interactions, thereby affecting inter-subunit communication that is thought to be essential for catalysis and allosteric regulation.

R443 resides in the small helix of the descending strand of the antenna that recoils (like a "molecular spring") as the catalytic cleft opens [14]. It is likely that substitution of S for R443 favors a closed enzyme conformation associated with severely decreased basal activity. ADP was able to activate the R443S-1 mutant enzyme, in agreement with the notion that ADP facilitates the opening of the active site or prevents hyper closure [14, 47].

Our data showing that substitution of Ser for R443 totally abrogated L-leucine activation could suggest that this mutation favors the closed enzyme conformation, as L-leucine was traditionally thought to bind at the active site [2]. According to this hypothesis, closure of the catalytic
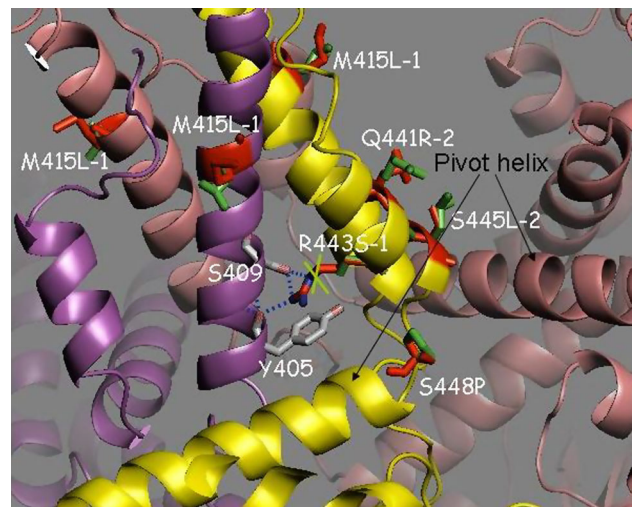
Fig. 5 Close-up of the hGDH 3D-structure in the antenna region of one trimer (open form; as in Fig. 2). Important residues discussed in the text are indicated and *colored* as in Fig. 4. Hydrogen-bonds are depicted as *blue dotted lines*. Substitution of S for R443 in hGDH2 is thought to disrupt the hydrogen bond that exists between R443 of one subunit and S409 of a neighboring subunit most probably resulting in closure of the catalytic cleft [36]. The figure was rendered using PyMOL (Color figure online)

cleft will prevent L-leucine from entering this site. Also, the fact that some minimal concentration of ADP is required to allow L-leucine to exert its effect could be consistent with the possibility that opening of the catalytic site by ADP is necessary for L-leucine to act. On the other hand, observations by Allen et al. [48] on *Tetrahymena* GDH and by Tomita et al. [20] on hGDH2 and *Thermus thermophilus* GDH showed that there could be an allosteric L-leucine site outside the active site (see also below).

Enzymatic assays with the M415L-1 mutant (the second evolutionary amino-acid substitution present in the antenna) showed that this mutant exhibited a basal catalytic activity similar to that of the parental wild-type hGDH1 [36]. Additional analyses revealed that the M415L-1 mutant exhibited an allosteric regulation pattern by ADP, GTP and estrogens that was comparable with that of the wild-type hGDH1 [36, 40] (Table 1). Analysis of the GDH structure also indicates that the residues involved in the M415L-1 mutation are surface residues and that their side chains are not involved in contacts with neighboring residues or co-factors (Fig. 5). This observation is consistent with the fact that this mutation does not affect the activity of the enzyme. On the other hand, Choi et al. [33] have suggested that the evolutionary mutations M415L-1 and R443S-1 acting in concert, as studied in the M415L/R443S-1 double hGDH1 mutant, are responsible for the different regulatory properties of the hGDH iso-enzymes. However, this double mutant did not acquire resistance to GTP, which is the major functional difference between

hGDH1 and hGDH2 and as indicated above relates to the G456A-1 change. Indeed, in subsequent studies, Choi et al. [41] reported that the M415L/R443S/G456A-1 triple mutant, which included the G456A-1 change in addition to the M415L-1 and R443S-1 changes, acquired the GTP inhibition pattern of hGDH2.

Mutagenesis Studies in the Antenna of hGDH2

Many of the HI–HA associated hGDH1 mutations that attenuate GTP inhibition localize to the antenna [14]. These antenna mutations do not alter the basal activity of hGDH1, with few exceptions, including the S448P-1 mutation [43, 49]. The functional consequences of mutations in the corresponding residues of hGDH2 are difficult to predict, as the G456A-1 evolutionary change has already made hGDH2 resistant to GTP. However, amino acid substitutions in this region of hGDH2 could affect the catalytic properties of the enzyme, given the functional importance of the antenna. We have accordingly introduced two HI–HA associated mutations (Q441R-2 and S445L-2) in the descending strand of the antenna and one (S448P-2) in the junction of the antenna with the pivot helix of hGDH2 [45] (Fig. 5).

Replacing Q441 by R and S445 by L in hGDH2 increased basal catalytic activity and enhanced activation by L-leucine [45]. In contrast, substitution of P for S448 in hGDH2 reduced basal activity [45]. The S448P-2 mutant displayed under baseline conditions 2.9 % of its maximal capacity (Table 1), with L-leucine activation being substantially lower for this mutant as compared to the wild-type hGDH2. However, the Q441R-2, S445L-2 and S448P-2 mutations had little effect on the allosteric regulation by ADP and GTP [45]. Of note, the Q441R-2 change occurs in nature in the Orangutan hGDH2 (Fig. 1), and as such its effect is not expected to be deleterious for this primate.

Modeling of the S445L-1 hGDH1 mutation predicts that the introduced L (considered to be a better helix former than serine) stabilizes the small α-helix of the antenna [14]. Similarly, replacement of Q441 by R could stabilize this α-helix. This could favor an open conformation of the active site, thereby counteracting the capacity of the evolutionary R443S-1 change to set the basal activity of hGDH2 to less than 10 % of its maximal. On the other hand, substitution of P for S448 could alter the flexibility of the loop between the small α-helix in the descending strand of the antenna and the pivot helix (Fig. 5) resulting in decreased basal activity. This has also been suggested for hGDH1, in which replacement of S448 by P (S448P-1) also attenuates GTP inhibition [43]. As the S448P-2 change in hGDH2 did not affect regulation by GTP and ADP, the molecular

mechanisms responsible for setting the level of basal activity and for allosteric regulation may be distinct.

Also, the present findings showing that the S448P-2 mutant, which, under baseline conditions, maintains about 3 % of its maximal activity, still exhibits some degree of activation by L-leucine, are consistent with the model suggested for the R443S-1 hGDH1 mutant, according to which the induced super-closed conformation prevents L-leucine from entering the catalytic cleft [36]. On the other hand, the wild-type hGDH2, by maintaining a low but measurable basal activity (2–8 % of maximal), is amenable to activation by L-leucine, as in this state the amino acid has access to the active site.

It has been recently shown that an amino acid substitution at position 445 in hGDH2 (S445A-2) accelerates Parkinson's disease onset [23]. In functional studies, the S445A-2 iso-enzyme showed a basal-specific activity that was substantially greater than that of the wild-type hGDH2, even though most of the other enzymatic properties of the two iso-enzymes were comparable [23] (Table 1).

Substitution of A for S445 is predicted to stabilize the small α-helix in the descending strand of the antenna [23]. Same as L, A is considered to be better α-helix former than S that occupies position 445 in both wild-type hGDH1 and hGDH2. Stabilization of the α-helix in the S445A-2 enzyme could favor an open active site conformation, thereby partially counteracting the minimization of basal activity conferred to hGDH2 by the evolutionary R443S-1 change. Thus, the S445A-2 change may be a gain-of-function mutation in hGDH2 [23].

The R443S/G456A-1 Double Mutant

As discussed above, the G456A-1 and R443S-1 changes, when introduced separately in hGDH1, confer increased resistance to GTP and decreased basal activity, respectively. As such, we asked whether R443S-1 and G456A-1 acting in concert may explain the differences in basal activity, allosteric regulation and thermo-stability of the wild type hGDH1 and hGDH2 iso-enzymes. In other words, we sought to determine if these two evolutionary amino-acid substitutions, acting in concert, were sufficient to functionally convert hGDH1 to hGDH2, especially since these two were among the first mutations to emerge after the retro-position event that gave birth to hGDH2 [17, 21] (Fig. 1).

Thus, we created a double hGDH1 mutant that had both amino acid changes in the same polypeptide chain. Functional analyses of the R443S/G456A-1 double mutant revealed a specific basal activity that was about tenfold lower than that of wild-type hGDH2 (and ∼100 times less than that of wild-type hGDH1), but slightly higher than that

of the R443S-1 single mutant [29] (Table 1). Concerning heat inactivation, the thermo-lability of the double R443S/G456-1 mutant was in-between that of wild type hGDH2 and the R443S-1 single mutant [29] (Table 1).

In terms of allosteric regulation, the R443S/G456A-1 double mutant was less sensitive to activation by ADP than the wild type hGDH2, but substantially more sensitive than the R443S-1 single mutant [29] (Table 1). ADP addition induced activation of the R443S/G456A-1 double mutant up to 5,000–6,000 %, which exceeded three times the respective ADP-induced increase in activity of the wild type hGDH2 and over 20 times the increase in activity of the wild type hGDH1 [29]. The R443S/G456A-1 double mutant was also found to be approximately as resistant to GTP inhibition as the G456A-1 mutant and the wild type hGDH2 and significantly more resistant than the wild-type hGDH1, and this was observed either in the presence or the absence of ADP (Table 1). Hill plot analyses of the GTP inhibition curves showed that the R443S/G456A-1 double mutant, depending on the ADP concentration, was characterized by either non-cooperativity (Hill coefficient about 1.0) or negative cooperativity (Hill coefficient < 1.0), a behavior that was similar to that of wild-type hGDH2 and quite different than the positively cooperative behavior of wild-type hGDH1 [29] (Table 1).

In conclusion, the enzymatic properties of the double R443S/G456A-1 mutant were in-between those of the wild type hGDH2 and the R443S-1 mutant, which meant that additional amino acid substitutions ought to be involved in the functional conversion of hGDH1 to hGDH2.

Mutagenesis Studies in the Glutamate Binding Domain of hGDH1 and hGDH2

On the basis on the mutagenesis studies in the pivot helix and the antenna described above, we showed that the GTP resistance and low basal activity of hGDH2 relates to the G456A-1 and R443S-1 mutations, respectively. However, these two mutations did not reproduce other functional properties of the wild-type hGDH2, as clearly shown also in the R443S/G456A-1 double mutant described above. For example, the wild-type hGDH2 can be stimulated by L-leucine in the absence of ADP and has increased ADP affinity compared to the R443S-1 mutant. Additional studies were needed to clarify the structural basis of the functional diversity of human GDHs.

Thus, we proceeded next by mutagenizing hGDH1 at sites of difference with hGDH2 in the glutamate binding domain (E34, R39, D142, I166, S174 and N498 were replaced by K, Q, E, N and S, respectively).

Substitution of S for N498 did not affect the properties of hGDH1, such as the allosteric regulation of the enzyme by GTP, ADP and estrogens [25, 40] (Table 1). GTP inhibition experiments produced IC_{50} and Hill coefficient values for the N498S-1 mutant comparable to those of the wild type hGDH1 enzyme [25] (Table 1). Comparable SC_{50} values were also obtained from ADP activation experiments comparing the N498S-1 and the wild-type hGDH1 enzymes (Table 1). These observations are consistent with the fact that N498 is not located in a tightly packed region of hGDH1 (data not shown).

Other functional analyses showed that the substitution of Q for R39 and N for S174 in hGDH1, rendered the enzyme somewhat less sensitive to estrogens, thus possibly counterbalancing (in conjunction with the G456A-1 change described above) the extreme estrogen sensitivity produced in hGDH2 by the R443S-1 mutation [40] (Table 1). Interestingly, the mutations rendering the enzyme more resistant to inhibition by estrogens appeared to more or less enhance its basal activity, and there seems to be a correlation of these properties [40].

Following up on initial crystallization and mutagenesis experiments in *Thermus thermophilus* GDH, Tomita et al. [20] performed site-directed mutagenesis studies in hGDH2 that made the enzyme resistant to L-leucine suggesting that hGDH2 uses an allosteric site at its glutamate binding domain for regulation by L-leucine. Specifically, replacement of R151 and D185 (thought to recognize the α-carboxyl group and the α-amino group of L-leucine, respectively; Fig. 6) made hGDH2 insensitive to L-leucine, suggesting that these residues directly recognize L-leucine. These R151M-2 and D185A-2 mutations also decreased the specific activity of the enzyme, suggesting that this subunit interface is also crucial for catalytic GDH activity. L-leucine could activate the enzyme by affecting domain opening and closing during the catalytic cycle, as it is believed that the core of the GDH hexamer contracts when the catalytic cleft closes and inversely expands when the catalytic cleft opens.

Mutagenesis Studies in the NAD$^+$ Binding Domain of hGDH1

With our questions still incompletely answered, we proceeded next to mutagenize hGDH1 at sites of difference with hGDH2 in the NAD$^+$ binding domain (G247, A321, S331, M370 were replaced by R, V, T and L, respectively).

Enzymatic assays carried out in crude tissue extracts showed that the S331T-1 and M370L-1 mutants exhibited a basal catalytic activity similar to that of the wild-type hGDH1. Also, the S331T-1 and M370L-1 mutants exhibited an allosteric regulation pattern by ADP and GTP that was comparable with that of the wild-type hGDH-1 [36] (Table 1). Other functional analyses showed that the
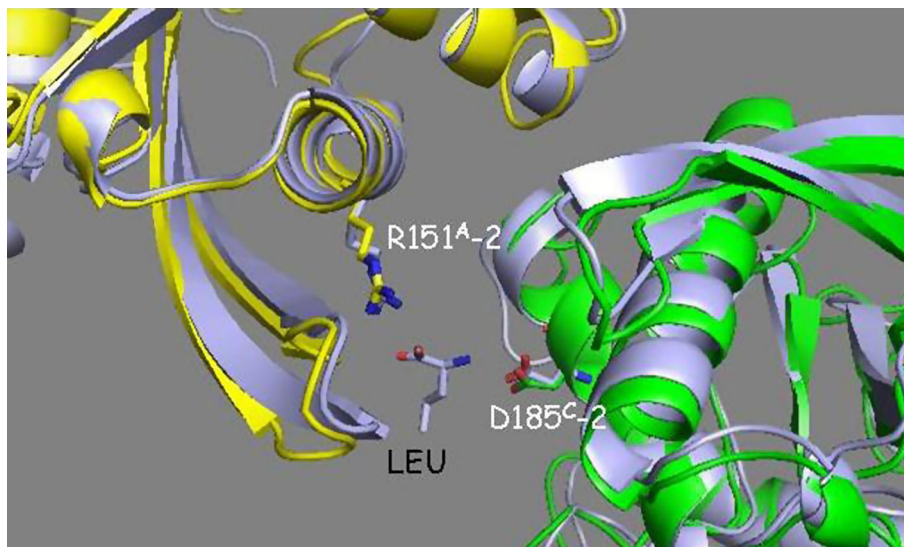
Fig. 6 Putative leucine-binding region of hGDH2 (from [20]). The superimposed crystal structures of the leucine bound form of the hetero-hexameric glutamate dehydrogenase from *Thermus thermophilus* (PDB code: 3AOE; [20]; in *light blue*) and the apo-form of hGDH1 (as in Fig. 2) are shown around one putative leucine-binding site. The orientation and coloring of the hGDH1 monomers are as in Fig. 2. Only two monomers are shown, for clarity. Residues R151-2 and D185-2 (thought to be involved in leucine binding in hGDH2 [20]) are indicated and depicted as stick-models. The figure was rendered using PyMOL (Color figure online)

M370L-1 substitution in hGDH1 rendered the enzyme somewhat less sensitive to estrogens, thus possibly counterbalancing (in conjunction with the G456A-1, R39Q-1 and S174N-1 changes described above) the extreme estrogen sensitivity produced by the R443S-1 mutation in hGDH2 [40] (Table 1). In contrast, the S331T-1 change did not significantly affect estrogen inhibition (Table 1).

Analysis of the GDH structure indicates that the residues involved in the S331T-1 mutation are surface residues and that their side chains are not involved in contacts with neighboring residues or co-factors (Fig. 3), an observation consistent with the fact that this mutation does not affect enzymatic activity. M370, involved in the mutation M370L-1, is also not in contact with any co-factors or substrates (Fig. 3). Its change to L is conservative and likely does not disturb the local packing of the molecule, in agreement with the absence of any change in activity.

Discussion

During the past 10 years, our studies employing site-directed mutagenesis of the *GLUD1* and *GLUD2* cDNAs, in addition to studies by other researchers, provided important insights into the molecular mechanisms that underlie the functional diversity of human GDHs. These studies revealed that the functional differences between hGDH1 and hGDH2 are mainly due to two evolutionary amino acid substitutions that occurred immediately after the emergence of hGDH2 and helped its survival under selection pressure (Fig. 1). The first change (G456A-1) made the enzyme resistant to GTP without altering its activation by ADP and L-leucine [25], whereas the second change (R443S-1) rendered the enzyme essentially inactive in the absence of allosteric effectors [36]. Although the activity of the R443S-1 mutant could be fully restored by ADP, this occurred at higher concentrations than those required for the wild-type hGDH2 iso-enzyme. Also, unlike the hGDH2 iso-enzyme, the R443S-1 mutant was not amenable to activation by L-leucine unless in the presence of ADP [36]. Furthermore, the R443S/G456A-1 double mutant or other combined mutants studied thus far could not reproduce all the properties of the wild-type hGDH2 enzyme [29], indicating that other amino-acid substitutions are involved in this evolutionary transition from hGDH1 to hGDH2.

Why the hGDH2 enzyme has evolved through the G456A-1 change to be extremely GTP resistant? It is widely accepted that intra-cellular GTP levels regulate multiple metabolic pathways [50]. Mammalian GDH1 is thought to be under tonic inhibition by GTP, as suggested by observations on patients with the HI/HA syndrome due to regulatory *GLUD1* mutations that attenuate GTP inhibition. In these patients, an over-active hGDH1 leads to excessive insulin release from the pancreatic beta cells, particularly in response to a protein-rich meal that increases L-leucine levels [38]. This entails increased glutamate deamination by the up-regulated enzyme to generate increased amounts of α-ketoglutarate in the Krebs cycle, leading to increased ATP formation and subsequently to insulin release. In the kidney,

enhanced glutamate deamination by GDH is shown to produce excess ammonia that enters the blood stream, probably accounting for the hyper-ammonemia observed in HI/HA syndrome [51]. As mitochondrial GTP levels are generally higher in brain, kidney and heart (in the order of 1.2–1.3 mM) than in other tissues, such as liver and muscle [52], GTP may not be a suitable modulator for GDH activity in these tissues. Also, hGDH2 may have evolved to perform another role in the testis, brain, and kidney where it is expressed [21]. This role in the nervous system could be metabolism of glutamate as a neurotransmitter irrespectively of the energy status of the cell. Thus, hGDH2 could produce or catabolize glutamate as a neurotransmitter even under conditions of high energy charge (high GTP levels due to enhanced Krebs cycle function), that are prone to fully inactivate hGDH1.

Why the hGDH2 enzyme has evolved through the R443S-1 change to have a very low basal activity that is responsive to activation by ADP and L-leucine? Total dependence on available ADP levels provides a novel molecular mechanism for the regulation of glutamate flux through the GDH pathway. This will permit the recruitment of the enzyme (possibly for metabolizing glutamate as a neurotransmitter) under conditions of low cellular energy (high ADP/ATP ratio), such as those occurring under glutamatergic neurotransmission that is highly energy consuming [10, 53, 54]. Traut [55] reported that, on the basis of data from several studies, the average concentration of ADP in human cells and fluids is 137 μM. However, the ADP concentration inside mitochondria is much higher (fluctuating between 1 and 9 mM) and depends on the energy status of the cell [52, 56]. On the other hand, it is expected that there are distinct micro-environments inside the mitochondria, with the ADP concentration being different among them [56, 57]. The ability of L-leucine to sensitize hGDH2 to ADP activation may permit the enzyme to respond to small changes in ADP concentration, even in the absence of an overt local energy deficit [31].

Is the fact that replacement of R443 by S, rendering hGDH2 more active at lower pH compared to hGDH1, of importance for glutamate metabolism in human tissues? The pH in the mitochondrial matrix is thought to remain lower (in the range of 7.5–8.2) than the cytosolic pH, since lowering the extra-mitochondrial pH causes an analogous reduction in the intra-mitochondrial pH in many cells [58–61]. We have observed that acidification substantially increases the $Km[NH_4^+]$ for both hGDH1 and hGDH2, favoring the oxidative deamination of glutamate by hGDHs [62]. This indeed is shown to occur in the kidney during systemic acidosis [63].

It is well known that the glutamate neurotransmitter action is terminated by uptake into glial cells [64]. In the salamander Muller cells (a type of retinal glial cell),

glutamate uptake generates intracellular acidification (pH drop from 7.2 to 7.0) due to counter-transport of OH– [64, 65]. These pH changes occur both in the cytosol and in the mitochondria-enriched distal process. This glutamate-induced acidification occurs in parallel with a rise in NAD(P)H that is thought to result from glutamate oxidation via GDH [65]. Likewise, the mitochondrial matrix pH drops significantly (to circa 7.2) in mouse astrocytes following the uptake of glutamate released from nerve endings during excitatory transmission [66]. In this respect, there is evidence that GDH works predominantly in the oxidative deamination direction in astrocytes exposed to glutamate [67–69]. Hence, the ability of hGDH2 to function well at pH 7.0, at least partially due to the R443S-1 change, may represent an adaptation of importance for the metabolism of neurotransmitter glutamate.

How is this association between glutamate levels and intra-mitochondrial pH achieved? Acidosis [59] or inhibition of the GDH activity [70] affects the transport of glutamate through cellular membranes. The inner membrane of human mitochondria contains two types of glutamate transporters, the aspartate/glutamate carrier and the glutamate carrier (GC), respectively [71]. Glutamate entering mitochondria by the aspartate/glutamate carrier is transaminated to aspartate (as part of the malate-aspartate shuttle) [72]. Glutamate using the GC to enter the mitochondria could be deaminated by GDH [72, 73]. Interestingly, transport of glutamate via the GC is associated with co-transport of H^+ across the mitochondrial membrane [71].

The emergence of the *GLUD2* gene coincides with a period of increase in size and in functional and structural complexity of the brain of the common ancestor of humans and other modern-day primates. While the precise biological advantage conferred by the emergence of the *GLUD2* gene needs to be elucidated, the present findings provide substantial insight into the molecular mechanisms that set basal activity levels and regulate the function of hGDH2 possibly permitting its adaptation to the unique conditions that prevail in the nerve and other tissues where it is expressed [10]. These include resistance to GTP inhibition, dependence on ADP for catalytic function, and ability to function efficiently in relatively low intracellular pH. While hGDH1 and hGDH2 are present at relatively high levels in human brain [21], their exact function there needs to be better understood. Immunocytochemical studies by Aoki et al. [74] revealed that GDH in rat brain is found mainly in astrocytes of regions associated with glutamatergic neurotransmission. Biochemical methods have shown substantial GDH activity in both astrocytes and neurons cultured from the cerebral cortex and the cerebellum of the mouse [75]. More recent studies [19, 21] have revealed that hGDH1 and hGDH2 are both expressed in human brain astrocytes. However, the exact role of these

iso-enzymes in nervous system metabolism and their functional and structural interaction remains a charming mystery.

References

1. Hudson R, Daniel R (1993) L-glutamate dehydrogenases: distribution, properties and mechanism. Comp Biochem Physiol B 106:767–792

2. Smith TJ, Stanley CA (2008) Untangling the glutamate dehydrogenase allosteric nightmare. Trends Biochem Sci 33:557–564

3. McKenna MC, Tildon JT, Stevenson JH, Huang X (1996) New insights into the compartmentation of glutamate and glutamine in cultured rat brain astrocytes. Dev Neurosci 18:380–390

4. McKenna MC (2007) The glutamate–glutamine cycle is not stoichiometric: fates of glutamate in brain. J Neurosci Res 85:3347–3358

5. Raimundo N, Baysal BE, Shadel GS (2011) Revisiting the TCA cycle: signaling to tumor formation. Trends Mol Med 17:641–649

6. Lambeth DO (2002) What is the function of GTP produced in the Krebs citric acid cycle? IUBMB Life 54:143–144

7. Shashidharan P, Clarke DD, Ahmed N, Moschonas N, Plaitakis A (1997) Nerve tissue-specific human glutamate dehydrogenase that is thermolabile and highly regulated by ADP. J Neurochem 68:1804–1811

8. Owen OE, Kalhan SC, Hanson RW (2002) The key role of anaplerosis and cataplerosis for citric acid cycle function. J Biol Chem 277:30409–30412

9. Sener A, Malaisse-Lagae F, Malaisse W (1981) Stimulation of pancreatic islet metabolism and insulin release by a nonmetabolizable amino acid. Proc Natl Acad Sci USA 78:5460–5464

10. Plaitakis A, Zaganas I (2001) Regulation of human glutamate dehydrogenases: implications for glutamate, ammonia and energy metabolism in brain. J Neurosci Res 66:899–908

11. Cooper AL (2012) The role of glutamine synthetase and glutamate dehydrogenase in cerebral ammonia homeostasis. Neurochem Res 37:2439–2455

12. Li M, Li C, Allen A, Stanley C, Smith T (2014) Glutamate dehydrogenase: structure, allosteric regulation, and role in insulin homeostasis. Neurochem Res. doi:10.1007/s11064-013-1173-2

13. Peterson PE, Smith TJ (1999) The structure of bovine glutamate dehydrogenase provides insights into the mechanism of allostery. Struct Fold Des 7:769–782

14. Smith TJ, Schmidt T, Fang J, Wu J, Siuzdak G, Stanley CA (2002) The structure of apo human glutamate dehydrogenase details subunit communication and allostery. J Mol Biol 318:765–777

15. Smith TJ, Peterson PE, Schmidt T, Fang J, Stanley CA (2001) Structures of bovine glutamate dehydrogenase complexes elucidate the mechanism of purine regulation. J Mol Biol 307:707–720

16. Shashidharan P, Michaelidis TM, Robakis NK, Kresovali A, Papamatheakis J, Plaitakis A (1994) Novel human glutamate dehydrogenase expressed in neural and testicular tissues and encoded by an X-linked intronless gene. J Biol Chem 269:16971–16976

17. Burki F, Kaessmann H (2004) Birth and adaptive evolution of a hominoid gene that supports high neurotransmitter flux. Nat Genet 36:1061–1063

18. Mavrothalassitis G, Tzimagiorgis G, Mitsialis A, Zannis V, Plaitakis A, Papamatheakis J, Moschonas N (1988) Isolation and characterization of cDNA clones encoding human liver glutamate dehydrogenase: evidence for a small gene family. Proc Natl Acad Sci USA 85:3494–3498

19. Spanaki C, Zaganas I, Kleopa KA, Plaitakis A (2010) Human GLUD2 glutamate dehydrogenase is expressed in neural and testicular supporting cells. J Biol Chem 285:16748–16756

20. Tomita T, Kuzuyama T, Nishiyama M (2011) Structural basis for leucine-induced allosteric activation of glutamate dehydrogenase. J Biol Chem 286:37406–37413

21. Zaganas I, Spanaki C, Plaitakis A (2012) Expression of human GLUD2 glutamate dehydrogenase in human tissues: functional implications. Neurochem Int 61:455–462

22. Ciomborowska J, Rosikiewicz W, Szklarczyk D, Makałowski W, Makałowska I (2013) Orphan retrogenes in the human genome. Mol Biol Evol 30:384–396

23. Plaitakis A, Latsoudis H, Kanavouras K, Ritz B, Bronstein JM, Skoula I, Mastorodemos V, Papapetropoulos S, Borompokas N, Zaganas I, Xiromerisiou G, Hadjigeorgiou GM, Spanaki C (2010) Gain-of-function variant in GLUD2 glutamate dehydrogenase modifies Parkinson's disease onset. Eur J Hum Genet 18:336–341

24. Colon A, Plaitakis A, Perakis A, Berl S, Clarke D (1986) Purification and characterization of a soluble and a particulate glutamate dehydrogenase from rat brain. J Neurochem 46:1811–1819

25. Zaganas I, Plaitakis A (2002) Single amino acid substitution (G456A) in the vicinity of the GTP binding domain of human housekeeping glutamate dehydrogenase markedly attenuates GTP inhibition and abolishes the cooperative behavior of the enzyme. J Biol Chem 277:26422–26428

26. Mastorodemos V, Kotzamani D, Zaganas I, Arianoglou G, Latsoudis H, Plaitakis A (2009) Human GLUD1 and GLUD2 glutamate dehydrogenase localize to mitochondria and endoplasmic reticulum. Biochem Cell Biol 87:505–516

27. McCarthy AD, Walker JM, Tipton KF (1980) Purification of glutamate dehydrogenase from ox brain and liver. Evidence that commercially available preparations of the enzyme from ox liver have suffered proteolytic cleavage. Biochem J 191:605–611

28. Yang S-J, Huh J-W, Hong H-N, Kim TU, Cho S-W (2004) Important role of Ser443 in different thermal stability of human glutamate dehydrogenase isozymes. FEBS Lett 562:59–64

29. Kanavouras K, Mastorodemos V, Borompokas N, Spanaki C, Plaitakis A (2007) Properties and molecular evolution of human GLUD2 (neural and testicular tissue-specific) glutamate dehydrogenase. J Neurosci Res 85:3398–3406

30. Plaitakis A, Metaxari M, Shashidharan P (2000) Nerve tissue-specific (GLUD2) and housekeeping (GLUD1) human glutamate dehydrogenases are regulated by distinct allosteric mechanisms. Implications for biologic function. J Neurochem 75:1862–1869

31. Plaitakis A, Spanaki C, Mastorodemos V, Zaganas I (2003) Study of structure–function relationships in human glutamate dehydrogenases reveals novel molecular mechanisms for the regulation of the nerve tissue-specific (GLUD2) isoenzyme. Neurochem Int 43:401–410

32. Zaganas I, Kanavouras K, Mastorodemos V, Latsoudis H, Spanaki C, Plaitakis A (2009) The human GLUD2 glutamate dehydrogenase: localization and functional aspects. Neurochem Int 55:52–63

33. Choi M-M, Kim E-A, Yang S-J, Choi SY, Cho S-W, Huh J-W (2007) Amino acid changes within antenna helix are responsible for different regulatory preferences of human glutamate dehydrogenase isozymes. J Biol Chem 282:19510–19517

34. Plaitakis A, Latsoudis H, Spanaki C (2011) The human GLUD2 glutamate dehydrogenase and its regulation in health and disease. Neurochem Int 59:495–509

35. Spanaki C, Zaganas I, Kounoupa Z, Plaitakis A (2012) The complex regulation of human glud1 and glud2 glutamate dehydrogenases and its implications in nerve tissue biology. Neurochem Int 61:470–481

36. Zaganas I, Spanaki C, Karpusas M, Plaitakis A (2002) Substitution of Ser for Arg-443 in the regulatory domain of human housekeeping (GLUD1) glutamate dehydrogenase virtually abolishes basal activity and markedly alters the activation of the enzyme by ADP and l-leucine. J Biol Chem 277:46552–46558

37. Mastorodemos V, Zaganas I, Spanaki C, Bessa M, Plaitakis A (2005) Molecular basis of human glutamate dehydrogenase regulation under changing energy demands. J Neurosci Res 79:65–73

38. Stanley CA, Lieu YK, Hsu BYL, Burlina AB, Greenberg CR, Hopwood NJ, Perlman K, Rich BH, Zammarchi E, Poncz M (1998) Hyperinsulinism and hyperammonemia in infants with regulatory mutations of the glutamate dehydrogenase gene. N Engl J Med 338:1352–1357

39. Lee E-Y, Yoon H-Y, Ahn J-Y, Choi SY, Cho S-W (2001) Identification of the GTP binding site of human glutamate dehydrogenase by cassette mutagenesis and photoaffinity labeling. J Biol Chem 276:47930–47936

40. Borompokas N, Papachatzaki M-M, Kanavouras K, Mastorodemos V, Zaganas I, Spanaki C, Plaitakis A (2010) Estrogen modification of human glutamate dehydrogenases is linked to enzyme activation state. J Biol Chem 285:31380–31387

41. Choi M, Hwang E, Kim E, Huh J, Cho S (2008) Identification of amino acid residues responsible for different GTP preferences of human glutamate dehydrogenase isozymes. Biochem Biophys Res Commun 368:742–747

42. Kelly A, Stanley C (2001) Disorders of glutamate metabolism. Ment Retard Dev Disabil Res Rev 7:287–295

43. Fang J, Hsu B, MacMullen C, Poncz M, Smith T, Stanley C (2002) Expression, purification and characterization of human glutamate dehydrogenase (GDH) allosteric regulatory mutations. Biochem J 363:81–87

44. Lee E-Y, Huh J-W, Yang S-J, Choi SY, Cho S-W, Choi HJ (2003) Histidine 454 plays an important role in polymerization of human glutamate dehydrogenase. FEBS Lett 540:163–166

45. Kanavouras K, Borompokas N, Latsoudis H, Stagourakis A, Zaganas I, Plaitakis A (2009) Mutations in human GLUD2 glutamate dehydrogenase affecting basal activity and regulation. J Neurochem 109:167–173

46. Banerjee S, Schmidt T, Fang J, Stanley CA, Smith TJ (2003) Structural studies on ADP activation of mammalian glutamate dehydrogenase and the evolution of regulation. Biochemistry 42:3446–3456

47. Petersen RC, Smith GE, Waring SC, Ivnik RJ, Tangalos EG, Kokmen E (1999) Mild cognitive impairment: clinical characterization and outcome. Arch Neurol 56:303–308

48. Allen A, Kwagh J, Fang J, Stanley CA, Smith TJ (2004) Evolution of glutamate dehydrogenase regulation of insulin homeostasis is an example of molecular exaptation. Biochemistry 43:14431–14443

49. Stanley CA (2011) Two genetic forms of hyperinsulinemic hypoglycemia caused by dysregulation of glutamate dehydrogenase. Neurochem Int 59:465–472

50. Meshkini A, Yazdanparast R, Nouri K (2011) Intracellular GTP level determines cell's fate toward differentiation and apoptosis. Toxicol Appl Pharmacol 253:188–196

51. Treberg JR, Clow KA, Greene KA, Brosnan ME, Brosnan JT (2010) Systemic activation of glutamate dehydrogenase increases renal ammoniagenesis: implications for the hyperinsulinism/hyperammonemia syndrome. Am J Physiol Endocrinol Metab 298:E1219–E1225

52. Wheeler LJ, Mathews CK (2011) Nucleoside triphosphate pool asymmetry in mammalian mitochondria. J Biol Chem 286:16992–16996

53. Attwell D, Laughlin SB (2001) An energy budget for signaling in the grey matter of the brain. J Cereb Blood Flow Metab 21:1133–1145

54. Schousboe A, Sickmann HM, Bak LK, Schousboe I, Jajo FS, Faek SAA, Waagepetersen HS (2011) Neuron–glia interactions in glutamatergic neurotransmission: roles of oxidative and glycolytic adenosine triphosphate as energy source. J Neurosci Res 89:1926–1934

55. Traut TW (1994) Physiological concentrations of purines and pyrimidines. Mol Cell Biochem 140:1–22

56. Metelkin E, Demin O, Kovacs Z, Chinopoulos C (2009) Modeling of ATP–ADP steady-state exchange rate mediated by the adenine nucleotide translocase in isolated mitochondria. FEBS J 276:6942–6955

57. Murthy MS, Pande SV (1985) Microcompartmentation of transported carnitine, acetylcarnitine and ADP occurs in the mitochondrial matrix. Implications for transport measurements and metabolism. Biochem J 230:657–663

58. Rottenberg H, Lee CP (1975) Energy dependent hydrogen ion accumulation in submitochondrial particles. Biochemistry 14:2675–2680

59. Schoolwerth A, LaNoue K, Hoover W (1984) Effect of pH on glutamate efflux from rat kidney mitochondria. Am J Physiol 246:F266–F271

60. Llopis J, McCaffery JM, Miyawaki A, Farquhar MG, Tsien RY (1998) Measurement of cytosolic, mitochondrial, and Golgi pH in single living cells with green fluorescent proteins. Proc Natl Acad Sci USA 95:6803–6808

61. Balut C, vandeVen M, Despa S, Lambrichts I, Ameloot M, Steels P, Smets I (2008) Measurement of cytosolic and mitochondrial pH in living cells during reversible metabolic inhibition. Kidney Int 73:226–232

62. Zaganas I, Pajecka K, Wendel Nielsen C, Schousboe A, Waagepetersen HS, Plaitakis A (2013) The effect of pH and ADP on ammonia affinity for human glutamate dehydrogenases. Metab Brain Dis 28:127–131

63. Schoolwerth AC, Nazar BL, LaNoue KF (1978) Glutamate dehydrogenase activation and ammonia formation by rat kidney mitochondria. J Biol Chem 253:6177–6183

64. Bouvier M, Szatkowski M, Amato A, Attwell D (1992) The glial cell glutamate uptake carrier countertransports pH-changing anions. Nature 360:471–474

65. Poitry S, Poitry-Yamate C, Ueberfeld J, MacLeish P, Tsacopoulos M (2000) Mechanisms of glutamate metabolic signaling in retinal glial (Móller) cells. J Neurosci 20:1809–1821

66. Azarias G, Perreten H, Lengacher S, Poburko D, Demaurex N, Magistretti PJ, Chatton J-Y (2011) Glutamate transport decreases mitochondrial pH and modulates oxidative metabolism in astrocytes. J Neurosci 31:3550–3559

67. Yu AC, Schousboe A, Hertz L (1982) Metabolic fate of 14C-labeled glutamate in astrocytes in primary cultures. J Neurochem 39:954–960

68. McKenna MC, Sonnewald U, Huang X, Stevenson J, Zielke HR (1996) Exogenous glutamate concentration regulates the metabolic fate of glutamate in astrocytes. J Neurochem 66:386–393

69. Sonnewald U, Westergaard N, Schousboe A (1997) Glutamate transport and metabolism in astrocytes. Glia 21:56–63

70. Whitelaw BS, Robinson MB (2013) Inhibitors of glutamate dehydrogenase block sodium-dependent glutamate uptake in rat brain membranes. Front Endocrinol (Lausanne) 4:123

71. Palmieri F (2013) The mitochondrial transporter family SLC25: identification, properties and physiopathology. Mol Asp Med 34:465–484

72. Berkich DA, Ola MS, Cole J, Sweatt AJ, Hutson SM, LaNoue KF (2007) Mitochondrial transport proteins of the brain. J Neurosci Res 85:3367–3377

73. Dennis SC, Clark JB (1977) The pathway of glutamate metabolism in rat brain mitochondria. Biochem J 168:521–527

74. Aoki C, Milner TA, Berger SB, Sheu KF, Blass JP, Pickel VM (1987) Glial glutamate dehydrogenase: ultrastructural localization and regional distribution in relation to the mitochondrial enzyme, cytochrome oxidase. J Neurosci Res 18:305–318

75. Zaganas I, Waagepetersen HS, Georgopoulos P, Sonnewald U, Plaitakis A, Schousboe A (2001) Differential expression of glutamate dehydrogenase in cultured neurons and astrocytes from mouse cerebellum and cerebral cortex. J Neurosci Res 66:909–913

76. Larkin MA, Blackshields G, Brown NP, Chenna R, McGettigan PA, McWilliam H, Valentin F, Wallace IM, Wilm A, Lopez R, Thompson JD, Gibson TJ, Higgins DG (2007) Clustal W and Clustal X version 2.0. Bioinformatics 23:2947–2948

77. Page R (1996) TreeView: an application to display phylogenetic trees on personal computers. Comput Appl Biosci 12:357–358